

THE USE OF SATELLITES IN NON-GEOSTATIONARY ORBITS FOR UNLOADING GEOSTATIONARY COMMUNICATIONS SATELLITE TRAFFIC PEAKS

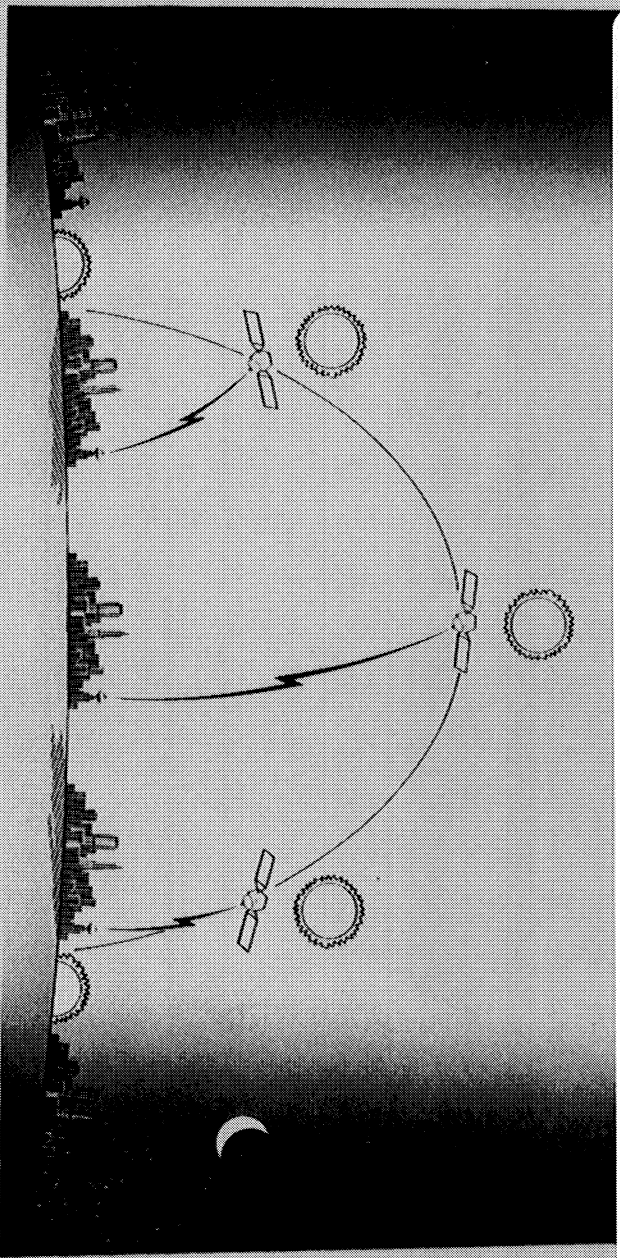
VOLUME 11 - TECHNICAL REPORT
MAY 1987

NASA
Lewis Research Center
Contract No. NAS3-24891

(NASA-CR-179597-VOL-2) THE USE OF
SATELLITES IN NON-GEOSTATIONARY ORBITS FOR
UNLOADING GEOSTATIONARY COMMUNICATION
SATELLITE TRAFFIC PEAKS. VOLUME 2: TECHNICAL
REPORT Final Report, Apr. (Fcid Aerospace

N87-21213

63/32 43553
Unclass



1. Report No. CR179597		2. Government Accession No.		3. Recipient's Catalog No.	
4. Title and Subtitle The Use of Satellites in Non-Geostationary Orbits for Unloading Geostationary Communication Satellite Traffic Peaks. Vol. II - Technical Report				5. Report Date May 1987	
				6. Performing Organization Code	
7. Author(s) K. Price, A. Turner, T. Nguyen, W. Doong, C. Weyandt				8. Performing Organization Report No. 650-60-26	
9. Performing Organization Name and Address Ford Aerospace & Communications Corp. 3939 Fabian Way Palo Alto, CA 94303				10. Work Unit No.	
				11. Contract or Grant No. NAS3-24891	
12. Sponsoring Agency Name and Address NASA, Lewis Research Center 21,000 Brookpark Road Cleveland, Ohio 44135				13. Type of Report and Period Covered Final . Apr 1986-Feb 1987	
				14. Sponsoring Agency Code	
15. Supplementary Notes NASA Contract Manager: Ms. Denise Ponchak One other volume prepared: Vol. I - Executive Summary					
16. Abstract <p>The part of the geostationary (GEO) orbital arc used for United States domestic fixed, communications service is rapidly becoming filled with satellites. One of the factors currently limiting its utilization is that communications satellites must be designed to have sufficient capacity to handle peak traffic loads, and thus are under utilized most of the time. A solution is to use satellites in suitable non-geostationary orbits to unload the traffic peaks.</p> <p>Three different designs for a non-geostationary orbit communications satellite system are presented for the 1995 time frame. The economic performance is analyzed and compared with geostationary satellites for two classes of service, trunking and customer premise service. The result is that the larger payload of the non-geostationary satellite offsets the burdens of increased complexity and worse radiation environment to give improved economic performance. Depending on ground terminal configuration, the improved economic performance of the space segment may be offset by increased ground terminal expenses.</p>					
17. Key Words (Suggested by Author(s)) Non-Geostationary Orbit Satellites Communication Satellite Economics			18. Distribution Statement General Release		
19. Security Classif. (of this report) Unclassified		20. Security Classif. (of this page) Unclassified		21. No. of Pages	
				22. Price*	

* For sale by the National Technical Information Service, Springfield, Virginia 22161

NASA Contract No. NAS3-24891

THE USE OF SATELLITES IN NON-GEOSTATIONARY
ORBITS FOR UNLOADING GEOSTATIONARY
COMMUNICATIONS SATELLITE TRAFFIC PEAKS

Volume II:
TECHNICAL REPORT

Prepared by
FORD AEROSPACE & COMMUNICATIONS CORPORATION
Western Development Laboratories Division
Spacecraft Systems Operation, Advanced Systems Department
3939 Fabian Way, Palo Alto CA 94303

Program Manager: Kent M. Price
Major Contributors: Andrew E. Turner
Tuan Nguyen
Wen Doong
Charles Weyandt

Prepared for
NASA, Lewis Research Center
Cleveland, OH 44135
May 1987

TABLE of CONTENTS

SECTION I – INTRODUCTION

1	Background	I – 1
2	Objectives of Study	I – 1
3	Approach	I – 1
3.1	Task 1 – Concepts Development	I-1
3.2	Task 2 – Systems Definition	I-2
3.3	Task 3 – Economic Comparisons	I-2
3.4	Task 4 – Technology Requirements	I-2
4	Organization of Report	I – 2

SECTION II – TRAFFIC MODEL

1	Introduction	II – 1
2	NASA Traffic Model	II – 1
2.1	Data Base	II-1
2.2	Methodology	II-1
2.3	Traffic by Service Category	II-2
2.4	Traffic by Location	II-2
3	Traffic by Time-of-Day	II – 2
3.1	Voice Traffic	II-2
3.1.1	Voice Traffic Data Base	II-2
3.1.2	Business Influence	II-3
3.1.3	Trunking and CPS Voice Services	II-4
3.2	Video Conferencing Traffic	II-4
3.3	Data Traffic	II-5
3.4	Video Broadcasting Traffic	II-5
3.5	Application to Zone Traffic	II-5
4	Traffic Model Results	II – 5
4.1	Inter-Zone Traffic	II-5
4.2	Intra-Zone Traffic	II-5
4.3	Total Traffic	II-5
4.4	Traffic Analysis	II-9

5	Sensitivity Analysis	II - 11
5.1	Introduction	II - 11
5.2	Total Traffic	II - 11
5.3	Distribution of Traffic	II - 11
5.4	Time of Day Analysis	II - 11
5.5	Tariffs	II - 11
5.6	Conclusions	II - 11

SECTION III - ANALYSIS OF SATELLITE ORBITS

1	Requirements	III - 1
2	Overview of Solutions	III - 1
2.1	Other GEO Solutions	III - 1
2.1.1	Closer Spacing in GEO	III - 1
2.1.2	Geosynchronous but not Geostationary	III - 2
2.1.3	Alternating Frequency Plan	III - 2
2.1.4	Combined Service Satellites	III - 2
2.1.5	Large Capacity Platforms	III - 2
2.1.6	Greater Available Bandwidth	III - 2
2.2	Super-Synchronous Satellites	III - 2
2.3	Sub-Synchronous Circular Orbits	III - 3
2.4	Sub-Synchronous Elliptic Orbits	III - 3
3	Orbital Mechanics	III - 3
3.1	Introduction	III - 3
3.2	Kepler's Laws	III - 5
3.3	Orientation of Orbit in Space	III - 5
3.3.1	Euler Angles	III - 5
3.3.2	Inclination	III - 5
3.3.3	Right Ascension of Ascending Node	III - 7
3.3.4	Argument of Perigee	III - 7
3.3.5	True Anomaly at Epoch	III - 7
3.4	Orbital Perturbations	III - 7
3.4.1	Introduction	III - 7
3.4.2	Nodal Regression	III - 8
3.4.3	Apsidal Rotation	III - 9
3.4.4	Luni-Solar Perturbations	III - 9
3.4.5	Atmospheric Drag	III - 11
3.4.6	Summary of Perturbations	III - 14
3.5	Earth Orbit and Sun Geometry	III - 14
4	Candidate Orbit Selection	III - 15
4.1	Introduction	III - 15
4.2	Constraint on Orbital Period	III - 16
4.3	Constraint on Apogee Altitude	III - 16
4.4	Single Satellite Configurations	III - 16

4.4.1	Circular Orbits	III - 16
4.4.2	Non-Circular Orbits	III - 20
4.4.3	Single Satellite Conclusions	III - 22
4.5	Multiple Satellite Constellations	III - 22
4.5.1	Molniya Orbit Systems	III - 22
4.5.2	Lower Altitude Satellites	III - 22
5	Analysis of Selected Orbits	III - 23
5.1	Introduction	III - 23
5.2	ACE Orbit	III - 23
5.2.1	General Description	III - 23
5.2.2	Size and Shape	III - 23
5.2.3	CONUS Coverage	III - 24
5.2.4	Motion of Satellite	III - 25
5.2.5	Worldwide Coverage	III - 25
5.3	STET Orbit	III - 26
5.3.1	General Description	III - 26
5.3.2	CONUS Coverage	III - 26
5.3.3	Worldwide Coverage by STET	III - 27
6	Conclusions	III - 27

SECTION IV - DELOADING PEAK TRAFFIC

1	Introduction	IV - 1
2	Magnitude of Traffic Deload	IV - 1
3	Deloading Methodology	IV - 1
4	STET Orbit Deloading	IV - 1
4.1	Intra-Zone Traffic	IV - 1
4.1.1	Eastern Zone	IV - 1
4.1.2	Central Zone	IV - 1
4.2	Inter-Zone Traffic	IV - 2
5	ACE Orbit Deloading	IV - 2
5.1	Intra-Zone Traffic	IV - 2
5.1.1	Eastern Zone	IV - 2
5.1.2	Central Zone	IV - 2
5.2	Inter-Zone Traffic	IV - 2
6	Analysis of Deloading	IV - 2
6.1	Summary of Deloading by Single Satellite	IV - 2
6.2	Visibility Constraints	IV - 6
6.3	Traffic Routing Constraints	IV - 6

7 Multiple Non-GEO Satellites	IV - 6
7.1 Introduction	IV-6
7.2 Methodology	IV-6
7.3 Multiple STET Satellites	IV-6
7.4 Multiple ACE Satellites	IV-9

8 Conclusions	IV - 9
----------------------	---------------

SECTION V - FORECAST OF 1990 TECHNOLOGY

1 Attitude Control Subsystem	V - 1
2 Communications Payload	V - 1
2.1 Antennas	V-2
2.2 Transponders and Receivers	V-2
2.3 On-Board Processing	V-2
3 Primary Power	V - 3
3.1 Batteries	V-3
3.2 Solar Cells	V-3
4 Propulsion Subsystem	V - 3
5 Structure and Mechanisms	V - 3
6 TT&C Subsystem	V - 4
7 Thermal Control	V - 4
8 Space Transportation	V - 4
9 Radiation Hardness	V - 5
10 Summary of Technology Developments	V - 5

SECTION VI - SYSTEM CONCEPTS

1 Introduction	VI - 1
2 Non-GEO System Issues	VI - 1
2.1 Antenna Coverage	VI-1
2.1.1 STET Satellite Antenna	VI-2
2.1.2 ACE Satellite Antenna	VI-4
2.2 Attitude Control	VI-4
2.2.1 Spin Stabilized Satellites	VI-4
2.2.2 3-Axis Satellites	VI-5
2.3 Battery Versus Solar Array Size	VI-5

2.4	Communications Capacity	VI-5
2.4.1	Potential Larger Capacity	VI-5
2.4.2	Problems with Frequency Reuse	VI-6
2.4.3	Non-GEO Payloads	VI-6
2.5	Intersatellite Links	VI-6
2.6	Launch Vehicle Capacity	VI-6
2.7	Orbital Drag at Perigee	VI-7
2.8	Polarization Tracking	VI-7
2.9	Radiation Effects	VI-7
3	Trunking Systems	VI - 8
3.1	Baseline Trunking System	VI-8
3.2	STET Trunking System	VI-8
3.3	ACE Trunking System	VI-9
4	CPS Systems	VI - 9
4.1	Baseline CPS System	VI-9
4.2	STET CPS System	VI-9
4.3	ACE CPS System	VI-10
5	Summary	VI - 10

SECTION VII - SYSTEM DEFINITION

1	Introduction	VII - 1
2	Trunking Systems	VII - 1
2.1	Baseline Trunking Satellite	VII-1
2.1.1	Design Overview	VII-1
2.1.2	C-Band FSS Payload	VII-7
2.1.3	Launch Requirements	VII-7
2.1.4	Space and Ground Segments	VII-7
2.2	STET Trunking Satellite	VII-7
2.2.1	Design Overview	VII-7
2.2.2	STET Satellite Differences	VII-7
2.2.3	Impact on STET Earth Terminals	VII-8
2.3	ACE Trunking Satellite	VII-9
2.3.1	Design Overview	VII-9
2.3.2	ACE Satellite Differences	VII-9
2.3.3	Impact on ACE Earth Terminals	VII-10
2.4	Alternate ACE Design (ACE*)	VII-10
2.4.1	Design Overview	VII-10
2.4.2	ACE* Satellite Differences	VII-10
2.5	Discussion of Trunking Systems	VII-11

1	Radiation Environment	A - 1
1.1	Location of Van Allen Belts	A - 1
1.2	Influence of Solar Activity	A - 2
1.3	Radiation Dose for Orbits	A - 2
2	Impact on Satellite	A - 3
2.1	Electronics	A - 3
2.2	Solar Array Design	A - 3

APPENDIX B - ANTENNA COVERAGE

LIST of FIGURES

II-1	Traffic by Time-of-Day	II - 3
II-2	Inter-Zone Traffic Versus Time-of-Day	II - 7
II-3	Intra-Zone Traffic Versus Time-of-Day	II - 8
II-4	Total CONUS Traffic Versus Time-of-Day	II - 10
II-5	Total CONUS Traffic Versus Time-of-Day, Alternate Scenario	II - 10
II-6	Intra-Zone Traffic Versus Time-of-Day, Alternate Scenario	II - 13
.		
III-1	Molniya Orbit Motion Relative to Sun	III - 4
III-2	ACE Orbit Motion Relative to Sun	III - 4
III-3	Elliptical Orbit Parameters	III - 6
III-4	Euler Angles i, Ω, ω , Specify Location of Orbit	III - 6
III-5	Equatorial Bulge of Earth	III - 8
III-6	Illustration of Nodal Regression	III - 8
III-7	Nodal Regression vs. Inclination	III - 9
III-8	Forces Causing Nodal Regression (F_1) and Apsidal Rotation (F_2)	III - 10
III-9	Apsidal Line Rotation	III - 10
III-10	Apsidal Rotation vs. Inclination	III - 10
III-11	Gravitational Force of Sun upon Satellite in Equatorial Orbit	III - 12
III-12	Diurnal Effect on Atmospheric Density	III - 12
III-13	Density Variation with Time	III - 13
III-14	Orbital Decay versus Ballistic Parameter	III - 13
III-15	Lifetime Versus Altitude	III - 14
III-16	Lifetime Versus Eccentricity	III - 14
III-17	Rotation of the Earth	III - 15
III-18	Earth's Motion Around the Sun	III - 15
III-19	Coverage Duration Versus Latitude for Circular Equatorial Orbits	III - 19
III-20	Apparent Satellite Motion in Different Circular Equatorial Orbits	III - 19
III-21	Apparent Paths of a Satellite in a 12 hr, Circular, 40° Inclined Orbit	III - 21
III-22	Coverage Times for Satellite in Triply Synchronous Orbit	III - 21
III-23	Geometry of ACE Orbit	III - 23
III-24	ACE Orbit Coverages: Apogees at 48° W and 120° W	III - 28
III-25	Coverage Duration Versus Ground Station Location for ACE Orbit	III - 28
III-26	Apparent Motion of ACE Satellite from Los Angeles	III - 29
III-27	Apparent Motion of ACE Satellite from Dallas	III - 29
III-28	Apparent Motion of ACE Satellite from Omaha	III - 30
III-29	Apparent Motion of ACE Satellite from Chicago	III - 30
III-30	Apparent Motion of ACE Satellite from Miami	III - 31
III-31	Apparent Motion of ACE Satellite from New York City	III - 31
III-32	Apparent Motion of ACE Satellite from Boston	III - 32
III-33	ACE Satellite Elevation Angle Versus Time	III - 32
III-34	Variation of Slant Range and Propagation Delay with Time (ACE)	III - 33
III-35	Range Rate and Doppler Shift of 6 GHz Signals Versus Time (ACE)	III - 33
III-36	Antenna Azimuth Slew Rates for ACE Orbit	III - 34
III-37	Antenna Elevation Slew Rates for ACE Orbit	III - 34

III-38	ACE Orbit Worldwide Coverage (Local Time)	III - 35
III-39	ACE Orbit Worldwide Coverage (Eastern Standard Time)	III - 35
III-40	STET Orbit Coverage Times for Different Cities	III - 36
III-41	Coverage Duration Versus Ground Station Location for STET Orbit	III - 36
III-42	Apparent Motion of STET Satellite from Los Angeles	III - 37
III-43	Apparent Motion of STET Satellite from Dallas	III - 37
III-44	Apparent Motion of STET Satellite from Omaha	III - 38
III-45	Apparent Motion of STET Satellite from Chicago	III - 38
III-46	Apparent Motion of STET Satellite from Miami	III - 39
III-47	Apparent Motion of STET Satellite from New York City	III - 39
III-48	Apparent Motion of STET Satellite from Boston	III - 40
III-49	Elevation Angle Versus Time for STET Orbit Satellite	III - 40
III-50	Variation of Slant Range and Propagation Delay with Time (STET)	III - 41
III-51	Range Rate and Doppler Shift of 6 GHz Signals Versus Time (STET)	III - 41
III-52	Antenna Azimuth Slew Rates for STET Orbit	III - 42
III-53	Antenna Elevation Slew Rates for STET Orbit	III - 42
III-54	Eclipse Durations for STET Orbit Satellites	III - 43
III-55	Worldwide Coverage of STET Satellite from 50° N Latitude	III - 43
.		
IV-1	Deloading of Intra-Zone Traffic by STET Orbit Satellite	IV - 3
IV-2	Deloading of Intra-Zone Traffic by ACE Orbit Satellite	IV - 3
IV-3	Deloading of E↔C Inter-Zone Traffic by STET Orbit Satellite, Case 1	IV - 4
IV-4	Deloading of E↔C Inter-Zone Traffic by STET Orbit Satellite, Case 2	IV - 4
IV-5	Deloading of E↔C Inter-Zone Traffic by ACE Orbit Satellite, Case 1	IV - 5
IV-6	Deloading of E↔C Inter-Zone Traffic by ACE Orbit Satellite, Case 2	IV - 5
IV-7	Deloading of Inter-Zone E↔P and C↔P Traffic, Case 1	IV - 7
IV-8	Deloading of Total CONUS Traffic by STET Orbit Satellite, Case 1	IV - 8
IV-9	Deloading of Total CONUS Traffic by STET Orbit Satellite, Case 2	IV - 8
IV-10	Deloading of Total CONUS Traffic by ACE Orbit Satellite	IV - 10
.		
VI-1	STET Coverage: 1.0° Beams	VI - 2
VI-2	STET Coverage: 1.5° Beams	VI - 2
VI-3	STET Coverage: 2.0° Beams	VI - 2
VI-4	STET Coverage: 0.67° Beams	VI - 3
VI-5	ACE Coverage: 3° Beams	VI - 4
VI-6	ACE Coverage: 2° Beams	VI - 4
.		
A-1	Inner and Outer Van Allen Belts	A - 1
A-2	Trapped Particle Distribution	A - 2
A-3	Total Dose Versus Shielding Thickness for Different Orbits	A - 4
A-4	Solar Array Parameters for GEO Orbit Satellite	A - 7
A-5	Solar Array Parameters for STET Orbit Satellite	A - 7
A-6	Solar Array Parameters for 8 Hour Orbit Satellite	A - 8
A-7	Solar Array Parameters for ACE Orbit Satellite	A - 8
.		
B-1	View of Earth from GEO Orbit (80° W, R = 6.62 R _⊕)	B - 3

B-2	View of Earth from STET Orbit (80° W, $R = 4.17 R_{\oplus}$)	B-3
B-3	View of Earth from ACE Orbit (76.6° W, $R = 2.5 R_{\oplus}$)	B-4
B-4	STET Satellite Rises (128.3° W); Boston at 10° Elevation	B-4
B-5	STET Satellite Overhead (80° W)	B-5
B-6	STET Satellite Sets (29.9° W); Chicago at 10° Elevation	B-5
B-7	ACE Satellite A.M. Rises (98.6° W and $R = 1.94 R_{\oplus}$); Boston at 10°	B-6
B-8	ACE Satellite A.M. Overhead (66.6° W and $R = 2.90 R_{\oplus}$)	B-6
B-9	ACE Satellite A.M. Sets (36.8° W and $R = 3.14 R_{\oplus}$); Chicago at 10°	B-7
B-10	ACE Satellite P.M. Rises (123.2° W and $R = 3.36 R_{\oplus}$); Boston at 10°	B-7
B-11	ACE Satellite P.M. Overhead (86.6° W and $R = 2.36 R_{\oplus}$)	B-8
B-12	ACE Satellite P.M. Sets (63.8° W and $R = 1.81 R_{\oplus}$); Chicago at 10°	B-8
B-13	Composite Coverage Pattern for STET Orbit Satellite Antenna	B-9
B-14	Composite Coverage Pattern for ACE Orbit Satellite Antenna	B-9

LIST of TABLES

I-1	Organization of Report	I-2
II-1	Peak Traffic Forecast for 2000	II-2
II-2	Traffic Distribution by Time Zone	II-2
II-3	Traffic Versus Time of Day	II-4
II-4	Inter-Zone Business Traffic Hours	II-4
II-5	Two-way Inter-Zone Traffic	II-6
II-6	Intra-Zone Traffic	II-9
II-7	Total CONUS Traffic	II-9
II-8	Inter-Zone Business Traffic Hours	II-11
II-9	Two-way Inter-Zone Traffic, Alternate Case	II-12
II-10	Alternate Scenario Traffic	II-14
III-1	Orbit Period Versus Altitude	III-5
III-2	Orbit Named by Inclination	III-7
III-3	Summary of Perturbations	III-14
III-4	Candidate Orbits	III-16
III-5	Characteristics of Candidate Orbits	III-17
III-6	Duration of Simultaneous Viewing	III-18
III-7	ACE Orbit Parameters	III-24
III-8	Apogee Longitudes for CONUS	III-24
III-9	CONUS City Locations	III-25
III-10	ACE Orbit Coverages	III-25
III-11	STET Orbit Parameters	III-26
III-12	STET Orbit Coverages	III-27
IV-1	Deloading Capacity (Gb/s)	IV-2
IV-2	Peak Traffic Deloading Performance	IV-11
V-1	TWTA Efficiency	V-2
V-2	Battery Comparison	V-3
V-3	Satellite Technology Developments (1990)	V-6
VI-1	Antenna Gain vs. STET Position	VI-3
VI-2	STET Antenna Parameters Versus Constituent Beam Size	VI-5
VI-3	ACE Antenna Parameters Versus Constituent Beam Size	VI-5
VI-4	Launch Vehicle Performance for GEO, STET, and ACE Orbit Satellites	VI-7
VI-5	Impact of Non-GEO Orbits on STET and ACE Satellite Systems	VI-11
VII-1	Baseline Trunking Satellite	VII-1
VII-2	Summary of Trunking Satellite Characteristics	VII-2
VII-3	Summary of CPS Satellite Characteristics	VII-2
VII-4	Baseline GEO Satellite Characteristics, Trunking Service	VII-3
VII-5	STET Satellite Characteristics, Trunking Service	VII-4

VII-6	ACE Satellite Characteristics, Trunking Service	VII - 5
VII-7	ACE* Satellite Characteristics, Trunking Service	VII - 6
VII-8	STET Trunking Satellite	VII - 8
VII-9	ACE Trunking Satellite	VII - 9
VII-10	Alternate ACE* Trunk Satellite	VII - 10
VII-11	Baseline CPS Satellite	VII - 13
VII-12	STET CPS Satellite	VII - 13
VII-13	ACE CPS Satellite	VII - 14
VII-14	Alternate ACE* CPS Design	VII - 16
VII-15	Baseline GEO Satellite Characteristics, CPS Service	VII - 19
VII-16	STET Satellite Characteristics, CPS Service	VII - 20
VII-17	ACE Satellite Characteristics, CPS Service	VII - 21
VII-18	ACE* Satellite Characteristics, CPS Service	VII - 22
.		
VIII-1	Capital Expenditures	VIII - 4
VIII-2	Rate of Return (DTRR)	VIII - 4
VIII-3	Transponder Prices (18% Return)	VIII - 5
VIII-4	Transponder Payloads for Different Satellite Designs	VIII - 6
VIII-5	Capital Expenditures for Trunking Satellites	VIII - 6
VIII-6	Capital Expenditures for CPS Satellites	VIII - 6
.		
.		
X-1	Transponder Prices (18% Return)	X - 1
.		
A-1	Orbital Parameters	A - 1
A-2	Normalized Total Radiation Dose	A - 3
A-3	Radiation Environment of Orbits	A - 3
A-4	System Level Projections for Radiation-Hardened Electronics Technology	A - 5
A-5	Solar Array Parameters (1 kW)	A - 6

Section I

INTRODUCTION

1 Background

The part of the geostationary (GEO) orbital arc used for United States domestic fixed communications service is rapidly becoming filled with satellites. One of the factors currently limiting its utilization is that communications satellites must be designed to have sufficient capacity to handle peak traffic loads, and thus are under-utilized most of the time.

A potential solution is to use satellites in suitable non-geostationary orbits to unload the traffic peaks. This approach may enable a significant increase in the effective utilization of the geostationary satellites. However, the cost of implementing the non-GEO orbit satellites must be less than the gain from increased utilization of the GEO satellites.

2 Objectives of Study

The overall objective of this study program is to assess the application, economic benefits, and technology and system implications of satellites in non-GEO orbits for off-loading peak traffic from GEO communications satellites.

3 Approach

The study is organized into four technical tasks.

1. Concepts Development
2. System Definition
3. Economic Comparisons
4. Technology Requirements Definition

These tasks are described below.

3.1 Task 1 – Concepts Development

The following concepts for satellite communications systems will be developed.

1. A system of GEO satellites only
2. An optimum combination of GEO plus non-GEO satellites

These concepts will address the United States domestic fixed-service traffic in the year 2000.

A baseline traffic model will be supplied to Ford Aerospace by NASA/LeRC. Ford Aerospace will parametrically vary the parameters of the traffic model, e.g. peak-to-average traffic, so as to assure conclusions for a range of traffic conditions.

Ford Aerospace will develop a GEO-only concept and at least two alternative non-GEO concepts for each of two representative systems.

1. A satellite system such as RCA Americom's Satcom system which provides a mix of fixed services (voice, video, data) and tends to be trunking service orientated.
2. A satellite system such as Satellite Business Systems which provides voice, data, and videoconferencing services and tends to provide business services directly to and from customers' premises.

The system concepts will be designed and developed on the basis of the technology state-of-the-art at the end of 1990. Ford Aerospace will forecast the state of technology at that time. It will be assumed that the satellites of each system are launched and become operational in the 1994 to 1997 time frame.

The concepts will be developed and compared on the basis of a system of satellites addressing

an appropriate portion of the year 2000 traffic. A design life of 12 years shall be assumed for all satellites. The definition of system architectures shall include a description of the following items:

- Number and location of nodes in the system, including both space and ground segments
- Number and sizes of satellite beams
- Network and control concepts
- System interconnectivity
- Functional block diagrams of communications hardware

The output of this task will be a detailed description of the alternate concepts and architectures along with a description of the rationale, assumptions, trade-offs, and selections made for each concept.

3.2 Task 2 – Systems Definition

For each of the system concepts developed in Task 1, the configurations of the satellites and earth terminals will be defined and described.

The differences between non-GEO and GEO satellites will be specifically addressed, including the following items:

- Degradation of solar array panels by Van Allen belt radiation
- Orbital drag at perigee
- Delta V required to achieve orbit

The output of this task will be a detailed technical description of each of the system configurations developed including rationale, assumptions, trade-offs, component selections, and design choices.

3.3 Task 3 – Economic Comparisons

An economic comparison between the GEO system and the GEO plus non-GEO systems defined in Task 2 will be performed. The economic assessment will include the following items:

- An estimate of the recurring and non-recurring costs.

Section	Task	Content of Section
I	–	Introduction
II	1	Traffic Model
III	1	Analysis of Satellite Orbits
IV	1	Deloading Peak Traffic
V	1	Forecast of 1990 Technology
VI	1	System Concepts
VII	2	System Definition
VIII	3	Economic Comparison
IX	4	Technology Requirements
X	–	Conclusions
A	2	Radiation Effects
B	2	Antenna Coverage

Table I-1: Organization of Report

- A life cycle cost analysis for each system.

A method for economic comparison will be developed such as cost per bandwidth-year or cost per channel in order to produce a valid comparison of systems.

3.4 Task 4 – Technology Requirements

Any enabling or critical technology required to implement the systems defined in Tasks 1 and 2 will be identified and described. The definition will be in quantitative form in order to provide specific guidance for NASA planning.

4 Organization of Report

The correspondence between sections of this report and program Tasks is shown in Table I-1. Appendix A contain discussion of radiation exposure and effects for the different orbits. Appendix B contains plots of the coverage area for different positions in the GEO and non-GEO orbits.

Section II

TRAFFIC MODEL

1 Introduction

This section presents the Task 1 results on the domestic fixed-service traffic in the year 2000. The baseline traffic model was supplied by NASA/Lewis Research Center and gives the traffic breakdown by category and the distribution of traffic over the contiguous United States (CONUS). Additional research was required to determine the distribution of traffic by time of day. The results are divided into the following sections:

- NASA Traffic Model Data
- Traffic by Time-of-Day Analysis
- Traffic Model Results
- Sensitivity Analysis

2 NASA Traffic Model

The projected satellite traffic for CONUS in the year 2000 is derived from the data developed on NASA/LeRC contract NAS3-24235, *Communication Platform Payload Definition (CPPD) Study*. (The reference is the CPPD Study Final Report, Vol. II - Technical Report, and Vol. III - Addendum, March 1986, NASA CR174929.)

2.1 Data Base

The baseline traffic model gives the U.S. domestic fixed-service satellite addressable traffic distribution by category and by location but does not contain information about distribution of traffic by time of day. With the exception of video broadcasting, satellite addressable traffic is defined to be between parties separated by at least 640 km (400 mi).

The following information is used from the NASA traffic model:

- Peak traffic breakdown by category:
 - Voice trunking
 - Voice customer premise service (CPS)
 - Data trunking
 - Data CPS
 - Video conferencing trunking
 - Video conferencing CPS
 - Broadcast video
- The peak traffic distribution by location in the four time zones:
 - Intra-zone traffic (within same zone)
 - Inter-zone traffic (between zones)

Trunking service uses high capacity links between a relatively few number of large ground stations. An example of trunking service is the RCA Americom Satcom system which provides a mix of voice, video, and data fixed services.

Customer premise service (CPS) provides business services directly to and from many business locations, and uses a large number of relatively small ground stations. An example of CPS is the Satellite Business System which provides voice, data, and videoconferencing services. Both trunking and CPS services are used in this study.

2.2 Methodology

The NASA traffic model is in 316 x 316 matrix form and gives the distribution of traffic among

Standard Metropolitan Statistical Areas (SMSAs). Ford Aerospace computer programs reduced the size of the matrix to 84 x 84 by mapping each of the SMSAs into one of 84 regions (CPPD Report, p. 4-29).

We use the same computer program to reduce the 84 x 84 matrix to a 4 x 4 matrix by mapping each of the 84 regions to one of the four time zones. The result is the distribution of satellite addressable traffic for voice, data, and video conferencing traffic among the four time zones for the year 2008.

We assume that the same relative traffic distribution applies to the year 2000. The magnitudes of the traffic are adjusted for the assumed rate of growth from 2000 to 2008.

2.3 Traffic by Service Category

The traffic forecast for United States domestic fixed satellite demand in the year 2000 is summarized in Table II-1 by category of service. The conversion to required digital capacity uses the CPPD Study criteria (CPPD Report, Subsection 4.8.5, p. 4-123, and Table 2.2.7-3, p. 2-37):

Half voice circuit (HVC) = 24 kb/s

Video conferencing channel = 2.1 Mb/s

Video broadcast channel = 29 Mb/s

These conversions are conservative. By the year 2000, use of more efficient digital coding schemes and removal of redundancy in the transmitted information may enable reduction in the equivalent digital capacity by a factor of two. This would not have an impact on the conclusions of this study which depend on the relative distribution of the traffic in time and space, and not on the absolute magnitude of the traffic.

2.4 Traffic by Location

Table II-2 shows the peak traffic distribution by time zone in units of Gb/s and percentage of total peak traffic. The total traffic is 208.6 Gb/s which is the total in Table II-1 minus the 4.6 Gb/s of broadcast video which is independent of the time of day. The intra-zone traffic

(over 640 km within the same time zone) refers to two-way (full voice) circuits while the inter-zone values are for half circuits. For example, there are table entries for E-to-C and C-to-E, both ways of a two-way conversation.

As shown in Table II-2, the traffic in and between the Eastern (E) and Central (C) time zones is 70% of the total traffic. The East intra-zone traffic itself accounts for 25% of the peak traffic. The East and Central traffic is the focus for unloading of peaks.

3 Traffic by Time-of-Day

The analysis of the behavior of different categories of traffic with respect to time of day is given. Time is measured on a 24 hour clock and refers to local time unless specified to be Eastern, Central, Mountain, or Pacific Zone time.

The best quantitative time of day traffic information available within the scope of this program is for voice traffic. This subsection presents this information and argues that it is a good estimate for the majority of satellite addressable traffic.

3.1 Voice Traffic

Voice traffic behavior is the best known since it has been studied over a long period of time by the telephone companies.

3.1.1 Voice Traffic Data Base

Figure II-1 gives the results of measurements of peak voice traffic magnitude versus time of day, and Table II-3 gives the traffic factor (normalized to unity) for one hour time periods over the day. The following points must be emphasized:

- Time scale is in local time and refers to the start of the one hour period in which peak traffic is measured.
- Values apply to one hour time periods.
- Values are for peak traffic reached during the one hour time period.

Category	Quantity	Traffic Units
Trunking Service:		
- Voice	6,814,000	HVC
- Data	3,178	Mb/s
- Videoconference	7,786	channels
CPS Service:		
- Voice	35,000	HVC
- Data	23,767	Mb/s
- Videoconference	439	channels
Broadcast Video	158	channels

Category	Mb/s	%
Trunking Service		
- Voice	163,536	76.71
- Data	3,178	1.50
- Video confer.	16,351	7.67
CPS Service		
- Voice	840	.39
- Data	23,767	11.15
- Video confer.	922	.43
Broadcast Video	4,582	2.15
Totals	213,176	100.00

Table II-1: Peak Traffic Forecast for 2000

Time Zone	Peak Traffic (Gb/s)				
To	E	C	M	P	Total
From					
E	52.4	38.4	5.0	10.2	106.1
C	38.4	18.3	4.0	7.6	68.2
M	5.0	4.0	.5	2.1	11.7
P	10.2	7.6	2.1	2.8	22.6

Time Zone	Peak Traffic (%)				
To	E	C	M	P	Total
From					
E	25.1	18.4	2.4	4.9	50.9
C	18.4	8.8	1.9	3.6	32.7
M	2.4	1.9	.3	1.0	5.6
P	4.9	3.6	1.0	1.3	10.8

Table II-2: Traffic Distribution by Time Zone

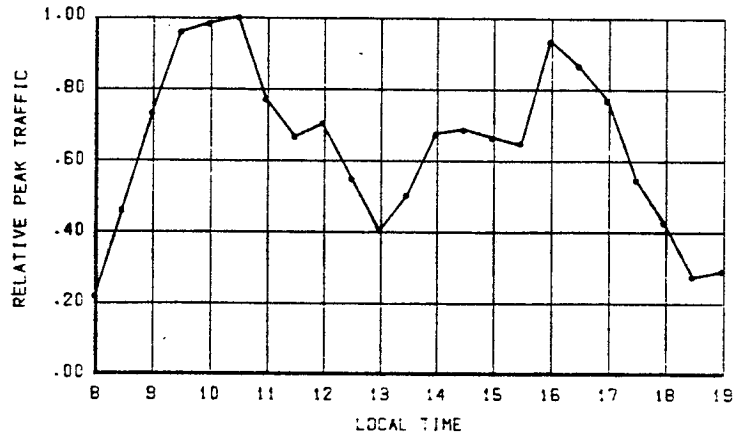


Figure II-1: Traffic by Time-of-Day

- Time scale of Figure II-1 is in local time and refers to the start of the one hour period in which peak traffic is measured.

This model is applicable to both calls within the same time zone (intra-zone) and calls between time zones (inter-zone). Satellite addressable traffic is defined as being over distances greater than 640 km.

The traffic model of Figure II-1 shows a rise in activity over the business day for the ten hours from 0830 to 1830 (6:30 pm). There are two peak traffic periods; one around 1100 in the morning and the other around 1630 in the afternoon.

The total CONUS satellite-addressable traffic is composed of traffic components from the four time zones, appropriately combined to account for the progressive one hour shift in local time across the time zones. The study assumes that the same time-of-day behavior (in local time) is applicable to each individual time zone.

3.1.2 Business Influence

As shown by the traffic model of Figure II-1, business traffic is dominant in defining voice traffic behavior versus local time of day:

8 am Traffic increases sharply at the start of the business day.

11 am Traffic peaks before lunch time.

4 pm Traffic peaks a second time before the end of the business day.

Local Time Period From - To	Relative Traffic Factor
0000 - 0100	.01
0100 - 0200	.00
0200 - 0300	.00
0300 - 0400	.00
0400 - 0500	.00
0500 - 0600	.01
0600 - 0700	.03
0700 - 0800	.05
0800 - 0900	.23
0830 - 0930	.45
0900 - 1000	.73
0930 - 1030	.95
1000 - 1100	.98
1030 - 1130	1.00
1100 - 1200	.76
1130 - 1230	.66
1200 - 1300	.70
1230 - 1330	.55
1300 - 1400	.41
1330 - 1430	.50
1400 - 1500	.67
1430 - 1530	.68
1500 - 1600	.66
1530 - 1630	.65
1600 - 1700	.93
1630 - 1730	.86
1700 - 1800	.77
1730 - 1830	.55
1800 - 1900	.43
1830 - 1930	.26
1900 - 2000	.29
2000 - 2100	.23
2100 - 2200	.14
2200 - 2300	.07
2300 - 2400	.03

Table II-3: Traffic Versus Time of Day

Between	Time (ET)
Eastern and Central	0900 - 1700
Eastern and Mountain	1000 - 1700
Eastern and Pacific	1100 - 1700
Central and Mountain	1000 - 1800
Central and Pacific	1100 - 1800
Mountain and Pacific	1100 - 1900

Table II-4: Inter-Zone Business Traffic Hours

6 pm Traffic falls sharply and then tails off into the evening.

Business activity also determines the difference between intra-zone and inter-zone traffic. Intra-zone traffic activity extends the entire working hours with significant traffic intensity values from 0800 to 1930 local time. Inter-zone traffic activity is restricted to matching business hours between time zones.

Table II-4 shows the restriction in hours for the inter-zone traffic, the tabulation being given in Eastern time (ET) for all cases. The assumption is that business activity only occurs between the hours of 8:00 am and 5:00 pm local time.

3.1.3 Trunking and CPS Voice Services

The time-of-day traffic model is from telephone companies and applies to both local and long distance voice traffic. Since long distance traffic is trunking traffic such as carried by the Satcom system, this traffic model applies directly to trunking services.

CPS traffic as carried by Satellite Business Systems is purely business traffic. Since the voice model is defined by business voice traffic, the same model can be applied to CPS. Thus trunking and CPS voice traffic follow the same traffic model with regard to peak traffic values.

3.2 Video Conferencing Traffic

Video conferencing traffic is a business service combining voice and image. It can be considered as an extension of voice traffic and therefore the voice traffic model applies.

3.3 Data Traffic

The volume of peak data traffic is 16% of peak voice traffic. Contrary to voice, there exists no valid study regarding data traffic behavior as a function of time of day. We have no information on the volume of interactive data versus the volume of delayed delivery data which could be carried during non-peak hours. However, interactive data traffic should have the same behavior as voice traffic regarding time of day.

For the purpose of this study, trunking and CPS data are assumed to have the same traffic model as voice traffic.

3.4 Video Broadcasting Traffic

Satellite video broadcasting traffic behavior makes up only 2% of the total traffic, with the majority of it extending 24 hours a day. Video broadcasting traffic will not be considered further in the study.

3.5 Application to Zone Traffic

The applicability of the same model to both intra and inter-zone calls means that the same traffic factors must be applied to the differing magnitudes of intra and inter-zone calls. Let α equal the value of traffic factor at hour H as given in Table II-3, and let:

T_{ii} = peak value of the intra-zone traffic for zone i ;

T_{ij} = peak value of the inter-zone traffic between zones i and j .

Then:

αT_{ii} = value of intra-zone traffic for zone i at hour H ;

αT_{ij} = value of inter-zone traffic between zones i and j at hour H .

The application of the business traffic hours criteria imposes the following constraint. The value of inter-zone traffic at hour H between zones i and j equals αT_{ij} with the condition that hour H falls within the business activity hours of zones i and j .

4 Traffic Model Results

4.1 Inter-Zone Traffic

Inter-zone traffic values are obtained by weighting the peak traffic values from Table II-2 with the traffic factor from Table II-3. However, there is the restriction that inter-zone traffic is exchanged only during the business hours of the related zone as per Table II-4. The results are given in Table II-5 for the six possible interconnections between the four time zones and the total inter-zone traffic.

Figure II-2 plots the results for the six possible inter-zone's traffic for Eastern time. The inter-zone traffic is completely dominated by the Eastern-Central traffic.

4.2 Intra-Zone Traffic

Intra-zone traffic values for each hour are obtained by weighting the peak traffic value from Table II-2 with the traffic factor for the time-of-day from Table II-3. The result is given in Table II-6 for each time zone together with the total intra-zone traffic for all time zones. Note that this traffic is two-way traffic.

Results for the four time zones are plotted in Figure II-3 in terms of Eastern time. The peaks for the different time zones have the same shape but different magnitudes. There is a progressive one hour shift in time of traffic peak from East to Central to Mountain to Pacific Zone. The majority of traffic is concentrated in the Eastern and Central time zones with the traffic in the Mountain and Pacific zones being relatively insignificant. Since the same time-of-day traffic model is used for inter as for intra-zone traffic, the peaks of Figure II-2 are similar to those of Figure II-3.

4.3 Total Traffic

The total of the intra and inter-zone peak traffic in Gb/s is given in Table II-7 for one hour time periods during the day. The peaks of the total traffic are typically 2/3 inter-zone traffic and 1/3 intra-zone traffic. Figure II-4 plots the total CONUS traffic. A scale of Gb/s and East-

Time Period (Eastern Time) From - To	PEAK TRAFFIC, Gb/s Between Time Zones						Total
	E↔C	E↔M	E↔P	C↔M	C↔P	M↔P	
0800 - 0900	0	0	0	0	0	0	0
0830 - 0930	0	0	0	0	0	0	0
0900 - 1000	36.8	0	0	0	0	0	36.8
0930 - 1030	53.7	0	0	0	0	0	53.7
1000 - 1100	65.6	6.1	0	3.8	0	0	75.5
1030 - 1130	74.8	7.3	0	5.6	0	0	87.7
1100 - 1200	66.7	7.5	10.1	6.8	9.1	2.0	102.3
1130 - 1230	63.7	8.1	11.4	7.8	11.0	2.9	104.8
1200 - 1300	56.0	8.5	14.7	7.0	11.3	3.5	100.8
1230 - 1330	46.4	7.8	15.4	6.7	12.2	4.0	92.4
1300 - 1400	42.6	5.9	14.2	5.9	12.7	3.6	84.8
1330 - 1430	40.3	5.8	15.4	4.8	11.7	3.4	81.5
1400 - 1500	41.4	6.9	14.6	4.4	8.8	3.0	79.3
1430 - 1530	45.3	6.2	13.7	4.2	8.8	2.5	80.6
1500 - 1600	51.0	5.4	13.9	4.3	10.4	2.3	87.3
1530 - 1630	51.0	5.8	12.3	4.7	9.3	2.2	85.3
1600 - 1700	61.0	8.1	13.7	5.3	8.1	2.2	98.4
1630 - 1730	0	0	0	5.3	8.7	2.4	16.5
1700 - 1800	0	0	0	6.4	12.1	2.7	21.2
1730 - 1830	0	0	0	0	0	2.7	2.7
1800 - 1900	0	0	0	0	0	3.3	3.3
1830 - 1930	0	0	0	0	0	0	0
1900 - 2000	0	0	0	0	0	0	0
2000 - 2100	0	0	0	0	0	0	0
2100 - 2200	0	0	0	0	0	0	0
Total	796.3	89.2	149.4	83.1	134.0	42.9	1,294.8

Table II-5: Two-way Inter-Zone Traffic

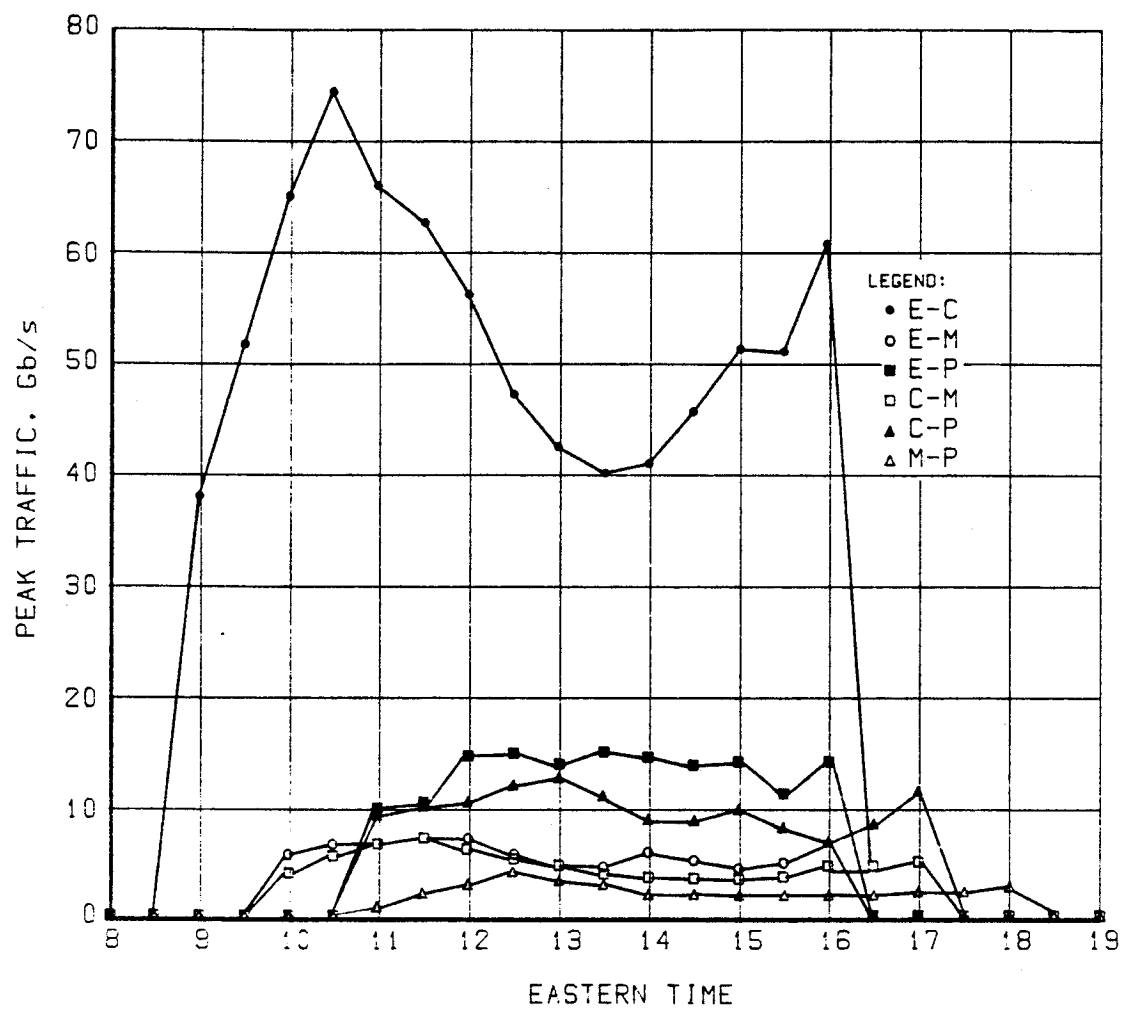


Figure II-2: Inter-Zone Traffic Versus Time-of-Day

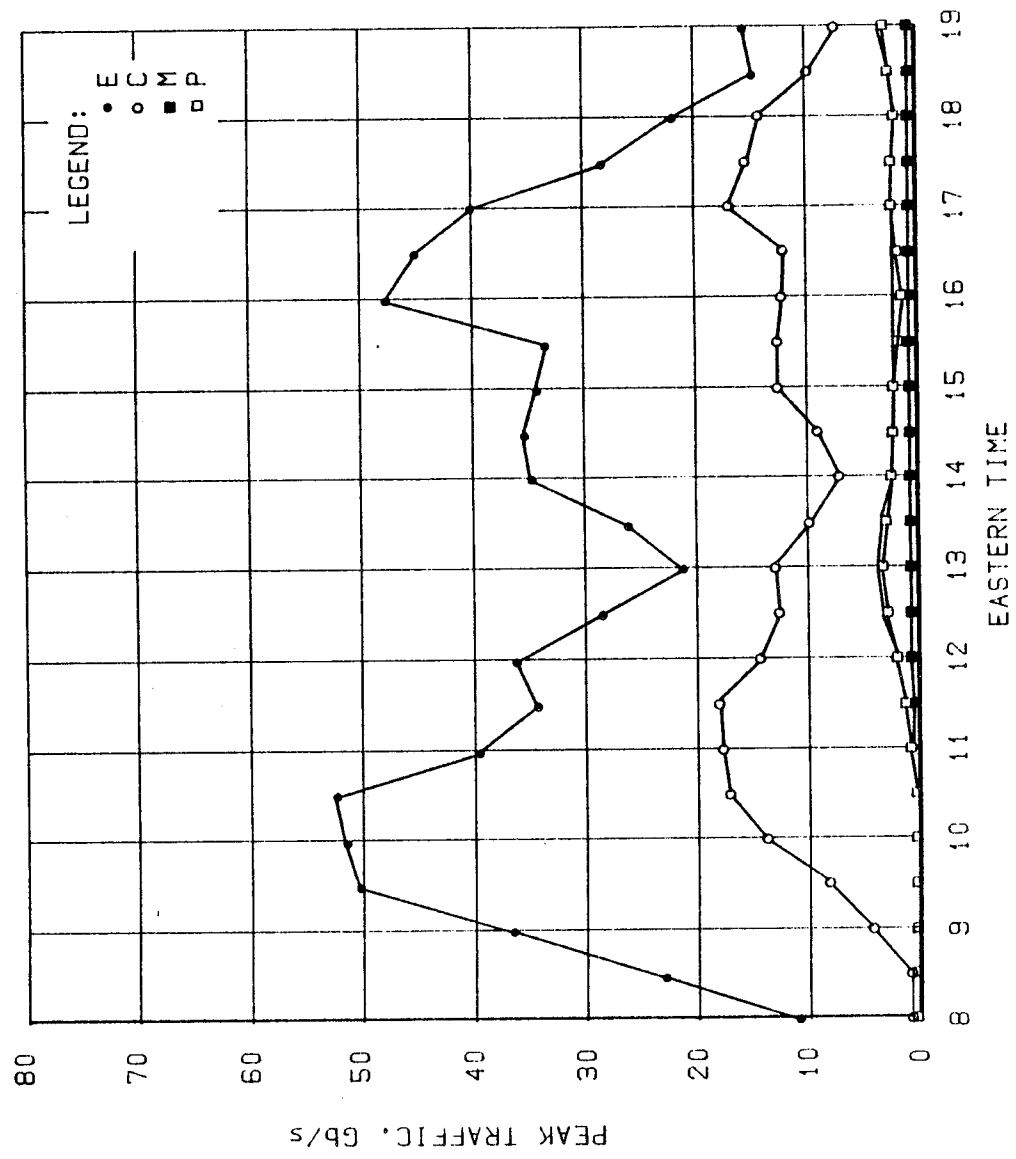


Figure II-3: Intra-Zone Traffic Versus Time-of-Day

Start of of 1 hr. Period (ET)	PEAK TRAFFIC (Gb/s)				
	Eas.	Cen.	Mtn.	Pac.	Total
0800	12.1	.6	0	0	12.6
0830	23.6	.9	0	0	24.5
0900	38.3	4.2	0	0	42.5
0930	49.8	8.3	0	0	58.1
1000	51.4	13.4	.1	.1	65.0
1030	52.4	17.4	.2	.1	70.2
1100	39.9	18.0	.4	.6	58.9
1130	34.6	18.3	.5	1.2	54.7
1200	36.7	13.9	.5	2.0	53.2
1230	28.8	12.1	.5	2.6	44.1
1300	21.5	12.8	.4	2.7	37.5
1330	26.2	10.0	.4	2.8	39.4
1400	35.1	7.5	.4	2.1	45.1
1430	35.7	9.2	.3	1.8	47.0
1500	34.6	12.3	.2	1.9	49.1
1530	34.1	12.5	.3	1.5	48.4
1600	48.8	12.1	.4	1.1	62.4
1630	45.1	11.9	.4	1.4	58.8
1700	40.4	17.1	.4	1.9	59.7
1730	28.8	15.8	.4	1.9	46.9
1800	22.6	14.1	.5	1.8	39.0
1830	13.6	10.1	.5	1.8	26.0
1900	15.2	7.9	.4	2.6	26.1
2000	12.1	4.8	.3	2.4	19.5
2100	7.3	5.3	.2	2.1	15.0

Table II-6: Intra-Zone Traffic

Time Period (Eastern time) From - To	PEAK TRAFFIC (Gb/s)		
	Intra	Inter	Total
0800 - 0900	12.6	0	12.6
0830 - 0930	24.5	0	24.5
0900 - 1000	42.5	36.8	79.3
0930 - 1030	58.1	53.7	111.8
1000 - 1100	65.0	75.5	140.5
1030 - 1130	70.2	87.7	157.9
1100 - 1200	58.9	102.3	161.2
1130 - 1230	54.7	104.8	159.5
1200 - 1300	53.2	100.8	154.1
1230 - 1330	44.1	92.4	136.5
1300 - 1400	37.5	84.8	122.3
1330 - 1430	39.4	81.5	120.8
1400 - 1500	45.1	79.3	124.4
1430 - 1530	47.0	80.6	127.6
1500 - 1600	49.1	87.3	136.4
1530 - 1630	48.4	85.3	133.7
1600 - 1700	62.4	98.4	160.4
1630 - 1730	58.8	16.5	75.3
1700 - 1800	59.7	21.2	80.9
1730 - 1830	46.9	2.7	49.6
1800 - 1900	39.0	3.3	42.3
1830 - 1930	26.0	0	26.0
1900 - 2000	26.1	0	26.1
2000 - 2100	19.5	0	19.5
2100 - 2200	15.0	0	15.0

Table II-7: Total CONUS Traffic

ern time is used. (Figure II-5 plots an alternate CONUS traffic scenario based on "extended business hours" - see Subsection II-5.4.)

Note that the peak traffic of 161 Gb/s is significantly less than the 208 Gb/s of Table II-1 (213 Gb/s minus 4.6 Gb/s broadcast video). This is due to the application of time-of-day analysis to the peak traffic.

4.4 Traffic Analysis

The total traffic plot of Figure II-4 suggests two possible non-GEO satellite coverages:

1. A single coverage from around 9 am to 5 pm ET (8 hr duration) could offload about half

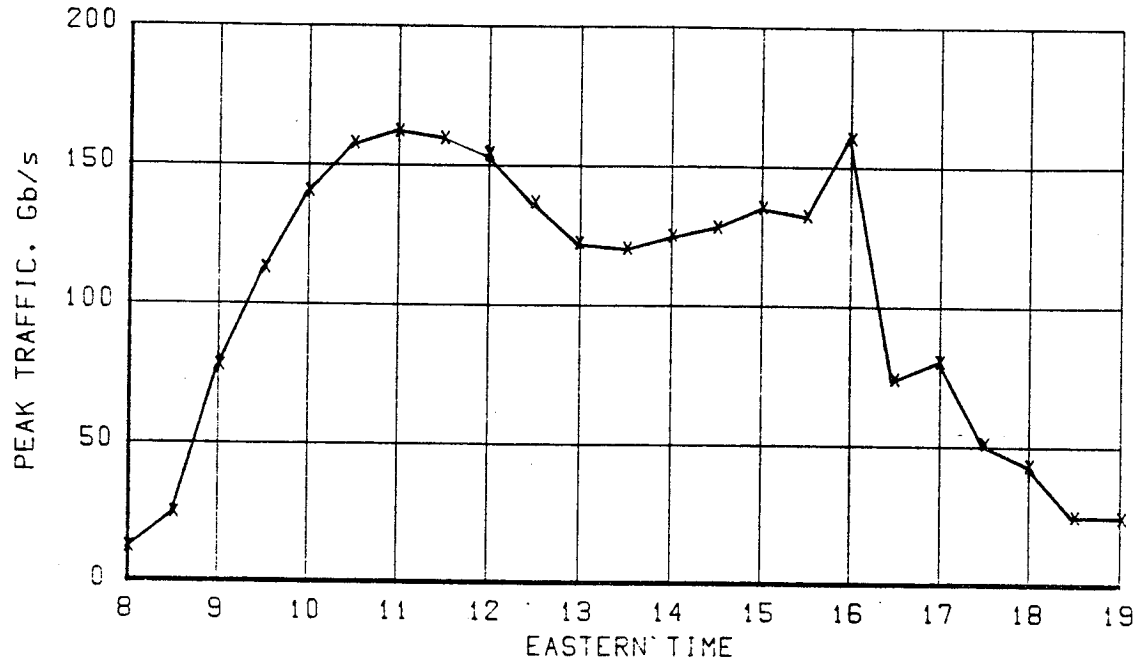


Figure II-4: Total CONUS Traffic Versus Time-of-Day

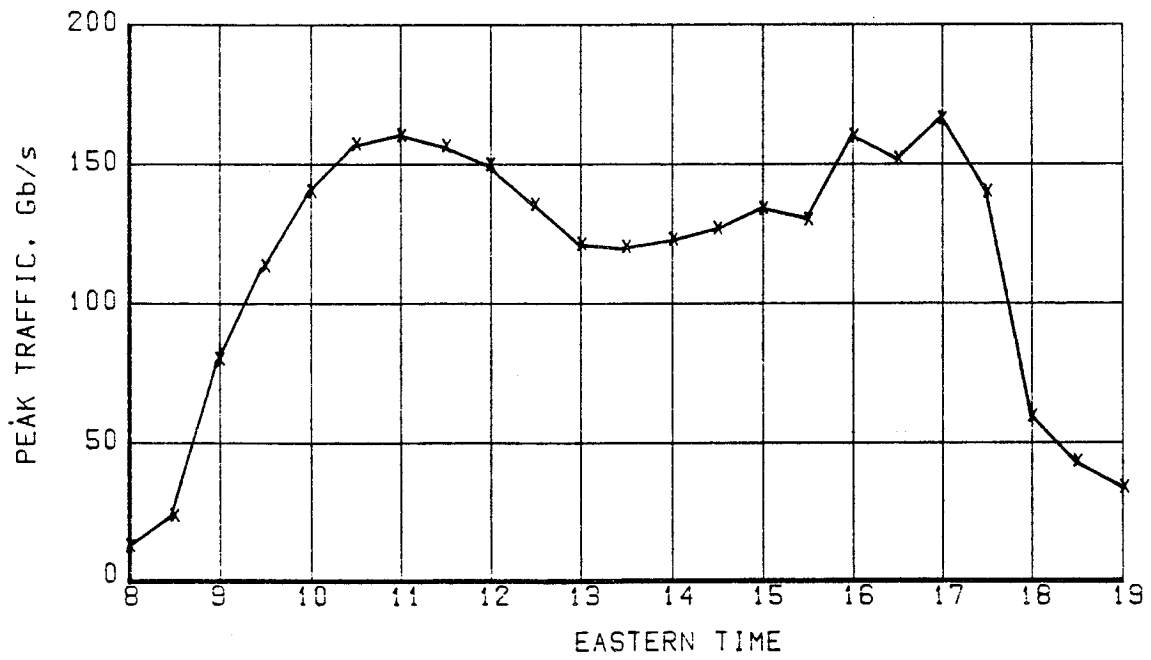


Figure II-5: Total CONUS Traffic Versus Time-of-Day, Alternate Scenario

the 160 Gb/s total.

2. A two peak coverage, with peaks of 3.5 hr duration separated by 4 hr, could offload about 25% of the 160 Gb/s total.

(Section IV gives an explanation of the methodology used to determine the amount of deloadable traffic.)

After analysis of candidate non-geostationary orbits in Section III, Section IV will choose the best match of possible orbits and traffic.

5 Sensitivity Analysis

5.1 Introduction

There are four major factors that influence the total traffic model of Figure II-4:

- Total magnitude of satellite traffic
- Geographical distribution of traffic
- Time-of-day distribution of traffic
- Tariffs versus time-of-day

5.2 Total Traffic

Although there is considerable debate about the magnitude of the satellite-addressable traffic in the year 2000, it is the time of day distribution of traffic that is important for this study. Variation in the total amount of traffic is expected to scale directly to variation in the amount of potential non-geostationary traffic.

5.3 Distribution of Traffic

The traffic follows the geographical location of businesses. The NASA traffic model has predicted the growth in SMSAs for the year 2000, and it is unlikely that significant geographical changes can occur in such a short time period.

5.4 Time of Day Analysis

The time-of-day analysis, being based on limited data, is the most likely factor to be in error. Accordingly, an alternative scenario based on the inter-zone traffic hours of Table II-8 is analyzed

Between	Time (ET)
Eastern and Central	0900 – 1830
Eastern and Mountain	1000 – 1830
Eastern and Pacific	1100 – 1830
Central and Mountain	1000 – 1930
Central and Pacific	1100 – 1930
Mountain and Pacific	1100 – 2030

Table II-8: Inter-Zone Business Traffic Hours

and displayed in Table II-9 and Figure II-6. (Table II-9 corresponds to Table II-5, and Figure II-6 corresponds to Figure II-2.)

Table II-10 and Figure II-5 give results analogous to the results of Subsection II-4.3 (Table II-7 and Figure II-4 respectively). The result is an extension of the afternoon peak by one hour into the evening and the requirement for a corresponding increase in satellite coverage time.

Note that for the case presented in Figure II-5, the duration of the peak traffic extends 1.5 hours into the evening. Since it is peak traffic that is plotted, there is no requirement that the areas under the curves in Figures II-4 and II-5 be equal.

5.5 Tariffs

Another factor that can influence traffic is the rate structure versus time of day. The current high rate period is for calls occurring between 8 am and 5 pm. If there were discounts for the time of the mid-day dip in peak traffic, it might level peak loads during the day. Also, deeper morning and evening discounts could offload daily peaks.

It is beyond the scope of this study to analyze the effect of tariffs on rates, but it is mentioned for completeness.

5.6 Conclusions

The double peak form of the total CONUS traffic as shown in Figures II-4 and II-5 is typical of the expected traffic. The majority of this traffic lies in the Eastern and Central time zones.

Time Period (Eastern Time) From - To	PEAK TRAFFIC, Gb/s Between Time Zones						Total
	E↔C	E↔M	E↔P	C↔M	C↔P	M↔P	
0800 - 0900	0	0	0	0	0	0	0
0830 - 0930	0	0	0	0	0	0	0
0900 - 1000	36.8	0	0	0	0	0	36.8
0930 - 1030	53.7	0	0	0	0	0	53.7
1000 - 1100	65.6	6.1	0	3.8	0	0	75.5
1030 - 1130	74.8	7.3	0	5.6	0	0	87.7
1100 - 1200	66.7	7.5	10.1	6.8	9.1	2.0	102.3
1130 - 1230	63.7	8.1	11.4	7.8	11.0	2.9	104.8
1200 - 1300	56.0	8.5	14.7	7.0	11.3	3.5	100.8
1230 - 1330	46.4	7.8	15.4	6.7	12.2	4.0	92.4
1300 - 1400	42.6	5.9	14.2	5.9	12.7	3.6	84.8
1330 - 1430	40.3	5.8	15.4	4.8	11.7	3.4	81.5
1400 - 1500	41.4	6.9	14.6	4.4	8.8	3.0	79.3
1430 - 1530	45.3	6.2	13.7	4.2	8.8	2.5	80.6
1500 - 1600	51.0	5.4	13.9	4.3	10.4	2.3	87.3
1530 - 1630	51.0	5.8	12.3	4.7	9.3	2.2	85.3
1600 - 1700	61.0	8.1	13.7	5.3	8.1	2.2	98.4
1630 - 1730	57.9	7.7	13.9	5.3	8.7	2.4	96.0
1700 - 1800	65.2	7.2	14.8	6.4	12.1	2.7	108.3
1730 - 1830	54.1	6.0	12.6	6.0	11.6	2.7	93.1
1800 - 1900	0	0	0	6.8	10.8	3.3	20.9
1830 - 1930	0	0	0	5.6	9.1	3.1	17.8
1900 - 2000	0	0	0	0	0	3.5	3.5
2000 - 2100	0	0	0	0	0	2.9	2.9
2100 - 2200	0	0	0	0	0	0	0
Total	973.5	110.2	190.7	101.5	165.4	52.4	1,593.8

Table II-9: Two-way Inter-Zone Traffic, Alternate Case

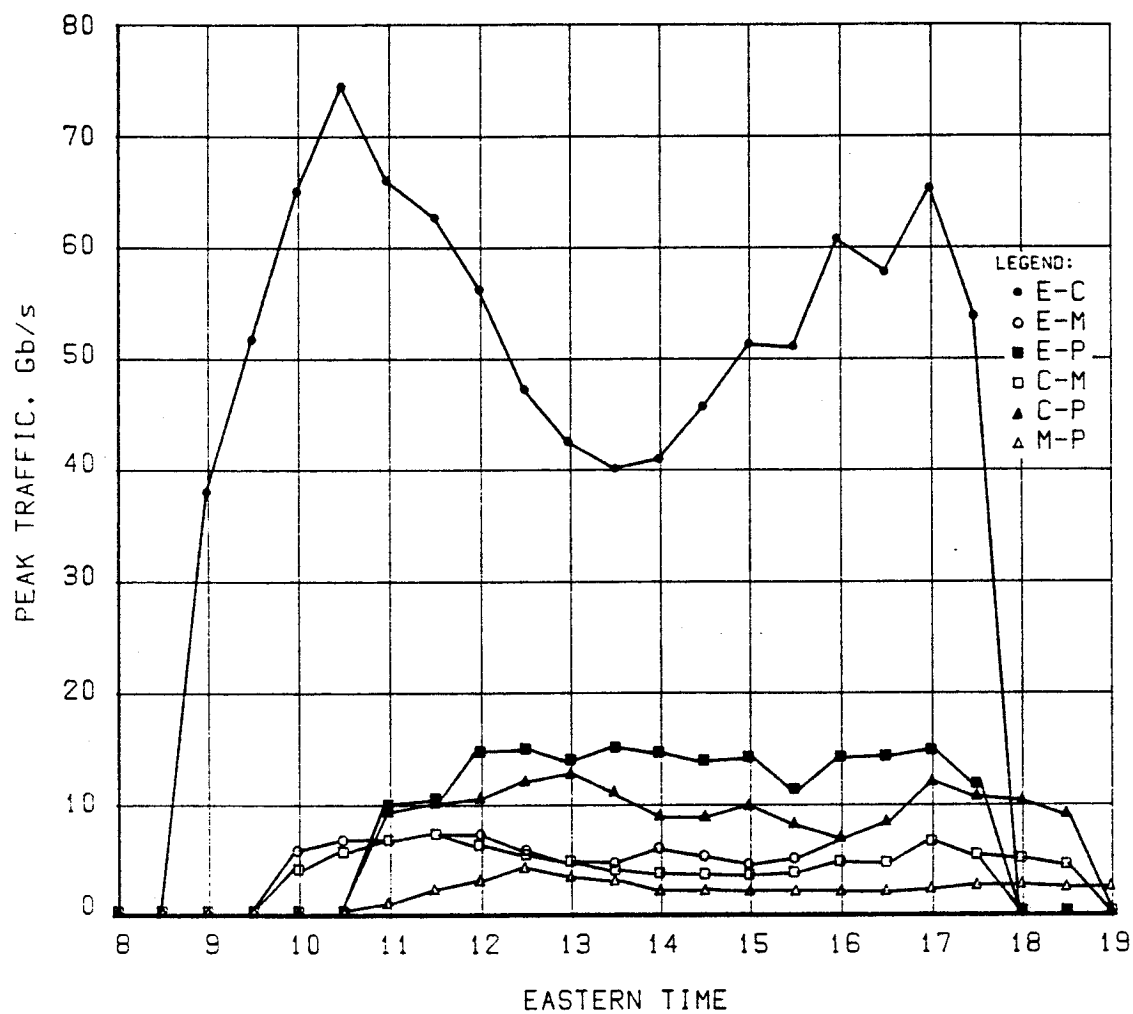


Figure II-6: Intra-Zone Traffic Versus Time-of-Day, Alternate Scenario

The feasibility of satellites or systems of satellites supplying 8 or 9 hours continuous coverage, or two 4 hour coverages separated by 4 hours, is investigated in the Section III.

The application of time-of-day traffic engineering to the total traffic of Table II-1 reduces the peak CONUS traffic from 208 Gb/s to 161 Gb/s (Figure II-4) or 168 Gb/s (Figure II-5), depending on traffic scenario.

Time Period (Eastern time) From - To	PEAK TRAFFIC (Gb/s)		
	Intra	Inter	Total
0800 - 0900	12.6	0	12.6
0830 - 0930	24.5	0	24.5
0900 - 1000	42.5	36.8	79.3
0930 - 1030	58.1	53.7	111.8
1000 - 1100	65.0	75.5	140.5
1030 - 1130	70.2	87.7	157.9
1100 - 1200	58.9	102.3	161.2
1130 - 1230	54.7	104.8	159.5
1200 - 1300	53.2	100.8	154.1
1230 - 1330	44.1	92.4	136.5
1300 - 1400	37.5	84.8	122.3
1330 - 1430	39.4	81.5	120.8
1400 - 1500	45.1	79.3	124.4
1430 - 1530	47.0	80.6	127.6
1500 - 1600	49.1	87.3	136.4
1530 - 1630	48.4	85.3	133.7
1600 - 1700	62.4	98.4	160.8
1630 - 1730	58.8	96.0	154.8
1700 - 1800	59.7	108.3	168.0
1730 - 1830	46.9	93.1	140.0
1800 - 1900	39.0	20.9	59.9
1830 - 1930	26.0	17.8	43.8
1900 - 2000	26.1	3.5	29.6
2000 - 2100	19.5	2.9	22.4
2100 - 2200	15.0	0	18.3

Table II-10: Alternate Scenario Traffic

Section III

ANALYSIS OF SATELLITE ORBITS

The analysis of candidate non-geostationary satellite orbits is organized into six subsections:

1. Requirements on Orbit
2. Overview of Solutions
3. Orbital Mechanics
4. Candidate Orbit Selection
5. Analysis of Selected Orbits
6. Conclusions

1 Requirements on Orbit

To off-load the daily peaks in geostationary communications traffic, the candidate satellite orbit should meet the following requirements:

- The satellite is in the correct position to service the daily traffic peaks:
 - The satellite (or other constellation member) is visible at the same time each day for the required period of time.
 - The satellite is above 10° elevation for the the traffic which it is servicing.
 - The satellite remains above 10° elevation for the region of CONUS being serviced for at least two hours each day.
- Redundancy is provided by the system.
- The non-GEO satellites do not physically or electrically interfere with existing satellites.
- The costs of the system are competitive.

2 Overview of Solutions

Solutions to the problem of geostationary arc crowding are discussed in the following categories:

1. Other GEO solutions
2. Super-synchronous orbits
3. Sub-synchronous circular orbits
4. Sub-synchronous elliptical orbits

The category of other GEO solutions is only mentioned for completeness. The scope of this study is to consider non-geostationary orbit solutions.

2.1 Other GEO Solutions

Although beyond the scope of this study, other GEO solutions to satellite congestion are possible and are listed for completeness.

2.1.1 Closer Spacing in GEO

The simplest though not necessarily the most desirable solution is to place additional satellites in the already crowded geostationary arc. The North American section of the arc is particularly crowded. Incidents have been recorded in which satellites have approached to within 10 km and passed each other in longitude. However, the probability of collisions is very low and the growing problem is one of interference.

The 1983 FCC *Orbital Assignment Order* specified that the 4° separation between satellites be reduced over time to 2° which corresponds to 1500 km separation at GEO. This places an increasing cost burden on the ground

station which must have a sufficiently large antenna to discriminate against signals from neighboring satellites. Use of 1° satellite spacing would again double the number of possible satellites, but place even greater requirements on the ground station.

2.1.2 Geosynchronous but not Geostationary

Geosynchronous means that the satellite has a rotational period around the earth equal to the earth's rotational period relative to the fixed stars - i.e. 23 h 56 min. Geostationary means geosynchronous plus the constraint that the satellite stays in the same place in the sky - i.e. it has 0° inclination and 0° eccentricity. (Practical considerations allow the geostationary satellite a small movement within a "dead" band such as $\pm 0.2^\circ$.) The ground antenna does not need to track the geostationary satellite, but the geosynchronous satellite would appear to move daily about a fixed position in the sky.

A possible solution to GEO arc crowding is to place several satellites in circular orbits around a single GEO arc position. This allows a two-dimensional spreading of satellite positions from the line of the geosynchronous orbit.

2.1.3 Alternating Frequency Plan

An interesting solution to interference between closely spaced satellites is to alternate the uplink/downlink frequencies of adjacent satellites. The same downlink or uplink frequency is then encountered every two satellites. Such a system would need careful coordination to avoid terrestrial interference problems.

If a ground station needed the ability to use satellites of opposite frequency plan, it would become more complex in order to service two sets of uplink/downlink frequencies at each frequency band. For example, C-band satellites could be either 6 GHz uplink/4 GHz downlink or 4 GHz uplink/6 GHz downlink.

2.1.4 Combined Service Satellites

Additional crowding can be avoided by use of new satellite designs such as the multi-frequency multi-service Insat satellites which combine FSS service, DBS and meteorological imaging.

2.1.5 Large Capacity Platforms

Another possibility is large geostationary platforms which combine the functions of many satellites and place much more capacity into one orbital position. Such large satellite designs will be assisted by the existence of the Space Station for assembly and the space-based orbital transfer vehicle for transport to GEO.

2.1.6 Greater Available Bandwidth

Another approach is to expand the frequency bandwidth available for satellite communications and thereby increase the communications capacity of a particular orbital position. The NASA Advanced Communications Technology Satellite will use the 2.5 GHz bandwidth available at Ka-band to supplement the 500 MHz at Ku-band and 500 MHz at C-band.

The World Administrative Radio Conference (WARC) 1985 *Allotment Plan* expands the C-band bandwidth by an additional 300 MHz and Ku-band by 500 MHz.

2.2 Super-Synchronous Satellites

At present, no commercial communications satellite uses a super-synchronous (higher than 36,000 km altitude) orbit. A single satellite in a super-synchronous orbit cannot provide daily coverage for CONUS at a constant time-of-day throughout the year since its orbital period is greater than 24 hours. (A special case exists for a satellite at the sun-earth gravitational equilibrium point which is several million miles from earth. This orbit is rejected for use by this study due to its excessive propagation time delay.)

However, a constellation of super-synchronous satellites, such as two satellites in 48 hour orbits, could provide coverage on alternate days. Disadvantages of super-synchronous satellites compared to geosynchronous satellites are as follows:

- Greater slant range and propagation delay
- Longer eclipse duration
- More on-orbit stationkeeping fuel.
- More accurate tracking by earth stations.

2.3 Sub-Synchronous Circular Orbits

At present, subsynchronous circular orbits are used by navigational satellites such as the Global Positioning System (GPS) but not generally by commercial communications satellites. Circular equatorial orbits whose periods are approximately equal to one day divided by an integer of 2 to 16 can be made sun synchronous and provide daily coverage at a constant time-of-day throughout the year. They are discussed in more detail in Subsection 5.3.

2.4 Sub-Synchronous Elliptic Orbits

All existing non-geostationary communications satellite systems involve constellations of several or more satellites to provide coverage throughout the day and throughout the year. As each satellite moves away from the coverage area, communications are handed off to another satellite. An example of such a system is the constellation of satellites operated in Molniya orbits by the USSR.

Each of the more than ten satellites in this Molniya constellation remains in view of the Soviet Union for approximately eight hours per day. A given satellite comes into view about four minutes earlier each day and departs from the coverage area four minutes earlier. Therefore, the time of day during which the satellite provides coverage changes throughout the year due to the earth's motion around the sun as shown by Figure III-1. The times of day that communications are handed off from one satellite to another also vary during the year.

A Molniya constellation cannot off-load daily traffic peaks unless it provides continuous coverage. This would require at least three times as many satellites for the same capacity as a constellation in which each member was always in

view during peak hours. Furthermore, no increased redundancy is provided by such a constellation since the velocity increment to transfer from one Molniya orbit to another is prohibitively large.

However, the ACE orbit, which is discussed in detail in Subsections II-4 and III-5.2, is both moderately elliptical and sun-synchronous. Figure III-2 shows how the position of the ACE orbit apogee remains constant with respect to the sun throughout the year.

3 Orbital Mechanics

3.1 Introduction

This discussion of orbital mechanics is divided into two parts:

- Kepler's laws
- Orientation of an orbit in space

The orbital motion of an earth satellite is principally governed by three laws determined empirically by Johannes Kepler:

1. The orbit of each satellite is an ellipse with the earth positioned at one of the two foci.
2. The line joining the satellite to the earth sweeps out equal areas in equal times.
3. The square of the period is proportional to the cube of the mean distance from the focus.

Perturbations due to the gravitational attraction of the sun, the moon, and the non-spherical mass distribution in the earth as well as other sources can cause the satellite to depart from the orbital trajectory predicted by Kepler. For all orbits under consideration, the effects of perturbations are small over the course of a single revolution.

The rate and the period of orbital motion are used to determine how often the satellite comes into view of a ground terminal, how long it remains in view, and how rapidly a ground antenna must be slewed to track it. The geometry of the orbit determines over which portions of the earth

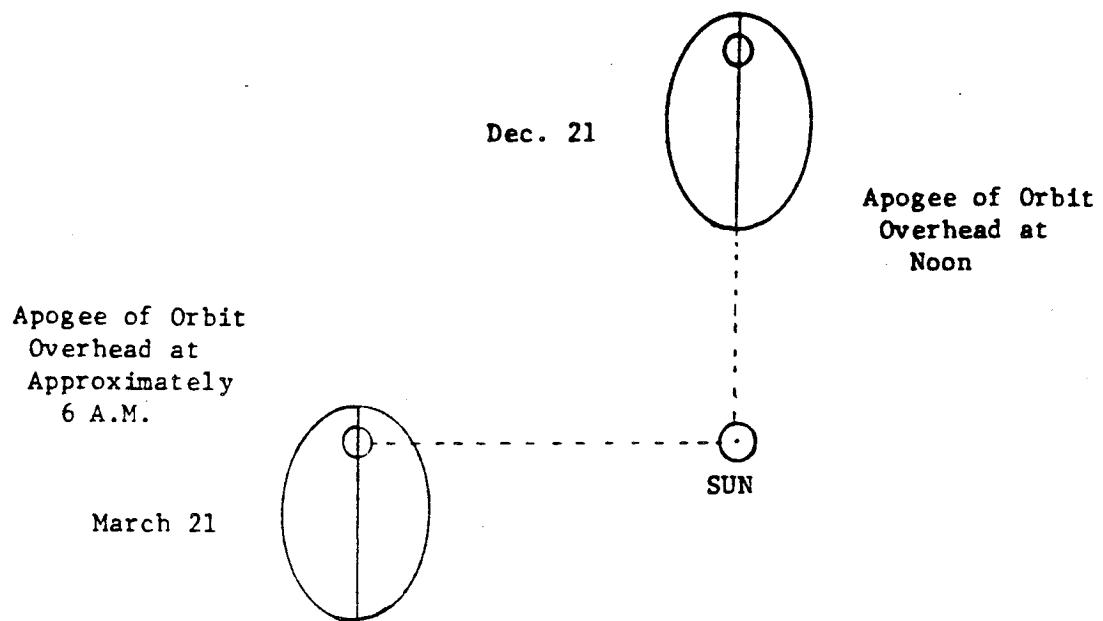


Figure III-1: Molniya Orbit Motion Relative to Sun

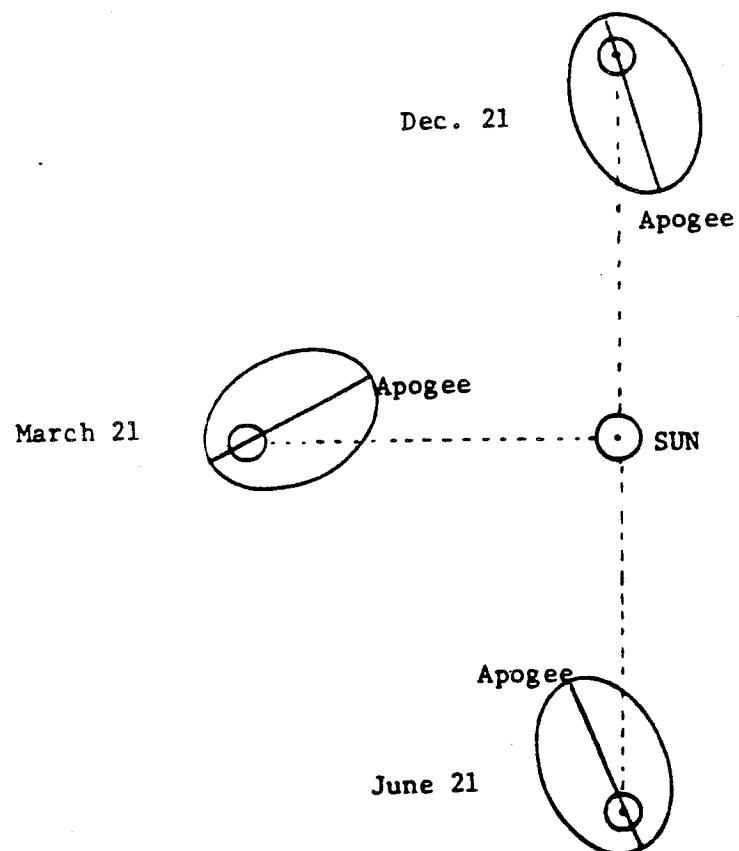


Figure III-2: ACE Orbit Motion Relative to Sun

the satellite passes. If orbital geometry is referenced to the sun, then the time-of-day when the satellite is in view of a particular ground station can be found.

3.2 Kepler's Laws

Kepler's First Law states that the orbital motion of an earth satellite is confined to a plane containing the center of the earth. A satellite orbit can lie in the plane of the earth's equator or it can be inclined to the equator so that the satellite overflies both the northern and southern hemispheres. However, it is not possible to make the satellite remain above the northern hemisphere at all times. The angle that the orbital plane makes with respect to the plane of the equator is known as the inclination of the orbit.

Kepler's Second Law relates the speed of the satellite in orbit to its radius from the center of the earth. A satellite in a circular orbit moves at the same rate of speed at each point. A satellite in an eccentric orbit moves at maximum speed when at minimum radius (perigee). It travels at minimum speed when it is most distant from the center of the earth (apogee).

Kepler's Third Law relates the size of an orbit to its period of revolution. The size of an orbit is determined by the length of its semi-major axis, which equals the radius for a circular orbit.

Figure III-3 illustrates the parameters of an elliptical orbit. The length of the semi-major axis of an orbit is equal to the arithmetic mean of its apogee and perigee radii. The period of revolution is given by the following formula where the period is in minutes of time and the semi-major axis a in kilometers.

$$Period = \left(\frac{a}{331.3} \right)^{1.5}$$

Table III-1 gives the orbital period as a function of semi-major axis and average altitude for the range of orbits under consideration for this study. The Van Allen inner and outer radiation belts lie at radii of 10,000 km and 23,600 km.

Orbital Period (h)	Average Radius (km)	Average Altitude (km)
1.5	6,653	282
2.0	8,060	1,689
4.0	12,795	6,424
6.0	16,766	10,395
8.0	20,310	13,939
12.0	26,614	20,243
18.0	34,874	28,503
23.93	42,170	35,799

Table III-1: Orbit Period Versus Altitude

3.3 Orientation of Orbit in Space

3.3.1 Euler Angles

The regions of the earth's surface which are overflown by the satellite are determined from the orientation of the orbit in space. The three Euler angles used to describe an orbit are shown in Figure III-4:

i - the inclination;

Ω - the right ascension of the ascending node;

ω - the argument of the perigee.

In addition, the true anomaly is used to locate the satellite within the orbit:

ν_0 - the true anomaly at epoch.

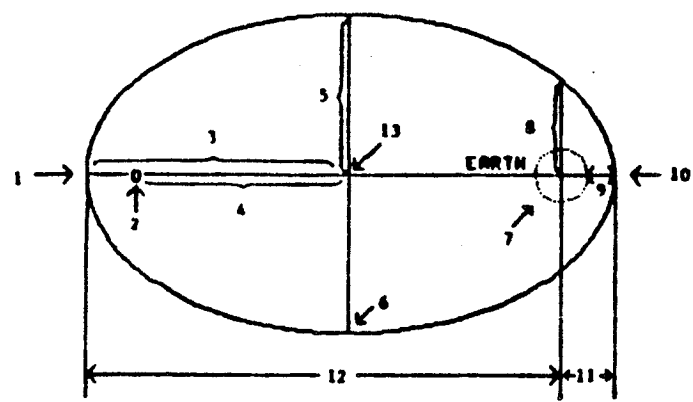
3.3.2 Inclination

The *inclination*, i , is the angle between the equatorial plane and the orbit plane. It is measured at the ascending node of the orbit (which is the point at which the satellite crosses the equator from south to north) and from the portion of the equatorial plane just to the east of the ascending node.

A satellite in an orbit with 0° inclination travels eastward around the equator. A satellite with inclination equal to 180° travels westward around the equator. Inclination cannot exceed 180° . As long as inclination is less than 90° , the satellite has some eastward motion as it crosses

ORIGINAL PAGE IS
OF POOR QUALITY

ORIGINAL PAGE IS
OF POOR QUALITY



1. Vertex (apogee)
2. Unoccupied focus
3. Semi-major axis " a "
4. Linear eccentricity " c "
5. Semi-minor axis " b "
6. Co-vertex
7. Occupied focus
8. Semi-latus rectum " p "
9. Perigee height " h_p "
10. Vertex (perigee)
11. Perigee radius " r_p "
12. Apogee radius " r_a "
13. Geometric center

Figure III-3: Elliptical Orbit Parameters

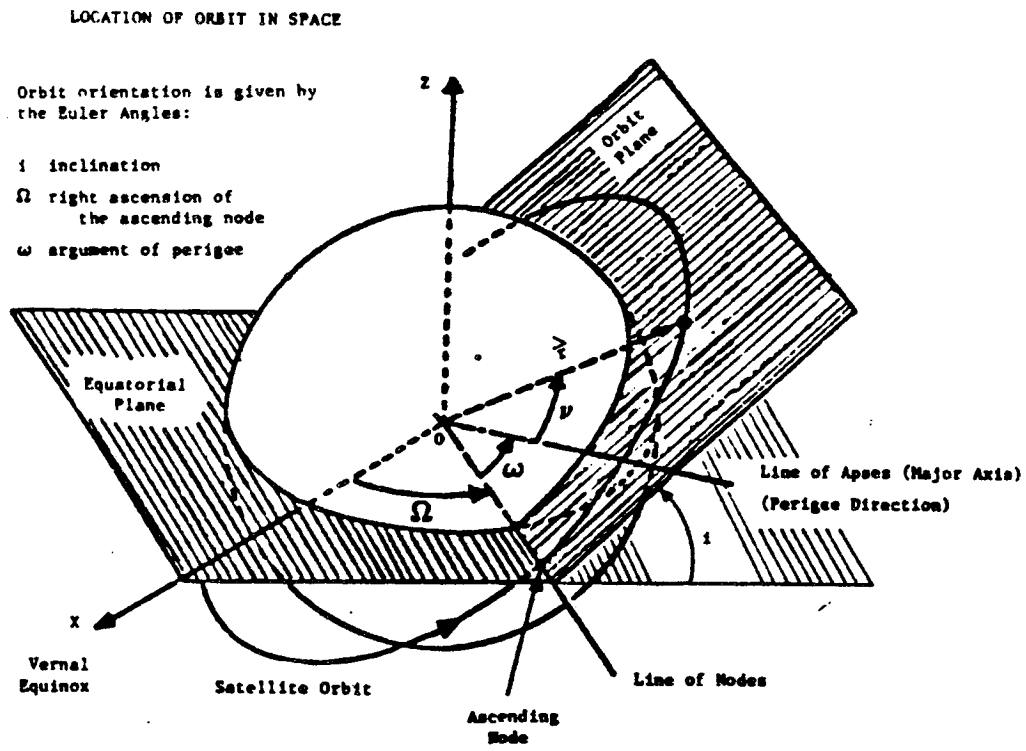


Figure III-4: Euler Angles i, Ω, ω , Specify Location of Orbit

Inclination Range (degrees)	Satellite Motion Towards	Orbit Type
$0^\circ \leq i < 90^\circ$	East	Prograde
90°	North-South	Polar
$90^\circ < i \leq 180^\circ$	West	Retrograde

Table III-2: Orbit Named by Inclination

the equator. This is the direction in which the earth rotates, accordingly such an orbit is said to be direct or *prograde*.

Inclinations greater than 90° lead to *retrograde* orbits, where the satellite revolves in the direction opposite to the earth's eastward rotation.

An orbital inclination of exactly 90° causes the satellite to travel either due north or due south in its orbit. This orbit carries the satellite directly over the north and south poles and is thus known as a *polar* orbit. Table III-2 summarizes the effects of inclination in determining orbital type.

The region overflown by a satellite in a prograde orbit is bounded by north and south latitudes equal to the inclination of the satellite's orbit. Satellites in retrograde orbits overfly regions bounded by latitudes equal to 180° minus the inclination. Therefore, the only satellites that can fly over every point on the surface of the earth are in orbits with inclination equal to 90° . Satellites in 0° or 180° inclination orbits never move north or south of the equator.

3.3.3 Right Ascension of Ascending Node

The *ascending node* is the point in the orbit where the satellite crosses the plane of the earth's equator when moving from south to north. It is located by means of its right ascension, an angle measured eastward around the equator from the Vernal Equinox of a given year, as shown in Figure III-4. The Greek letter Ω is used to denote the right ascension of the ascending node.

The *vernal equinox* is the direction from the Earth to the sun at the instant the sun appears

to cross the plane of the earth's equator on the first day of Spring. It forms the basis for the coordinate reference system by which satellite orbits are oriented in space, since it varies in direction by only a tiny fraction of a degree from year to year. This coordinate system is known as the *geocentric equatorial* coordinate system.

The point at which the satellite crosses the plane of the earth's equator moving in a southerly direction is known as the *descending* node. The line connecting the nodes is referred to as the *line of nodes*. The *antinodes* of an orbit are the points at which the satellite reaches its maximum northerly and southerly latitudes.

3.3.4 Argument of Perigee

The *argument of perigee*, ω , is an angle measured around the satellite orbit from the ascending node to the perigee. As shown in Figure III-4, the argument of perigee is measured in the direction of satellite motion.

The line connecting the perigee and the apogee of the orbit is known as the *line of apsides*. The orientation of the line of apsides with respect to the line of nodes is given by the argument of perigee.

3.3.5 True Anomaly at Epoch

The position of the satellite within the orbit is given by its true anomaly ν as shown in Figure III-4. This is an angle measured from the perigee around the orbit to the satellite in the direction of orbital motion. True anomaly at epoch, ν_0 , gives the position of the satellite at a particular epoch of time. It completes the set of elements needed to describe a satellite orbit.

3.4 Orbital Perturbations

3.4.1 Introduction

If the only force on a satellite were the gravitational attraction towards the center of the earth, its orbit would be said to be "ideal". All of Kepler's laws would be obeyed and the size, shape, and orientation in space of the orbit would remain constant.

However, other forces act on satellites. Some forces are gravitational such as those due to the sun, the moon, or the non-uniform distribution of matter within the earth itself. Other perturbations include those due to atmospheric drag or the pressure of sunlight on the satellite.

Only the perturbations which affect orbits in the range of interest are discussed. Of these, only perturbations which are of major importance in mission analysis are covered in detail. Other perturbations can be corrected during the spacecraft's mission lifetime by the use of a small quantity of stationkeeping propellant.

The following orbital perturbations are discussed:

- Nodal regression
- Apsidal rotation
- Luni-solar perturbations
- Atmospheric drag

Finally, Table III-3 gives a summary of the effects of these perturbations on the orbital elements.

3.4.2 Nodal Regression

As its name indicates, *nodal regression* causes the line of nodes of the orbit to rotate. It is caused by the oblateness of the earth, which is shown with an exaggerated scale in Figure II-5. The equatorial radius is 6,378 km versus 6,357 km for the polar radius. (The mean earth radius is 6,371 km). The equatorial bulge distorts the path of a satellite when it crosses the equator.

For purposes of discussion, consider the distortion of the satellite's path to be a sharp bend as the satellite nears the equator. The attractive force bends the satellite trajectory northward as the satellite approaches the equatorial plane from the south. As the satellite leaves the equatorial plane, it is bent southward back into its original inclination. The net result of this zig-zag motion is that the ascending node shifts in the direction opposite to that of the satellite motion, as shown in Figure III-6.

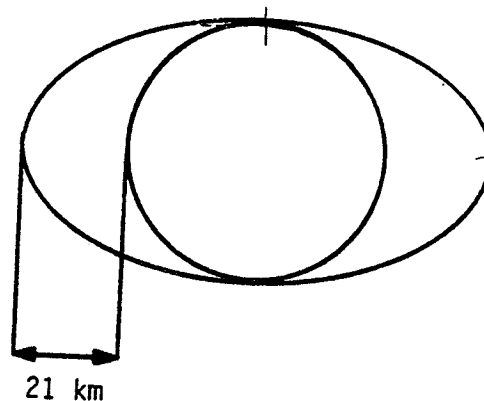


Figure III-5: Equatorial Bulge of Earth

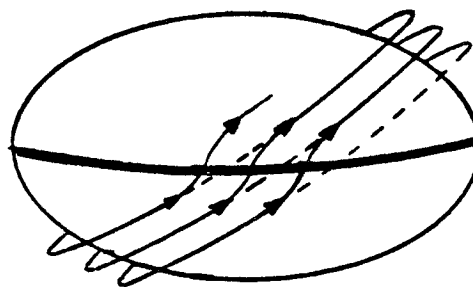


Figure III-6: Illustration of Nodal Regression

The node moves westwards if the orbital inclination is between 0° and 90° (prograde orbit), and moves eastwards if the orbital inclination is between 90° and 180° (retrograde orbit). The magnitude of the nodal regression effect depends on the size, shape, and inclination of the orbit. Very large orbits or polar orbits do not experience significant nodal regression effects. Figure III-7 presents plots of nodal regression rates as a function of orbital inclination.

3.4.3 Apsidal Rotation

Apsidal rotation alters the argument of perigee of a satellite orbit. The force F on the satellite due to the equatorial bulge can be resolved into two components, F_1 which is perpendicular to the plane of the orbit and F_2 which is in the orbital plane (Figure III-8).

The force perpendicular to the orbit plane causes the orbital plane to precess like a gyroscope. It is this normal component of the force which produces the regression of the nodes. The component of the force in the orbit plane causes the line of apsides to rotate from one orbit to the next as shown in Figure III-9.

The apsidal rotation is similar to regression of the nodes in that its rate decreases with increasing altitude and changes with inclination. However, it differs in that low inclinations produce an apsidal rotation in the direction of satellite motion, and near polar orbits have a rotation direction that is opposite the direction of satellite motion. Thus there are two inclinations, 63.4° and 116.6° , where there is no apsidal rotation at all (Figure III-10). These inclinations are used for some missions where the position of apogee must remain fixed in space, such as Molniya communications satellites.

3.4.4 Luni-Solar Perturbations

The gravitational attractions of the sun and the moon perturb the orbits of interest to this study. The principal effect of these luni-solar perturbations is to alter inclination, unless the orbit lies in the plane of the ecliptic in which case the effect on inclination is small. (The ecliptic is the plane of the earth's orbit around the sun.)

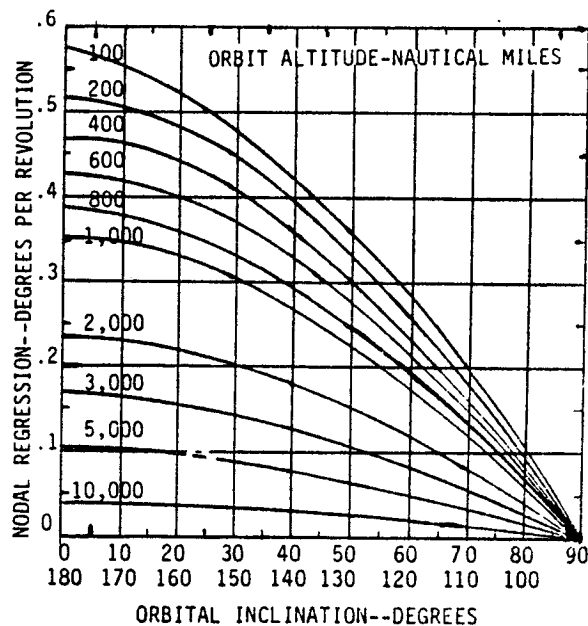
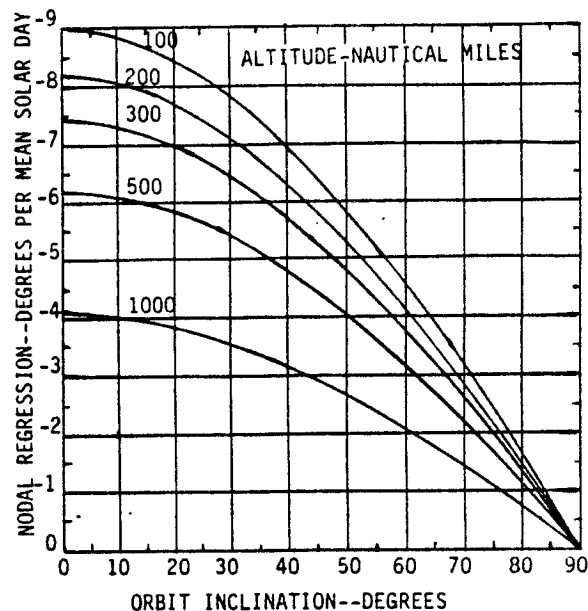


Figure III-7: Nodal Regression vs. Inclination

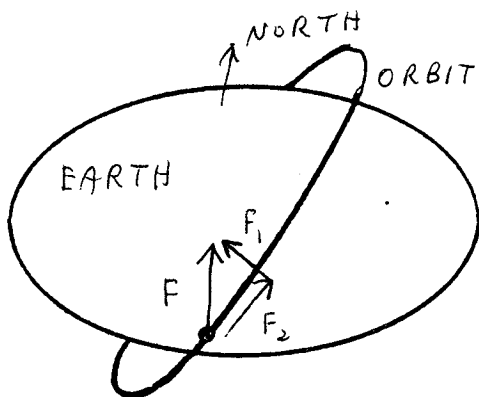


Figure III-8: Forces Causing Nodal Regression (F_1) and Apsidal Rotation (F_2)

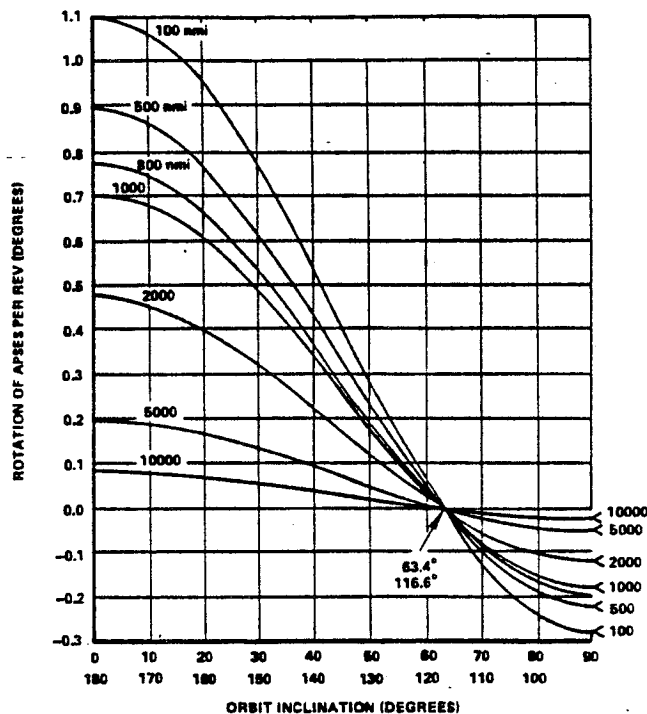


Figure III-10: Apsidal Rotation vs. Inclination

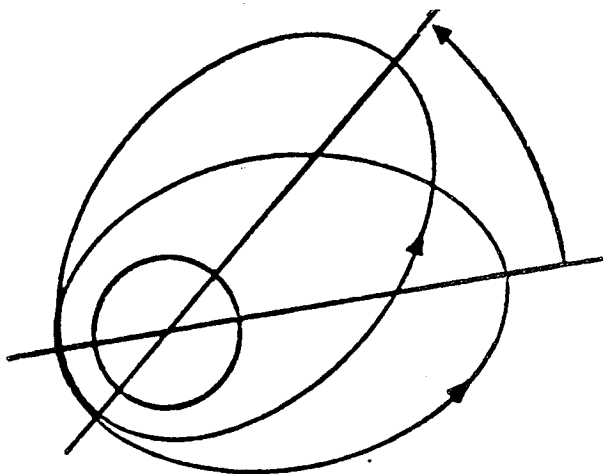


Figure III-9: Apsidal Line Rotation

For nodal regression and apsidal rotation, the orbital perturbations can be minimized by judicious selection of orbital elements (Subsection 3.3.2). However, this is not the case for luni-solar perturbations unless orbits are made relatively small (low altitude), which reduces the satellite coverage area. Stationkeeping maneuvers using the satellite thrusters are necessary.

The gravitational forces of the sun and the moon attract the satellite at every point in the orbit. However, the magnitudes of these attractive forces vary with position in the orbit. It is this differential gravitational effect which perturbs orbital inclinations.

As shown in Figure III-11, the gravitational field of the sun attempts to align the satellite's orbital plane with the plane of the ecliptic. During the summer, the sun's attractive force is stronger at point *B* than point *A*, resulting in the arc of the orbit being raised in the vicinity of point *B* and lowered near point *A* below the plane of the equator. The same effect occurs in winter with the net result that the sun's gravity

operates to increase orbital inclination throughout the year.

The moon's gravity has a similar net effect since its orbit plane is inclined by only 5.2° with respect to the ecliptic plane. The effect of lunar gravity is actually greater than that of the sun. The gravitational attraction of the moon on the satellite varies over a greater range, since the distance from the satellite to the moon changes by a larger fractional amount than the distance from the satellite to the sun changes.

These perturbations are resisted by the orbital angular momentum of the satellite, which resists changes in orientation in the manner of a gyroscope. The angular momentum of an orbit increases as its size (specifically its semi-latus rectum length) is increased. However, the differential gravitational effects due to the sun and the moon increase even more rapidly as the orbit is made larger. For circular equatorial orbits, the rate of change of orbital inclination varies linearly with orbital period.

Spacecraft orbital elements are specified to lie within dead bands. As inclination increases, the limits of the dead band are approached and stationkeeping maneuvers must be made using the on-board thrusters. Thrusting is done in a direction perpendicular to the orbit plane to reset inclination. For equatorial orbits this is referred to as north-south stationkeeping.

For circular equatorial orbits, the annual north-south stationkeeping velocity increment depends linearly upon orbital semi-major axis and varies with orbital period by the following equation:

$$\Delta V_{\text{annual}} \doteq 50 \tau^{2/3} \text{ m/s/yr} \quad (\text{III} - 1)$$

where

ΔV_{annual} is the annual velocity increment in meters per second per year.

τ is the orbital period in days.

3.4.5 Atmospheric Drag

Atmospheric drag has little or no effect on the orbits of interest to this study. It acts to reduce

the semi-major axis and eccentricity of the orbit, until eventually the satellite reaches such a low altitude that it burns up on account of air friction. Atmospheric drag is the limiting factor on the lifetime of low altitude satellites.

Air density drops off so rapidly with increasing height that high altitude satellites are unaffected by atmospheric drag. For medium altitude satellites, atmospheric effects are usually not significant unless the satellite is large and has low density like Echo passive communications satellites. Atmospheric density is reduced by half each time an observer increases altitude by approximately 5 km.

The effect of atmospheric resistance to satellite motion depends on the geometry and internal structure of the satellite. A satellite shaped like a bullet encounters less resistance than one shaped like a barn door, even if they both have the same mass and frontal area, and move through air of the same density.

Density varies with time as well, having a number of cycles of various durations as well as short-lived effects which occur at irregular intervals. There is a daily or diurnal variation in the profile of the atmosphere because the sun heats up the air on the day side of the earth, causing it to expand upwards. This in turn increases the density of the upper atmosphere. There is a 27 day cycle in atmospheric density, a seasonal variation between summer and winter, an annual variation, and an 11 year cycle. Magnetic storms and solar flares can also heat the atmosphere.

The solar ultraviolet radiation impinging on the atmosphere reaches its maximum at local noon and heats the atmosphere which results in an increase in density at satellite altitudes. This effect upon density is usually referred to as the diurnal or day-night effect, and results in a distribution of density called the diurnal bulge (Figure III-12). This bulge follows the path of the sun but lags by approximately 30° in longitude because of the rotation of the earth and the time constant of the atmosphere to solar heating. The point of maximum density therefore occurs at about 2 p.m. local time. The minimum value occurs on the night side of the earth at approximately 4 a.m. local time. This effect

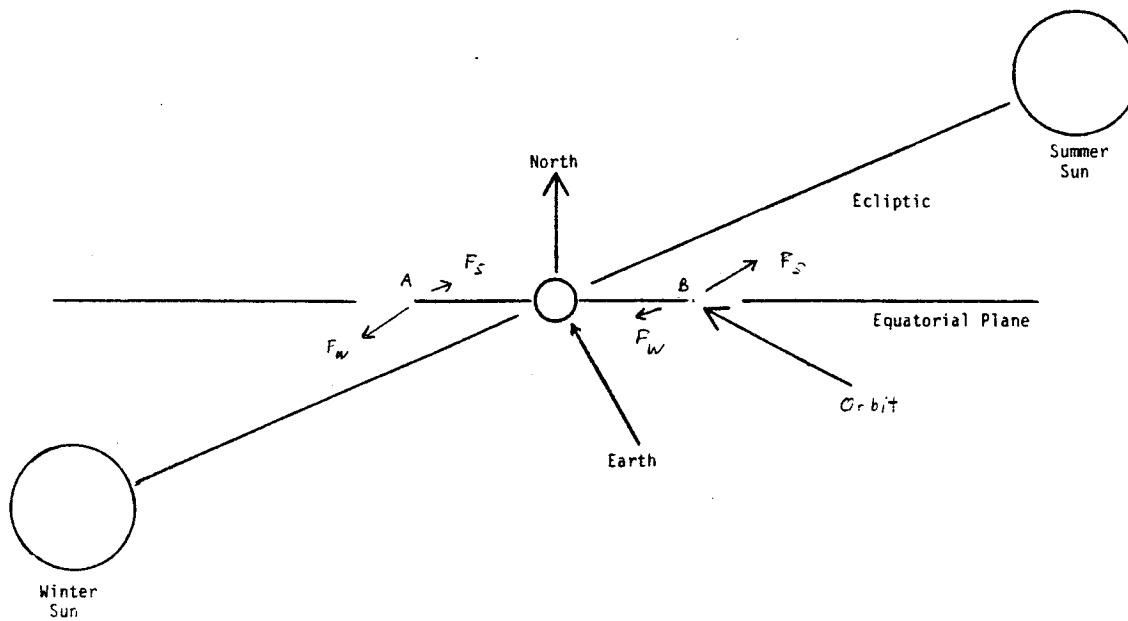


Figure III-11: Gravitational Force of Sun upon Satellite in Equatorial Orbit

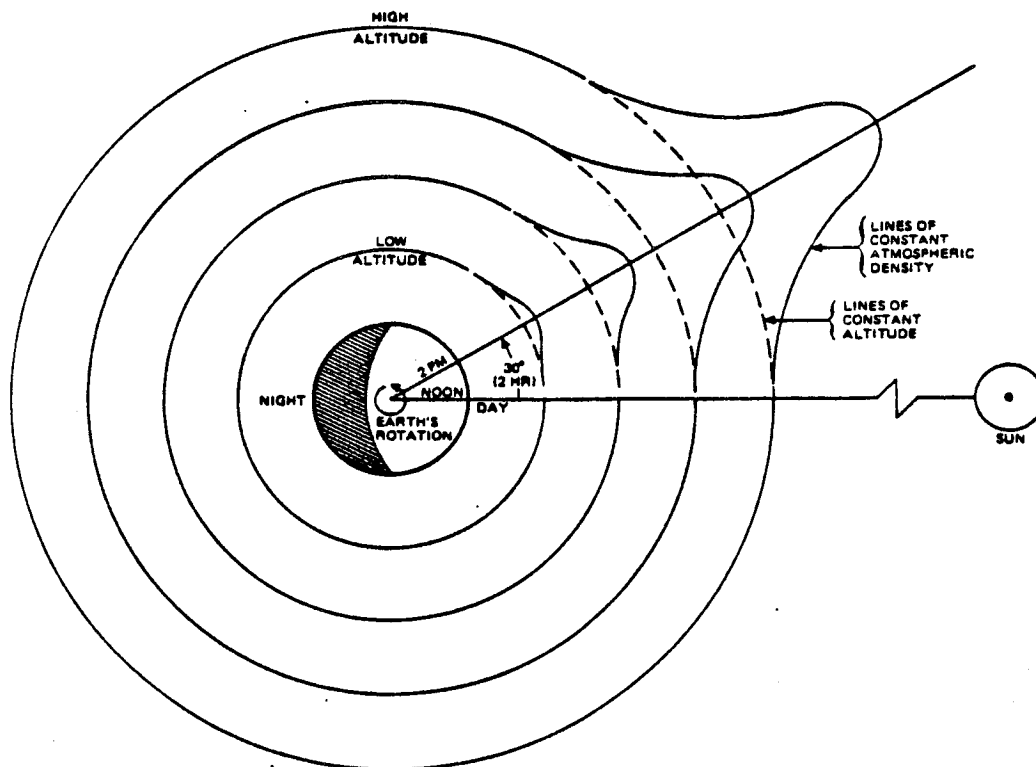


Figure III-12: Diurnal Effect on Atmospheric Density

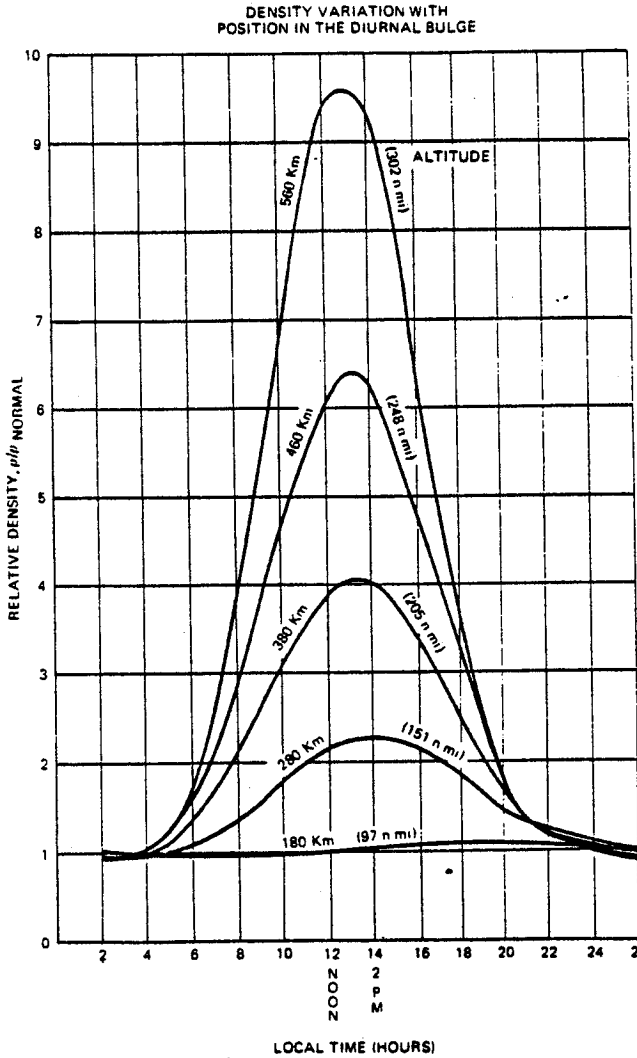


Figure III-13: Density Variation with Time

is also seasonal because the diurnal bulge is alternately located in the northern and southern hemispheres during the local summer.

As an example of the magnitude of the diurnal effect, the minimum and maximum values of atmospheric density at an altitude of 180 km vary by about 20% due to diurnal heating. The effect at higher altitude is much greater, as shown in Figure III-13.

The ease with which the satellite penetrates the atmosphere is measured by using the ballistic parameter β , which is given by the following equation:

$$\beta = \frac{W}{C_D A} \quad (III - 2)$$

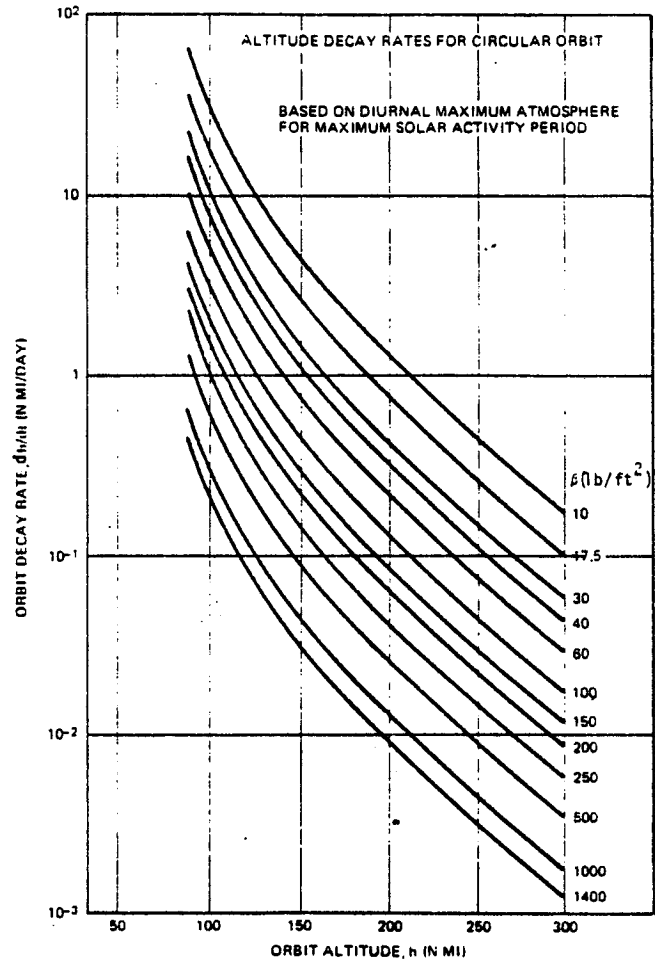


Figure III-14: Orbital Decay versus Ballistic Parameter

where

β is the ballistic parameter.

W is the satellite mass at sea level.

C_D is the satellite drag coefficient.

A is the satellite frontal area.

The ballistic parameter of the satellite affects the orbital decay rate. Satellites with high ballistic parameters penetrate the atmosphere more easily. Figure III-14 shows the orbital decay rate versus orbital altitude for different values of the ballistic parameter. Small, massive satellites stay in orbit longer than large, light ones.

Orbital Element	Affected by	Source of Perturb.	Unaffected Orbits
a	Air drag	Atmosphere	High alt.
e	Air drag	Atmosphere	High alt.
i	Luni-solar	Sun, moon	none
Ω	Nodal regression	Earth's oblateness	Polar, ($i = 90^\circ$)
ω	Apsidal regression	Earth's oblateness	Molniya ($i = 63^\circ$, $i = 116^\circ$)

Table III-3: Summary of Perturbations

Figure III-15 shows the effects of atmospheric drag on satellite lifetimes for a constant ballistic parameter ($\beta = 100 \text{ lb/ft}^2$) and an atmospheric model for a period of high solar activity (AODC 1959 atmospheric model). Figure III-16 shows the orbital lifetime of satellites in orbits with different eccentricities. The variation in lifetime due to satellite ballistic parameter or atmospheric density is not taken into account.

3.4.6 Summary of Perturbations

Table III-3 gives a summary of the perturbations discussed in this subsection and their effects on the orbital elements listed below:

- a – semi-major axis
- e – eccentricity
- i – inclination
- Ω – right ascension of the ascending node
- ω – argument of perigee

3.5 Earth Orbit and Sun Geometry

The position of the satellite within the orbit and the orientation of the orbit with respect to the sun determines the local time-of-day when the satellite overflies a particular geographic region. It is therefore crucial to control these factors to enable the satellite to off-load daily peaks in the geostationary communications traffic.

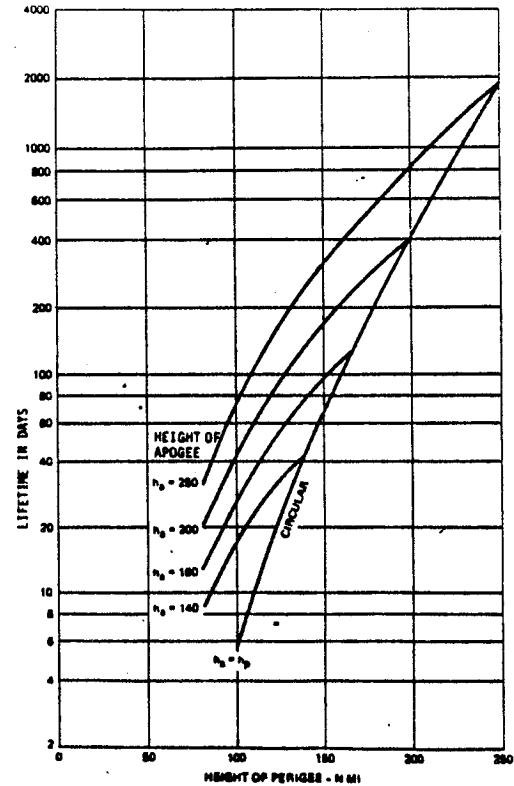


Figure III-15: Lifetime Versus Altitude

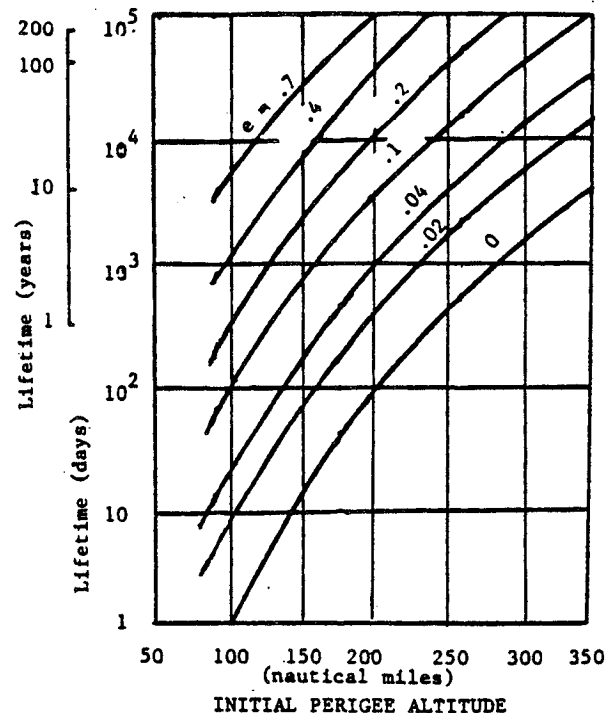


Figure III-16: Lifetime Versus Eccentricity

The earth's rotation on its axis and its orbital motion about the sun are of interest. A satellite orbiting the earth can revolve in a manner similar to the earth's rotation as shown in Figure III-17. The geocentric equatorial coordinate system introduced in Subsection 3.3.3 is specified by the vernal equinox earth-sun direction and the earth's north polar axis direction.

The earth's orbital motion around the sun causes the sun to appear to move annually with respect to the geocentric-equatorial coordinate system. Figure III-18 illustrates this effect. A polar orbit with the ascending node located in the vernal equinox direction is also shown. An observer on the equator could watch the satellite in this polar orbit pass overhead at 6 p.m. local time on the winter solstice and at noon on the vernal equinox. Thus the annual apparent motion of the sun plays a role in the selection of candidate orbits for offloading geostationary traffic peaks which occur at a constant time of day.

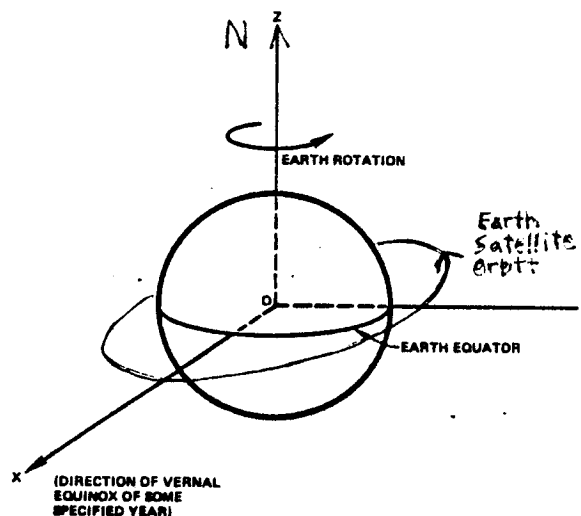


Figure III-17: Rotation of the Earth

4 Candidate Orbit Selection

4.1 Introduction

The principles of orbital mechanics are applied in this subsection to select orbits suitable for offloading daily peaks in the geostationary communications traffic.

First a number of candidate orbits are chosen for which CONUS satellite visibility is assured for each day of the year. In addition, a satellite in each orbit must follow the same arc across the sky from the view of a ground observer, regardless of the time of year. This simplifies the task of tracking the satellite and assures that the satellite is in view of a particular ground terminal at least once each day.

Table III-4 classifies the candidate orbits by eccentricity (circular and non-circular) and inclination (equatorial plane and inclined orbits). Table III-5 lists the characteristics of eight candidate orbits.

The candidate orbits are compared and the most advantageous selected for further discussion. This discussion is presented in Section 5

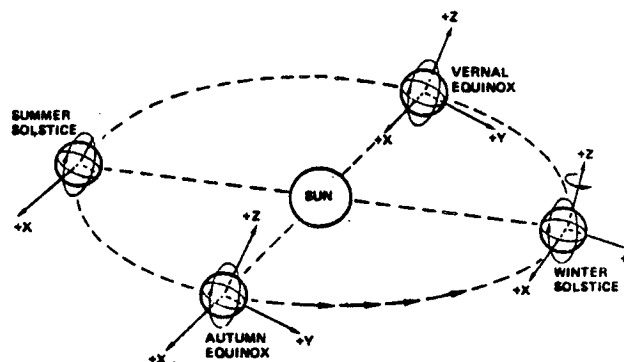


Figure III-18: Earth's Motion Around the Sun

	Equatorial	Inclined
Circular	GEO 12 h 8 h 6 h Retro 12 h	(none)
Non-circ.	ACE	3-synchronous Molniya

Table III-4: Candidate Orbits

and includes satellite coverage hours and tracking antenna look angles for major CONUS cities.

4.2 Constraint on Orbital Period

To enable the satellite to be in view of CONUS at certain hours of the day, the number of orbits made during the day must be an integer plus or in some cases minus a very small fraction. This fraction allows for the apparent annual motion of the sun discussed in Section 3.4 as well as the effects of orbital perturbations.

The number of orbits made during the day is approximately equal to any integer between one and sixteen. The orbital period is given by the following equation:

$$\tau \doteq \frac{24}{n} \text{ hours} \quad (III - 3)$$

where

$$n = 1, 2, 3, \dots 16.$$

The semi-major axis of the orbit is set by the orbital period:

$$a \doteq 42,164 \left(\frac{1}{n} \right)^{2/3} \text{ km} \quad (III - 4)$$

The exact value of the semi-major axis must be determined individually for each candidate orbit due to sun geometry and perturbation consideration.

4.3 Constraint on Apogee Altitude

At some point in the orbit the satellite must reach a sufficiently great altitude to simultaneously view the whole of CONUS. In other words, the satellite must be at an elevation of 10° or greater for any CONUS ground observer.

If the orbital inclination is 40° or greater, the satellite can overfly the geographical center of CONUS. From such a position, an altitude of 1,900 km gives all CONUS coverage. For an equatorial orbit an altitude of 9,500 km is required to enable satellite viewing from the northeasterly and northwesterly regions of CONUS.

Orbital apogee radius must therefore exceed 8,300 km for an orbit with inclination of 40° or greater and 16,000 km for equatorial orbits.

Circular equatorial orbits must have semi-major axes of at least 16,000 km, restricting them to periods of 5.6 hr or more. Certain inclined circular orbits can have semi-major axes as low as 8,300 km and periods as short as two hours. However, constraints arising from the annual apparent motion of the sun eliminate inclined circular orbits from consideration for single satellite constellations.

Eccentric equatorial orbits with periods of less than five hours can provide all-CONUS viewing in their apogee regions and merit further discussion.

4.4 Single Satellite Configurations

The most advantageous configurations for commercial use can be made to provide CONUS coverage at one or both of the daily geostationary communications traffic peaks with a single satellite. Service can be inaugurated with the completion of on-orbit testing by the first satellite launched. A single satellite is of use throughout the year and ground antenna tracking patterns can remain the same all year.

4.4.1 Circular Orbits

Equatorial Orbits. As viewed from the earth, a satellite in a non-geosynchronous circular equatorial orbit appears to follow the same arc across the sky every day of the year. If the orbital pe-

	Equatorial Orbits						Inclined Orbits	
	Circular					Elliptic	Elliptical	
	Prograde				Retrograde			
	GEO 24 hr	STET ^e 12 hr	8 hr	6 hr	12 hr	ACE ^f 4.8 hr	Molniya 12 hr	3-synch. 3 hr.
Eccentricity	.0	.0	.0	.0	.0	.49	.73	.3467
Inclination (degrees)	0	0	0	0	0	0	63.4	116.6
Apogee (km)	42,164	26,590	20,300	10,760	26,640	21,480	45,950	14,220
Apogee altitude (km)	35,786	20,210	13,900	10,380	20,620	15,100	39,580	7,480
Perigee (km)	—	—	—	—	—	7,410	7,170	6,900
Perigee altitude (km)	—	—	—	—	—	1,030	790	520
Period (hr:min)	23:56	11:59	7:59	3:59	12:01	4:48	11:58	3:00
Revs. per solar day	1	2	3	4	2	5	2	8
Offloads daily peaks?	yes	yes	yes	yes	yes	yes	no	yes
Eclipses (days/yr)	88	150	240	290	150	365	> 0 ^a	≥ 0 ^a
Max. Eclipse Time (min)	72	56	50	45	56	26 ^a	> 0 ^a	40
Crosses CONUS Zenith?	no	no	no	no	no	no	yes	yes
Crosses GEO arc?	yes	no	no	no	no	no	yes	yes
Max. 2-way time delay (s)	.25	.15	.10	.07	.15	.12	.27	.05
Velocity increments (m/s)								
STS to orbit ^c	4,200	4,000	3,900	3,780	> 5,000 ^b	3,200	3,360	7,100
12 yr stationkeeping	600	380	290	240	380	100 ^d	100 ^d	100 ^d

Table III-5: Characteristics of Candidate Orbits

- a. Exact value depends on position of apsidal line with respect to earth-sun line.
- b. Assumes bi-elliptic transfer requiring translunar plane change maneuver.
- c. Assumes orbital inclination of 28.5°.
- d. Estimated.
- e. STET means Sun-synchronous Twelve-hour Equatorial orbit.
- f. ACE means Apogee at Constant time-of-day Equatorial orbit.

Orbit	Hours in view of both cities	
	Boston & Omaha	Boston & Los Angeles
Prograde 12 hr	6.0	4.7
Prograde 8 hr	2.6	2.0
Prograde 6 hr	1.4	1.1
Retrograde 12 hr	2.0	1.6
Retrograde 8 hr	1.3	1.0

Table III-6: Duration of Simultaneous Viewing

riod is constrained as per Subsection 4.2, the satellite is at the same point in its arc at the same time each day. Thus circular equatorial orbits are attractive candidates for this study.

Orbits can be either prograde or retrograde. However, the retrograde equatorial orbit is less attractive since it provides shorter coverage duration and requires a higher launch velocity increment.

Figure III-19 displays coverage durations for candidate circular equatorial orbits for ground terminals at different latitudes, assuming a minimum satellite elevation angle of 10° . The prograde 12-hour orbit (STET orbit) provides by far the longest time in view.

Figure III-20 displays the satellite apparent motion for circular equatorial retrograde orbits of 24, 12, and 8 hour durations, as viewed by a ground observer at 30° N latitude. The retrograde 24-hour orbit was not considered since its apparent position coincides with the geostationary arc from the perspective of a ground terminal.

Table III-6 gives the duration of simultaneous visibility in Boston/Omaha and Boston/Los Angeles for satellites in different circular equatorial orbits. Only the prograde orbits with periods of eight hours or longer provide sufficiently long time-in-view of distant CONUS cities to warrant further consideration by this study.

Inclined Orbits. A satellite in an inclined circular orbit follows the same path in the sky if a constraint on its period is maintained. However, the time-of-day at which the satellite reaches a

particular point in its arc changes by approximately four minutes each day.

A small adjustment to the orbital period can make the satellite cross the observer's meridian of longitude at the same local time each day. However, now the satellite does not follow the same arc across the sky throughout the year.

Figure III-21 shows the path followed by a satellite in a 12 hour orbit inclined 40° to the equator. Paths are shown at 90 day intervals. Although the path changes during the year, the satellite is in view at a constant time-of-day each day of the year

A satellite whose orbital period is constrained in this manner follows a different arc across the sky each day unless the orbit is equatorial. A different segment of the orbit is in view each day. At one time of year the orbit segment to the north of the equatorial plane is in view during the mid-afternoon. Approximately six months later this particular orbit segment is in view before dawn. A segment of the orbit to the south of the equator could be in view at mid-afternoon if satellite altitude is sufficiently great and orbital inclination is sufficiently low.

The nodal regression perturbation introduced in Subsection 3.3.1 could conceivably be employed to produce a situation where the satellite is in view at a constant time-of-day and follows the same arc across the sky as viewed from the earth. Such an orbit would be retrograde for this perturbation to generate an eastward motion of the line of nodes equal in angular rate to the mean apparent annual motion of the sun (i.e. sun synchronous). The orbital radius cannot exceed 12,400 km which corresponds to a period of 3.8 hours.

The conclusion is that inclined circular orbits are unsuitable for unloading peak geostationary communications satellite traffic with single satellite configurations. An orbit of this class with sufficiently large altitude for full CONUS visibility for a useful duration of time can provide either constant time-of-day coverage or constant path in the sky throughout the year, but not both.

ORIGINAL PAGE IS
OF POOR QUALITY

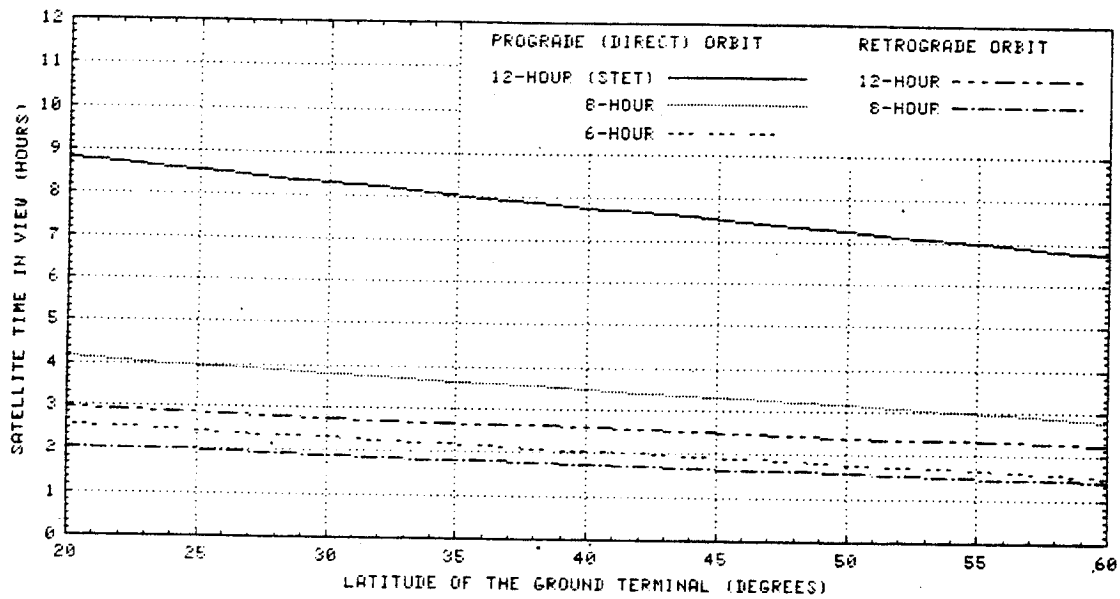


Figure III-19: Coverage Duration Versus Latitude for Circular Equatorial Orbits

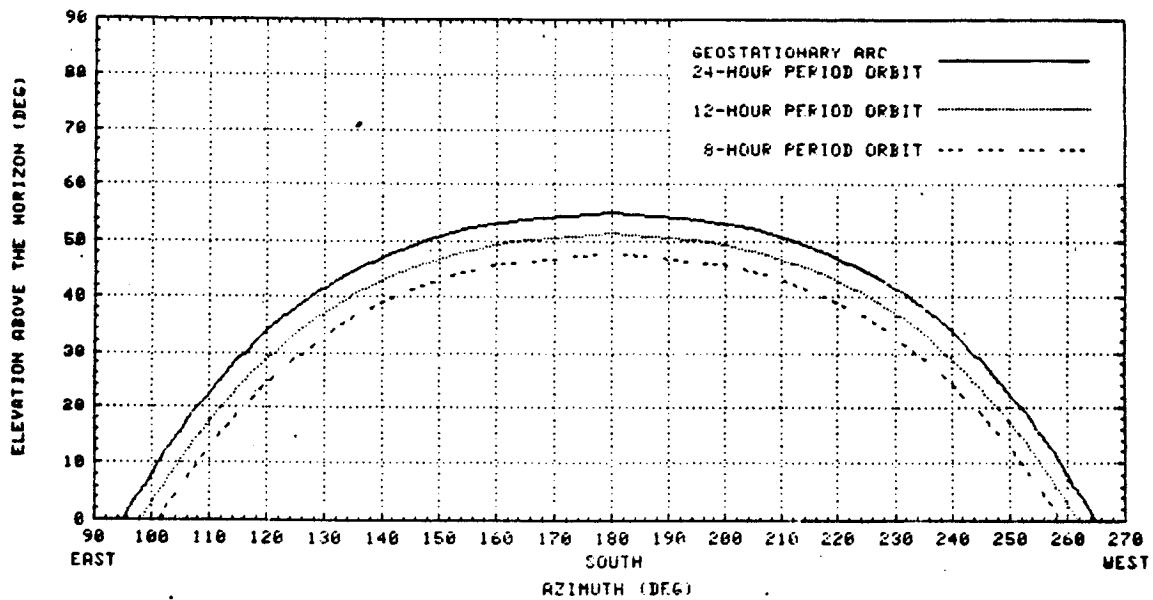


Figure III-20: Apparent Satellite Motion in Different Circular Equatorial Orbits

4.4.2 Non-Circular Orbits

Eccentric orbits are attractive since the satellite spends a larger fraction of its orbital period near apogee where its altitude is high, its speed is low, and it is most easily tracked from the ground. However, there are only three inclinations for which the apogee region can be maintained above a specified parallel of latitude for a moderate to high eccentricity orbit. One of these inclinations must be used if the ground terminal antenna is to track the satellite in the same manner throughout the year.

Suitable inclinations include those of Molniya orbits discussed in Subsection 3.2.2 (63.4° and 116.6°) and 0° . For eccentric orbits of other inclinations, the apogee latitude of the satellite varies throughout the year due to apsidal rotation. The apogee subsatellite point or point on the earth's surface directly beneath the satellite at apogee is located in the southern hemisphere half the time.

Apsidal rotation cannot be negated using nodal regression effects, even though they appear to operate in opposite directions for certain orbital inclinations. Apsidal rotation causes the line of apsides or major axis of the orbit to rotate within the orbit plane, while nodal regression generates a rotation of the orbit plane itself in an easterly or westerly direction. Unless the orbit is equatorial, these motions are not coplanar. For all equatorial orbits, the apsidal rotation rate is nearly twice the nodal regression rate.

Inclined Orbits. The orientation of the Molniya orbit in space is affected by nodal regression. Constant time of day viewing can only be assured by a retrograde Molniya orbit, where the apogee region moves east due to nodal regression even though the apogee latitude remains constant. This is opposite to the direction of the annual apparent motion of the sun.

A candidate for further consideration is a particular retrograde Molniya orbit known as the *triply synchronous orbit*, so named because three parameters are synchronized:

1. The orbital period is synchronized to $1/8$

that of the earth. For every single earth rotation, the satellite makes 8 orbits.

2. The nodal regression rate is set to the mean solar annual apparent angular rate. This allows the satellite to overfly a position on the earth at the same time each day.
3. The apsidal rotation is set to zero.

Three hours is the maximum period for which a sun-synchronous orbit can be produced with this orbital inclination and still satisfy the period constraint of Subsection 4.2. Figure III-22 displays CONUS city coverage durations for this orbit. Maximum coverage duration for any city is 1.5 hours.

Equatorial Orbits. Conditions are more favorable for equatorial eccentric orbits. As will be discussed in Subsection 5.2, one such orbit (ACE) can be found with a sufficiently great apogee altitude for full CONUS viewing and the appropriate geometry for constant time of day coverage throughout the year.

For 0° inclination (an equatorial orbit), the apsidal rotation causes the apogee to move eastwards around the equator. However, nodal regression induces a westward motion of the apogee since the line of nodes and the line of apsides both lie in the equatorial plane. They are separated by the argument of perigee angle, which increases with time at almost precisely twice the rate at which the line of nodes moves westward, resulting in a net easterly motion of the apogee segment of the orbit.

By the judicious selection of orbital elements the apogee segment can be made to move eastward at an angular rate equal to that of the apparent mean annual rate of the sun's motion. This assures constant time of day viewing of the apogee segment of the orbit. Applying the orbital period constraint introduced in Section 4.2 generates the Apogee at Constant time of day Equatorial (ACE) Orbit, which is discussed in detail in Subsection 5.2.

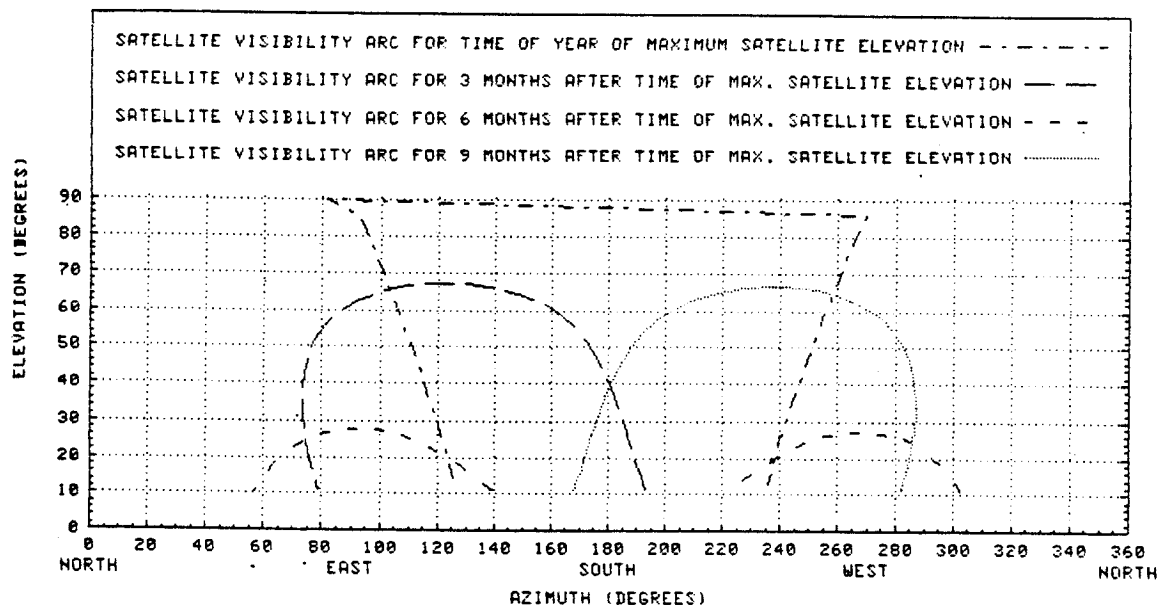


Figure III-21: Apparent Paths of a Satellite in a 12 hr, Circular, 40° Inclined Orbit

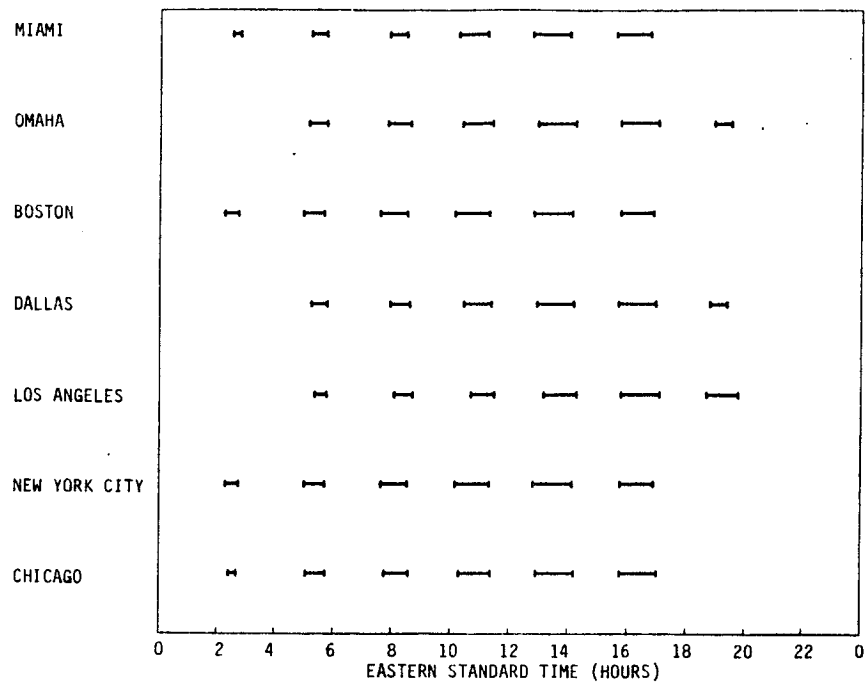


Figure III-22: Coverage Times for Satellite in Triply Synchronous Orbit

4.4.3 Single Satellite Conclusions

Only equatorial orbits and the triply synchronous orbit can provide the necessary constant time of day satellite coverage throughout the year. The triply synchronous orbit and retrograde equatorial orbits are not recommended due to relatively short visibility times and large launch velocity increments.

Three circular and one eccentric equatorial orbits possess sufficient advantages to warrant consideration. Of the circular orbits, the prograde orbit with a 12 hour period has the longest visibility time and is recommended for use by this study. It is known as the STET or Sun-synchronous Twelve hour Equatorial Orbit. The one eccentric orbit recommended is the ACE or Apogee at Constant time of day Equatorial Orbit.

4.5 Multiple Satellite Constellations

The largest multiple satellite constellation providing services at present is the Molniya system operated by the U.S.S.R. Certain geostationary satellites are operated together by cross-linking communications among them. Each satellite in a GEO constellation is capable of constant time of day service throughout the year, while Molniya constellation members are not. A dozen or more Molniya satellites must be operated at once in order to provide round-the-clock coverage.

4.5.1 Molniya Orbit Systems

The Soviet Union has launched over eighty satellites into Molniya orbits since 1965. Over a dozen are operated at any given time to provide round-the-clock coverage which is necessary to provide constant time of day coverage throughout the year.

Figure III-1 illustrates that the apogee of a Molniya satellite overhead at noon in December is overhead at approximately 6 am in March. Due to the earth's rotation around the sun, the satellite ground coverage time is 4 minutes earlier each day.

The Molniya constellation makes use of groups of satellites in different orbital planes to provide

constant time-of-day coverage. Each group of satellites shares a common ascending node right ascension. Communications are handed off from one satellite to another approximately every six hours in a constellation with four orbit planes. The hand-off times vary throughout the year and occur four minutes earlier each day.

A particularly serious problem with Molniya systems is redundancy since the failure of a single satellite can jeopardize year round coverage. A constellation of several Molniya satellites must be used to provide constant time of day coverage. Furthermore, a number of different orbit planes are required and the velocity increment necessary to transfer from one plane to another is prohibitively large. If used, on-orbit spares must be provided for each orbital plane. Ground spares provide better flexibility but depend on launch vehicle availability.

4.5.2 Lower Altitude Satellites

Low to medium altitude satellite orbits provide a rich study area for certain types of communications services. Advantages include the relative ease of access of certain low orbits, the short slant ranges from ground terminals, and the rapidity with which a satellite in such an orbit can overfly widely separated regions of the world.

Satellite orbits up to 40° inclination and altitudes up to a few thousand kilometers are accessible for low cost launches. In comparison, sun synchronous orbits are more difficult to achieve. Equatorial orbits are not attractive for low altitude constellations due to poor visibility at high latitudes and the difficulty of achieving these orbits from non-equatorial launch sites.

Low/medium altitude constellations will not be considered further in this study due to the limited coverage times provided by a single satellite. It is true that a large number (i.e. several hundred) of satellites interconnected with each other could provide service. However, individual satellites would need to be very inexpensive. This is a subject for another study.

5 Analysis of Selected Orbits

5.1 Introduction

The following two orbits are selected for use in offloading daily traffic peaks:

- Apogee at Constant time-of-day Equatorial (ACE) orbit
- Sun-synchronous Twelve-hour Equatorial (STET) orbit

The analysis of these orbits is given in this subsection.

5.2 ACE Orbit

5.2.1 General Description

ACE orbit is the abbreviation for Apogee at Constant time-of-day Equatorial orbit. The ACE orbit is sun-synchronous and highly eccentric, with the satellite completing five revolutions per day. The satellite depends upon a continuing perturbation of its orbit to overfly the same area of the earth at the same time each day.

A 4.8 hour orbital period enables a single satellite to be used for both the morning traffic peak and on the next orbit the afternoon traffic peak. Due to the high eccentricity ($\epsilon = 0.49$) of the orbit, the satellite loiters in its apogee portion, remaining in view for over two hours. It then moves rapidly through the perigee portion during the time between the two traffic peaks.

If an orbit is unperturbed, the satellite reaches apogee at a different local (sun) time each day just as the Molniya satellite does (Figure III-1). The effect of apsidal rotation, however, causes the apogee of the ACE orbit to move eastwards at an angular rate of approximately one degree per day. This matches the earth's orbital angular rate around the sun (360° per year), enabling a satellite in the ACE orbit to reach apogee at the same time each day with minimal station-keeping (Figure III-2).

5.2.2 Size and Shape

The size and shape of the ACE orbit are constrained by the dependence of the apsidal rota-

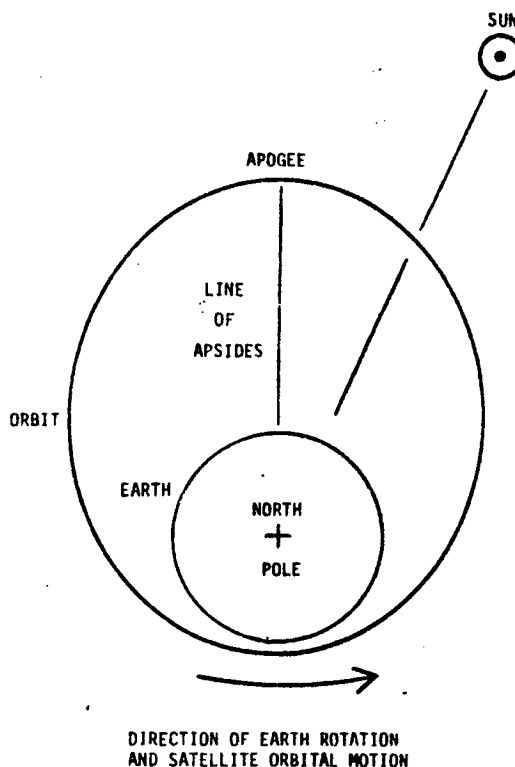


Figure III-23: Geometry of ACE Orbit.

tion and nodal regression rates on orbital dimensions. Only an orbit whose period is one-fifth of a day or less is sufficiently small to have a suitably large apsidal rotation rate. Orbits whose periods are one-seventh of a day or less have apsidal rotation rates which are excessively large. Thus the one-fifth and one-sixth day periods are the only possible choices in order to maintain apogees at constant solar times.

Figure III-23 displays the geometry of the orbit. The semi-major axis is constrained by its 4.8 h period to be approximately 14,440 km. The shape of the orbit is constrained by the need to move the apogee by 1° per day to an eccentricity of 0.49. The line of apsides retains approximately the same orientation with respect to the earth-sun line throughout the year. Table III-7 summarizes the parameters of the orbit for the one-fifth and one-sixth day period orbits.

The one-sixth day period orbit does not appear to be advantageous due to its low apogee altitude and the short period of time during which it can provide communications. Its semi-major axis is constrained by its 4 hour period to be ap-

1/5 Day Period		
Parameter	Value	Unit
Period	4.79	h
Semi-major axis	14,445	km
Eccentricity	.49	
Inclination	0.0	°
Perigee radius	7,410	km
Perigee altitude	1,030	km
Apogee radius	21,480	km
Apogee altitude	15,100	km
Nodal regression	-.986	°/day
Apsidal rotation	1.972	°/day

1/6 Day Period		
Parameter	Value	Unit
Period	4.0	h
Semi-major axis	12,780	km
Eccentricity	.23	
Inclination	0.0	°
Perigee radius	9,840	km
Perigee altitude	3,460	km
Apogee radius	15,710	km
Apogee altitude	9,340	km
Nodal regression	-.986	°/day
Apsidal rotation	1.972	°/day

Table III-7: ACE Orbit Parameters

Apogee	Longitude	Visibility Limits	
		at 50° N	
1	48° W	6° W	90° W
2	120° W	78° W	162° W
3	168° E	150° W	126° E
4	96° E	138° E	54° E
5	24° E	66° E	18° W

Table III-8: Apogee Longitudes for CONUS

proximately 12,780 km. The shape of the orbit is constrained to an eccentricity of 0.23. Apogee altitude is therefore only 9,340 km, which is too low for useful communications coverage. Altitude limits for orbits are discussed in Subsection III-4.3. A satellite in this orbit could be useful for meteorological or other purposes and could be the subject of another study.

5.2.3 CONUS Coverage

A satellite in the ACE orbit has five apogee crossings each day, with each crossing occurring above a particular point on the equator. These points are separated by one-fifth the circumference of the earth or 72° of longitude and remain fixed throughout the year. Table III-8 lists apogee longitudes for a possible configuration of the ACE orbit for good CONUS visibility. The limits of satellite visibility for a site at apogee longitude and 50° N latitude are also tabulated.

Very good coverage for CONUS peak times is afforded by a satellite in an ACE orbit which reaches apogee above 48° W and 120° W at 11:50 am and 4:37 pm eastern time respectively.

Table III-9 gives the latitude and longitude of seven major traffic cities (marked with asterisks) located at the extremes of CONUS. The coverage pattern for the seven cities is shown in Figure III-24 for this ACE orbit. Table III-10 gives the coverage times and duration (satellite above 10° elevation angle) for the first and second apogees of this ACE orbit for the cities.

As seen from Table III-10, the coverage pattern characteristics vary with ground station longitude as well as latitude. Figure III-25 shows

City	Latitude (° N)	Longitude (° W)
San Francisco	37.5	122.3
Los Angeles*	34.0	118.2
Denver	39.5	105.0
Dallas*	32.5	96.5
Omaha*	41.2	96.0
Chicago*	41.5	87.5
Miami*	25.5	80.2
New York City*	40.4	73.5
Boston*	42.2	71.0

Table III-9: CONUS City Locations

City	1st Apogee 48° W Coverage Hours (ET)		
	Begin	End	Duration
San Francisco	0945	1032	.76
Los Angeles*	0944	1053	1.15
Denver	0950	1138	1.79
Dallas*	0948	1222	2.56
Omaha*	0853	1109	2.27
Chicago*	0956	1232	2.61
Miami*	0951	1301	3.17
New York City*	1000	1300	3.00
Boston*	1002	1301	2.98

City	2nd Apogee 120° W Coverage Hours (ET)		
	Begin	End	Duration
San Francisco	1458	1814	3.26
Los Angeles*	1459	1818	3.33
Denver	1514	1823	3.15
Dallas*	1518	1830	3.20
Omaha*	1426	1726	3.00
Chicago*	1540	1829	2.80
Miami*	1539	1838	2.98
New York City*	1613	1834	2.33
Boston*	1627	1833	2.10

Table III-10: ACE Orbit Coverages

the variation in coverage duration as a function of ground terminal location and apogee longitude of the satellite.

5.2.4 Motion of Satellite

The ACE orbit satellite is in continuous motion with respect to any ground terminal. A ground station observes the satellite to move across the sky following the same arc each day. Since the motion is the same each day, the ground station can track the satellite in the same manner on any day of the year. This is an advantage of the ACE orbit over the Molniya orbit. However, due to the elliptical orbit, the motion in the ACE orbit is non-uniform with position in the orbit.

Figures III-26 to III-32 display the apparent motions of an ACE orbit satellite from seven cities. The satellite moves from west to east and remains over 5° away from the geostationary arc for the worst case at Miami (7° at New York City). The satellite never approaches the zenith.

Figure III-33 displays the elevation of the satellite as a function of time for seven cities. The satellite is visible across CONUS for the afternoon peak. West coast visibility is limited during the morning peak, but west coast traffic is also limited at this time.

Figure III-34 shows how the slant range and one-way signal propagation delay vary with time. Geostationary satellites have a constant range and propagation delay of that is typically 38,150 km and 127 ms respectively (Chicago viewing satellite at 90° W).

The range rate and doppler shift of signals at a frequency of 6 GHz are shown in Figure III-35.

The azimuth and elevation antenna slew rates for terminals in seven cities are shown in Figures III-36 and III-37.

5.2.5 Worldwide Coverage

The ACE orbit satellite is visible daily for at least two hours for every point on the earth's surface below 50° latitude. Figure III-38 shows the local time of day an ACE satellite is above 10° for an orbit with apogees at 48° W, 120° W, 168° W, 96° E, and 24° E. Thus coverage can be

provided during the local business day throughout the world. Figure III-39 provides worldwide coverage information referenced to Eastern Standard Time.

Use of the ACE orbit satellite to service widely separated geographical regions is an attractive possibility. European, Mideastern, Asian, and American customers can all use the same satellite, filling its capacity over half of its service lifetime. There are also short periods when the satellite is in view of both the East Coast of the United States and Western Europe, and longer periods when the satellite is in view of both Eastern Asia and the Mideast or the Mideast and Europe.

5.3 STET Orbit

5.3.1 General Description

A satellite in the Sun-synchronous Twelve-hour Equatorial Orbit (STET) depends only on the specific value of its orbital period to bring it into view of its service region at the same time each day. The orbit is circular and does not depend on perturbations to enable the satellite to carry out its mission. Furthermore, the path of the satellite across the sky is the same each day, greatly simplifying tracking. The number of orbital revolutions the STET satellite makes during the day is equal to two plus a small fraction which accounts for the annual motion of the sun and orbital perturbations.

During the day the sun is observed to move eastward with respect to the fixed stars. This apparent solar annual motion is approximately $.986^\circ$ per day or 360° per year due to the earth's orbital motion. The STET orbit satellite travels through an angle of 720.986° per day, or $.986^\circ$ more than two full orbital revolutions. Thus the satellite's orbital position as measured at a constant time of day advances eastward to match the annual apparent solar motion. The STET orbit satellite is in view of its coverage area at noon on every day of the year because it is astride the projection of the earth-sun line in the equatorial plane at twelve hour intervals.

Since the STET satellite travels 720.986° in 24 hours, its orbital period is 11 hr 59 min. Circular

Parameter	Value	Unit
Period	12	h
Eccentricity	0	
Inclination	0.0	$^\circ$
Radius	26,590	km
Altitude	20,210	km

Table III-11: STET Orbit Parameters

equatorial orbits with periods of approximately eight or six hours can also provide constant time of day coverage throughout the year. However, coverage duration is much shorter than for the twelve hour STET orbit, as shown in Figure III-19. Table III-11 summarizes the STET orbital parameters.

5.3.2 CONUS Coverage

Figures III-40 and III-41 and Table III-12 display the times for which a STET satellite could be used to provide coverage for major CONUS cities. Simultaneous coverage of all cities is only provided from 9:29 am to 2:13 pm EST, a period of 4 hr 44 min. Figures III-42 through III-48 show the apparent motions of the STET satellite (positioned such that it passes over New York at 1 pm EST) from major CONUS cities. The satellite moves from west to east and remains a constant 3° away from the geostationary arc for the worst case at Miami (5° at New York).

Figure III-49 shows the elevation angle of a STET satellite as a function of time. Figure III-50 displays the slant ranges from an earth terminal and the one-way signal propagation delay. provided in The variation of range rates and signal doppler shifts for each city are given in Figure III-51. Figures III-52 and III-53 show the azimuth and elevation tracking rates for different earth station locations.

Eclipse duration information is shown in Figure III-54. The eclipses do not occur when the satellite is providing geostationary communications traffic peak of-loading. This is implicit in the requirement for sun synchronous communications coinciding with the business day hours.

City	Coverage Hours (ET)		
	Begin	End	Duration
Los Angeles	0715	1413	8.14
Dallas	0740	1542	8.21
Omaha	0757	1529	7.71
Chicago	0830	1602	7.68
Miami	0833	1655	8.48
New York City	0915	1700	7.76
Boston	0929	1706	7.63

Table III-12: STET Orbit Coverages

5.3.3 Worldwide Coverage by STET

The STET orbit satellite overflies every point on the equator and is visible for over seven hours between 50° N and 50° S latitudes. However, the timings of these coverage periods are not advantageous for many geographical regions.

Figure III-55 displays coverage times for various parts of the world. A satellite visible throughout the midday hours in CONUS appears only at night in Europe and from mid-afternoon through the evening in Japan. Only at the longitude of India and Central Asia does the STET Orbit Satellite servicing CONUS appear during the midday hours.

6 Conclusions

Two suitable satellite orbits have been described: the ACE orbit in Subsection 5.2 and the STET orbit in Subsection 5.3. Section IV describes the traffic deloading possibilities with satellites using these orbits.

There are three major differences between the ACE and STET orbits:

1. The minimum separation (Miami) from the plane of the GEO arc is 3° for the STET and 5.6° for the ACE satellite.
2. The duration of coverage for the STET satellite is around 8 h from a single location versus the ACE coverage of 3 h, followed by a 3 h gap of no coverage, and then another 3 h coverage.

3. The ACE orbit is lower than the STET orbit and requires less energy to reach.

In addition, the radiation environment of the two orbits is different as discussed in Appendix A.

ORIGINAL PAGE IS
OF POOR QUALITY

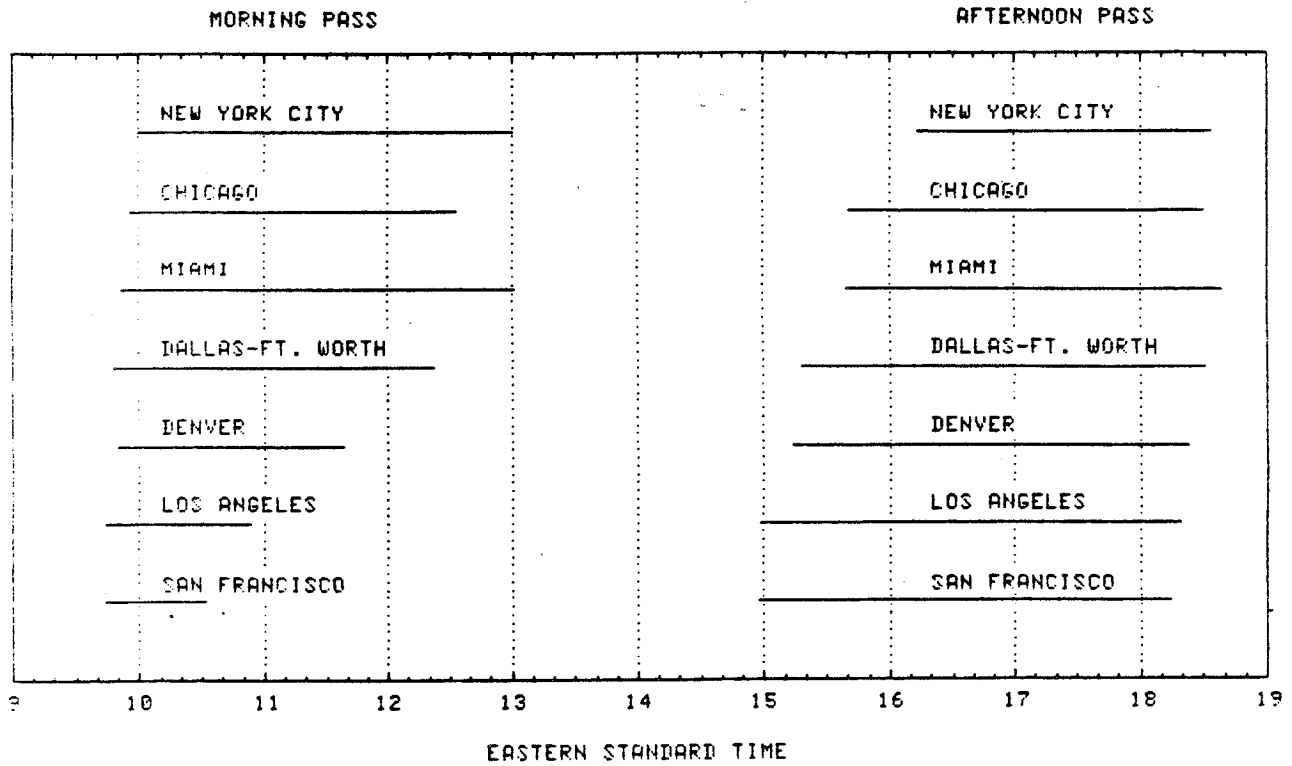


Figure III-24: ACE Orbit Coverages: Apogees at 48° W and 120° W

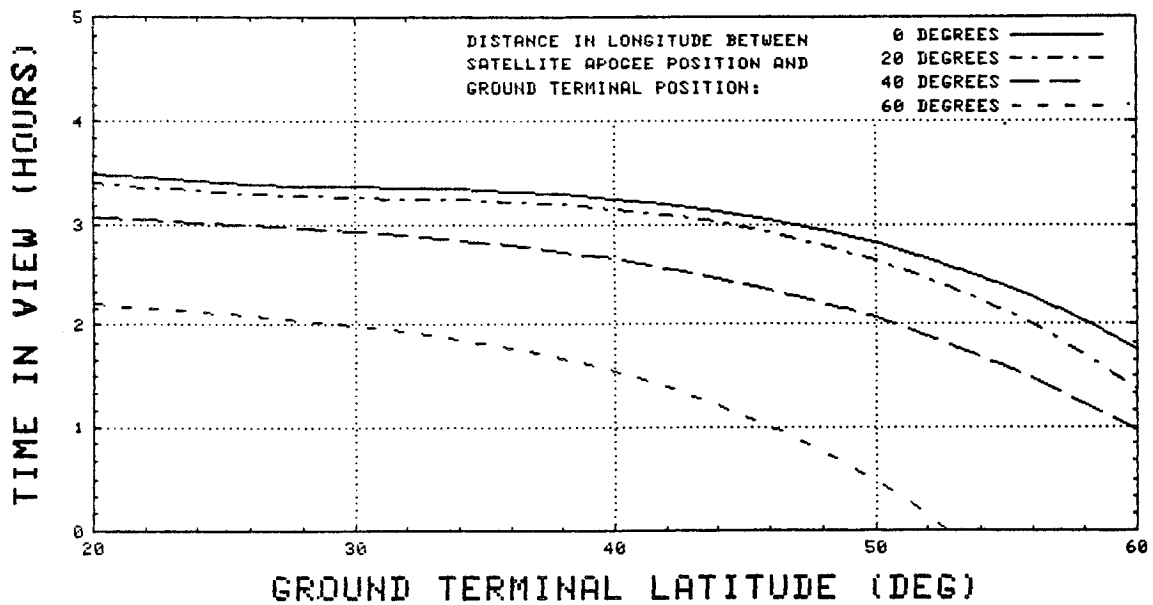


Figure III-25: Coverage Duration Versus Ground Station Location for ACE Orbit

ORIGINAL PAGE IS
OF POOR QUALITY

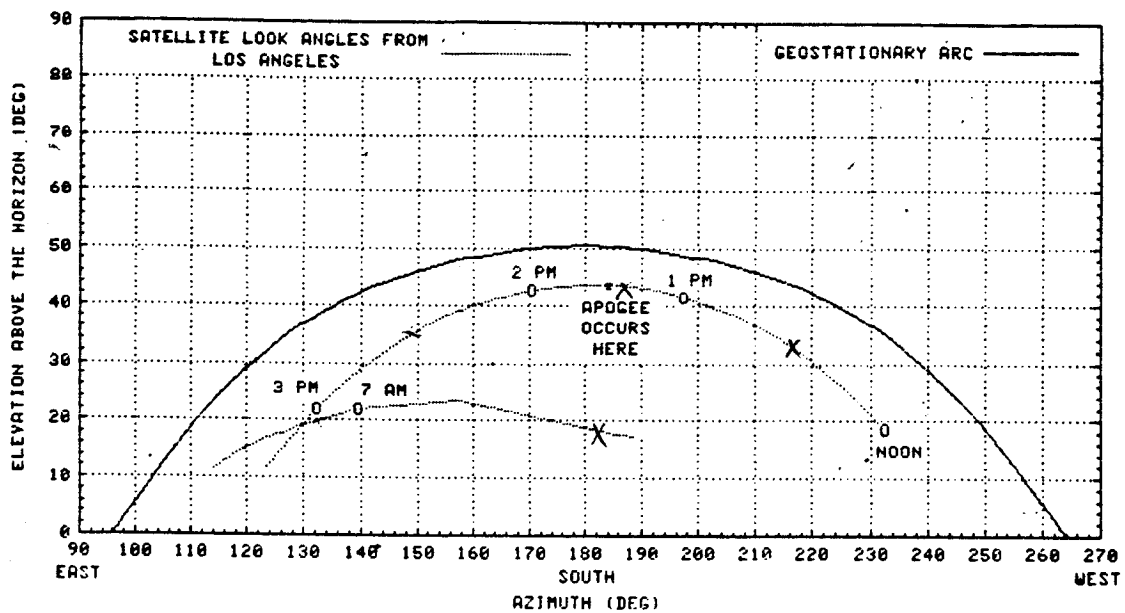


Figure III-26: Apparent Motion of ACE Satellite from Los Angeles

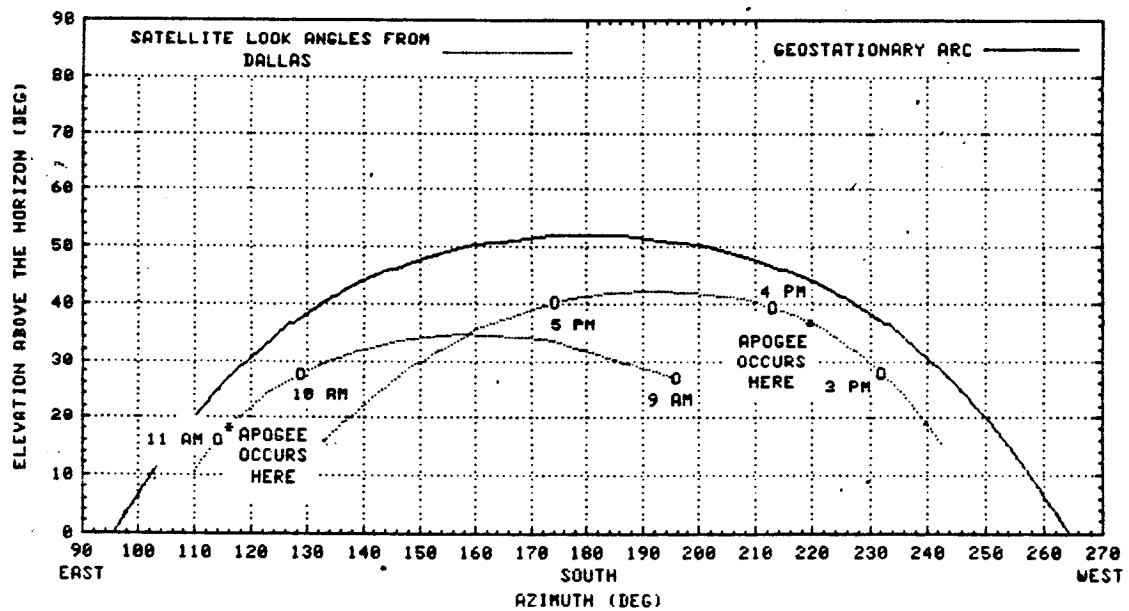


Figure III-27: Apparent Motion of ACE Satellite from Dallas

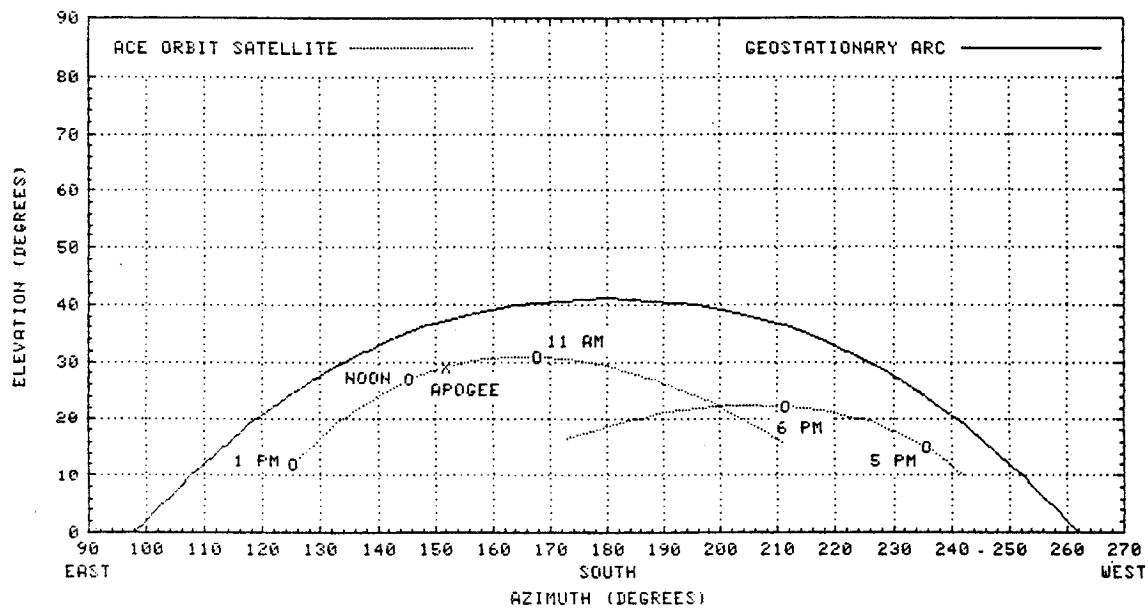


Figure III-28: Apparent Motion of ACE Satellite from Omaha

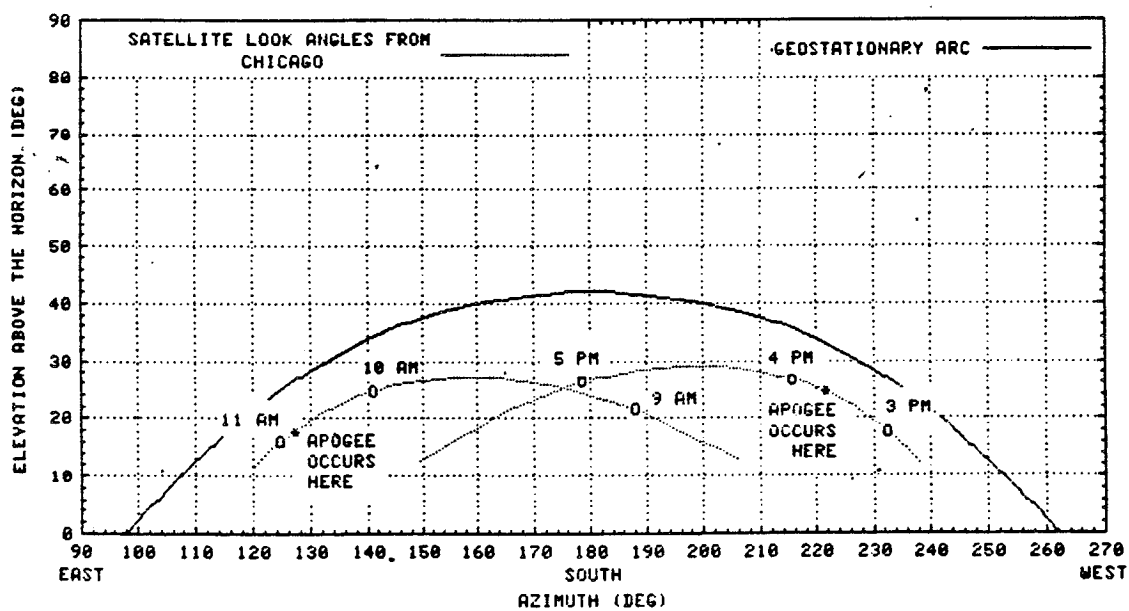


Figure III-29: Apparent Motion of ACE Satellite from Chicago

ORIGINAL PAGE IS
OF POOR QUALITY

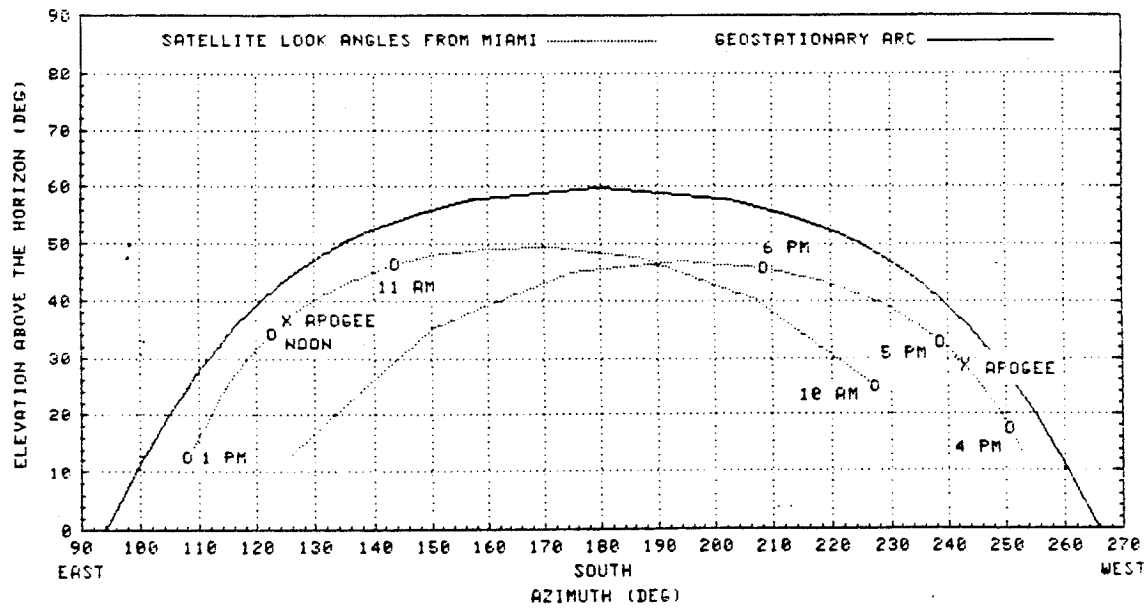


Figure III-30: Apparent Motion of ACE Satellite from Miami

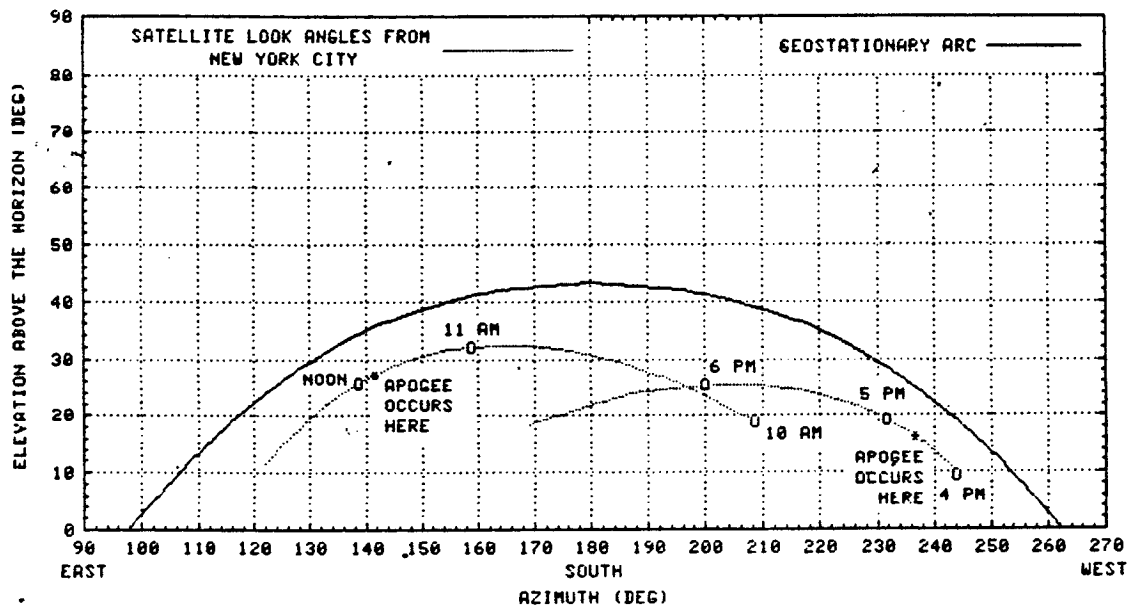


Figure III-31: Apparent Motion of ACE Satellite from New York City

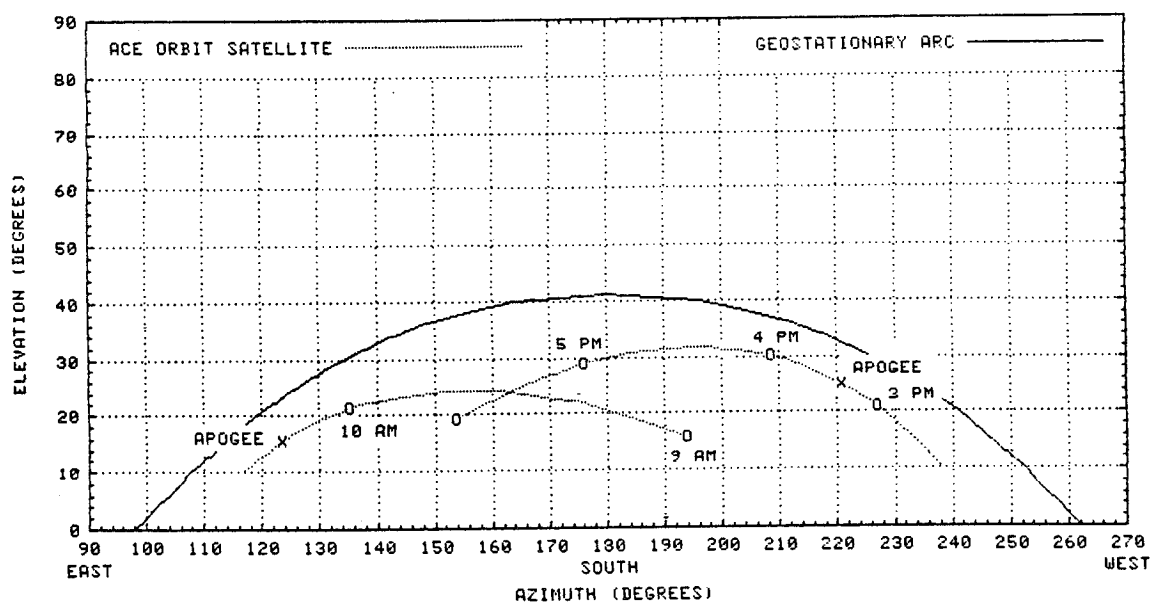


Figure III-32: Apparent Motion of ACE Satellite from Boston

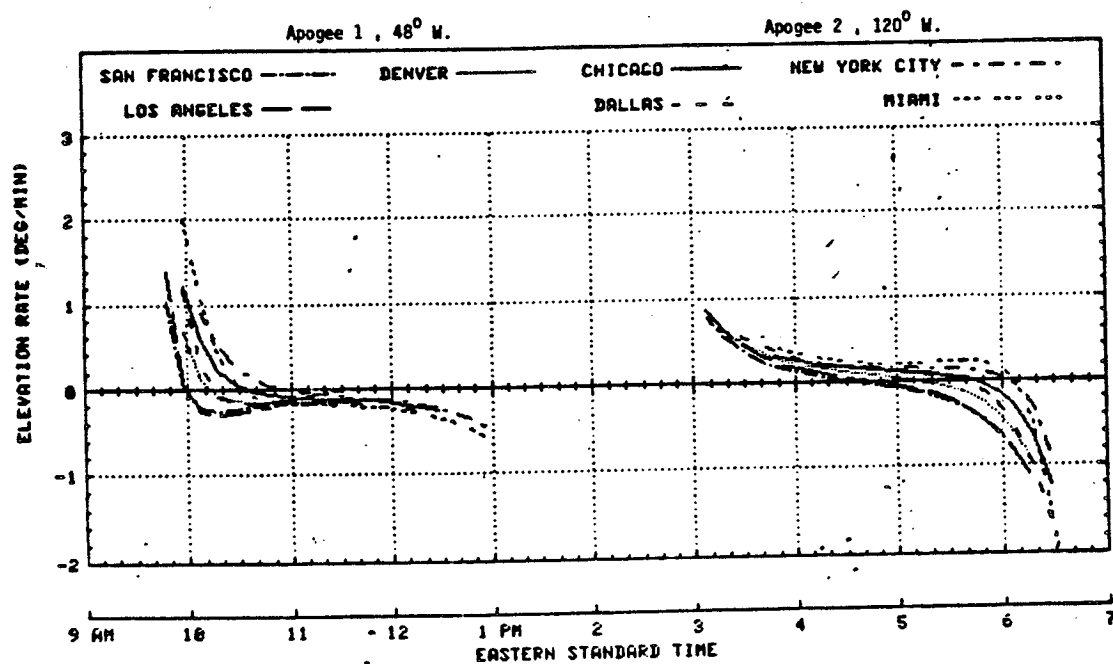


Figure III-33: ACE Satellite Elevation Angle Rate-of-Change with Time

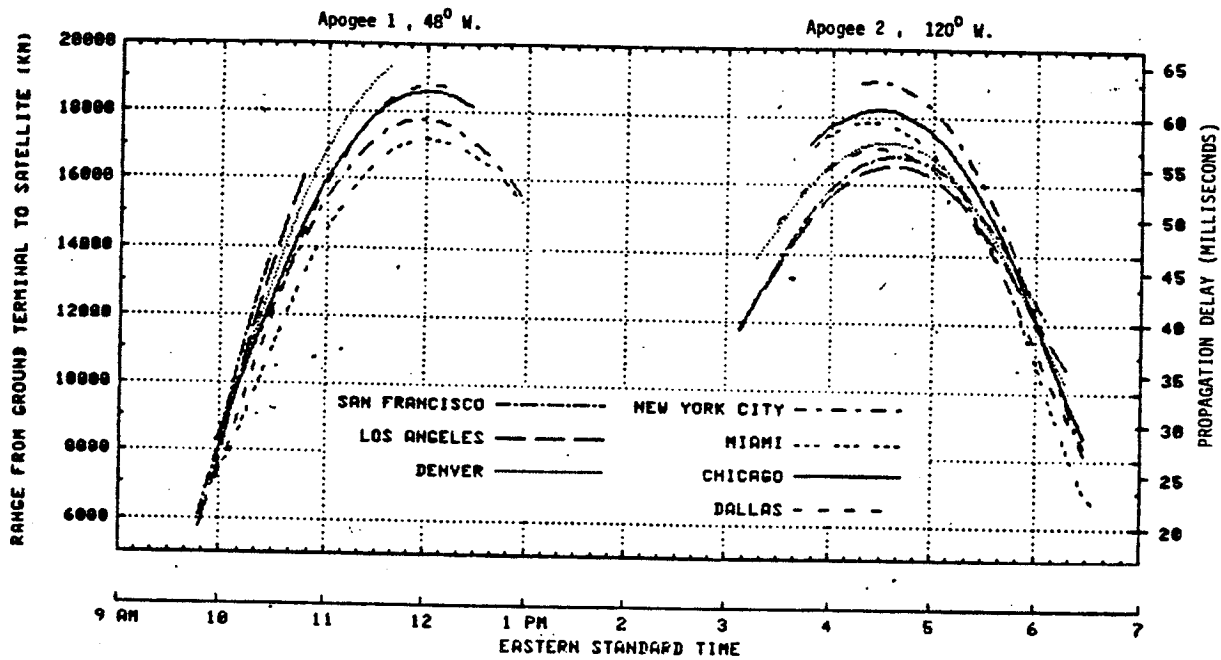


Figure III-34: Variation of Slant Range and Propagation Delay with Time (ACE)

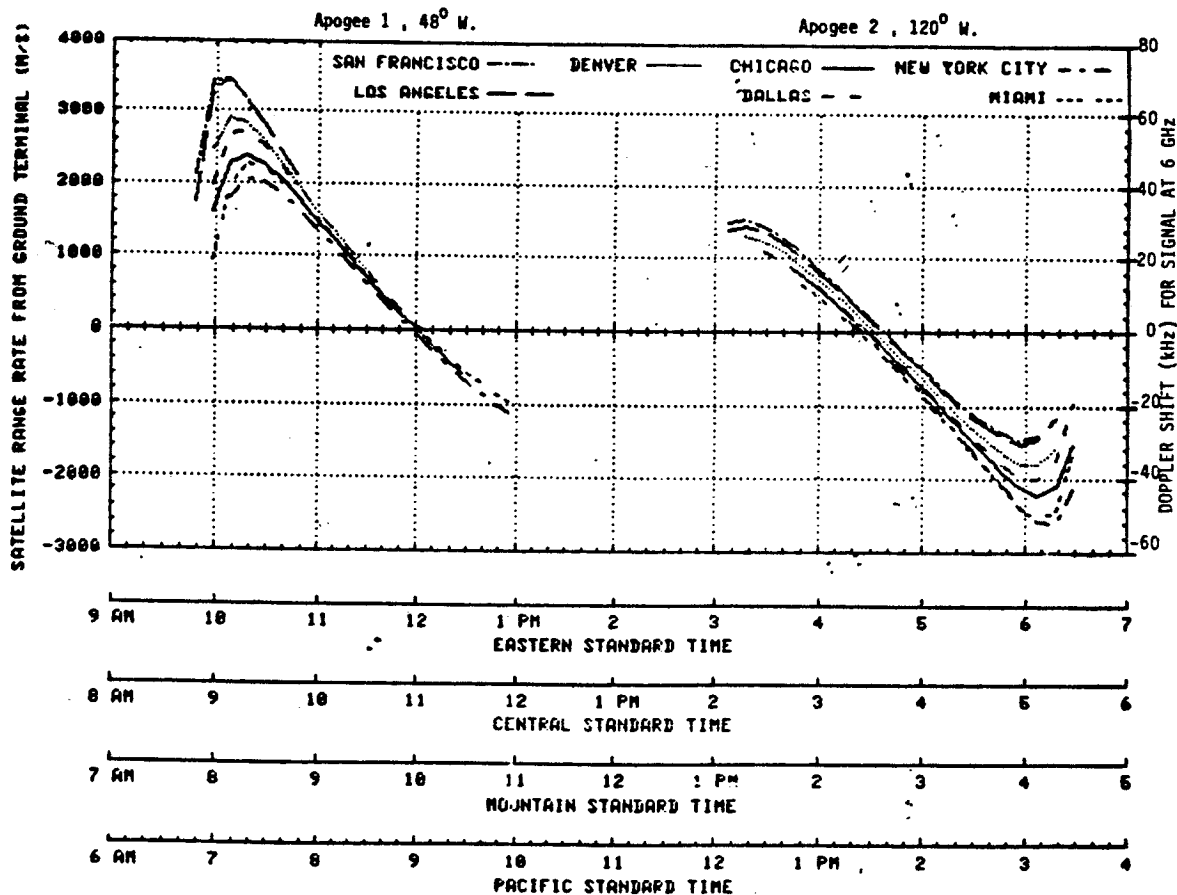


Figure III-35: Range Rate and Doppler Shift of 6 GHz Signals Versus Time (ACE)

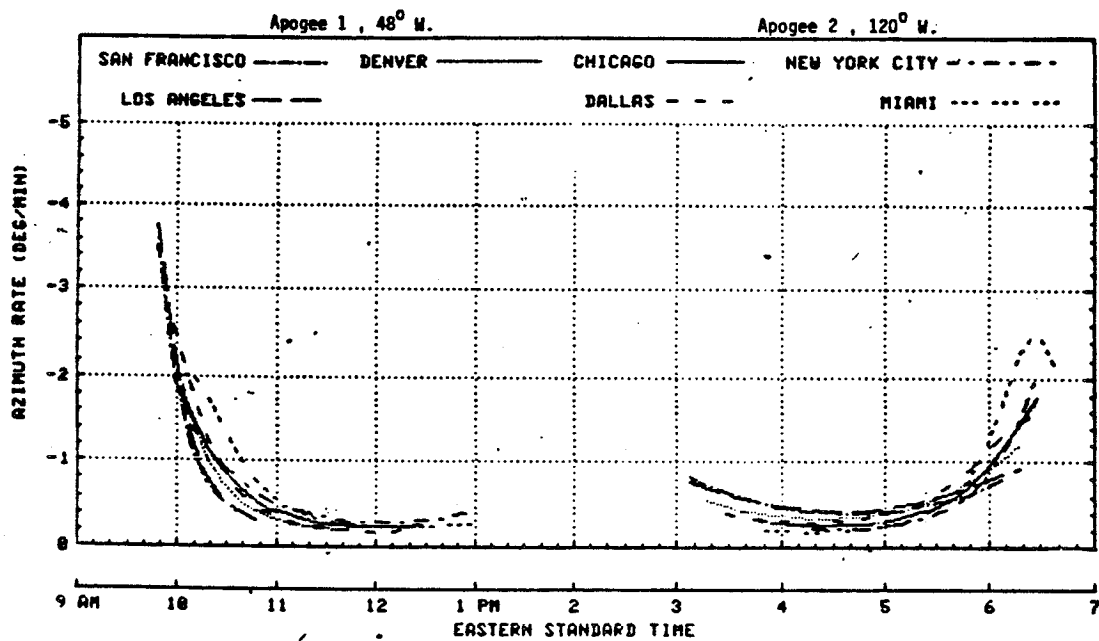


Figure III-36: Azimuth Tracking Rates for ACE Orbit

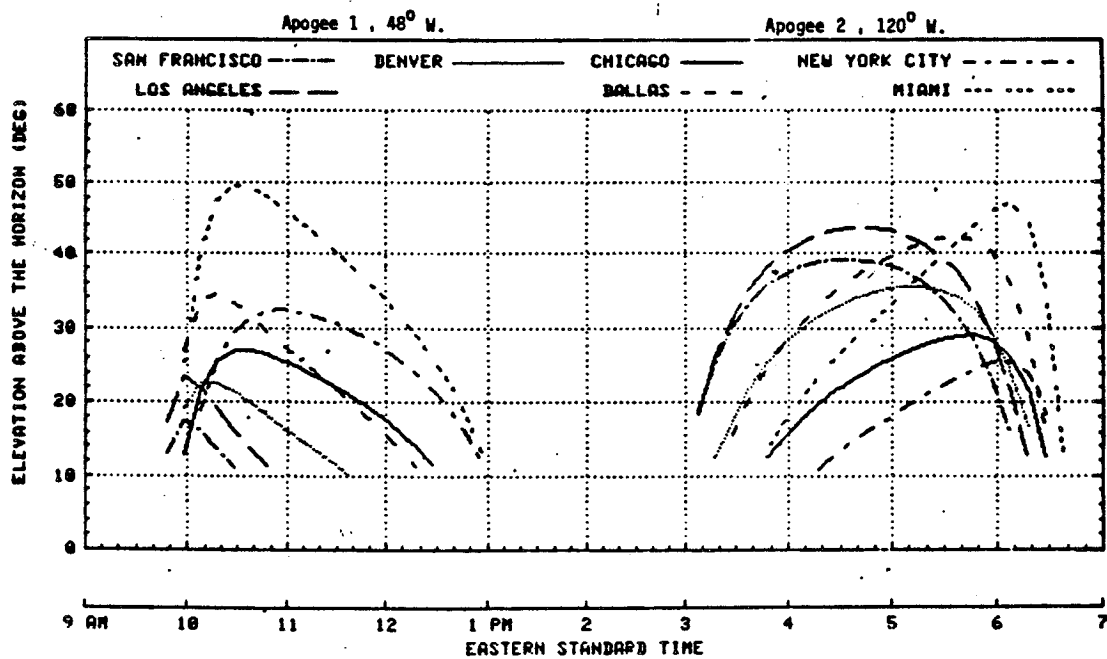


Figure III-37: Elevation Angle Versus Time for ACE Orbit

Figure III-39: ACE Orbit Worldwide Coverage (Eastern Standard Time)

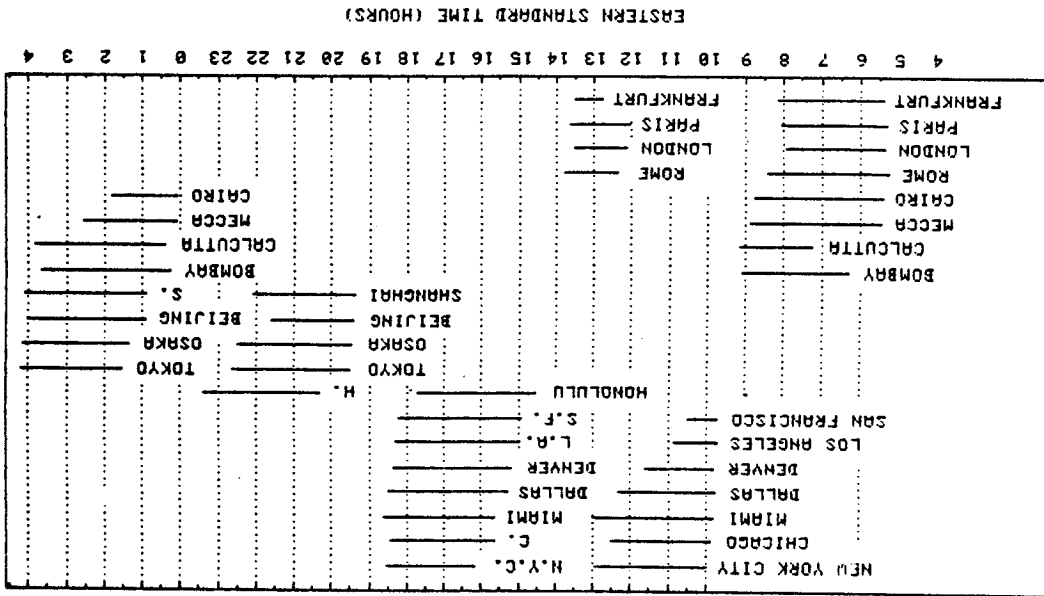
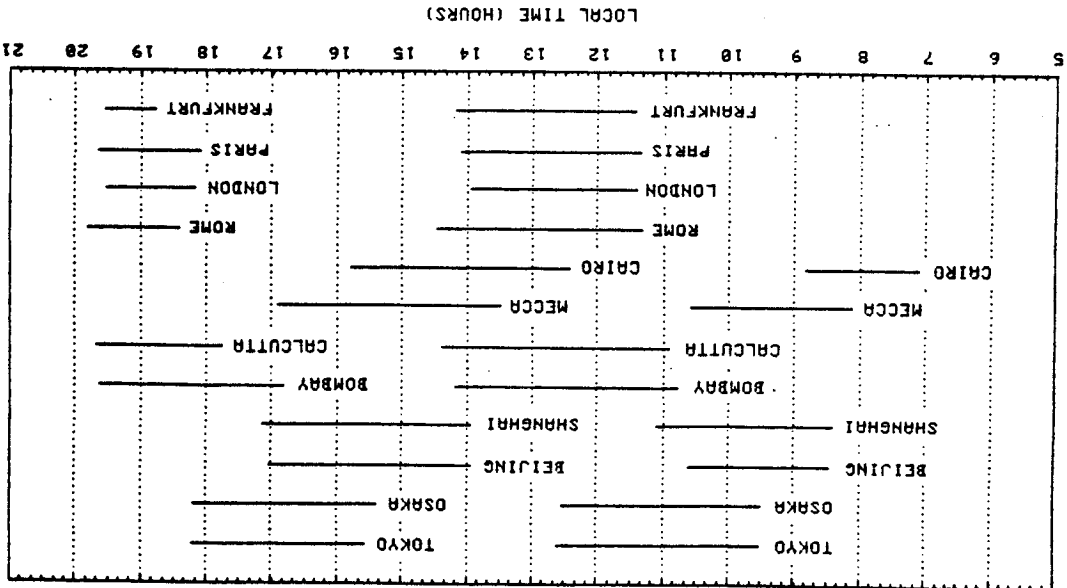


Figure III-38: ACE Orbit Worldwide Coverage (Local Time)



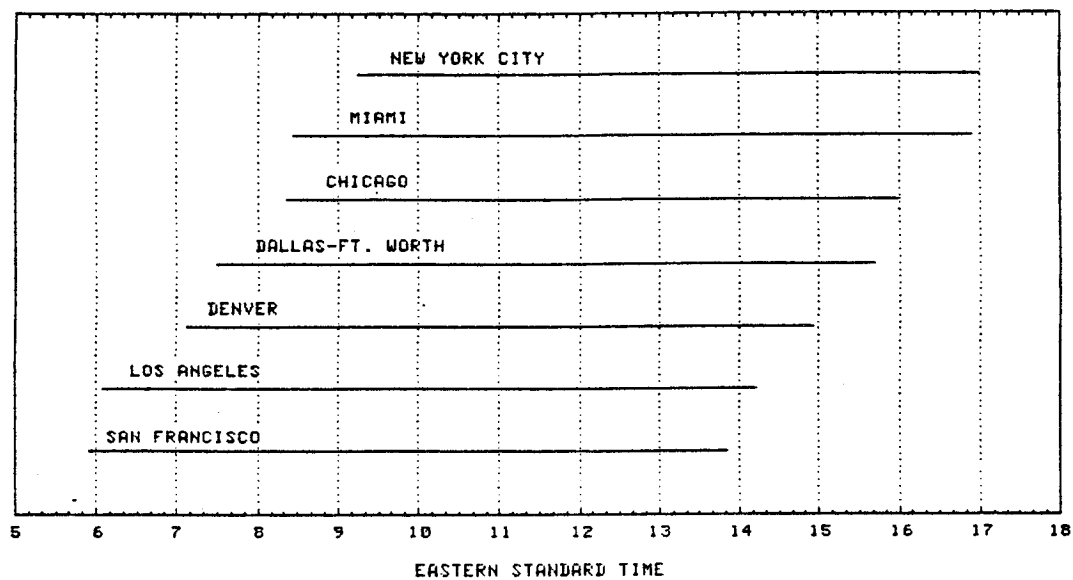


Figure III-40: STET Orbit Coverage Times for Different Cities

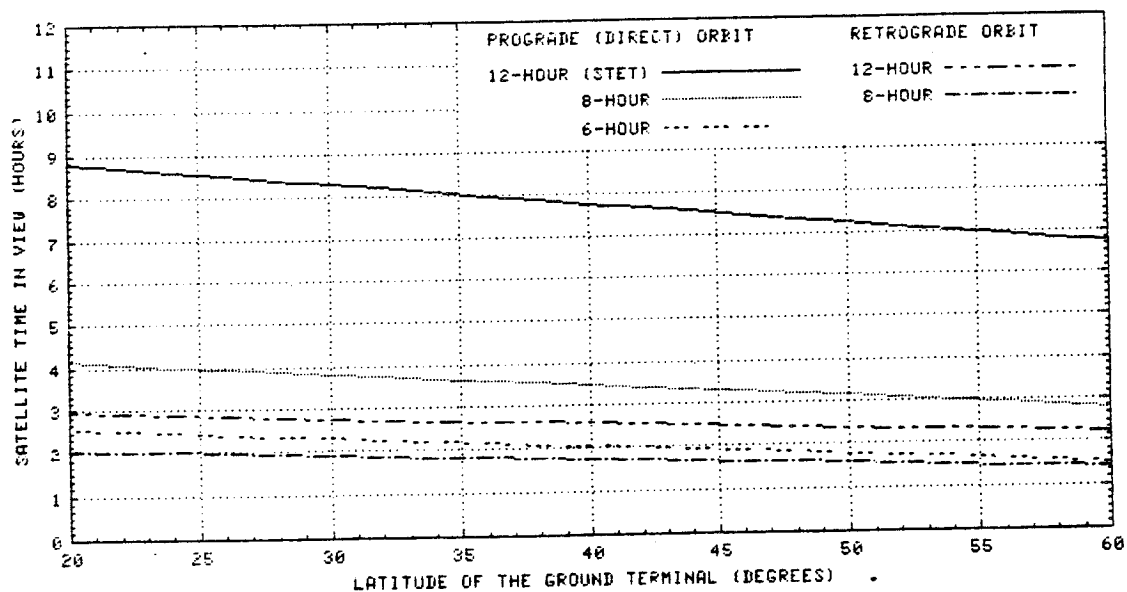


Figure III-41: Coverage Duration Versus Ground Station Location for STET Orbit

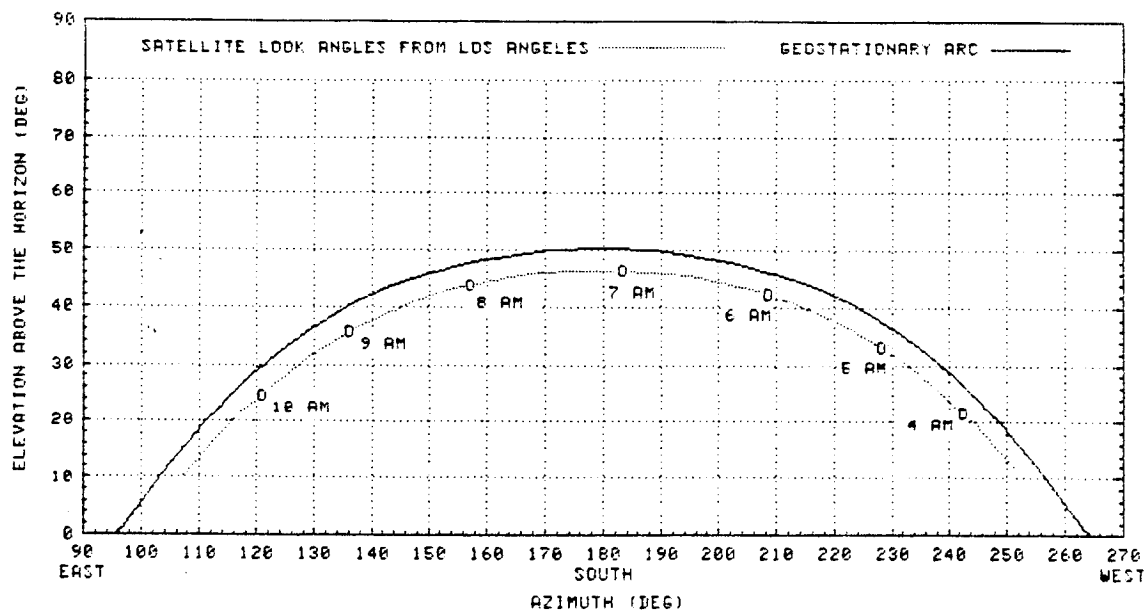


Figure III-42: Apparent Motion of STET Satellite from Los Angeles

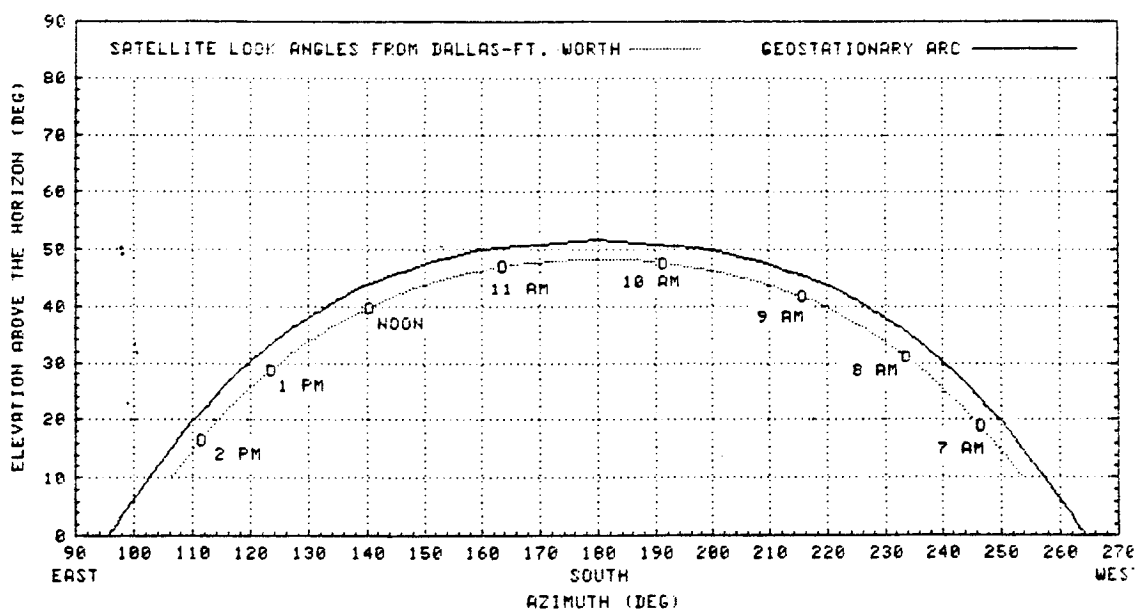


Figure III-43: Apparent Motion of STET Satellite from Dallas

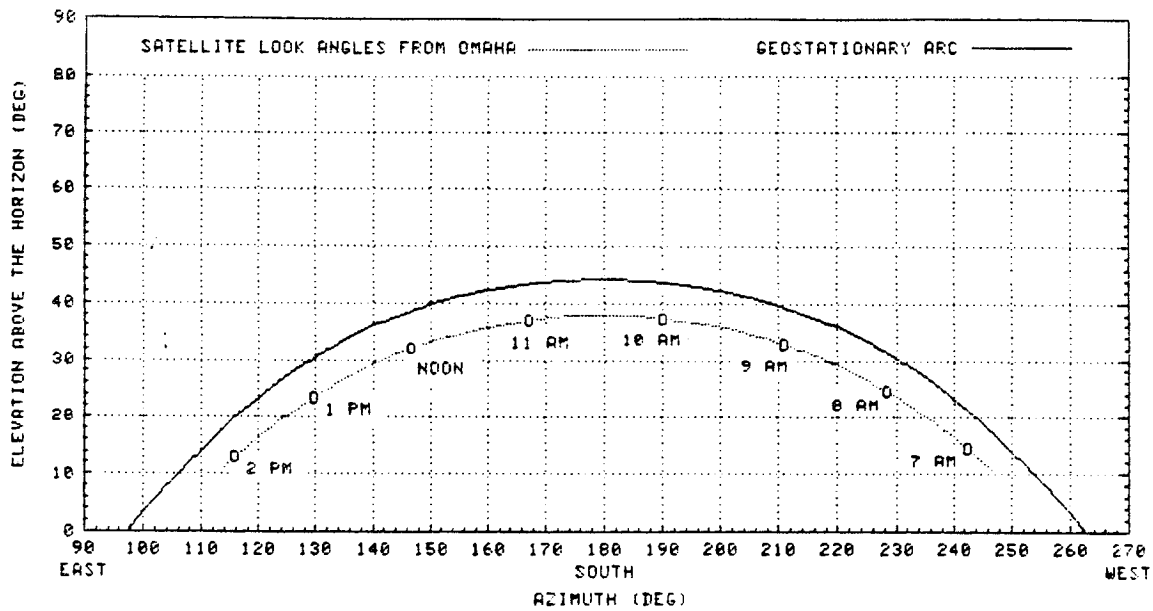


Figure III-44: Apparent Motion of STET Satellite from Omaha

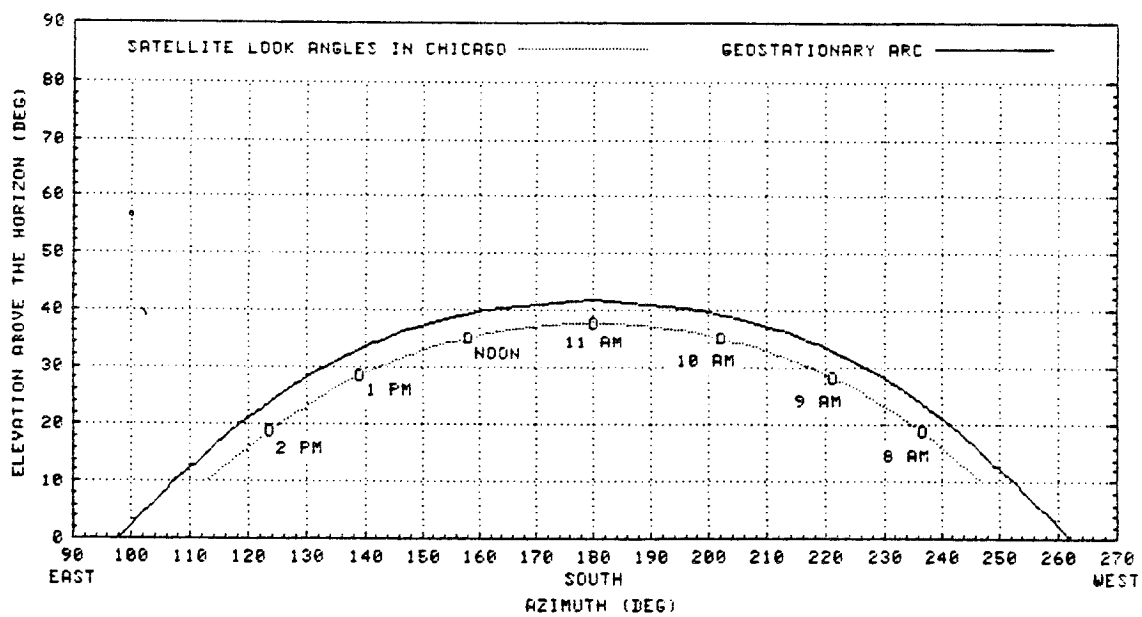


Figure III-45: Apparent Motion of STET Satellite from Chicago

ORIGINAL PAGE IS
OF POOR QUALITY

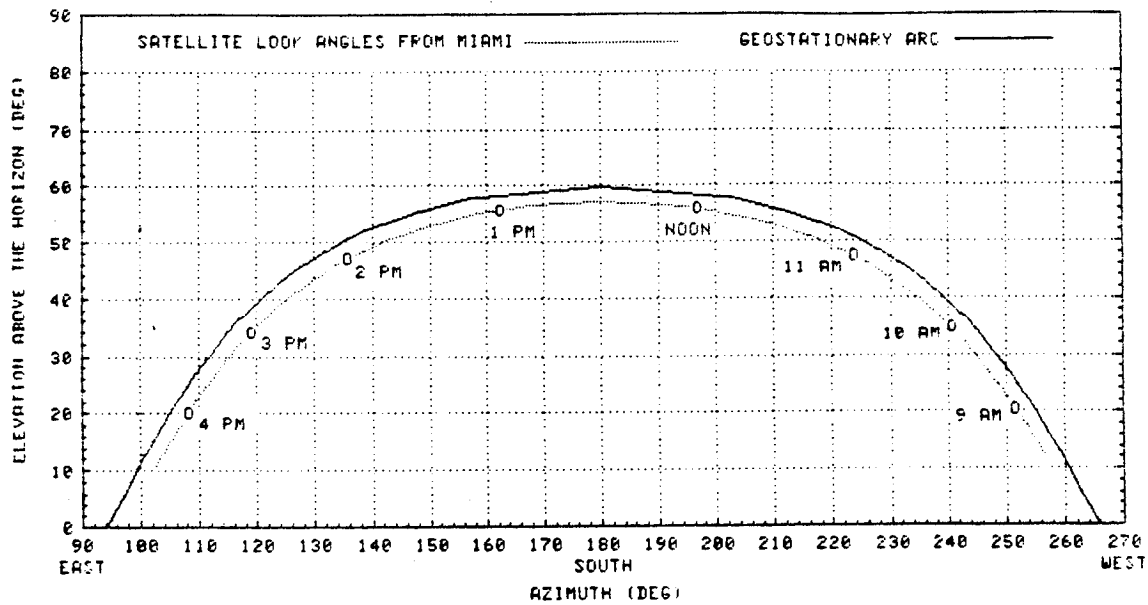


Figure III-46: Apparent Motion of STET Satellite from Miami

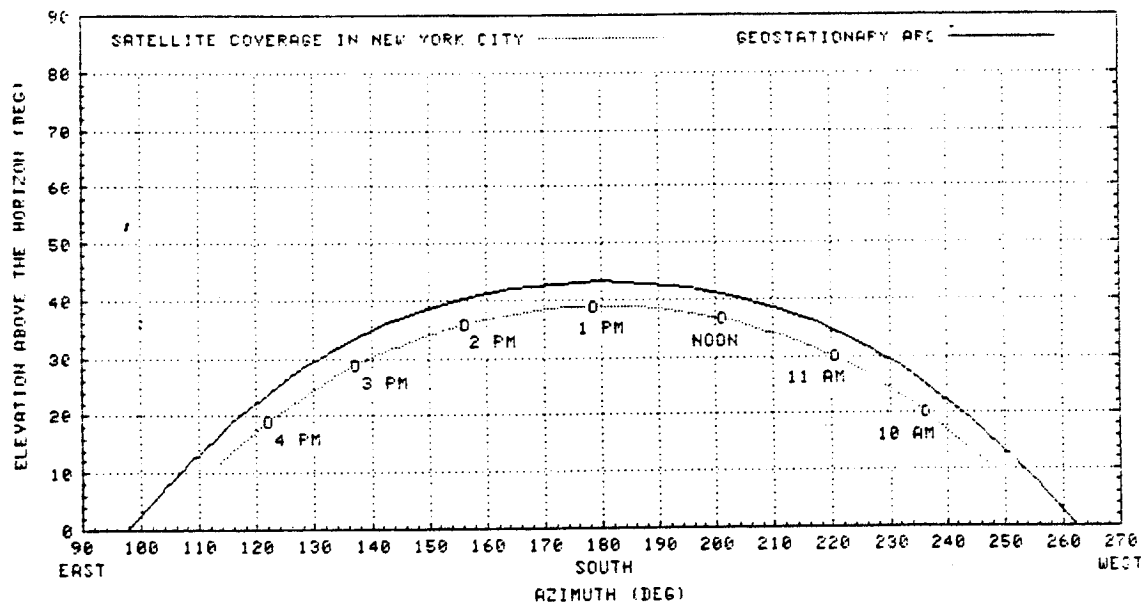


Figure III-47: Apparent Motion of STET Satellite from New York City

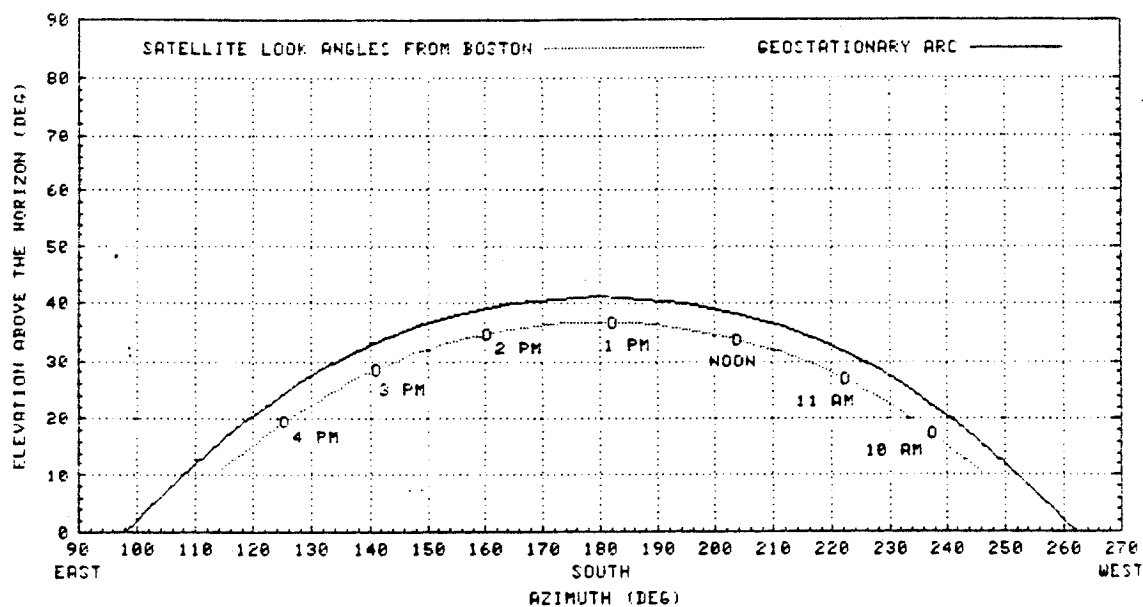


Figure III-48: Apparent Motion of STET Satellite from Boston

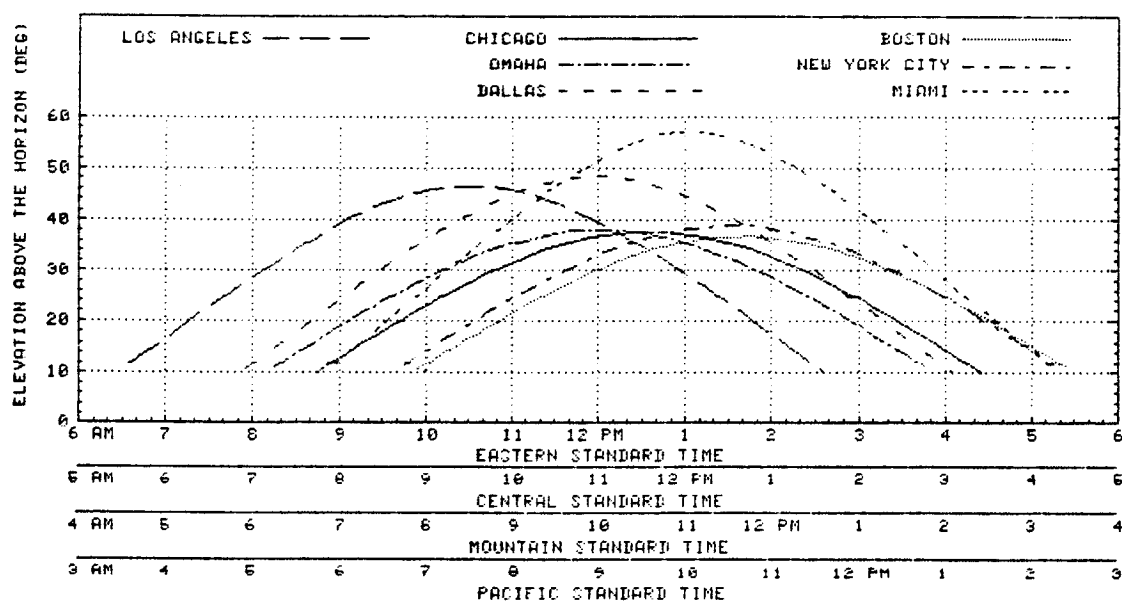


Figure III-49: Elevation Angle Versus Time for STET Orbit Satellite

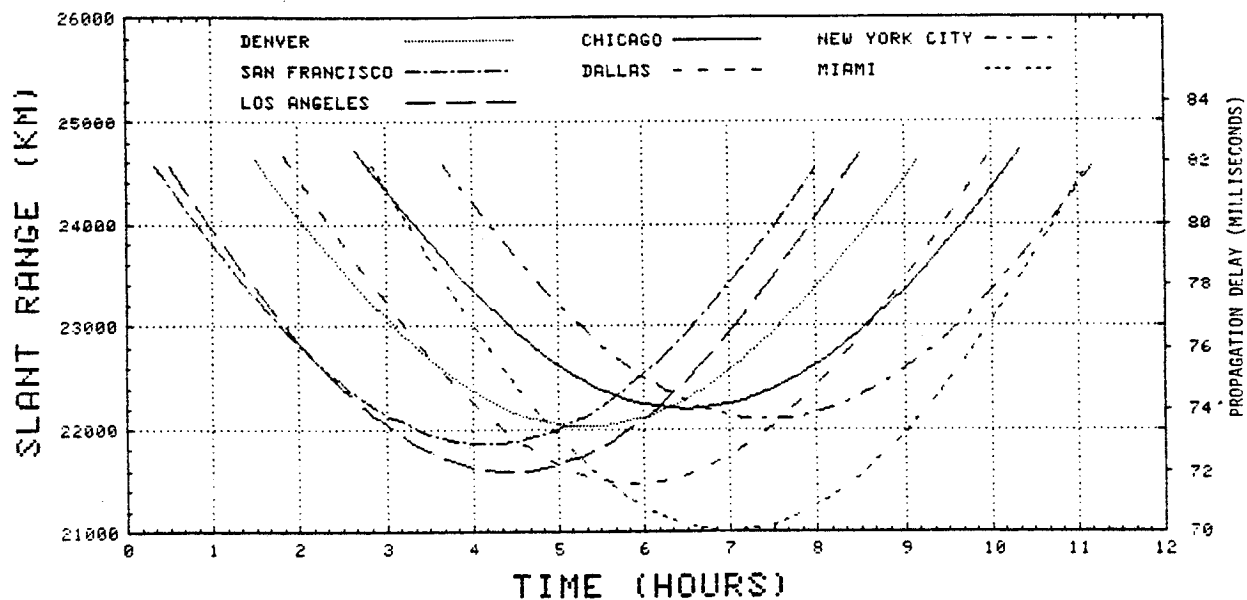


Figure III-50: Variation of Slant Range and Propagation Delay with Time (STET)

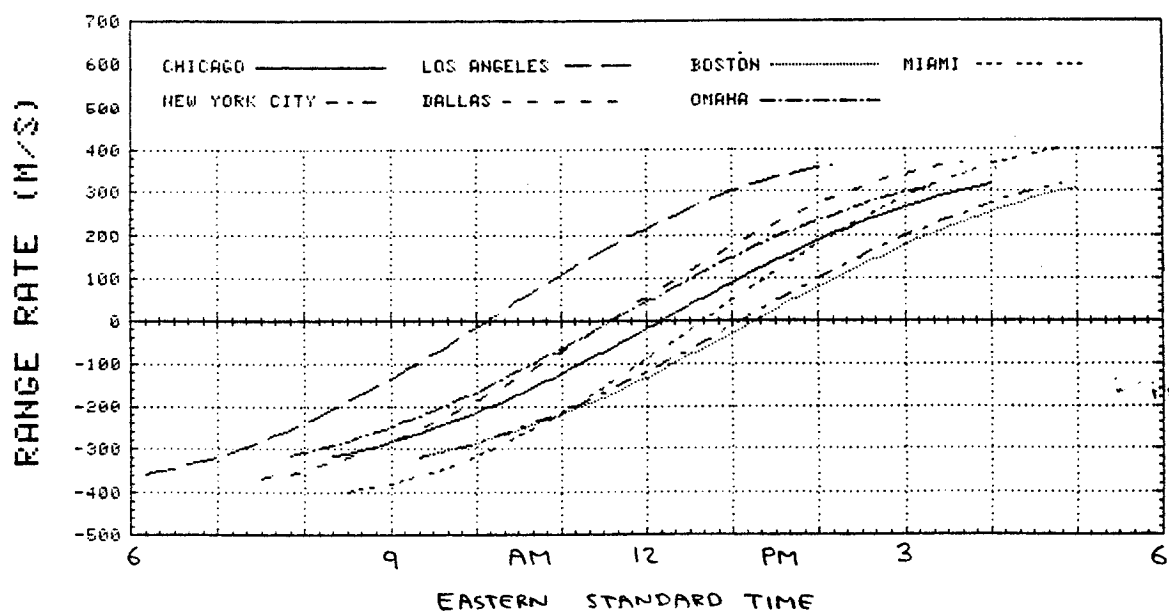


Figure III-51: Range Rate and Doppler Shift of 6 GHz Signals Versus Time (STET)

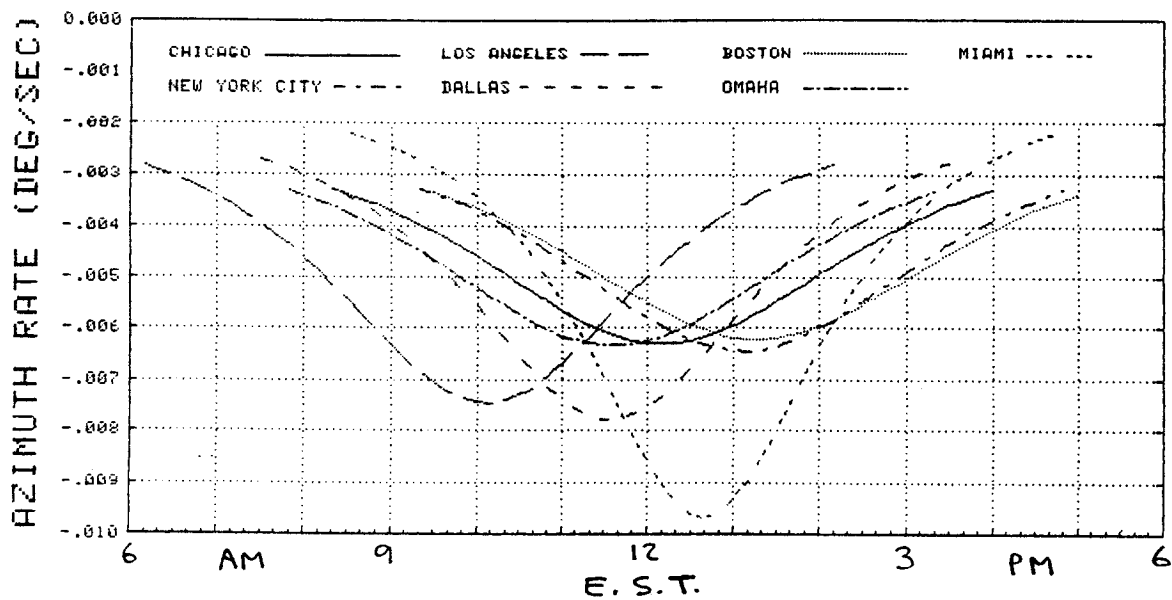


Figure III-52: Azimuth Tracking Rates from Different Ground Stations for STET Satellite

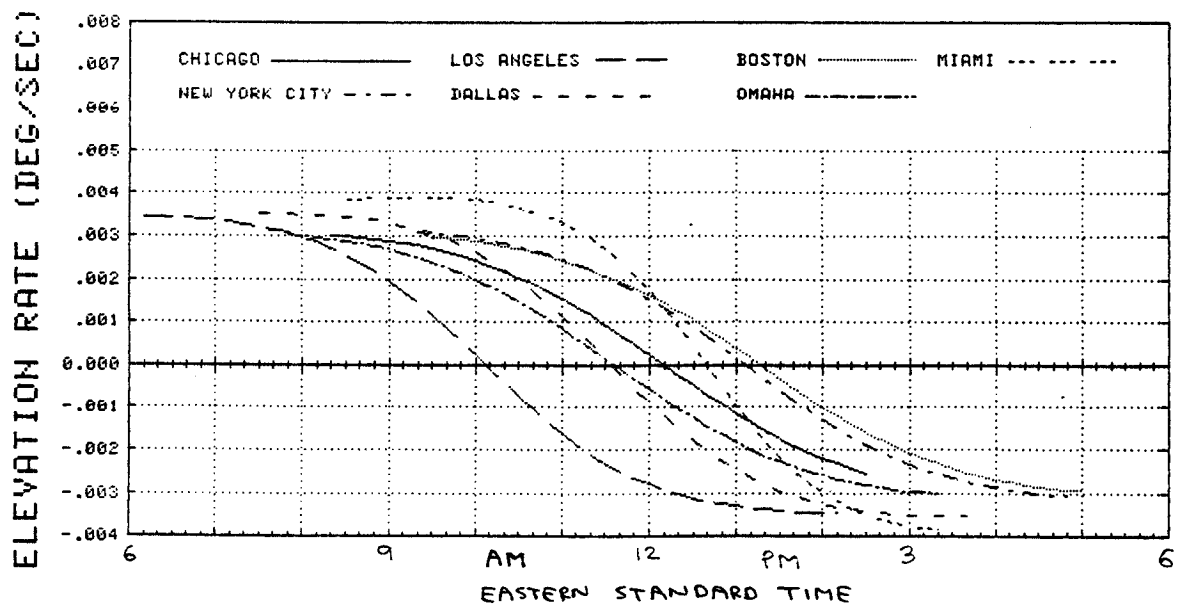


Figure III-53: Elevation Tracking Rates from Different Ground Stations for STET Satellite

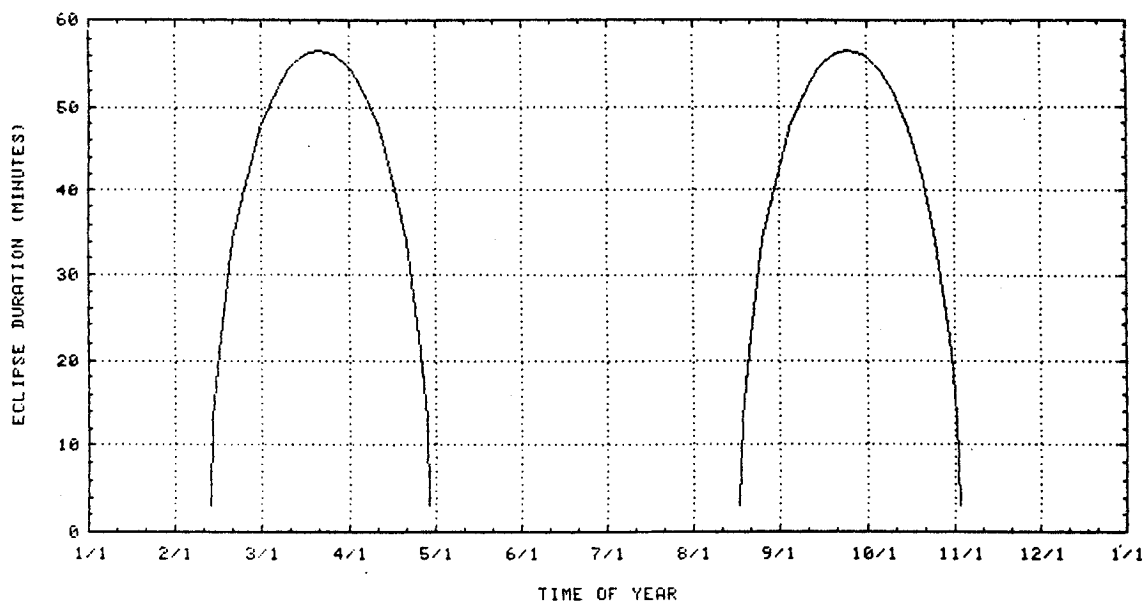


Figure III-54: Eclipse Durations for STET Orbit Satellites

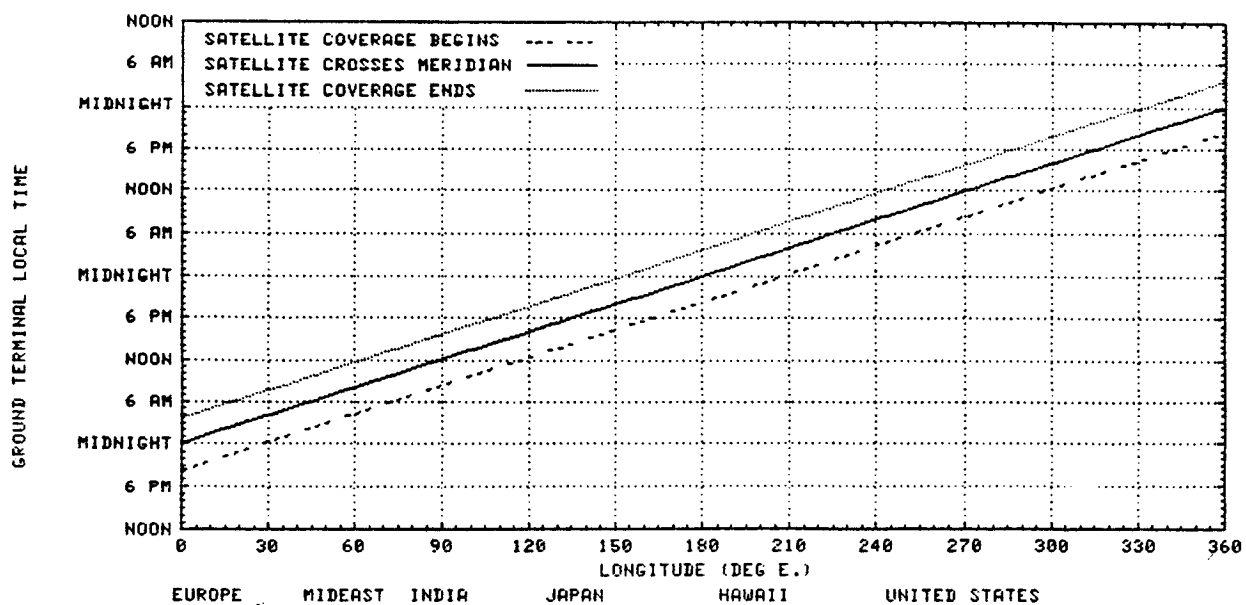


Figure III-55: Worldwide Coverage of STET Satellite from 50° N Latitude

Section IV

DELOADING PEAK TRAFFIC

1 Introduction

The traffic analysis and orbit analysis are now combined to determine how much traffic can be deloaded by non-GEO satellites from GEO satellites. Section II has presented in Figures II-4 and II-5 alternate scenarios for peak traffic versus time-of-day. Section III has identified two promising orbits, the ACE (Subsection III-5.2) and the STET (Subsection III-5.3) for deloading peak traffic. This section considers how much traffic can be deloaded by satellites in these orbits.

2 Magnitude of Traffic Deload

A peak CONUS traffic of 160 Gb/s requires from 1,100 to 5,500 equivalent 36 MHz transponders, depending on the coding and modulation used. Assuming that individual satellites using 1990 technology at C and/or Ku-bands have 36 transponders, this peak traffic will require 30 to 150 such satellites of 5 to 1 Gb/s capacity each.

The ratio of the number of non-GEO to GEO satellites in a closed system will simply equal the amount of traffic deloaded. However, due to differences from GEO satellites, it is likely that an organization such as Intelsat will take the initiative and establish a network of non-GEO only satellites clustered in formation leading and following the sun around the earth.

3 Deloading Methodology

Figures II-4 and II-5 show two small peaks of several hours duration superimposed on the broad daily peak of 8 to 10 hours duration. For purposes of deloading, the alternative capacity must

be available for the entire duration of the deloading.

The non-GEO satellite visibility period must coincide with the peak deloading period. Since the satellite visibility period varies for different ground positions, a further parameter to be considered is the location of the traffic. A satellite can pass traffic between two points only while visible from both points.

4 STET Orbit Deloading

The STET orbit is a 12 hour circular equatorial plane orbit and is described in Subsection III-5.3.

4.1 Intra-Zone Traffic

The greatest single segment (25%) of CONUS satellite addressable traffic falls in the Eastern Time Zone with the Central Time Zone having 9% (Table II-2).

4.1.1 Eastern Zone

A satellite in the STET orbit is visible for a period of 7 h 40 min from New York and 8 h 30 min from Miami, and 7 h 30 min from the entire Eastern Time Zone. A satellite could be positioned to provide coverage from 0915 to 1645 ET (Eastern Time), and deload 10 Gb/s in the morning and 6 Gb/s in the afternoon. Figure IV-1 illustrates the deloading of intra-zone traffic by a satellite in the STET orbit.

4.1.2 Central Zone

The same satellite is visible in the Central Time Zone about 50 minutes earlier from 0830 to 1600 ET. The period of visibility is 7 h 30 min

and does not allow deloading of the afternoon peak busy hour, as shown in Figure IV-1.

The maximum traffic the satellite can deload is the difference of peak traffic between the morning and afternoon, or 1.2 Gb/s (Table II-6).

4.2 Inter-Zone Traffic

Table II-2 shows that 18% of the peak traffic is between the Eastern and Central Time Zone. A STET orbit satellite is visible to both Eastern and Central Zones for a period of 6 h 30 min, or from 0915 to 1545 ET. This visibility is insufficient to cover the afternoon peak period of inter-zone traffic.

Figures IV-3 and IV-4 show the optimum deloading possible for the two traffic cases. Maximum deloading capacity is equal to the difference of peak traffic between morning and afternoon peaks (Tables II-5 and II-10 for the two traffic cases), and is equal to 13.8 Gb/s and 9.6 Gb/s respectively.

5 ACE Orbit Deloading

The ACE orbit is a highly eccentric orbit with five revolutions per day. It is described in Subsection III-5.2.

5.1 Intra-Zone Traffic

The ACE orbit with apogees at 60°W and 132°W is chosen.

5.1.1 Eastern Zone

The satellite in ACE orbit is visible to New York for a period of 3 h 40 min followed by an interruption of 3 h 40 min and is visible again for 1 h 37 min. Visibility from Miami is better; 3 h 15 min visibility, 2 h 50 min interruption, and 2 h 26 min visibility.

Assuming the visibility for the Eastern Time Zone is the same as for New York, the deloading capability of the ACE satellite is shown in Figure IV-2. The deload capacity is 14 Gb/s for the morning peak and 12 Gb/s for the afternoon peak.

Traffic	STET		ACE	
	Case 1	Case 2	Case 1	Case 2
E Intra	10.0	10.0	14.0	14.0
C Intra	1.2	1.2	1.0	1.0
E-C Inter	13.8	9.6	10.8	10.8
Total	25.0	20.8	25.8	25.8

Table IV-1: Deloading Capacity (Gb/s)

5.1.2 Central Zone

The satellite in ACE orbit is visible to Chicago at the same time New York time with a cycle of 2 h 50 min visibility, 3 h 15 min interruption, and 2 h 26 min visibility.

This visibility covers the morning and afternoon traffic periods as shown in Figure IV-2. Afternoon coverage, however, does not match the afternoon peak period and deloading capacity is only around 1 Gb/s.

5.2 Inter-Zone Traffic

A satellite in ACE orbit is visible to both Eastern and Central Time Zones from 0830 to 1130 and then again from 1530 to 1710 ET.

Figure IV-5 shows the deload possible for Case 1 traffic. Although the afternoon visibility is sufficient to cover the afternoon peak traffic, the visibility is useless due to the restriction in morning visibility. Deloading capacity is restricted to 10.8 Gb/s.

Figure IV-6 shows the deload possible for Case 2 traffic. The deload capacity is similar to Case 1 traffic.

6 Analysis of Deloading

6.1 Summary of Deloading by Single Satellite

The deloading capacity of a single (or multiple satellites at approximately the same orbital locations) is summarized for the STET and ACE orbits in Table IV-1.

The deloading capacity of satellites in STET and ACE orbits are the same for the Case 1 traf-

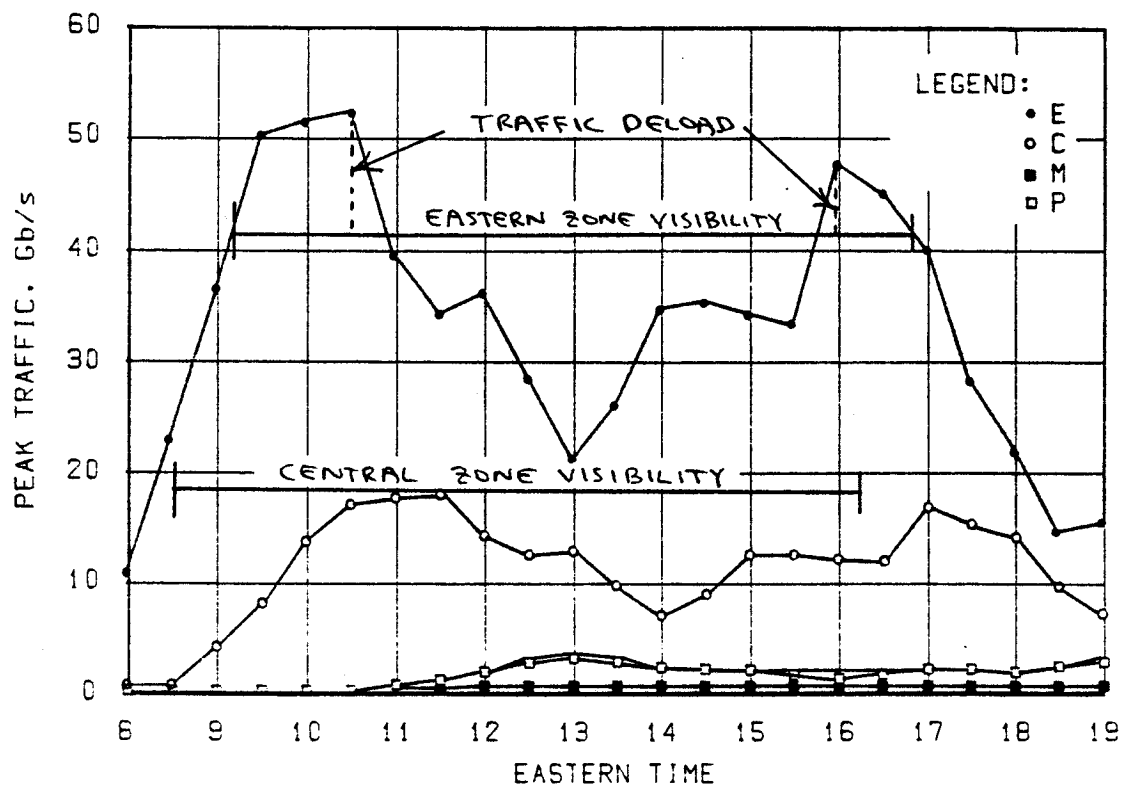


Figure IV-1: Deloading of Intra-Zone Traffic by STET Orbit Satellite

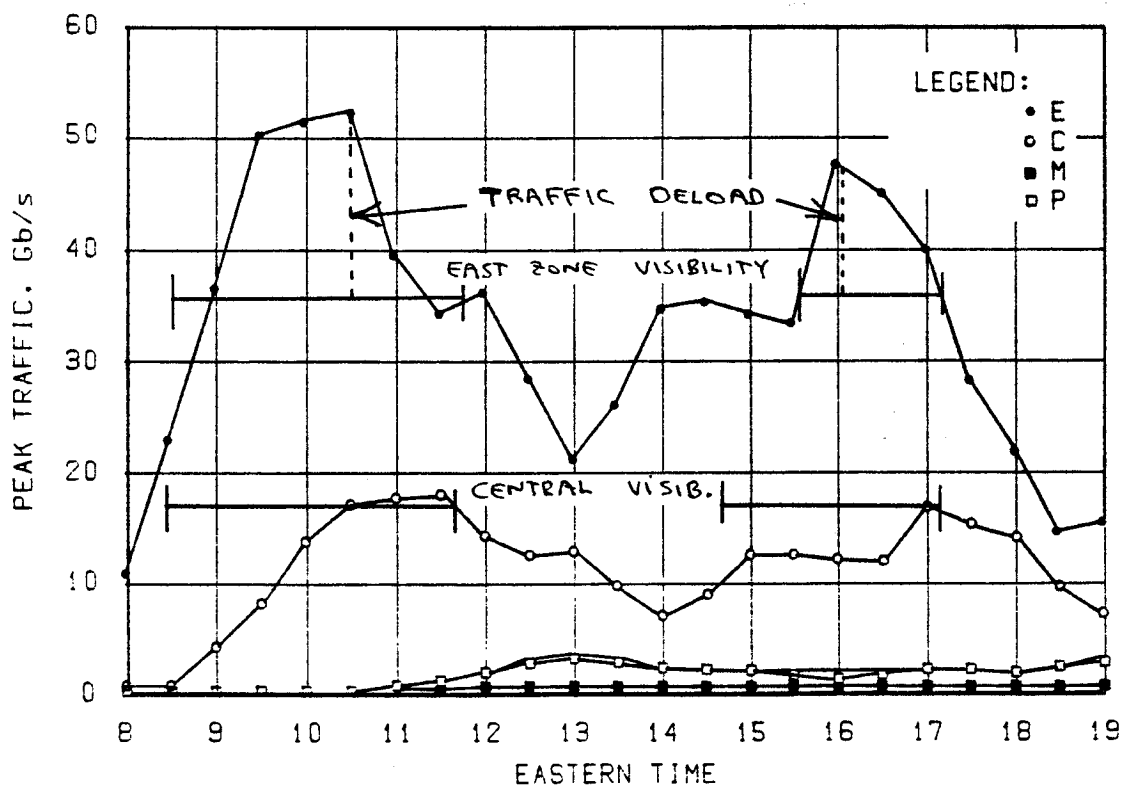


Figure IV-2: Deloading of Intra-Zone Traffic by ACE Orbit Satellite

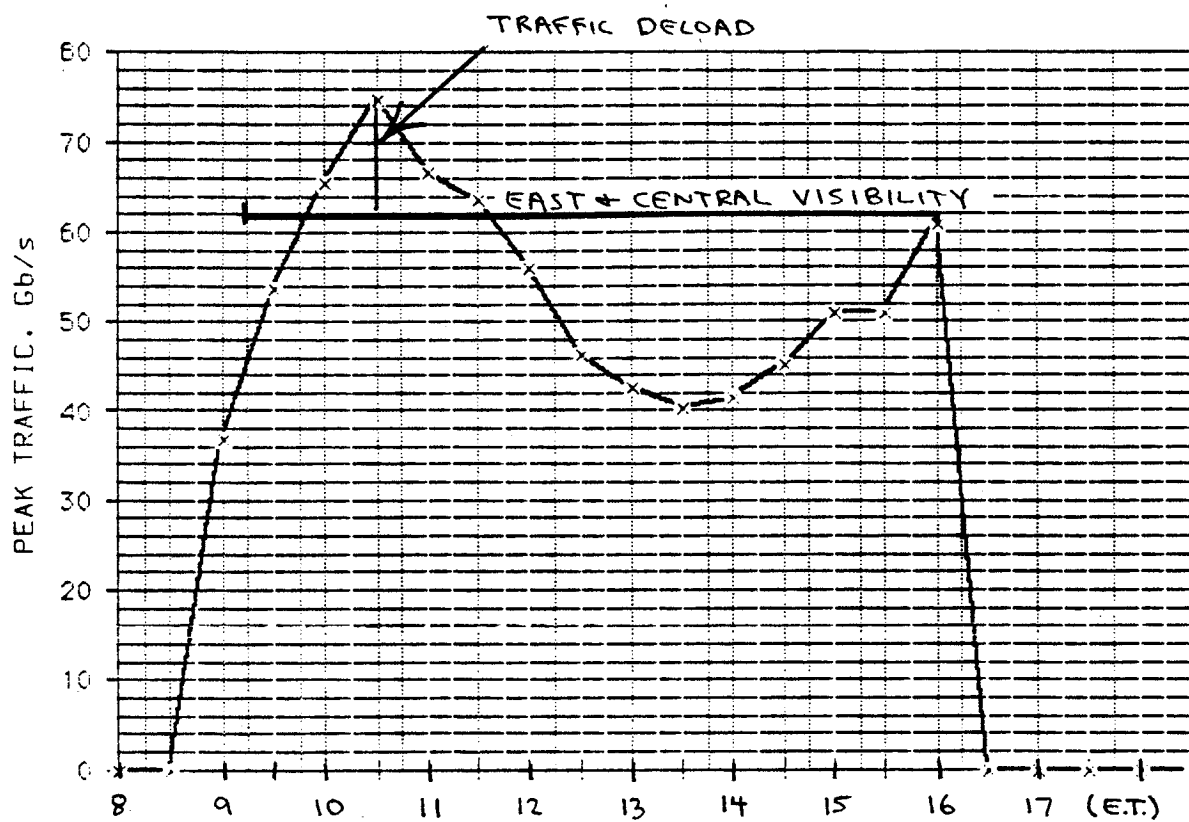


Figure IV-3: Deloading of E↔C Inter-Zone Traffic by STET Orbit Satellite, Case 1

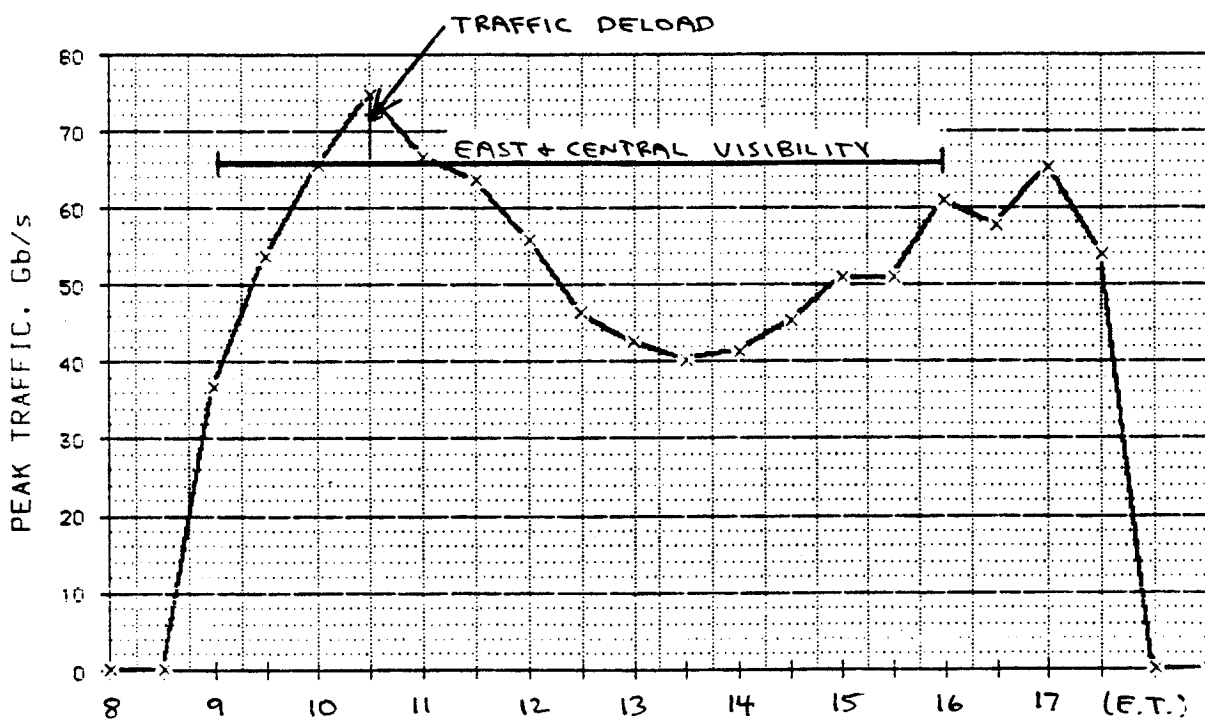


Figure IV-4: Deloading of E↔C Inter-Zone Traffic by STET Orbit Satellite, Case 2

ORIGINAL PAGE IS
OF POOR QUALITY

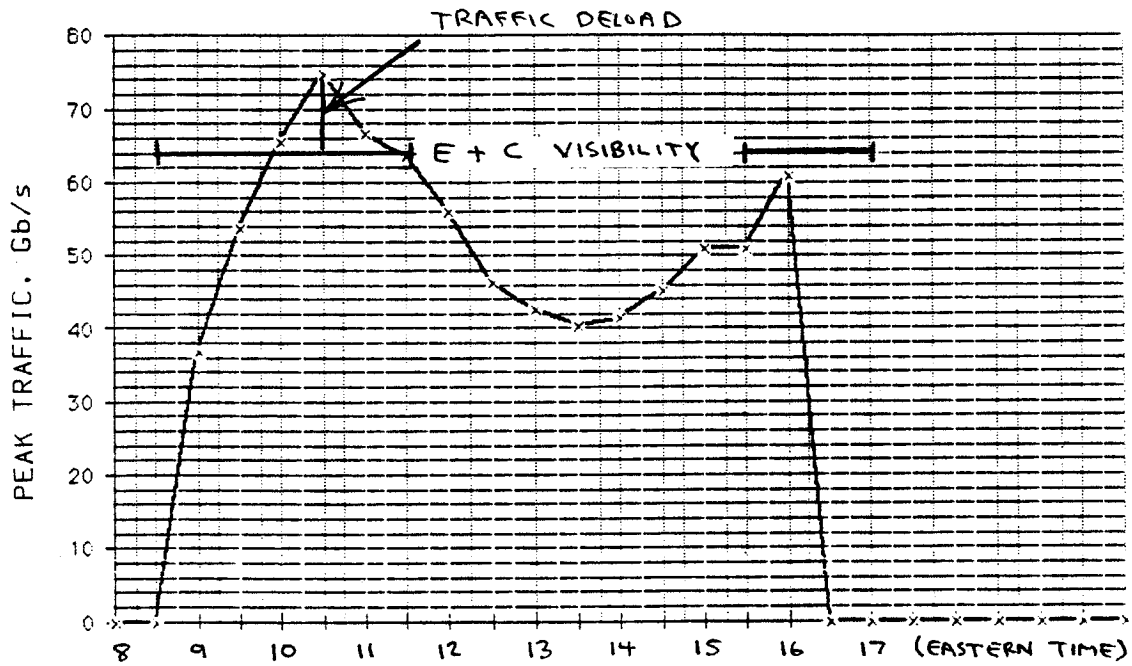


Figure IV-5: Deloading of E↔C Inter-Zone Traffic by ACE Orbit Satellite, Case 1

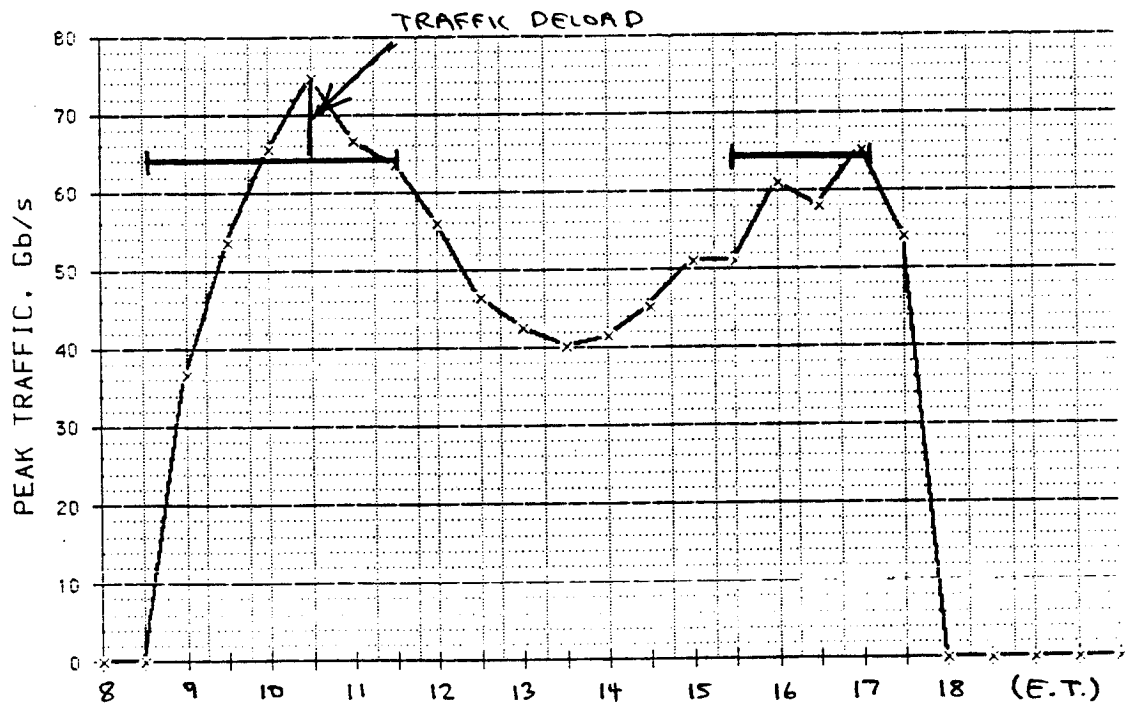


Figure IV-6: Deloading of E↔C Inter-Zone Traffic by ACE Orbit Satellite, Case 2

fic, but STET is slightly worse for the Case 2 traffic. Total deloading is around 10% to 12% of the peak capacity of 208.5 Gb/s (Table II-1), and 13% to 16% of the time-engineered peak of 161 Gb/s (Subsection II-4.3).

6.2 Visibility Constraints

Deloading with a single non-GEO satellite is severely constrained by the visibility coverage that the single satellite provides for different time zones. Both STET and ACE orbits do not provide enough continuous coverage (i.e. 10 to 12 hours) over the entire CONUS to arbitrarily deload any desired amount of traffic.

The visibility constraint is further illustrated by looking at the next most significant traffic, the inter-zone traffic from E-P and from C-P. Figure IV-7 illustrates the situation for Case 1 traffic. Since Pacific Time is 3 hours behind Eastern Time, the STET coverage of the Pacific Zone is early, from 0520 to 1315. The corresponding ACE coverages are from 0815 to 1000 and from 1335 to 1700. As seen from Figure IV-7, STET covers only part of the morning peak with very little deloading, and no traffic can be deloaded by the ACE satellite.

6.3 Traffic Routing Constraints

When traffic deloading is restricted to certain time zones, constraints are placed on the routing of traffic. For the case of deloading only intra-zone Eastern and Central traffic, and E-C inter-zone traffic, the following routing conditions should be met:

- A special trunk group should be established by the Common Carrier (such as ATT or MCI) for deloading to the non-GEO satellite.
- Only calls originating from the Eastern or Central Time Zones and terminated to the Eastern or Central Time Zones can be routed for deloading to this special trunk group.
- Traffic can be deloaded only during the satellite visibility period relative to this traffic.

This routing is selected by origination, destination, and time-of-day. Although modern stored program control switching machines can be programmed for such routing, its implementation on a large scale may pose problems for Common Carriers.

7 Multiple Non-GEO Satellites

7.1 Introduction

The next solution for obtaining greater deloading capacity is a system of several non-GEO satellites queuing in time so that the coverage time can be extended. This solution is potentially less attractive than a single long-coverage satellite in that two or more non-GEO satellites are required to do the work of one GEO satellite.

7.2 Methodology

The total CONUS traffic has been given in Table II-7 and Figure II-4 for Case 1 and Table II-9 and Figure II-5 for the Case 2 traffic scenario.

The methodology applicable to total CONUS is to engineer for total CONUS coverage. With CONUS coverage, no complex routing is required. It suffices that separate trunk groups for deloading traffic to the satellite be established. Extra traffic to be deloaded will automatically be routed to such trunk groups irrespective of origination, destination, and time-of-day.

7.3 Multiple STET Satellites

The visibility period for a STET satellite covering all of CONUS (i.e. seen simultaneously from San Francisco to New York) is about 4 h 40 min. Coverage of CONUS traffic by two STET satellites queuing with a little overlap is shown in Figure IV-8 for Case 1 and Figure IV-9 for the Case 2 traffic scenario. For Case 1, the deloading level is 91 Gb/s, while for Case 2 the maximum deloading capacity is 72 Gb/s.

ORIGINAL PAGE IS
OF POOR QUALITY

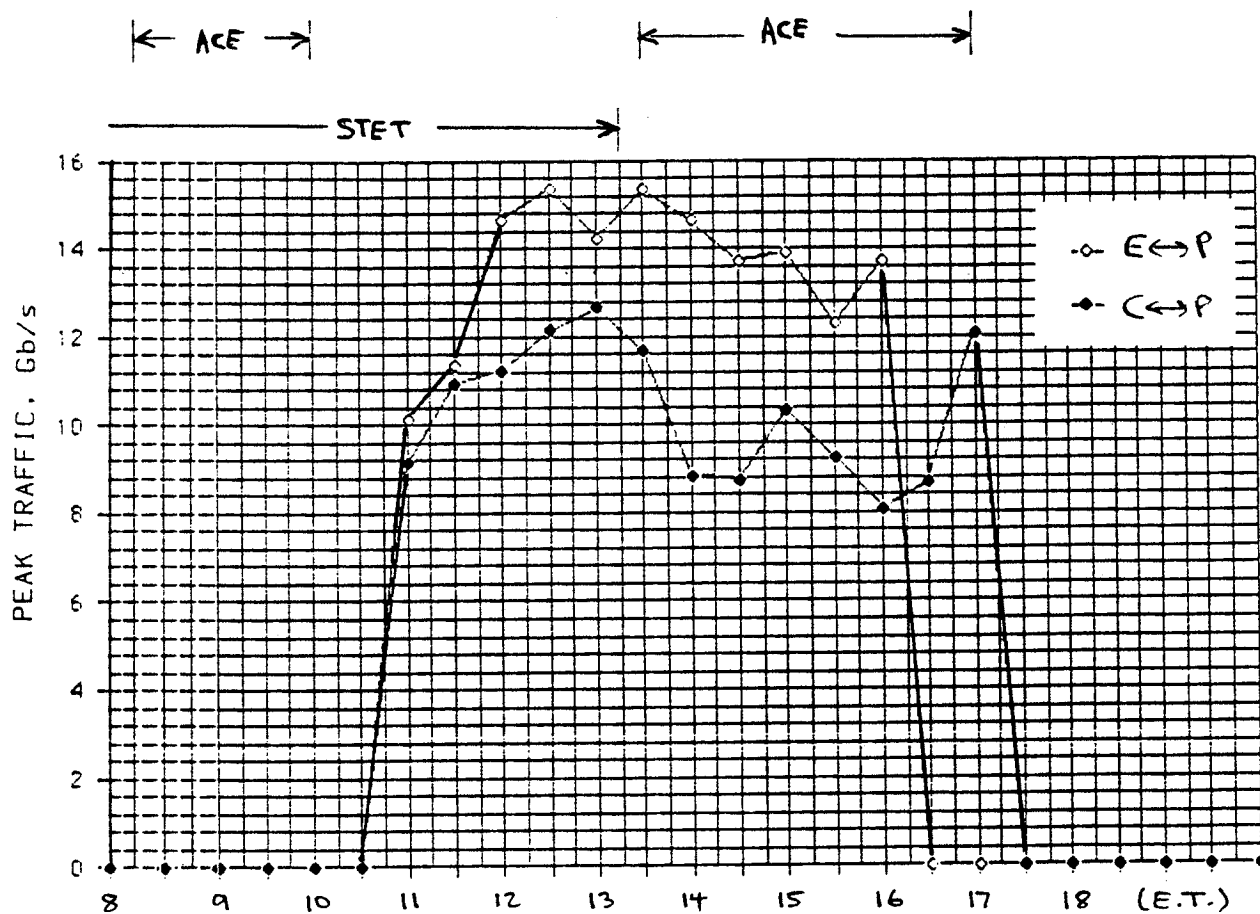


Figure IV-7: Deloading of Inter-Zone $E \leftrightarrow P$ and $C \leftrightarrow P$ Traffic, Case 1

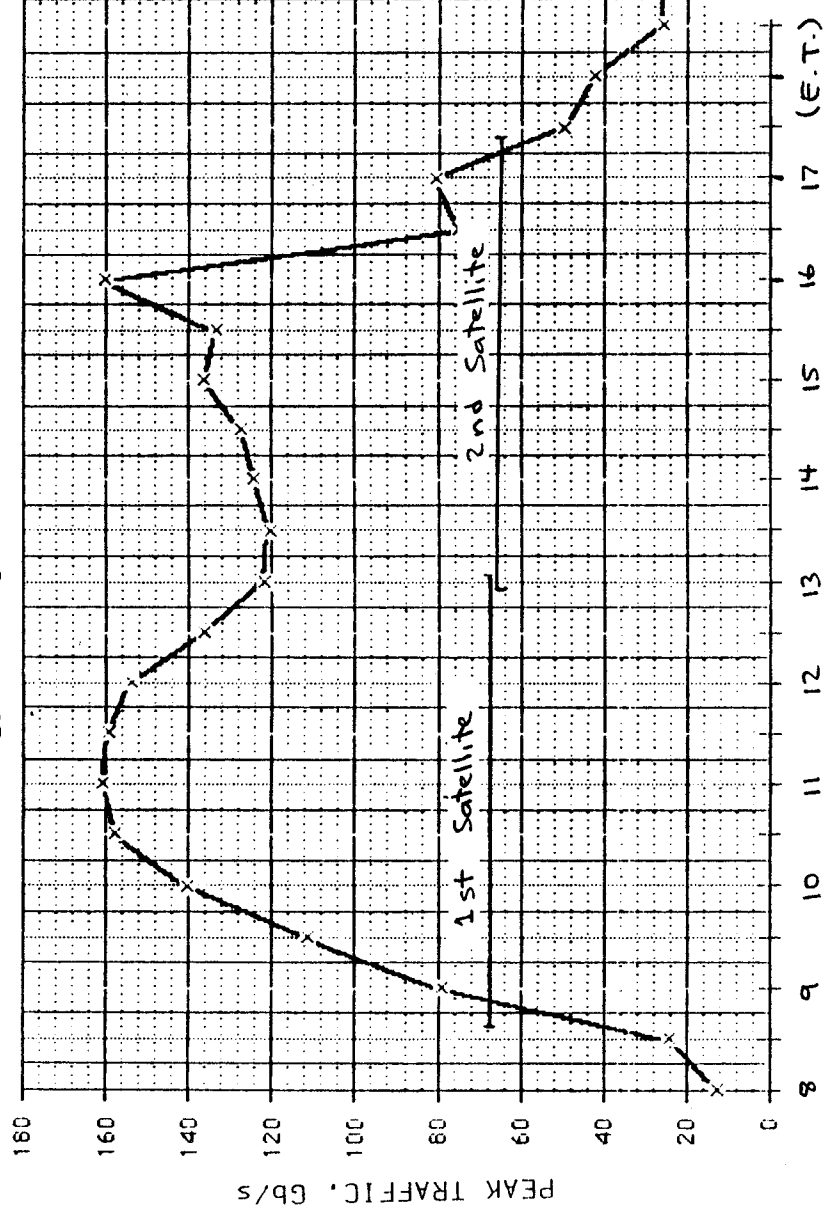


Figure IV-8: Deloading of Total CONUS Traffic by STET Orbit Satellite, Case 1

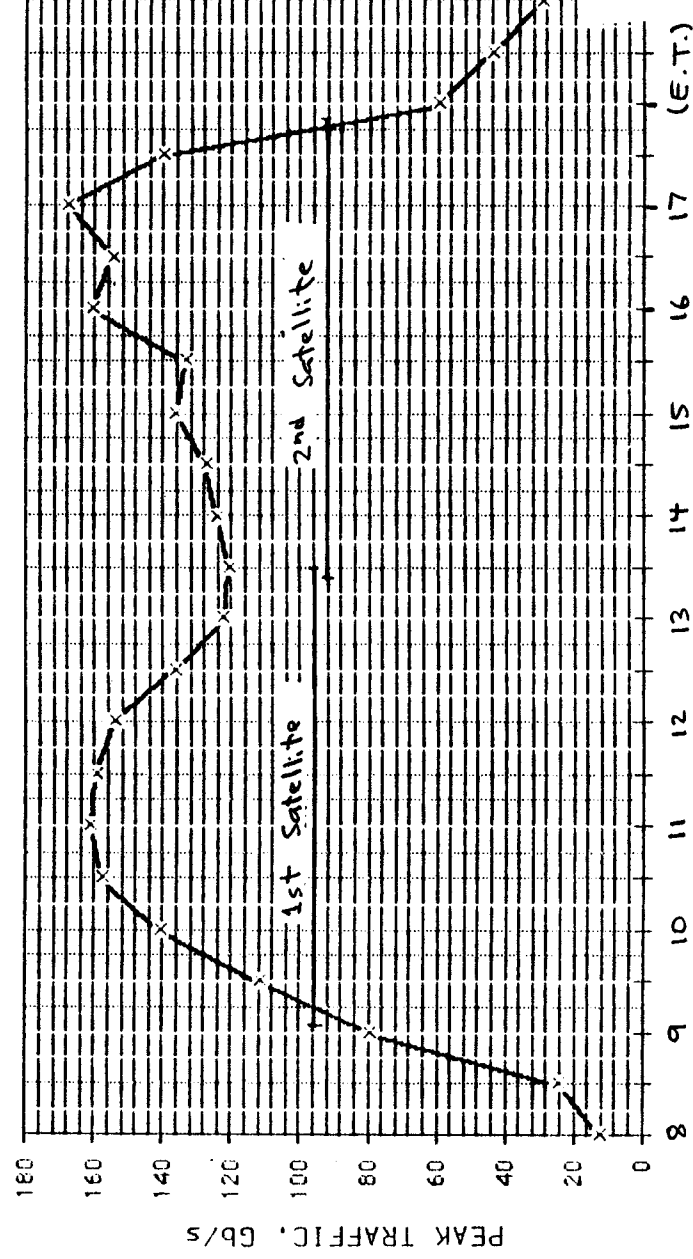


Figure IV-9: Deloading of Total CONUS Traffic by STET Orbit Satellite, Case 2

7.4 Multiple ACE Satellites

Satellites in ACE orbits with 60° and 132°W apogees provide best CONUS coverage. Visibility of this orbit covering all of CONUS is made up of a first visibility period of 1 h 25 min, an interruption of 5 h 40 min, and a second visibility period of 1 h 15 min. Coverage is shown in Figure IV-10 for both traffic cases.

As shown by the top line in Figure IV-10, four satellites can not cover the morning and afternoon traffic peaks without leaving a gap. However, as shown by the lower line, five satellites can provide a total continuous coverage of 13 h 20 min and a total deloading capacity of over 140 Gb/s.

This case is practically equivalent to a single GEO satellite, but the penalty is that five times as many satellite are required to do the work the GEO satellites.

8 Conclusions

Table IV-2 summarizes the various peak traffic deloading possibilities. Results are presented in percent deload relative to the peak traffic of 208.6 Gb/s.

The first case called *Time-of-day* engineering requires no satellite and was described in Subsection II-4.3. It requires that the time-of-day shift in traffic be considered in the analysis required communications capacity. It is beyond the scope of this study to discuss further.

The basic restriction in providing deloading capacity is the time the satellite is visible to the potential users. Traffic analysis gives a requirement of from 7 to 10 hours continuous coverage, depending on coverage area and amount of deload desired. However, the number of possible orbits is limited by the requirement for being sun synchronous (i.e. satellite is at the same place in the sky at the same time each day) and for using little stationkeeping fuel, and a single non-GEO orbit satellite cannot supply as much coverage as would be desirable.

One non-GEO satellite location cannot provide full CONUS deloading. However, two satellites (with sufficient capacity) in the STET or-

bit can deload 35% to 44% of the peak traffic. However, the economics of having two non-GEO satellites do the work of one GEO satellite may not be attractive.

One non-GEO satellite, in STET or ACE orbit, can provide substantial deloading of Eastern and Central intra-zone traffic and E↔C inter-zone traffic. System concepts for these cases are developed and defined in Sections VI and VII, and the economics of the resulting non-GEO satellites are analyzed in Section VIII.

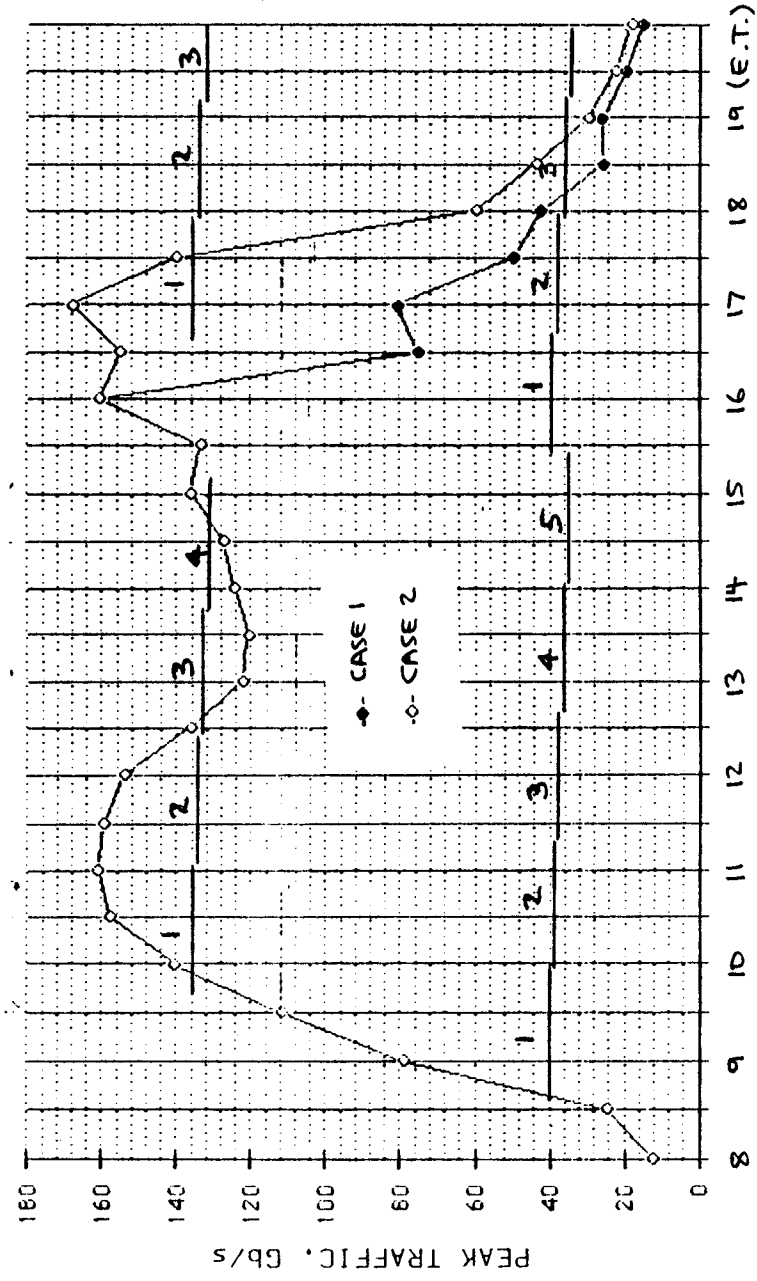


Figure IV-10: Deloading of Total CONUS Traffic by ACE Orbit Satellite

Deload Method	Peak Traffic Deloaded (Gbits/s)							
	Eastern		Central		E↔C		Total CONUS	
	Intra-zone		Intra-zone		Inter-zone			
	1	2	1	2	1	2	1	2
Time-of-day engineering	—	—	—	—	—	—	47.4	40.6
One STET	10.0	1.3	13.8	9.6	25.0	20.8	0.0	0.0
One ACE	14.0	1.0	10.8	10.8	25.8	25.8	0.0	0.0
Two STET							91.2	72.0
Two ACE							0.0	0.0
Five ACE							141.2	148.0

Deload Method	Percent Peak Traffic Deloaded (of 208 Gb/s)							
	Eastern		Central		E↔C		Total CONUS	
	Intra-zone		Intra-zone		Inter-zone			
	1	2	1	2	1	2	1	2
Time-of-day engineering	—	—	—	—	—	—	22.7	19.5
One STET	4.8	4.8	0.6	0.6	6.6	4.6	0.0	0.0
One ACE	6.7	6.7	0.5	0.5	5.2	5.2	0.0	0.0
Two STET							43.7	34.5
Two ACE							0.0	0.0
Five ACE							67.7	70.9

Table IV-2: Peak Traffic Deloading Performance

Section V

FORECAST OF 1990 TECHNOLOGY

This section forecasts the technology state-of-the-art existing at the end of 1990. It is assumed that this level of technology is used for satellites launched and becoming operational in the 1994 to 1997 time. Section VI uses this technology to develop satellite system concepts.

An assessment is made of the expected state-of-the-art status of communications satellite systems and operations for U. S. domestic FSS systems based on the 1990 technology level. The assessment considers each of the seven communications satellite subsystems:

1. Attitude Control
2. Communications Payload
3. Primary Power
4. Propulsion
5. Structure and Mechanisms
6. Telemetry, Tracking, and Command
7. Thermal Control

Also assessed will be the following:

8. Space transportation
9. Radiation hardness

1 Attitude Control Subsystem

The business-as-usual attitude and orbit control subsystems contain a variety of autonomous and manual control modes. During basic on-orbit operation, as many as 20 people (over three shifts) are required for manual control of attitude and orbit parameters. The number of people could be reduced to 6 if some basic jobs could be

made autonomous. The station keeping or orbit control, which has the highest manual control requirements, could be made autonomous by advances being made in navigation and computer software and hardware. The reliability of this type of autonomy is currently being studied through various programs.

Use of the TDRSS relay satellites would allow contact to be kept with the satellite even when on the other side of the earth from the control station. Use of the planned global positioning system (GPS) network of satellites will allow constant and more accurate position determination. Together, GPS and TDRSS will simplify the support required for initial positioning in orbit and for attitude determination during the lifetime of the satellite.

The recently-developed ring laser gyroscope has several advantages over conventional gyros:

- Higher accuracy;
- Reduced calibration time; and
- Quicker start-up.

At present the ring laser gyro is heavier, uses more power, and is more expensive than a conventional gyro. However, developments of this technology are expected to overcome these problems by 1990. It is forecast that the ring laser gyro will be used rather than the digital integrated rate assembly (DIRA) for sensing of satellite attitude.

2 Communications Payload

Due to development of higher strength materials and increased compactness of electronic components, a 15% mass reduction for the payload is projected for 1995 launches.

2.1 Antennas

Modest technical advances are projected over the next decade for the antenna subsystem, but they will be offset by the increased performance requirements imposed by closer orbital spacings. Increased component efficiency will be offset by the reduced antenna efficiency of tapered illumination functions required to control sidelobes.

Antenna subsystem development costs will be reduced by improved analysis programs that allow skipping of the breadboard antenna design step.

Antenna manufacturing costs will be reduced by near field range facilities which allow faster and more accurate adjustment of the antenna subsystem.

The development of higher strength materials will allow a 10% reduction in antenna subsystem mass for 1995 launches. However, increased frequency reuse will require smaller beam sizes which require larger diameter antennas. Use of the Shuttle limits the diameter of a solid reflector to 15 ft (4.5 m), which corresponds to 1.25° C-band and 0.30° Ku-band beam sizes. The Ka-band reflector size is limited to 4 m, corresponding to a 0.3° beam size, by the overall satellite pointing accuracy.

2.2 Transponders and Receivers

Most significant advances in the transponder subsystem will be in the area of better device performance – lighter and more efficient traveling wave tube amplifiers (TWTAs) and solid state power amplifiers (SSPAs) and better noise figure low noise amplifiers (LNAs).

Table V-1 gives TWTA efficiency (dc to rf power) predictions for 1985 and 1995 launched satellites. The 50 W per transponder required at Ku-band will be supplied by a TWTA with an expected 10 year lifetime for 1995 launches.

Solid state power amplifiers (SSPA) will be available with 10 W per device at C-band and 35% efficiency for satellites launched in 1995. SSPA have advantages of increased reliability and lifetime, and much less mass than the equivalent TWTA. A satellite with 36 10 W C-band channels would require 1030 W of dc power for

Frequency Band	Efficiency, %	
	1985	1995
C	48	63
Ku	37	53
Ka	29	45

Table V-1: TWTA Efficiency

SSPAs versus 570 W for TWTAs. For 1995 satellites, SSPAs will be preferred for C-band use.

LNAs using GaAs FETs will be available for 1995 with 2.5 dB noise figures, a 1 dB improvement from 1985. The most significant change for receivers will be in a 50% mass reduction due to large scale integration techniques.

The development of dielectric filters and oscillators will allow a great reduction in transponder subsystem mass.

Improvements in modulation techniques, particularly digital coding schemes, will allow more efficient use of the available bandwidth.

MMIC technology has the potential to greatly reduce payload mass and add capability, but is judged to be immature for commercial satellite launches in 1995.

2.3 On-Board Processing

The most dramatic change in technology could be in the area of on-board signal processing due to advances in VHSIC (Very High Speed Integrated Circuit) technology and high speed digital control systems. Benefits can be achieved in the areas of:

- Increased connectivity;
- Increased capacity;
- Increased communications link efficiency;
- Increased flexibility.

Increased connectivity via switch matrices is postulated for satellites launched in 1995, but on-board signal demodulation is judged to be immature technology.

Type	Year	DOD (%)	Power/weight (W hr kg ⁻¹)
NiCad	1985	55	21.3
NiH	1985	70	24.5
NiH	1989	70	31.0
NaS	1992	70	58.0
NaS	1995	70	70.0

Table V-2: Battery Comparison

3 Primary Power

3.1 Batteries

The standard method of power storage in commercial satellites has been the nickel cadmium (NiCad) battery. In 1984, the Intelsat V and G-Star satellites became the first commercial satellites to use nickel hydrogen (NiH) batteries. The main advantage of the NiH over the NiCad battery is its higher depth of discharge (DOD) which effectively increases its power to weight ratio.

The sodium sulfur (NaS) battery is presently under development and promises to have a power to weight ratio three times the NiCad battery. Although the NaS battery operates at a temperature of 350° C, the required technology exists. Table V-2 compares battery performance for different launch years. The NaS battery is the preferred technology for 1995 satellites.

3.2 Solar Cells

Current practice uses silicon (Si) solar cells with 13.5% BOL efficiency. Developments are underway to reduce cell thickness and thus mass. Although thin cells are more expensive to manufacture, the reduced mass will give a lower overall cost in geosynchronous orbit.

The gallium arsenide (GaAs) cell, currently under development, has a 21% BOL efficiency and is relatively impervious to radiation, but is 2.5 times heavier than silicon and much more expensive. For 1995 launches, GaAs may be equal to Si cells for space applications (same on-orbit cost for equal capacity), but will only be used when area available for solar cells is limited (as

for a high power spinner satellite) or on account of its increased radiation hardness.

The 1990 solar collector technology for commercial satellites will remain silicon, but collector mass should be reduced by 25% for similar capacity systems.

4 Propulsion Subsystem

Two types of propulsion systems are being used today:

- Hydrazine station keeping system plus solid-propellant apogee motor;
- A bipropellant system [nitrogen tetroxide (N₂O₄) and monomethylhydrazine (MMH)] used for both station keeping and apogee motor firing.

The hydrazine thruster has the advantage of being able to supply smaller force-time increments of thrust. However, the biprop system results in mass savings due to the higher specific impulse of the fuel and is the preferred technology, allowing less fuel mass or longer station keeping time with a given fuel mass. The biprop technology will be assumed for 1990 technology-base satellites.

Hydrazine thruster performance can be improved by heating the fuel at the thruster. Devices known as augmented catalytic thrusters (ACTs) will be available with 50% more specific impulse than today. However, significant electric power is required to operate these thrusters (20 kW for a 1 kg thruster). Systems requiring solid apogee motors will use this technology for station keeping, but bipropellant systems remain the preferred technology.

5 Structure and Mechanisms

Business-as-usual satellite structures are primarily constructed of aluminum or aluminum honeycomb materials with two main exceptions:

- If the satellite has a mass problem due to launch vehicle constraints, some structure may be manufactured from either graphite

fiber reinforced plastic (GFRP) or beryllium.

- Parts of the satellite critical to thermal distortions, such as antenna related structures, are usually constructed from GFRP due to its extremely low coefficient of thermal expansion.

However, the additional expense of these exotic materials will continue to keep their use to a minimum for commercial communications satellites.

Higher strength graphite materials will be available for satellites launched in 1995 and should reduce mass by 10%. However, for the major part of the satellite, there will be no use of new structural technology.

Satellite appendages are typically deployed with one-shot spring motor devices or electromechanical actuators. No significant changes are expected for 1995 launches.

6 TT&C Subsystem

Little technology change is expected in the telemetry, tracking, and command (TT&C) subsystem for satellites launched in 1995. At present TT&C takes place at C-band. However, a number of new satellites are planning to use Ku-band since C-Band is becoming saturated with users. Likewise, as more satellites shift to Ku-band, there may need to be a shift to Ka-band with consequent rain attenuation problems. For 1995, C and Ku bands will be adequate.

7 Thermal Control

Present satellites use passive thermal control plus heater augmentation. Passive radiators are mounted on the north or south-facing panels of a 3-axis satellite or on the despun portion of a spinner satellite. These systems are relatively inexpensive, but are heavy and limited in capacity per radiator area.

New generation satellites may incorporate heat pipes with passive or active pumping to reduce mass and improve thermal dissipation capacity. A single phase pump system using freon

fluid has been demonstrated which is efficient up to 4 kW dissipation. A pumped heat pipe system has more accurate temperature control than a passive system, but this is not a critical factor for communications systems which can typically tolerate $\pm 50^\circ \text{C}$.

The passive heat pipe rather than the pumped system is the preferred technology for 1995 FSS systems. It has:

- Greater design maturity;
- Higher reliability and life;
- Less complex integration.

Heat pipes are imbedded within the honeycomb structure of the equipment panel for best efficiency, minimum system weight, and less complex spacecraft integration.

Radiators fixed to the body of the spacecraft rather than deployable radiators are preferred due to their lower weight and cost, and higher reliability. Deployable radiators would be used only if adequate area does not exist for fixed radiators.

8 Space Transportation

The Ariane launch vehicle places the satellite in a highly elliptical orbit known as a geosynchronous transfer orbit (GTO) with a perigee altitude of 200 km and an apogee altitude of 36,000 km. A high thrust apogee kick motor (AKM) is then used to circularize the GTO orbit. Finally, fine orbit adjustments are made.

The Space Transportation System (STS) or Shuttle places a payload in low earth orbit (LEO) at an altitude of 260 km. Further means are then required to transport the payload to geosynchronous earth orbit (GEO), which is a circular orbit of 36,000 km altitude. The STS is expected to be available again in 1995 only for selected commercial or government communications satellites.

It is expected that expendable launch vehicles (ELVs) will be developed and increasingly available by 1995.

Another alternative method of transportation from LEO (or GTO) is the integral perigee stage,

which is controlled directly from the satellite. This results in lower mass and significantly reduced launch costs. A new development will be the ground based orbital transfer vehicle (OTV) which is scheduled to become operational in 1995.

The space-based (SB) OTV is scheduled to become operational in 1998, and should have a dramatic effect on upper stage launch costs. The SB-OTV will be based at the Space Station and will not have to be carried up from earth for each use. It will be reusable and return from GEO orbit via aerobraking to conserve fuel. The capacity of the SB-OTV is planned to be 12,000 kg, which will allow much larger satellites to be put into orbit.

9 Radiation Hardness

Radiation resistance of satellite components is of increasing concern for military satellite programs, and has led to an accelerated effort to produce satellite components that are more radiation resistant. Appendix A, Table A-4, gives an overview of the expected improvement of the hardness level of available piece parts for the 1990s time frame.

Predictions are that the harder piece parts using 1990 technology will require only half the shielding thickness to survive the same radiation dose as current parts.

10 Summary of Technology Developments

The anticipated technology developments for each subsystem are summarized in Table V-3 along with the anticipated technical benefits. The bottom line is that satellites will have a significant improvement in payload capacity, perhaps by 50%, which will allow a reduction in transponder lease cost by 33% (approximately 4% per year).

Category	Change	Benefit
Structure	None	
Thermal	Passive heat pipes	Reduced mass of thermal subsystem. Higher thermal dissipation.
Propulsion	Bipropellant system	Reduced fuel mass.
Attitude Control	Use of GPS & TDRSS Ring laser gyro	More accurate and faster position determination. Increased reliability, less calibration time.
Power	NaS batteries Thinner Si solar cells GaAs solar cells	Improved power/weight ratio. Reduction in mass. Greater efficiency (21% vs 13%)
TT&C	None	
Comm. Payload	Better design tools Near field testing More efficient TWTAs SSPAs at C-band Improved modulation VHSIC & microprocessors High strength materials Large scale integration	Reduced development time & cost. Reduced testing time. Less power required. Greater reliability and lifetime, less mass More efficient use of given bandwidth. Better capacity for processing and switching. 15% mass reduction for antenna subsystem 15% mass reduction for electronic components
Space Transport	ELVs Ground-based OTV Space-based OTV	Reduced launch costs. Reduced launch costs. Greater launch capacity.
Rad. Hardness	Harder piece parts	Increased radiation resistance. Reduced shielding weights.

Table V-3: Satellite Technology Developments (1990)

Section VI

SYSTEM CONCEPTS

1 Introduction

This section uses the traffic analysis of Section II and the orbit analysis of Section III as a basis for proposing non-GEO satellite concepts. These concepts are defined in sufficient detail in the next section (Section VII) to allow economic comparison with the baseline GEO satellite system in Section VIII.

The following system concepts are developed:

1. Trunking System Concepts:

- Baseline GEO system
- STET satellite system
- ACE satellite system

2. Customer Premise Service Concepts:

- Baseline GEO system
- STET satellite system
- ACE satellite system

The baseline GEO system is defined in order to allow economic performance comparison of the non-GEO and GEO systems. Mixed GEO/non-GEO systems are not explicitly considered since it is believed that initial non-GEO systems will be separate entities selling communications services.

2 Non-GEO System Issues

The following potential differences between GEO and non-GEO satellite systems are discussed before system concepts are developed.

1. Antenna coverage
2. Attitude control

3. Battery versus solar array capacity
4. Communications capacity
5. Intersatellite links
6. Launch vehicle capacity
7. Orbital drag at perigee
8. Polarization tracking
9. Radiation environment effects

2.1 Antenna Coverage

Appendix B gives plots of required antenna coverage for the non-GEO ACE and STET orbits, and compares coverage with that of the GEO satellite. The following points are evident:

- The lower altitude non-GEO satellites have a wider antenna coverage angle than a GEO satellite (Figures B-1 through B-3). The resultant antenna has lower gain and a smaller diameter.
- As the STET (Figures B-4 through B-6) and ACE (Figures B-7 through B-12) satellites change orbital position, the size and shape of the coverage area changes. This suggests a more complex reconfigurable antenna may be required. Alternately, antennas with composite patterns as shown in Figures B-13 and B-14 could be used.

A GEO satellite has a fixed coverage area which can be readily divided to obtain frequency reuse. The antenna system can be optimized for the mission and there is generally no need to alter the coverage pattern with time.

In contrast, the non-GEO satellite rises and sets with the consequent cosine elevation angle shortening of one dimension of the coverage region. In theory, the satellite antenna pattern could be reconfigured to follow the apparent change in shape of the coverage region. The resulting increase in antenna gain could compensate for the increased atmospheric loss at low elevation angles.

A reconfigurable antenna usually requires a penalty on the satellite in terms of mass, volume, and power consumption. Future satellites using direct radiating phased arrays with MMIC components to control amplitude and phase would pay less penalty since much of the required hardware would be in place.

For the time frame (1990 technology) and application (low-cost commercial communications) considered in this study, partial reconfigurability using ferrite variable power dividers (VPDs), ferrite variable phase shifters (VPSs), and ferrite switches could be considered. Clusters of feed horns in a multiple beam antenna (MBA) could be switched in and out to give gross pattern changes with less impact on the satellite.

2.1.1 STET Satellite Antenna

Figures B-3 through B-6 of Appendix B show how the apparent size of the eastern half-CONUS coverage area changes with satellite position. Figure B-13 gives the composite coverage pattern whose envelope encloses all possible coverage region shapes.

Figures VI-1 through VI-3 show how the STET composite coverage of Figure B-13 is fitted by different composite beams. Table VI-2 gives the antenna size and number of feeds for composite beams ranging from 0.67° to 2° . A certain number of "primary" feeds are required to direct energy on the coverage area and an additional number to the south for sidelobe control.

Since the apparent separation of the STET satellite from other satellites in the geostationary arc decreases for lower earth station latitude, the sidelobes to the south of CONUS must be carefully controlled to avoid interference with non-CONUS earth stations using GEO satellites. This requires an additional row of feed elements

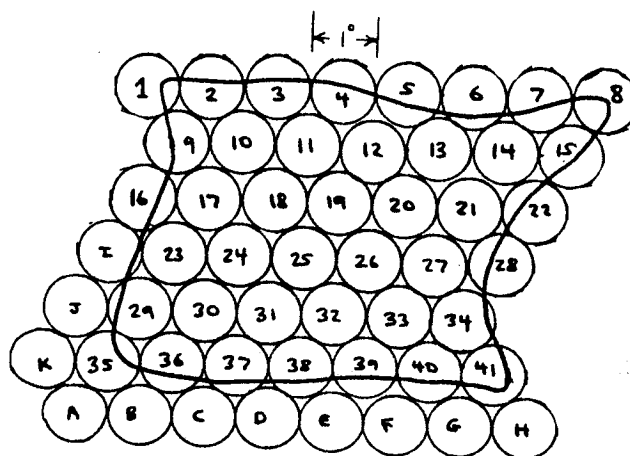


Figure VI-1: STET Coverage: 1.0° Beams

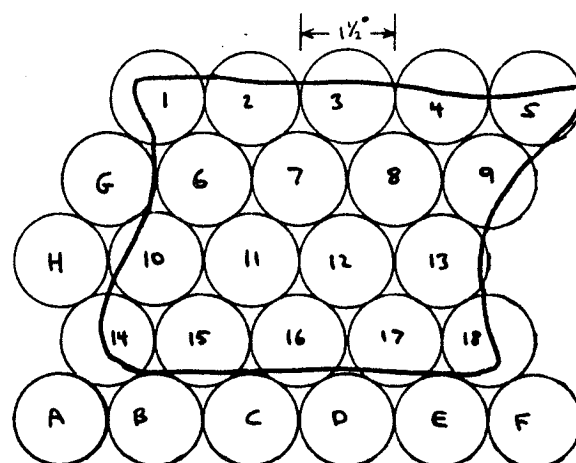


Figure VI-2: STET Coverage: 1.5° Beams

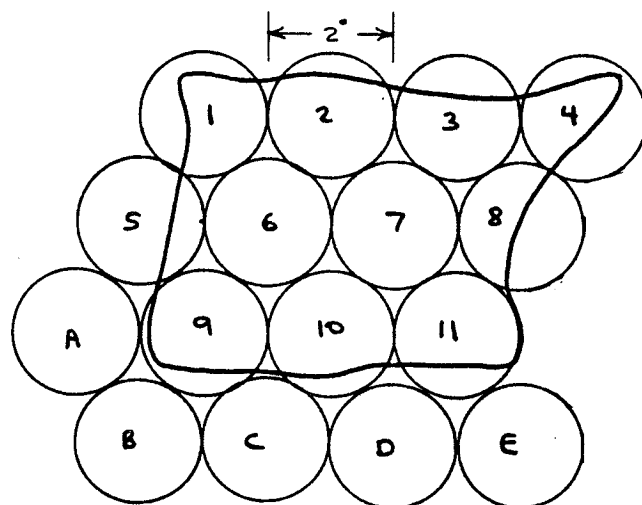


Figure VI-3: STET Coverage: 2.0° Beams

Satellite Position (° W)	Coverage Area (° ²)	Antenna Gain (dB)	
		1°	2°
128	14	30.1	29.3
110	20	28.6	27.5
80	21	28.5	27.1
50	13	29.3	28.6
30	7	31.6	31.1
Composite	27	27.0	26.7

Table VI-1: Antenna Gain vs. STET Position

(shown by letters rather than numbers in the figures). This study assumes that high latitude sidelobes are not a problem. However, if their suppression is required, additional feeds are required to control them.

Table VI-1 gives the apparent change in coverage area as the STET satellite rises in the West (128° W), passes overhead (80° W), and sets in the East (30° W). The composite coverage area and antenna gains with 1° and 2° composite beams are also given. In general, smaller composite beams give a better fit to the coverage contours and provide higher gain. However, the comparison among gains at different satellite positions depends on how well the particular beam size and pattern fits the desired coverage region.

A fully reconfigurable antenna with the indicated beam size could follow the gain changes of Table VI-1, but would experience 1 to 2 dB loss if implemented with VPSs and VPDs. The potential gain from reconfiguring the STET antenna may be offset by additional losses in the beam forming network. At Ku-band the increased effect of the atmosphere at low elevation angles makes limited reconfigurability attractive in order to increase satellite antenna gain by 1 dB at low elevation angles.

C-Band STET Antenna

The choice of C-band antenna for the STET satellite is an MBA with 1.5° constituent beams and 3.2 m diameter. (The constituent beam is the basic building block from which the composite coverage pattern is constructed.) Approx-

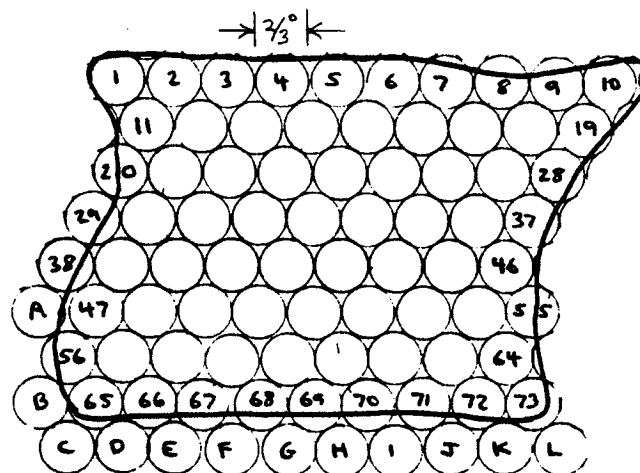


Figure VI-4: STET Coverage: 0.67° Beams

imately 26 feed horns (18 for primary pattern and 8 for sidelobe control) form the composite pattern as shown in Figure VI-2. Gain is approximately 27 dB and is equivalent to a GEO satellite antenna of 1.8 m providing CONUS coverage with 31 dB gain but 4 dB more space loss. Full reconfigurability is supplied in order to obtain three times frequency reuse.

However, consideration of the PAM D perigee stage launch envelope (large sunshield) limits maximum antenna size to 2.9 m. This has only a small effect on the performance parameters given above. (The beam size is 1.7° and there are two 22-element fully reconfigurable feed arrays.)

Ku-Band STET Antenna

The choice of Ku-band antenna for the STET satellite is an MBA with 0.67° constituent beams and 2.3 m diameter. Approximately 85 feed horns as shown in Figure VI-4 are used for primary illumination and sidelobe control. Due to the excessive loss due to rainfall at low elevation angles, it is judged necessary to include a limited, switched reconfigurability for rising and setting coverages from 10° to 30° elevation angles. Antenna performance should equal the GEO orbit satellite antenna (2.4 m diameter). However, low elevation angle gain increases about 1.5 dB even with BFN losses.

A fully reconfigurable antenna is required to obtain the necessary isolation for three or more times frequency reuse.

2.1.2 ACE Satellite Antenna

Figures B-7 through B-12 of Appendix B show how the apparent size of the eastern half-CONUS coverage area changes with satellite position. Figure B-14 gives the composite coverage pattern whose envelope encloses all possible coverage region shapes.

The analysis for the ACE orbit is more complex than that for the STET orbit satellite due to the addition of varying satellite range to the coverage region foreshortening at low elevation angles. Fortunately these effects partially offset each other since the satellite apogee occurs when the satellite is over the coverage area. When the satellite is at lower altitudes and the apparent coverage area increases, it is also at low elevation angle and the coverage region size is foreshortened.

Figures VI-5 and VI-6 show the ACE composite coverage region with 3° and 2° beam sizes. The antenna gain and number of feeds is given in Table VI-3. Using a composite pattern, the antenna performance at apogee is 19 dB gain versus the 31 dB of an equivalent GEO satellite. The difference in space loss is 7 dB, leaving a 5 dB performance disadvantage for the ACE composite pattern antenna.

The conclusion is that a fully reconfigurable antenna is required for the ACE satellite antenna in order to avoid a 5 dB link margin loss. The C-band system uses 2.0° composite beams with a 2.4 m antenna. The Ku-band system uses 2° composite beams with a 0.8 m antenna. Link performance is equivalent to the GEO system when the satellite is above the coverage area due to the additional BFN losses being offset by improved antenna efficiency. At low elevation angles, performance is improved by 2 dB compared to when the satellite is on the meridian, and the additional margin can be used to offset weather effects.

2.2 Attitude Control

The rising and setting of the satellite requires that the pointing direction of the satellite antenna be continuously changed during times of coverage. This is true regardless of the reference

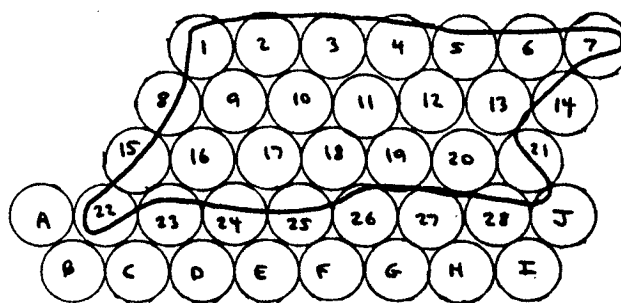


Figure VI-5: ACE Coverage: 3° Beams

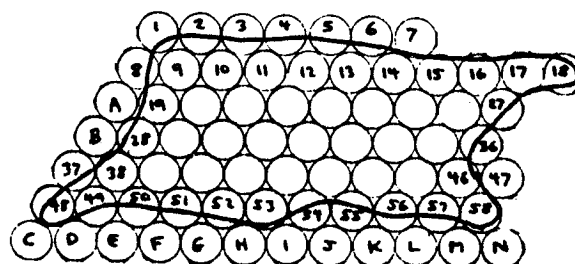


Figure VI-6: ACE Coverage: 2° Beams

frame to which the satellite is fixed, even with gravity gradient stabilization. In addition, the antenna may be pointed to minimize the composite coverage pattern envelope. The range of pitch motion required for each coverage region pass is 25° for the STET and 37° for the ACE orbit satellite.

Since both the STET and ACE satellites are closer to the earth, an earth sensor with a wider field of view is needed. There is no mass change for the STET orbit, but the ACE orbit requires a panoramic earth sensor with a 1 kg mass increase.

2.2.1 Spin Stabilized Satellites

Attitude control simply requires that the antenna platform is despun at a different rate for the STET satellite. For the ACE satellite there is a slightly varying despin rate with additional control electronics required to change the despin rate.

Constituent Beam Size (°)	Ant. Dia. (m)		Number of Feeds			EOC Gain (dB)
	C-band	Ku-band	Primary	Sidelobe	Total	
0.67	—	2.3	73	12	85	28.0
1.00	4.8	1.5	41	11	52	27.0
1.50	3.2	1.0	18	8	26	27.1
2.00	2.4	0.8	11	5	16	26.7

Table VI-2: STET Antenna Parameters Versus Constituent Beam Size

Constituent Beam Size (°)	Ant. Dia. (m)		Number of Feeds			EOC Gain (dB)
	C-band	Ku-band	Primary	Sidelobe	Total	
2.00	2.4	0.8	58	14	72	19.7
3.00	1.6	0.5	28	10	38	19.1

Table VI-3: ACE Antenna Parameters Versus Constituent Beam Size

2.2.2 3-Axis Satellites

The proposed solution for the 3-axis satellite is to use a reaction wheel to provide small increments of attitude control for the satellite. The estimated impact is 4 kg mass and 15 W electric power.

2.3 Battery Versus Solar Array Size

Since there is no requirement for communications during solar eclipse for the non-GEO satellite, the battery capacity can be reduced to the level of the satellite "housekeeping power" which is typically 15% of full power. Thus approximately 85% of the GEO satellite battery mass (0.26 kg/Ah for NaS) can be saved by the non-GEO satellites.

A better approach is to reduce solar cell area by increasing battery capacity. This is possible since the non-GEO satellite provides communications for only 8 hr a day, and the worst case eclipse scenario results in sunlight on the solar arrays 22 hr per 24 hr. The solar array is sized to provide the full amount of housekeeping power but only 8/22 of the communications power. Battery capacity is sized to provide the other 14/22 communications power for the 8 hr of communications. (In other words, of the 22

hours of sunlight, the 14 hours falling during times of non-communications are stored in batteries for use during the 8 hours of communications.)

The impact on the power system is a reduction in solar cell area by 50% and an increase in battery capacity by 5 to 8 times. This exchange is favorable if the total cost of solar cells is more than 8 to 14 times the total cost of batteries. (This may be true for the ACE satellites where the radiation environment requires an 85% increase in solar array size or for spinner satellites which have 2.5 times the solar array area of a 3-axis design.)

Solar array area can also be reduced by use of higher efficiency GaAs solar cells. However, the 18% GaAs efficiency (versus 12% Si) is offset by its greater thickness, density, and cost. GaAs is projected to be used only where there are limits on available area for solar cells.

2.4 Communications Capacity

2.4.1 Potential Larger Capacity

Geostationary satellites are typically designed with a communications capacity determined by launch vehicle capacity as well as mission requirements. Any savings in mass can be turned

there is considerable impact on the ACE orbit but not very much on the STET orbit satellites (Table A-5). The ACE orbit satellite requires 85% more area and thicker coverglass compared to the equivalent GEO satellite.

3 Trunking Systems

This subsection proposes the trunking system concepts which are defined in detail in Section VII and whose economic performance is analyzed in Section VIII.

These trunking systems supply a mix of fixed services (voice, video, data) from a relatively few number of larger ground stations. The function of a trunking system is to transmit prepackaged, bulk information over a relatively long distance. Such service tends to use wide bandwidth channels and larger earth terminals. The satellites use end-of-1990 technology, are launched in the 1994 to 1997 time frame, and address a portion of the year 2000 traffic.

A small C-band satellite design (Galaxy 4) is selected for the following reasons.

- For a given required coverage area on earth, C-band systems are more economical than Ku-band systems. (Trunking systems of the 1990s will be in direct competition competition with fiber optics.)
- The CPS design is required to use Ku-band due to considerations of terrestrial interference. For purpose of using different satellite designs, a C-band system is selected for the trunking application.
- The lower power of the C-band system allows use of a smaller bus which can be a spinner design. (Again this is different from the larger, high power Ku-band design which favors a three axis satellite design.)

3.1 Baseline Trunking System

The baseline system to be used for economic comparison is a C-band geosynchronous satellite system based on the Galaxy 4 design, but updated from 1982 to 1990 technology. The system consists of two in-orbit satellites and one

ground spare. General features of the baseline system are as follows.

- 24 ea. 9 W, 36 MHz, C-band transponders
- Two full CONUS coverages
- 1.8 m antenna with 7-element feed array
- EIRPs: 35 dBW (Full CONUS)
- 560 kg, 800 W, spinner satellite design
- STS/PAM D launch

The design concept is to provide a low cost system that is compatible with existing C-band ground stations, and that can compete with terrestrial systems for some point-to-point services as well as supply broadcast services.

3.2 STET Trunking System

The STET non-GEO system differs from the baseline system in the following respects.

- 130 kg more mass can be placed in STET orbit using the same PAM D upper stage. The design approach is to change the transponder configuration.
- A 2.9 m satellite antenna with a 22 element fixed feed array provides a composite coverage beam. (This is slightly smaller than the chosen 3.2 m size of paragraph VI-2.1.1, but is the maximum size allowable for STS/PAM D launch.)
- Change in transponder configuration (i.e. number, bandwidth, and power).
- Additional radiation shielding of electronic components (100 mil aluminum equivalent).
- Additional 15% solar cell area to compensate for increased radiation degradation.
- Reduced solar array area on account of low duty cycle, but at the cost of increased battery capacity.
- Tracking (position and polarization) required of ground stations.

3.3 ACE Trunking System

The ACE non-GEO system differs from the baseline system in the following respects.

- An integral upper stage can be used instead of the PAM D perigee stage.
- The number of transponders is double that of the GEO satellite.
- 2.4 m satellite antenna with a 38 element fully reconfigurable feed array.
- Additional 40 W power required for reconfigurable antenna.
- Additional 85% solar cell area and coverglass mass for radiation protection.
- Reduced solar array area on account of low duty cycle, but at the cost of increased battery capacity.
- Tracking (position and polarization) required of ground stations.
- Alternately, an smaller perigee stage can be used instead of the PAM D, but the payload is the same as the GEO satellite.

4 CPS Systems

This subsection proposes the CPS (customer premise service) system concepts which are defined in detail in Section VII and whose economic performance is analyzed in Section VIII.

These CPS systems provide business services (voice, data, videoconferencing) directly to customer premises. There are a relatively large number of small ground stations, possibly sharing a transponder on a TDMA basis. The satellites use end-of-1990 technology, are launched in the 1994 to 1997 time frame, and address a portion of the year 2000 traffic.

4.1 Baseline CPS System

The baseline system to be used for economic comparison is a Ku-band geosynchronous satellite system consisting of two in-orbit satellites and one ground spare. The satellite design is

based on the Satcom K2, updated to 1990 technology, but using a payload and operational concept similar to the SBS system. General features of the baseline system are as follows.

- 24 ea. 50 W, 54 MHz Ku-band transponders
- East, West, and full CONUS coverages
- EIRPs: 46 dBW (CONUS) and 49 dBW (E/W CONUS)
- 1,020 kg, 2,900 W, 3-axis satellite design
- STS/PAM D2 launch

The design concept is to provide a system that is has sufficient EIRP to allow use of relatively small (1.2 m to 1.8 m), low cost ground stations on the business customer's premises. Ku-band is required in order to allow ground station transmissions without restrictions of interference with ground microwave facilities.

4.2 STET CPS System

The STET non-GEO system differs from the baseline system in the following respects.

- 240 kg more mass can be placed in STET orbit. The design approach is to change the transponder configuration.
- 2.3 m satellite antenna with a 85 element feed array with full reconfigurability for use at low elevation angles (additional mass and power required).
- EIRP improvement of 1.5 dB at low elevation angles.
- Reaction wheel plus small amount of fuel used for attitude control.
- Additional radiation shielding of electronic parts (100 mil aluminum equivalent).
- Additional 15% solar cell area.
- Less battery capacity since there are no communications during eclipses.
- Tracking (position and polarization) required of ground stations.

4.3 ACE CPS System

The ACE non-GEO system differs from the baseline system in the following respects.

- The number of transponders is double that of the GEO satellite.
- A 0.8 m satellite antenna with a 72 element fully reconfigurable feed array is used (additional mass and power required).
- EIRP improves 2 dB at low elevation angles.
- Reaction wheel plus small amount of fuel used for attitude control.
- Additional solar cell area of 85% and cover-glass mass for radiation protection.
- Solar array area reduced 50% and battery capacity increased on account of low duty cycle for communications power (8 hr per 24 hr).
- Tracking (position and polarization) required of ground stations.
- Alternately, a smaller perigee stage can be used instead of the PAM D2, but the payload is the same as the GEO satellite.

5 Summary

The appropriate choice of satellite system definition as given in the next section (Section VII) depends on characteristics of the non-GEO orbit as regards to communications.

The significant differences of the non-GEO orbits (compared to the GEO orbit) on the satellite system are summarized as follows.

- Satellite coverage region
 - Larger area (steradians)
 - Area changes with time
- Satellite services
 - Service area restricted to half CONUS
 - Communications supplied 8 out of 24 hr

- Difficult to reuse frequency band
- Larger satellite separations allow use of higher transmit powers (reduced adjacent satellite interference)

- Radiation environment
 - Shielding of electronics
 - Degradation of solar cells
- Satellite orientation and position
 - More attitude control
 - Less station-keeping fuel
 - Earth terminal must track satellite position and polarization
- Launch
 - Less energy required

The impact of these differences on the satellite is reflected in mass changes which are directly related to costs. Table VI-5 summarizes the impacts on the satellite system.

For an equivalent payload, it is clear that the non-GEO satellite has more mass, and thus the non-GEO satellite costs more than its GEO counterpart. However, this is offset by reduced STS launch cost and perigee stage cost. A key factor is to select a communications payload that takes advantage of the non-GEO orbit, and thereby can give additional revenue to the non-GEO system transponder.

The next section (Section VII) defines the satellite system, and Section VIII does the detailed economic comparison using a *Financial Model* of commercial communications satellite systems.

Component	Impact on Satellite System	
	STET Orbit	ACE Orbit
Antenna:	Closer to earth implies smaller antenna. Variable coverage region shape implies: – less gain, potential interference; – need for reconfigurable antenna Small efficient beams imply larger antenna.	ditto ditto Reconfigurable antenna required. ditto
Attitude control:	More mass for reaction wheels (3-axis). Additional attitude control fuel (3-axis).	ditto ditto More mass for earth sensor.
Power:	Battery mass can be reduced by 85%. Alternately, solar array area can be reduced 50% and battery capacity increased. Radiation environment requires 15% increase in solar cell area. More power for attitude control (3-axis). More power for reconfigurable antenna.	ditto ditto 85% increase solar cells. ditto ditto
Propulsion:	Smaller apogee motor.	ditto Possible integral upper stage.
Structure:	Larger satellite needs more structure mass.	ditto Electronics radiation shielding.
Launch Vehicle:	+33% dry mass into orbit for same vehicle. Or smaller perigee and apogee motors and less STS fuel and volume.	110% more dry mass into orbit. ditto
Earth terminal:	Position tracking capability. Polarization vector tracking capability.	ditto ditto

Table VI-5: Impact of Non-GEO Orbits on STET and ACE Satellite Systems

Section VII

SYSTEM DEFINITION

1 Introduction

This section defines and describes the configurations of satellites and earth terminals for each of the system concepts developed in Section VI.

1. Trunking System Concepts:

- Baseline GEO system
- STET satellite system
- ACE satellite system

2. Customer Premise Service Concepts:

- Baseline GEO system
- STET satellite system
- ACE satellite system

Table VII-2 summarizes the definitions of the three types of trunking systems, and Table VII-3 summarizes the definitions of the three types of CPS systems.

The satellite costs are explained in Section VIII and include 12% G&A expense and 12% manufacturer's fee. (The cost excludes launch costs, perigee stage costs, launch operations, mission operations, and insurance.)

2 Trunking Systems

The definitions of the three types of trunking systems proposed in Subsection VI-3 are summarized in Table VII-2. Tables VII-4 through VII-7 give more details of the GEO, STET, and ACE orbit satellite designs. The following paragraphs discuss the baseline trunking system design and the differences of the STET and ACE satellite designs from the baseline.

Component	Mass (kg)
Attitude control	25
Power	117
Propulsion	48
Structure	98
Thermal	20
TT&C	27
Payload - Antenna	20
- Transponder	80
Margin	10
Total (dry mass)	445
Stationkeeping fuel	100
Attitude control fuel	15
Total (BOL mass)	560

Table VII-1: Baseline Trunking Satellite

2.1 Baseline Trunking Satellite

2.1.1 Design Overview

A small spin stabilized satellite design based on the HS-376 bus is chosen for the baseline trunking system concept. The payload consists entirely of C-band transponders. Table VII-1 gives the breakdown of satellite mass by subsystem for this design. The communications payload is divided into antenna and transponder parts for purposes of comparisons.

Table VII-4 summarizes the baseline trunking satellite design which is a spin stabilized satellite of 560 kg beginning-of-life (BOL) mass, C-band payload, and STS/PAM D launch. The use of 1990 technology gives mass and power savings that allow higher power transponders and greater redundancy to meet the 12 year lifetime than on the original HS-376 bus on Galaxy 4.

Parameter	GEO	STET	ACE	ACE*
Baseline satellite type:	HS-376	-	-	-
Design life (yr)	12	12	12	12
BOL mass (kg)	560	690	990	560
Payload mass (kg)	100	160	260	124
- Antenna (kg)	20	60	80	44
- Transponder (kg)	80	100	180	80
EOL power (W)	830	520	800	465
Stabilization	spin	spin	spin	spin
Frequency	C-band	C-band	C-band	C-band
Number of transponders	24	30	48	24
Transponder bandwidth (MHz)	36	36	36	36
Transponder power (W)	9	9	9	9
Antenna coverages:	2	3	4	2
EIRP, half CONUS (dBW)	38	38	38	38
Launch vehicle(s):	Ariane 4 STS/PAM D	Ariane 4 STS/PAM D	Ariane 4 STS/PAM D	Ariane 4 STS/Star 37
Satellite Cost (\$M, 1986)	39.3	48.6	73.4	44.2

Table VII-2: Summary of Trunking Satellite Characteristics

	GEO	STET	ACE	ACE*
Baseline satellite type:	Satcom K2	-	-	-
Design life (yr)	12	12	12	12
BOL mass (kg)	1,020	1,260	1,820	990
Payload mass (kg)	277	379	549	282
- Antenna (kg)	29	49	53	34
- Transponder (kg)	248	330	496	248
EOL power (W)	2,900	3,800	3,000	1,600
Stabilization	3-axis	3-axis	3-axis	3-axis
Frequency	Ku-band	Ku-band	Ku-band	Ku-band
Number of transponders	24	32	48	24
Trans. bandwidth (MHz)	54	54	54	54
Transponder power (W)	50	50	50	50
Antenna coverages:	3	4	6	3
EIRP, half CONUS (dBW)	49	49	49	49
Launch vehicle(s):	Ariane 4 STS/PAM D2	Ariane 4 STS/PAM D2	Ariane 4 STS/PAM D2	Ariane 4 STS/PAM D
Satellite Cost (\$M, 1986)	53.7	66.5	94.5	59.6

Table VII-3: Summary of CPS Satellite Characteristics

Baseline satellite type:	Galaxy 4 (HS-376)
EIRP (half CONUS):	38 dBW
Lifetime:	12 yr
Launch vehicle:	Ariane 4 or STS/PAM D
Frequency band and bandwidth:	C-band, 500 MHz
- receive:	5.925 - 6.425 GHz
- transmit:	3.7 - 4.2 GHz
Antenna	
- type:	Offset parabolic, dual gridded
- number:	1
- size:	1.8 m
- mass:	20 kg
- feed array:	2 arrays, 7 elements each
- coverage (2 beams):	CONUS
- polarization:	H and V, linear
- dc power:	None
Transponders	
- type:	SSPA
- number:	24
- power:	9 W
- bandwidth:	36 MHz
- SSPA redundancy:	11 for 8
- receiver redundancy:	4 for 2
- mass:	80 kg
- dc power:	700 W
Spacecraft	
- type:	Spin stabilized
- size (stowed):	dia. = 2.2 m, length = 2.9 m
- mass, BOL/dry:	560/445 kg
includes station/attitude fuel:	115 kg
- power (EOL) at summer solstice:	830 W
- primary power:	Solar cells (thin silicon)
- batteries:	NaS, 50 Ah, (15 kg)
- attitude and station keeping:	Hydrazine thrusters (ACTS)
- attitude pointing accuracy:	$\pm 0.05^\circ$
- apogee motor:	Solid propellant

Table VII-4: Baseline GEO Satellite Characteristics, Trunking Service

EIRP (half CONUS):	38 dBW
Lifetime:	12 yr
Launch vehicle:	Ariane 4 or STS/PAM D
Frequency band and bandwidth:	C-band, 500 MHz
– receive:	5.925 – 6.425 GHz
– transmit:	3.7 – 4.2 GHz
Antenna	
– type:	Offset parabolic, dual gridded, fully reconfigurable.
– number:	1
– size:	2.9 m
– mass:	60 kg
– feed array:	2 arrays, 22 elements each
– coverage (3 beams):	East half CONUS; N, Central, S
– polarization:	H and V, linear
– dc power:	30 W
Transponders	
– type:	SSPA
– number:	30
– power:	9 W
– bandwidth:	36 MHz
– SSPA redundancy:	11 for 8
– receiver redundancy:	4 for 2
– mass:	100 kg
– dc power:	875 W
Spacecraft	
– type:	Spin stabilized
– size (bus):	dia. = 2.2 m, length = 2.9 m
– mass, BOL/dry:	690/585 kg
includes station/attitude fuel:	105 kg
– power (EOL) at summer solstice:	520 W
– primary power:	Solar cells (thin silicon)
– batteries:	NaS, 210 Ah (56 kg)
– attitude and station keeping:	Hydrazine thrusters (ACTS)
– attitude pointing accuracy:	$\pm 0.1^\circ$
– apogee motor:	Solid propellant

Table VII-5: STET Satellite Characteristics, Trunking Service

EIRP (half CONUS):	38 dBW
Lifetime:	12 yr
Launch vehicle:	Ariane 4 or STS/PAM D
Frequency band and bandwidth:	C-band, 500 MHz
– receive:	5.925 – 6.425 GHz
– transmit:	3.7 – 4.2 GHz
Antenna	
– type:	Offset parabolic, dual gridded, fully reconfigurable
– number:	1
– size:	2.4 m
– mass:	80 kg
– feed array:	2 arrays, 72 elements each
– coverage (4 beams):	East half CONUS; from N to S.
– polarization:	H and V, linear
– dc power:	40 W
Transponders	
– type:	SSPA
– number:	48
– power:	9 W
– bandwidth:	36 MHz
– SSPA redundancy:	11 for 8
– receiver redundancy:	4 for 2
– mass:	180 kg
– dc power:	1,400 W
Spacecraft	
– type:	Spin stabilized
– size (bus):	dia. = 2.2 m, length = 2.9 m
– mass, BOL/dry:	990/945 kg
– includes station/attitude fuel:	45 kg
– power (EOL) at summer solstice:	800 W
– primary power:	Solar cells (GaAs)
– batteries:	NaS, 320 Ah (86 kg)
– attitude and station keeping:	Hydrazine thrusters (ACTS)
– attitude pointing accuracy:	Variable speed despun platform
– apogee motor:	$\pm 0.1^\circ$ Solid propellant

Table VII-6: ACE Satellite Characteristics, Trunking Service

EIRP (half CONUS):	38 dBW
Lifetime:	12 yr
Launch vehicle:	Ariane 4 or STS/STAR 37FM
Frequency band and bandwidth:	C-band, 500 MHz
– receive:	5.925 – 6.425 GHz
– transmit:	3.7 – 4.2 GHz
Antenna	
– type:	Offset parabolic, dual gridded, fully reconfigurable
– number:	1
– size:	1.6 m
– mass:	44 kg
– feed array:	2 arrays, 72 elements each
– coverage (4 beams):	East half CONUS; from N to S.
– polarization:	H and V, linear
– dc power:	20 W
Transponders	
– type:	SSPA
– number:	24
– power:	9 W
– bandwidth:	36 MHz
– SSPA redundancy:	11 for 8
– receiver redundancy:	4 for 2
– mass:	80 kg
– dc power:	780 W
Spacecraft	
– type:	Spin stabilized
– size (bus):	dia. = 2.2 m, length = 2.9 m
– mass, BOL/dry:	560/515 kg
– includes station/attitude fuel:	45 kg
– power (EOL) at summer solstice:	465 W
– primary power:	Solar cells (GaAs)
– batteries:	NaS, 160 Ah (42 kg)
– attitude and station keeping:	Hydrazine thrusters (ACTS) Variable speed despun platform
– attitude pointing accuracy:	$\pm 0.1^\circ$
– apogee motor:	Solid propellant

Table VII-7: ACE* Satellite Characteristics, Trunking Service

A spin stabilized design is chosen for the baseline trunking satellite for the following reasons:

- Both spin stabilized and 3-axis satellite designs are desired to be analyzed by the study. The CPS satellite design is much larger and favors the 3-axis design.
- The small size of the trunking satellite may favor, and certainly allows a spin stabilized design.

2.1.2 C-Band FSS Payload

This payload is similar to the Scenario II C-band FSS concept developed under NASA Contract No. NAS3-24235, *Communication Platform Payload Definition Study* (see NASA CR174929, Vol. II - Technical Report, p. 5-23). There is two times frequency reuse via horizontal and vertical polarized beams. There are 24 C-band transponders with 9 W power and 36 MHz bandwidth.

The 1.8 m C-band antenna consists of a dual-gridded offset-fed reflector and two 7-element feed arrays for each polarization. Both transmit and receive bands use the same feed array.

The C-band transponders uses SSPAs with 35% dc to RF power efficiency. SSPA redundancy is increased to 11-for-8 (versus 5-for-4 in the CPPD study) in order to obtain a 12 yr lifetime. The receiver has low noise GaAs FETs with 1.5 dB noise figure, monolithic gain blocks, and dielectric oscillators. The multiplexers use dielectric resonator filters.

2.1.3 Launch Requirements

The STS/PAM D combination allows launch of 560 kg BOL (445 kg dry) into GEO orbit. The mass as loaded in the Shuttle (BOL mass + apogee fuel + perigee motor + cradle) is 4,100 kg (9,020 lb). The required length in the Shuttle is 2.51 m (99 in).

2.1.4 Space and Ground Segments

A satellite system consisting of two in-orbit, operating satellites with one ground spare is used. The ground segment consists of the usual satellite control facilities (shared among missions),

and the communications earth terminals. For the trunking mission applications, medium to large C-band earth stations (5 m to 11 m) which are distributed over the coverage region population centers are used.

2.2 STET Trunking Satellite

2.2.1 Design Overview

Table VII-5 summarizes the STET trunking satellite design which is a modification of the baseline GEO design. An increase in payload mass is possible because of reduced station-keeping fuel requirements and increased launch capability for satellites in this orbit (see Table VI-4). The payload is adjusted to give a satellite that still is launched using the STS/PAM D combination. Due to limitations in time the satellite is visible, coverage is restricted to the eastern half of CONUS.

The payload mass is increased by putting more transponders on the satellite. The number of transponders is increased from 24 (GEO) to 30, requiring three times frequency reuse.

2.2.2 STET Satellite Differences

The differences of the STET orbit satellite design compared to the baseline GEO trunking design concept are discussed by subsystem. Table VII-8 summarizes the subsystem mass for the STET trunking satellite design compared to the baseline GEO design. The 130 kg mass increase for the STET orbit satellite is the maximum possible that can be launched by the STS/PAM D.

The antenna has a diameter of 2.9 m, a 1.7° beam size, and is fully reconfigurable. The payload is increased to 30 SSPA transponders with 36 MHz bandwidth and 9 W power versus the baseline GEO satellite 24 transponders with 36 MHz bandwidth and 9 W power. There is three times frequency reuse, either with three regions (North, Central, and South) or one half-CONUS beam with 2 separate N and S spots. The EIRP of the smaller beams is 3 dB or more.

Attitude Control Subsystem

Similar to the baseline GEO design, the use of

Satellite Component	Mass (kg)	
	Change	Total
Attitude	0	25
Power	+14	131
Propulsion	0	48
Structure	+33	131
Thermal	+5	25
TT&C	0	27
Antenna	+40	60
Transponders	+20	100
Margin	+28	38
Total (dry mass)	+140	585
Stationkeeping fuel	-10	90
Attitude control fuel	0	15
Total (BOL mass)	+130	690

Table VII-8: STET Trunking Satellite

spin stabilization requires that the antenna platform be despun in order to remain pointed at the earth. The only difference of the STET satellite is a slightly different, fixed despun rate.

Payload for Communications

The antenna size is increased from the 1.8 m baseline to 2.9 m (+20 kg). A fully reconfigurable feed array is used, resulting in a mass increase of 20 kg. The change in number of transponders gives a mass increase of 20 kg.

Power Subsystem

The reconfigurable antenna requires 30 W power. The change in transponder number gives a 175 W power increase compared to the baseline GEO satellite. Also an additional 15% solar cell area is required to compensate for the increased degradation of the STET orbit radiation environment.

The impact of the radiation on the spinner solar array can be offset by the use of more batteries as discussed in Subsection VI-2.3. The required solar array output can be reduced by 50% and the battery capacity increased to 210 Ah since the satellite requires communications power only 8 hours out of the day.

Compared to the baseline GEO satellite, the

net result for the STET spinner is an increase in battery mass of 41 kg and an decrease in solar array mass of 27 kg. The net result is a mass increase of 14 kg for the power subsystem.

Structure Subsystem

The additional radiation shielding to the equivalent level of 100 mils aluminum adds 10 kg. Sizing to accommodate the increased payload adds another 23 kg.

Thermal Subsystem

An additional 5 kg mass is required.

Station and Attitude Control Fuel

The STET orbit satellite requires 10 kg less stationkeeping fuel than the equivalent GEO orbit satellite. No additional attitude control fuel is required.

Launch Size

The STS/PAM D combination allows launch of 690 kg BOL (600 kg dry) into STET orbit. This is an increase of 130 kg BOL (140 kg dry mass) over the comparable GEO launch. The mass as loaded in the Shuttle (BOL mass + apogee fuel + perigee motor + cradle) is 4,230 kg (9,306 lb). The required length in the Shuttle is 3.61 m (142 in).

2.2.3 Impact on STET Earth Terminals

Earth stations are required to follow the daily motion of the satellite across the sky. Since the motion is predictable and the same each day, this can be done by programmed tracking. The earth terminal requires two axis motion capability, preferably with a tilted polar axis so as to allow uniform motion about one axis only (most of the time). The larger (11 m) earth terminals are likely to have these capabilities. The smaller sizes (5 m) may have a significant cost impact in order to implement tracking.

Polarization also must be tracked by the earth terminal. This can be accomplished at low cost by a mechanical feed horn rotator or electromagnetic electric field rotator in the feed horn, using table look-up information.

Satellite Component	Mass (kg)	
	Change	Total
Attitude	+1	26
Power	+178	295
Propulsion	0	48
Structure	+76	174
Thermal	+20	40
TT&C	0	27
Antenna	+60	80
Transponders	+100	180
Margin	+65	75
Total (dry mass)	+500	945
Stationkeeping fuel	-70	30
Attitude control fuel	0	15
Total (BOL mass)	0	990

Table VII-9: ACE Trunking Satellite

2.3 ACE Trunking Satellite

2.3.1 Design Overview

Table VII-6 summarizes the ACE trunking satellite design. The satellite dry mass is increased by 500 kg on account of the increased launch capacity of the PAM D perigee stage for the ACE orbit

A fully reconfigurable antenna with 2.4 m diameter and 2° beam size is used. The transponder configuration is increased to 48 SSPA transponders with 36 MHz bandwidth and 9 W power. Four times frequency reuse is required either with one half-CONUS beam plus three spot beams or four regional spot beams.

2.3.2 ACE Satellite Differences

The differences of the ACE orbit satellite design compared to the baseline GEO trunking design concept are discussed by subsystem.

Table VII-9 summarizes the subsystem mass for the ACE trunking satellite design compared to the baseline GEO design. The reduced stationkeeping fuel requirements and increased launch capability for this orbit (see Table VI-4) allow a larger payload.

Attitude Control Subsystem

The ACE orbit satellite requires a varying antenna despin rate depending on position in the orbit. The change is relatively slow and is predictable. There is no mass impact. An additional 1 kg is required for a panoramic earth sensor.

Payload for Communications

The antenna size is increased from the 1.8 m baseline to 2.4 m (+10 kg), and the feed array is fully reconfigurable (+50 kg). The transponder mass is increased by 80 kg and there is an additional 20 kg in switches for interconnections among the four coverage regions.

Power Subsystem

An additional 40 W power is required for the reconfigurable antenna and an additional 700 W is required by the transponders.

An additional 85% solar cell area is required to compensate for the increased degradation of the ACE orbit radiation environment, as well as 43 kg/kW additional mass for coverglass. (This figure reflects the fact that 2.5 times as many cells are required for the spinner versus the 3-axis design.)

Since the payload requires communications power only 8 hours out of the day, the impact of the ACE radiation environment on the spinner solar array can be offset by the use of more batteries as discussed in Subsection VI-2.3.

The net result is a required solar array output of 800 W and battery capacity of 320 Ah. Compared to the baseline GEO satellite, the mass impact for the ACE spinner is an increase in battery mass of 71 kg, an increase in solar array mass by 72 kg, and an increase in solar array coverglass mass of 35 kg. The total power subsystem mass increase is 178 kg.

Use of GaAs solar cells has approximately the same mass impact and may be required on account of the limited area for solar cells on the spinner satellite.

Structure Subsystem

Sizing to accommodate the increased payload adds 76 kg.

Thermal Subsystem

An additional 20 kg mass is required by the increased number of transponders.

Station and Attitude Control Fuel

The ACE orbit satellite requires 70 kg less station-keeping fuel than the equivalent GEO orbit satellite. No additional attitude control fuel is required.

Launch Size

The STS/PAM D combination allows launch of 990 kg BOL (945 kg dry) mass into ACE orbit, an increase of 430 kg BOL (500 kg dry mass) over the comparable GEO launch. The mass as loaded in the Shuttle (BOL mass + apogee fuel + perigee motor + cradle) is 4,530 kg (9,966 lb). The required length in the Shuttle is 3.61 m (142 in).

2.3.3 Impact on ACE Earth Terminals

Earth stations are required to follow the daily motion of the satellite across the sky. Since the motion is predictable (the same each day), this can be done by programmed tracking. The earth terminal requires two axis motion capability, preferably with a tilted polar axis so as to allow motion about one axis only. (Note that in contrast to STET orbit satellites, ACE orbit satellite motion is not uniform but is the same each day.) The larger (11 m) earth terminals are likely to have these capabilities. The smaller sizes (5 m) may have a significant cost impact in order to implement tracking.

Polarization also must be tracked by the earth terminal. This can be accomplished at low cost by a mechanical feed horn rotator or electromagnetic electric field rotator in the feed horn, using table look-up information.

2.4 Alternate ACE Design (ACE*)

2.4.1 Design Overview

The alternate ACE design concept, called the ACE*, keeps the same GEO payload mass but can use a smaller perigee motor. The transpon-

Satellite Component	Mass (kg)	
	Change	Total
Attitude	+1	26
Power	+46	163
Propulsion	0	48
Structure	0	98
Thermal	0	20
TT&C	0	27
Antenna	+24	44
Transponders	0	80
Margin	-1	9
Total (dry mass)	+70	515
Stationkeeping fuel	-70	30
Attitude control fuel	0	15
Total (BOL mass)	0	560

Table VII-10: Alternate ACE* Trunk Satellite

der configuration is the same as that for the baseline GEO satellite. A antenna has a 1.6 m diameter, 3° beam size, and two 38-element feed arrays.

2.4.2 ACE* Satellite Differences

Table VII-10 summarizes the subsystem mass for the alternate ACE trunking satellite design compared to the baseline GEO design. The reduced stationkeeping fuel requirements and increased launch capability for this orbit (see Table VI-4) allow use of a smaller perigee stage.

Attitude Control Subsystem

The ACE orbit satellite requires a varying antenna despin rate depending on position in the orbit. The change is relatively slow and is predictable. There is no mass impact. An additional 1 kg is required for a panoramic earth sensor.

Payload for Communications

The antenna size is decreased from the 1.8 m GEO baseline to 1.6 m (-4 kg) and the feed array is fully reconfigurable (+28 kg). The transponder configuration is the same as the baseline.

Power Subsystem

An additional 20 W power is required for the reconfigurable antenna. An additional 85% solar cell area is required to compensate for the increased degradation of the ACE orbit radiation environment, as well as 43 kg/kW additional mass for coverglass.

The impact of the ACE radiation environment on the spinner solar array can be offset by the use of more batteries as discussed in Subsection VI-2.3. The required solar array output is reduced by 50% to 425 W and the battery capacity increased to 160 Ah since the satellite requires communications power only 8 hours out of the day.

Compared to the baseline GEO satellite, the mass impact for the ACE* spinner design is an increase in battery mass of 28 kg with the same solar array size. There is also an increase in solar array coverglass mass of 18 kg, giving a total power subsystem mass increase of 46 kg.

Station and Attitude Control Fuel

The ACE orbit satellite requires 70 kg less station-keeping fuel than the equivalent GEO orbit satellite. No additional attitude control fuel is required.

Launch Size

Total BOL mass is 560 kg, the same as the baseline GEO satellite. The mass as loaded in the Shuttle (BOL mass + apogee fuel + perigee motor + cradle) is 3,300 kg (7,260 lb). The required length in the Shuttle is 2.51 m (99 in).

A Morton Thiokol STAR 37FM solid rocket is used as perigee stage. Its dimensions are 37" diameter by 67" length versus the PAM D 48" dia. by 72" long. Since the satellite plus perigee stage sits vertical in the Shuttle bay, the Shuttle length is the same as for the baseline GEO satellite launch. However, this perigee stage has considerably less mass and is less expensive than the PAM D. A launch cradle for use in the Shuttle must be made rather than rented as for the PAM D.

2.5 Discussion of Trunking Systems

Table VII-2 gives a summary of the Trunking System definitions. All Trunking Satellite designs are spin stabilized. The main design drivers of the non-GEO designs compared to the GEO design are as follows:

- Larger mass can be launched into orbit.
- "Smart" antenna systems are required to follow changes in coverage region size and shape.
- Solar array size is doubled for ACE orbit on account of radiation environment. This is particularly difficult for spinner satellites which already require 2.5 times more solar cell area than a 3-axis satellite due to geometry.
- Solar array size can be reduced at the expense of increased battery mass on account of the low communications duty cycle (8 hr per 24 hr).

For the STET satellite, the number of transponders increases slightly and it is expected that economic performance will be about the same as the GEO satellite.

For the ACE satellite, the number of transponders is doubled and a significant performance improvement is expected. However, the power subsystem becomes large and requires use of GaAs solar cells on account of the limited solar cell area on the spinner satellite.

The ACE* satellite is relatively simple in that it keeps the same number of transponders as the GEO satellite, but uses a smaller perigee motor. Considering the small mass penalty of the ACE orbit, its economic performance should be very similar to the GEO satellite.

3 CPS Systems

The definitions of the three types of CPS systems are summarized in Table VII-3. Tables VII-15 through VII-18 give more details of the GEO, STET, and ACE orbit satellite designs. All CPS systems are based on a 3-axis satellite with high power Ku-band transponders.

mass as loaded in the Shuttle (BOL mass + apogee fuel + perigee motor + cradle) is 6,870 kg (15,114 lb). The required length in the Shuttle is 3.61 m (142 in).

3.2.3 Impact on STET Earth Terminals

Earth stations are required to follow the daily motion of the satellite across the sky. Since the motion is predictable (the same each day), this can be done by programmed tracking. The earth terminal requires two axis motion capability, preferably with a tilted polar axis so as to allow uniform motion about one axis only (most of the time). There is a significant cost impact in order to implement tracking on the CPS earth terminals.

Polarization also needs to be tracked by the earth terminal. This is easily accomplished by a mechanical feed horn rotator or electromagnetic electric field rotator in the feed horn.

3.3 ACE CPS Satellite

3.3.1 Design Overview

Table VII-17 summarizes the ACE CPS satellite design. The approach for the ACE orbit satellite is to increase the payload to the limit of the PAM D2 perigee stage.

The transponder configuration is 48 TWTAs with 54 MHz bandwidth and 50 W power. Antenna size is considerably smaller (1.0 m versus 2.4 m) than the baseline due to the closer distance to earth. However, a fully reconfigurable antenna is required to allow for the changing coverage region shape and to partially compensate (2 dB) for increased atmospheric attenuation at low elevation angles. The six times frequency reuse is obtained by utilizing the capabilities of the reconfigurable antenna.

The configuration of the payload is a particularly difficult decision for this satellite. The launchable dry mass is more than double compared to the baseline GEO satellite (1,742 kg versus 831 kg). Simple addition of high power transponders is difficult for two reasons.

- It is difficult to get more frequency reuses due to the charging size and shape of the

Satellite Component	Mass (kg)	
	Change	Total
Attitude	+4	43
Power	+443	626
Propulsion	0	82
Structure	+120	273
Thermal	+50	100
TT&C	0	27
Antenna	+24	53
Transponders	+248	496
Margin	+42	42
Total (dry mass)	+931	1,742
Stationkeeping fuel	-131	30
Attitude control fuel	0	15
Total (BOL mass)	-30	1,820

Table VII-13: ACE CPS Satellite

coverage area.

- The radiation environment places an almost two times mass penalty on the solar array mass; coverglass thickness increases by 17 kg/kW and 85% greater cell area is required.

The conclusion is that this orbit is well suited to carrying a more complex payload such as reconfigurable antennas, regenerative repeaters, digital signal processors, and switches. However, for purposes of comparison with the other concepts, an increased number of transponders is used for the payload.

3.3.2 ACE Satellite Differences

Table VII-13 summarizes the differences in subsystem mass for the ACE trunking satellite design compared to the baseline GEO design. The reduced stationkeeping fuel requirements and increased launch capability for satellites in this orbit (see Table VI-4) allow use of the larger payload.

The major impact lies in the degradation of solar cells in the ACE orbit radiation environment. For this reason a lower power payload is better suited to this orbit. Fortunately, the low communications duty cycle (8 hr per 24 hr) allows a

compensating reduction in solar array capacity.

Attitude Control Subsystem

An additional 4 kg mass is required for the additional reaction wheel required for attitude control.

Payload for Communications

The antenna size is decreased from the 1.8 m baseline to 1.0 m (-16 kg) and the feed arrays are larger and fully reconfigurable (+40 kg). The transponder configuration is 248 kg heavier than that of the baseline GEO satellite.

Power Subsystem

An additional 60 W power is required for the reconfigurable antenna and 15 W power for attitude control operations with the reaction wheel. The change in number of transponders requires 2,530 W more power.

An additional 85% solar cell area is required to compensate for the increased degradation of the ACE orbit radiation environment, as well as 17 kg/kW additional mass for coverglass (3-axis satellite).

The impact of the ACE radiation environment on the spinner solar array can be offset by the use of more batteries as discussed in Subsection VI-2.3. The required solar array output can be reduced by approximately 50% to 3,000 W and the battery capacity increased to 990 Ah since the satellite uses communications power only 8 hours out of the day.

Compared to the baseline GEO satellite, the net result for the ACE satellite is an increase in battery mass of 216 kg while the solar array mass increases 176 kg plus 51 kg for the coverglass. The net power subsystem mass increase is 443 kg.

Structure

The structure mass increases by 120 kg on account of the larger satellite mass.

Thermal

The thermal subsystem mass increases by 50 kg.

Station and Attitude Control Fuel

This ACE orbit satellite requires 131 kg less station-keeping fuel than the baseline GEO orbit satellite. No additional attitude control fuel is required.

Launch Size

The STS/PAM D2 combination allows launch of 1,820 kg BOL (1,742 kg dry) into ACE orbit. This is an increase of 800 kg BOL (931 kg dry mass) over the comparable GEO launch. The mass as loaded in the Shuttle (BOL mass + apogee fuel + perigee motor + cradle) is 7,430 kg (16,346 lb). The required length in the Shuttle is 2.51 m (99 in). (Note that this is less than the baseline GEO case which requires the large sunshield on account of its 2.4 m antenna.)

3.3.3 Impact on ACE Earth Terminals

Earth stations are required to follow the daily motion of the satellite across the sky. Since the motion is predictable (the same each day), this can be done by programmed tracking. The earth terminal requires two axis motion capability, preferably with a tilted polar axis so as to allow motion about one axis only. (Note that in contrast to STET orbit satellites, ACE orbit satellite motion is not uniform. However, it is still predictable.) There is significant cost impact in order to implement tracking on the CPS earth terminals.

Polarization also needs to be tracked by the earth terminal. This is easily accomplished by a mechanical feed horn rotator or electromagnetic electric field rotator in the feed horn.

3.4 Alternate ACE CPS Satellite

3.4.1 Design Overview

An alternate approach for the ACE orbit satellite, called the ACE*, is to use a smaller perigee stage with the same payload mass as GEO. The reduced stationkeeping fuel requirements and increased launch capability for satellites in this orbit (see Table VI-4) allow use of the PAM D perigee stage rather than the baseline PAM D2. Table VII-14 summarizes the differences in sub-

Satellite Component	Mass (kg)	
	Change	Total
Attitude	+4	43
Power	+123	306
Propulsion	0	82
Structure	-3	150
Thermal	0	50
TT&C	0	27
Antenna	+5	34
Transponders	0	248
Margin	+5	5
Total (dry mass)	+134	945
Stationkeeping fuel	-164	30
Attitude control fuel	0	15
Total (BOL mass)	-30	990

Table VII-14: Alternate ACE* CPS Design

system mass for this alternate ACE* CPS satellite design compared to the baseline GEO design.

3.4.2 ACE* Satellite Differences

The transponder configuration is the same as the baseline GEO satellite. Antenna size is considerably smaller (0.8 m versus 2.4 m) than the baseline due to the closer distance to earth. However, a fully reconfigurable antenna is required to allow for the changing coverage region shape and to partially compensate (2 dB) for increased atmospheric attenuation at low elevation angles. Three times frequency reuse is obtained by utilizing the capabilities of the reconfigurable antenna.

Attitude Control Subsystem

An additional 4 kg mass is required for the additional reaction wheel required for attitude control.

Payload for Communications

The antenna size is decreased from the 1.8 m baseline to 0.8 m (-18 kg), and the feed arrays are fully reconfigurable (+23 kg). The transponder configuration remains the same as the baseline GEO satellite.

Power Subsystem

An additional 40 W power is required for the reconfigurable antenna and 15 W power for attitude control operations with the reaction wheel. The change in transponder configuration has no impact on power requirements.

An additional 85% solar cell area is required to compensate for the increased degradation of the ACE orbit radiation environment, as well as 17 kg/kW additional mass for coverglass (3-axis satellite).

The impact of the ACE radiation environment on the spinner solar array can be offset by the use of more batteries as discussed in Subsection VI-2.3. The required solar array output can be reduced to 1,600 W and the battery capacity increased to 560 Ah since the satellite uses communications power only 8 hours a day.

Compared to the baseline GEO satellite, the net result for the ACE satellite is an increase in battery mass of 96 kg while the solar array area stays the same. However, the solar array coverglass mass increases 27 kg, giving a total power subsystem mass increase of 123 kg.

Structure

The structure mass decreases by 3 kg on account of the smaller satellite mass.

Station and Attitude Control Fuel

This ACE orbit satellite requires 164 kg less station-keeping fuel than the baseline GEO orbit satellite. No additional attitude control fuel is required.

Launch Size

A PAM D perigee stage is used instead of the baseline PAM D2. The STS/PAM D combination allows launch of 990 kg BOL (945 kg dry) into ACE orbit. This is an change of -30 kg BOL (+134 kg dry mass) over the comparable GEO launch (using the PAM D2). The mass as loaded in the Shuttle (BOL mass + apogee fuel + perigee motor + cradle) is 4,530 kg (9,966 lb). The required length in the Shuttle is 2.51 m (99 in), the same as the baseline since the PAM D is 48" diameter by 72" long versus 63" dia. by 72"

long for the PAM D2. Thus the same length is used in the Shuttle but the mass is less.

3.5 Discussion of CPS Systems

Table VII-3 gives a summary of the CPS system definitions. All CPS designs are 3-axis satellites. The main design drivers of the non-GEO designs compared to the GEO design are as follows:

- Larger mass can be launched into orbit.
- "Smart" antenna systems are required to follow changes in coverage region size and shape.
- Solar array size is doubled for ACE orbit on account of radiation environment.
- Solar array size can be reduced at the expense of increased battery mass on account of the low communications duty cycle (8 hr per 24 hr).

For the STET satellite, the number of transponders increases and it is expected that performance will improve slightly due to economies of scale.

For the ACE satellite, the number of transponders is doubled and a significant performance improvement is expected. However, the power subsystem becomes large and is dominated by 264 kg of NaS batteries. There are also two 90-element reconfigurable antennas.

The ACE* satellite is relatively simple in that it keeps the same number of transponders as the GEO satellite, but uses a smaller perigee motor. Considering the small mass penalty of the ACE orbit, its economic performance should be very similar to the GEO satellite.

4 Summary

The system definitions which are used for the economic comparison of the next section (Section VIII) are summarized in Tables VII-2 and VII-4 through VII-7 for the trunking systems, and in Tables VII-3 and VII-15 through VII-18 for the CPS systems.

4.1 Satellite Payload

A further discussion of satellite payload is in order. The concepts defined in this section have used similar types of communication payloads for the non-GEO as for the GEO orbit satellites. This selection is made in part because of the study direction to investigate the use of non-GEO satellites to unload GEO satellite traffic peaks. Thus the emphasis is on duplicating GEO system performance.

However, the key (other than an overly crowded GEO arc) to use of non-GEO satellites lies in the discovery of a communications service that the non-GEO satellite can more advantageously supply than the GEO satellite. The payloads defined in this section do not address this task.

4.2 STET Versus GEO Satellites

From the standpoint of satellite design, the penalties associated with the STET orbit (more complex antenna, radiation shielding) are balanced by the increased payload which allows more transponders. Thus while satellite cost increases, satellite revenues also increase. Thus economic performance should be similar to the GEO design if the STET transponders can be sold for a similar price to the GEO transponders.

4.3 ACE Versus GEO Satellites

The penalties associated with the ACE orbit (more complex antenna, doubling of power subsystem mass) are considerable, but are more than offset by a doubling in payload mass. There is a large potential for increased satellite economic performance.

4.4 Spinner Versus 3-Axis Satellites

Generally speaking, the spinner satellite design has a cost advantage over the 3-axis design for smaller satellites. However, for the ACE orbit, the spinner design must be of low power due to the double effects of the radiation environment and the spinner geometry. Thus the spinner de-

sign is not suited for ACE orbit CPS applications.

4.5 Trunking Versus CPS Satellites

The non-GEO orbits appear to be more suitable for trunking applications (than for CPS) due to the fewer number of ground stations and the fact that larger ground stations are likely to have a tracking capability.

For CPS applications that are uplink power limited, there is potential for the non-GEO satellites to have better EIRP than GEO satellites due to decreased space loss. However, the antenna system has to be designed to subdivide the coverage area into smaller pieces.

Both trunking and CPS non-GEO satellites suffer less time delay of the communications signal — .15 s for the STET and .12 s for the ACE versus the .25 s up-down delay for the GEO satellite signal.

Baseline satellite type:	Satcom K2
EIRP (half CONUS):	49 dBW
Lifetime:	12 yr
On-board switching:	Among coverage regions
Launch vehicle:	Ariane 4 or STS/PAM D
Frequency band and bandwidth:	Ku-band, 500 MHz
– receive:	14.0 – 14.5 GHz
– transmit:	11.7 – 12.2 GHz
Antenna	
– type:	Offset parabolic, dual gridded
– number:	1
– size:	2.44 m
– mass:	29 kg
– feed array:	2 arrays, 80 elements each
– coverage (3 beams):	CONUS and E & W CONUS
– polarization:	H and V, linear
– dc power:	None
Transponders	
– type:	TWTA
– number:	24
– power:	50 W
– bandwidth:	54 MHz
– TWTA redundancy:	11 for 8
– receiver redundancy:	6 for 3
– mass:	248 kg
– dc power:	2,530 W
Spacecraft	
– type:	3-axis stabilized
– size (bus):	1.57 x 2.18 x 1.77 m
– mass, BOL/dry:	1,020/811 kg
includes station/attitude fuel:	209 kg
– power (EOL) at summer solstice:	2,900 W
– primary power:	Solar cells (thin silicon)
– batteries:	NaS, 180 Ah (48 kg)
– thermal control:	Heat pipes
– attitude and station keeping:	Hydrazine thrusters (ACTS)
– attitude pointing accuracy:	±0.07°
– apogee motor:	Solid propellant

Table VII-15: Baseline GEO Satellite Characteristics, CPS Service

EIRP (half CONUS):	49 dBW
Lifetime:	12 yr
On-board switching:	Among coverage regions
Launch vehicle:	Ariane 4 or STS/PAM D2
Frequency band and bandwidth:	Ku-band, 500 MHz
- receive:	14.0-14.5 GHz
- transmit:	11.7-12.2 GHz
Antenna	
- type:	Offset parabolic, dual gridded, fully reconfigurable.
- number:	1
- size:	2.3 m
- mass:	49 kg
- feed array:	2 arrays, 80 elements each
- coverage (4 beams):	East half CONUS; from N to S
- polarization:	H and V, linear
- dc power:	40 W
Transponders	
- type:	TWTA
- number:	32
- power:	50 W
- bandwidth:	54 MHz
- TWTA redundancy:	11 for 8
- receiver redundancy:	6 for 3
- mass:	330 kg
- dc power:	3,370 W
Spacecraft	
- type:	3-axis stabilized
- size (bus):	1.57 x 2.18 x 1.77 m
- mass, BOL/dry:	1,260/1,087 kg
includes station/attitude fuel:	173 kg
- power (EOL) at summer solstice:	3,800 W
- primary power:	Solar cells (thin silicon)
- batteries:	NaS, 40 Ah (12 kg)
- thermal control:	Heat pipes
- attitude and station keeping:	Hydrazine thrusters (ACTS)
- attitude pointing accuracy:	$\pm 0.07^\circ$
- apogee motor:	Solid propellant

Table VII-16: STET Satellite Characteristics, CPS Service

EIRP (half CONUS):	49 dBW
Lifetime:	12 yr
On-board switching:	Among coverage regions
Launch vehicle:	Ariane 4 or STS/PAM D
Frequency band and bandwidth:	Ku-band, 500 MHz
– receive:	14.0-14.5 GHz
– transmit:	11.7-12.2 GHz
Antenna	
– type:	Offset parabolic, dual gridded, fully reconfigurable.
– number:	1
– size:	1.0 m
– mass:	53 kg
– feed array:	2 arrays, 90 elements each
– coverage (6 beams):	East half CONUS; spot beams.
– polarization:	H and V, linear
– dc power:	60 W
Transponders	
– type:	TWTA
– number:	48
– power:	50 W
– bandwidth:	54 MHz
– TWTA redundancy:	11 for 8
– receiver redundancy:	6 for 3
– mass:	496 kg
– dc power:	4,060 W
Spacecraft	
– type:	3-axis stabilized
– size (bus):	1.57 x 2.18 x 1.77 m
– mass, BOL/dry:	1,820/1,742 kg
includes station/attitude fuel:	45 kg
– power (EOL) at summer solstice:	3,000 W
– primary power:	Solar cells (thin silicon)
– batteries:	NaS, 990 Ah (264 kg)
– thermal control:	Heat pipes
– attitude and station keeping:	Hydrazine thrusters (ACTS)
– attitude pointing accuracy:	±0.07°
– apogee motor:	Solid propellant

Table VII-17: ACE Satellite Characteristics, CPS Service

EIRP (half CONUS):	49 dBW
Lifetime:	12 yr
On-board switching:	Among coverage regions
Launch vehicle:	Ariane 4 or STS/PAM D
Frequency band and bandwidth:	Ku-band, 500 MHz
– receive:	14.0-14.5 GHz
– transmit:	11.7-12.2 GHz
Antenna	
– type:	Offset parabolic, dual gridded, fully reconfigurable.
– number:	1
– size:	0.8 m
– mass:	34 kg
– feed array:	2 arrays, 72 elements each
– coverage (3 beams):	East half CONUS; from N to S.
– polarization:	H and V, linear
– dc power:	40 W
Transponders	
– type:	TWTA
– number:	24
– power:	50 W
– bandwidth:	54 MHz
– TWTA redundancy:	11 for 8
– receiver redundancy:	6 for 3
– mass:	248 kg
– dc power:	2,530 W
Spacecraft	
– type:	3-axis stabilized
– size (bus):	1.57 x 2.18 x 1.77 m
– mass, BOL/dry:	990/945 kg
– includes station/attitude fuel:	45 kg
– power (EOL) at summer solstice:	1,600 W
– primary power:	Solar cells (thin silicon)
– batteries:	NaS, 560 Ah (144 kg)
– thermal control:	Heat pipes
– attitude and station keeping:	Hydrazine thrusters (ACTS)
– attitude pointing accuracy:	$\pm 0.07^\circ$
– apogee motor:	Solid propellant

Table VII-18: ACE* Satellite Characteristics, CPS Service

Section VIII

ECONOMIC COMPARISON

1 Introduction

This section presents an economic comparison between the GEO and non-GEO systems presented in Section V and defined in Section VI. The economic assessment is based on the Financial Model for commercial communications satellite systems developed by Ford Aerospace and Coopers and Lybrand under NASA/LeRC contract number NAS3-24253, *Communications Satellite Systems Operations with the Space Station*.

The Financial Model is described in Subsection 2 and the methodology used to determine economic performance in Subsection 3. Subsections 4 and 5 give the economic performance of the different satellite systems.

- Trunking systems:
 - Baseline GEO system
 - STET non-GEO system
 - ACE non-GEO system
- Customer premise systems:
 - Baseline GEO system
 - STET non-GEO system
 - ACE non-GEO system

Subsection 6 summarizes the conclusions.

2 Financial Model

The communications satellite financial model (the Model) describes quantitatively the economics of the space segment of U. S. domestic Fixed Satellite Service (FSS) communication

satellite systems. The Model describes the economic status of the system throughout the lifetime of the satellite beginning with its design and continuing through its construction, launch, and commercial operations. Ground terminals and terrestrial system costs are excluded from consideration except for those systems required for satellite telemetry, tracking, and control.

A detailed description and operators manual for the Model is found in the Final Report for NASA/LeRC contract number NAS3-24253, *Communications Satellite Systems Operations with the Space Station*.

2.1 Model Assumptions

Model assumptions consist of the various input data necessary to operate the Model. They can be grouped in six categories which are discussed in turn.

1. System characteristics
2. Capital expenditures
3. Revenues
4. Operating expenditures
5. Financing activities
6. Taxes

2.1.1 System Characteristics

The first step in determining system economic performance is to describe the satellite system characteristics which drive both revenues and costs. These characteristics have been discussed in Section VII and summarized in Tables VII-1 and VII-2.

2.1.2 Capital Expenditures

A capital expenditure is normally an outflow of cash which is generated from debt or equity and is used to obtain an asset with a useful life usually exceeding one year. For a satellite operator, capital expenditures are comprised of the following costs.

- Satellite
- Perigee stage
- Launch (STS or Ariane)
- Launch operations
- Mission operations
- Launch insurance

The cash outflows for capital expenditures are predetermined by milestone billing schedules negotiated between the operator and the manufacturer for the satellite and related services. The major categories of capital expenditures are discussed in the following paragraphs.

Satellite Costs

Satellite costs are developed from the Ford Aerospace database using the PRICE H cost model. The PRICE (Parametric Review of Information for Costing and Evaluation) H (Hardware) Model is a computerized method for deriving cost estimates of electronic and mechanical hardware assemblies and systems.

In order to use PRICE H, the first step is to create and store the hardware parametric data. Separate data files are created for the seven satellite subsystems.

- Attitude control
- Power
- Propulsion
- Structure
- Thermal
- TT&C
- Payload (Antenna and Transponder)

PRICE H outputs another category, integration and test, which is based on the input data.

The second step involves an interaction between the user and the PRICE H model to calibrate the PRICE H output. The Ford Aerospace satellite cost database is used to validate the satellite costs.

A G&A expense of 12% and manufacturer's fee of 12% is added to the PRICE H output to determine the satellite cost which is an input to the Model. The cost excludes STS launch costs, perigee stage costs, launch operations, mission operations, and launch insurance.

Perigee Stage Costs

Separate perigee stages are assumed to be provided by the PAM D and the PAM-D2. Prices and payment schedules for these stages are determined from McDonnell Douglas published prices.

Launch Costs

The STS launch cost is calculated based on the load factor and anticipated launch date. The launch costs in the Model are priced using current NASA rates and escalation factors. The launch cost is assumed to be contracted directly by the operator with NASA, and thereby avoids an allocation of the manufacturer's G&A expense and fee.

Launch and Mission Operations

Launch support and mission operations costs are derived from Ford Aerospace experience. These costs include installation of the satellite in the launch vehicle and telemetry, tracking, and control during launch and checkout and during station keeping operations.

Launch Insurance

It is assumed that launch insurance in the 1994 time frame will be priced at 20% of insured value for typical GEO satellites with a good history of success. This price assumes that the industry has had successful launches and placements of satellites in service sufficient to allow a drop in rates from the present level of 30% (if available).

Rates for the STET and ACE orbit satellites are assumed to be 20%, the same as their GEO counterparts. However, non-GEO satellites may encounter insurance problems due to their unique aspects.

Payment Schedules

This study assumes that 90% of the total contract value is paid during satellite construction and the remaining 10% is paid at completion of checkout with a warranty payback.

2.1.3 Revenues

Project revenues are affected by five related factors.

1. Characteristics of transponder
 - Bandwidth
 - Frequency band of operation
 - Power
 - Transponder type
2. Degradation of satellite
 - Transponder availability
3. Market factors
4. Price of transponder
5. Utilization of satellite

2.1.4 Operating Expenditures

An operating expenditure is a cost incurred in the normal operations of the firm to sustain and support day to day activities. There are four categories of operating expenditures in this model.

- Life insurance
- Other expenditures
- Rate of inflation
- Telemetry, tracking, and control

2.1.5 Financing Assumptions

General Balance Sheet financing is assumed. This means that the sources of funds come from internally generated equity and general company debt. A debt-to-total asset ratio of 45% is assumed.

Money is borrowed as needed during the construction period. During this time, the principal accrues and only interest is paid. Once the satellite becomes operational, level monthly payments of principal and interest are made for five years.

The interest rate charged during the construction period and during operation is assumed to be variable and equivalent to the prime rate plus two points. The prime rate is assumed to be 9% for satellites launched in 1994.

2.1.6 Tax Assumptions

All tax computations are based on the 1985 Internal Revenue Code, and it is assumed that the owner/operator is a U.S. corporation. All tax benefits are utilized at the marginal tax rates when generated. These benefits consist of investment tax credits and depreciation.

The tax code had a major revision in 1986, and as of the end of 1986 there is new discussion of a change in maximum tax rates. Since the evolution of the tax code to the 1990s is not clear, the 1985 code is used for the purpose of economic comparisons of satellite systems. This is not a significant factor for comparisons of similar systems.

2.2 Financial Analysis

The Financial Model provides the user with three measurements of economic performance.

- Net present value of project
- Internal rate of return on equity
- Dual terminal rate of return on equity

The internal rate of return (IRR) for an investment is that rate which, when used to discount both positive and negative cash flows back to time zero, results in a present value equal to

zero. Once generated, an investment's IRR is an effective means of comparing alternative investments (regardless of the magnitude) and can also be used to evaluate individual transactions by comparing the IRR to the investor's marginal cost of capital or investment rate.

The dual terminal rate of return (DTRR) will be used for evaluation of economic performance in this study. The DTRR is similar in concept to the IRR computation except that positive cash flows are reinvested at the target rate (i.e. 18%) and not the DTRR rate. The net result is a more conservative estimate of improvements in economic performance.

3 Methodology

The methodology used to compare economic performance of GEO and non-GEO satellite systems is as follows.

- Start with 1985 GEO satellite designs
- Predict end-of-1990 technology
- Evolve 1985 GEO satellites to 1994 launch date designs
 - These are the “baseline” GEO trunking and CPS designs described in Section VII.
- Use the Financial Model to calculate the baseline satellite system initial rate-of-return (DTRR).
- Adjust the baseline transponder price until the rate of return equals 18%.
 - The results are basic transponder prices of \$1.65 M/yr (C-band, 9 W, 36 MHz) and \$2.14 M/yr (Ku-band, 50 W, 54 MHz).
- Modify the baseline GEO satellite designs as per the system definitions of Section VII.
 - The results are the STET and ACE non-GEO designs for trunking and CPS applications.

Satellite Design	Capital Cost, \$M	
	Trunking	CPS
GEO	81.47	116.58
STET	94.41	134.49
ACE	127.24	172.65
ACE*	88.05	110.12

Table VIII-1: Capital Expenditures

Satellite Design	Rate of Return, %	
	Trunking	CPS
GEO	18.00	18.00
STET	18.13	19.43
ACE	20.47	20.98
ACE*	17.79	18.42

Table VIII-2: Rate of Return (DTRR)

- Use the Financial Model to determine economic performance of the non-GEO satellite designs:
 - Rates of return for non-GEO designs.
 - Non-GEO transponder prices which give 18% rate of return.

Table VIII-1 compares the total capital expenditures in 1986 dollars for the different satellite designs. Capital expenditures are for one satellite and include satellite cost, STS launch cost, perigee stage cost, launch support cost, mission operations, and launch insurance at 20% (details given in Tables VIII-5 and VIII-6).

Table VIII-2 gives the dual terminal rate-of-return (DTRR) for the six satellite types that are analyzed, based on a fixed transponder price of \$1.65 M yearly lease fee for C-band (9 W, 36 MHz) and \$2.14 M for Ku-band (50 W, 54 MHz) transponders.

Table VIII-3 turns the question around and gives the transponder price corresponding to an 18% rate-of-return (DTRR) for the eight satellite types that are analyzed. This is perhaps more reasonable since in an open market, the non-GEO transponders would be expected to sell at a discount from their GEO counterparts.

Satellite Design	Transponder Price (\$M/yr)	
	Trunking	CPS
GEO	1.65	2.14
STET	1.63	1.84
ACE	1.27	1.56
ACE*	1.69	2.05

Table VIII-3: Transponder Prices (18% Return)

4 Economic Performance

4.1 Summary of Payloads

Table VIII-4 summarizes the transponder payloads on the different satellite designs. Note that the same types of transponders are used on the different trunking and CPS designs respectively. The assumed lease fee per transponder-year is based on an 18% rate-of-return as given in Table VIII-3.

4.2 Capital Expenditures

The capital expenditures for the three trunking systems (baseline GEO, STET, and ACE) are detailed in Table VIII-5, and the three CPS systems are given in Table VIII-6. The considerable variation in satellite costs among the GEO, STET, and ACE designs is simply related to the number of transponders in the payload. There is variation in STS launch costs based on length and mass of the satellite plus perigee stage. There are also changes in perigee motor costs depending on what is used. The mission operations become more expensive for shorter period orbits due to the necessity to only make orbital adjustments while the satellite is in view of the control station; (i.e. more time is required for mission operations). Launch insurance is calculated at 20% (effective 24% of all capital costs except insurance).

4.3 Rates of Return

The Financial Model considers expenditures and revenues to calculate rate of return (DTRR) on investment. The results are given in Table VIII-

2. It is evident that a better rate of return is obtained with the non-GEO compared to the baseline GEO satellite. This is primarily due to the use of the greater payload to generate additional revenues and the consequent economies of scale of larger payload satellites.

It is evident from comparison of the GEO and ACE* designs (same payload) that there is little intrinsic difference in economic performance between orbits. The savings in launch costs are balanced by the costs of the ACE orbit (i.e. complex antenna and oversize solar arrays). In addition there are further ground terminal costs for the non-GEO satellite systems which have not yet been considered (see Subsection VIII-4.5).

4.4 Transponder Prices

Table VIII-3 indicates the potential for transponder price reductions for the non-GEO orbit designs. The tabulated transponder lease fees are adjusted to give the operator a uniform 18% dual terminal rate of return (DTRR). For example, the CPS ACE design could be priced \$0.58 M/yr less than the CPS GEO design and still make an 18% return on investment.

Although the tabulated prices for the ACE* trunking and CPS designs and the STET trunking design are competitive with the baseline GEO transponder prices, there probably must be an incentive (i.e. lower prices) to use these designs. This is particularly true since additional costs for a tracking ground terminal have not yet been considered. However if the GEO arc is full, there is no penalty (other than a tracking ground terminal) for use of these non-GEO designs and they may be acceptable.

More interesting are the STET CPS concept which has a 14% price reduction and the trunking and CPS ACE designs which have 23% and 27% transponder price reductions respectively. These reductions may be enough to make a carrier prefer the non-GEO system.

4.5 Ground Terminal Costs

The consideration of ground terminal costs can be approached by considering how much additional expense is required to build a new ground

Satellite System			Transponders			
System	Orbit	Freq. Band	Number	Power (W)	Bandwidth (MHz)	Lease Fee (\$ M/yr)
Trunking	GEO	C	24	9	36	1.65
	STET	C	30	9	36	1.63
	ACE	C	48	9	36	1.27
	ACE*	C	24	9	36	1.69
CPS	GEO	Ku	24	50	54	2.14
	STET	Ku	32	50	54	1.84
	ACE	Ku	48	50	54	1.56
	ACE*	Ku	24	50	54	2.05

Table VIII-4: Transponder Payloads for Different Satellite Designs

Capital Expenditure	Cost in \$ M, (1986)			
	GEO	STET	ACE	ACE*
Satellite cost	39.30	48.60	73.40	44.20
STS launch cost	16.01	22.46	22.46	15.93
Perigee cost	6.20	6.20	6.20	3.00
Launch support cost	1.63	1.63	1.63	1.63
Mission operations	2.56	3.20	3.80	3.80
Launch insurance	15.77	18.27	24.63	16.46
Total	81.47	94.41	127.24	85.05

Table VIII-5: Capital Expenditures for Trunking Satellites

Capital Expenditure	Cost in \$ M, (1986)			
	GEO	STET	ACE	ACE*
Satellite cost	53.70	66.50	94.50	59.60
STS launch cost	25.43	26.43	28.41	17.58
Perigee cost	10.70	10.70	10.70	6.20
Launch support cost	1.63	1.63	1.63	1.63
Mission operations	2.56	3.20	3.80	3.80
Launch insurance	22.56	26.03	33.41	21.31
Total	116.58	134.49	172.65	110.12

Table VIII-6: Capital Expenditures for CPS Satellites

terminal that can track the non-GEO designs. Other issues such as siting may be important but are more difficult to quantify and are not considered. (For instance, can the earth station "see" to within 10° of the horizon, and are the permissible ground transmit flux density limits exceeded?)

The ground terminal tracking requirements are to follow the non-GEO satellite across the sky while it is above 10° elevation angle. The general path is a few degrees below the geostationary arc. The motion is uniform for the STET orbit and varying for the ACE orbit satellite. The satellite motion is the same every day; i.e. the satellite is in the same place in the sky at the same time each day. Thus a programmed track capability is adequate. A beacon autotrack system is not required.

4.5.1 Trunking Ground Terminals

A large (11 m) trunking terminal may cost \$500,000 to \$1 M, and the non-GEO tracking requirements cost an additional \$50,000. The large terminal usually has a full motion capability and the only changes are the slow retrograde motion and the programmed track mode. For the trunking systems, two transponders may be utilized by only two ground terminals with full duplex transmission. This scenario can be analyzed from the viewpoint of the ground terminal operator for a \$1.6 M/yr transponder, 18% desired return on investment, and 12 yr lifetime. The additional 10% ground terminal cost plus additional maintenance of \$10,000/yr is equivalent to a \$0.03 M/yr transponder lease fee.

The conclusion is that this cost is not significant for the trunking transponder user. (However, other considerations such as siting will certainly make the GEO transponder the preferred choice unless there are some financial incentives for non-GEO transponder use.)

4.5.2 CPS Ground Terminals

The situation is quite different for CPS systems where many thousands of very small aperture terminals (VSATs) may share one transponder. VSATs have a size of 1.2 m or 1.8 m and are

covered by a blanket FCC license that is not site specific. The small terminal has the same tracking requirements although its gain is lower (and hence it has lower required tracking accuracy) than the large trunking terminal.

Motion capability is not present on VSATs which may cost from \$2,000 to \$10,000. It is estimated that an additional \$1,000 may be required to implement tracking for a \$5,000 VSAT. The implementation of tracking is likely to become an increasing burden for lower cost VSATs. The only reason the estimate is as low as \$1,000 is that a production run of 10,000 or more is estimated for a VSAT design.

Consider a scenario of 1,000 VSATs sharing a \$2 M/yr transponder with an 18% desired return on investment and 12 yr lifetime. The ground terminals cost \$5,000 each, with an additional \$1,000 being required for non-GEO tracking. Analysis shows that the additional ground terminal cost plus maintenance of \$200/yr/terminal is equivalent to a \$0.32 M/yr transponder lease fee.

For this scenario the conclusion is that the non-GEO transponder cost should be reduced from \$2.14 M (GEO) to \$1.82 M in order to allow for the additional operator expense of \$0.32 M/yr for the tracking ground terminal. This analysis would need to be carried out with actual numbers for the real system under consideration since it is very sensitive to the parameters used.

5 Conclusions

Conclusions of the economic analysis are as follows.

- Non-GEO satellites are competitive with GEO satellites.
- The STET orbit used for CPS service allows a 14% transponder price reduction.
- The ACE orbit allows about 25% transponder price reduction for both trunking and CPS service.
- The ground system impact of tracking the non-GEO satellite is not significant econom-

ically for the trunking system but can require a 15% transponder price reduction for the CPS VSAT system in order to compensate for the user's increased ground terminal costs.

Section IX

TECHNOLOGY REQUIREMENTS

1 Introduction

This section identifies and describes any enabling or critical technology required to implement the systems concepts proposed and defined in Sections VI and VII. In particular, technology shortfalls are given from the state-of-the-art expected to be achieved by the end of 1990 (Section V), assuming a business-as-usual advancement.

The following technologies are discussed.

- Antennas with reconfigurability
- Intersatellite links
- Solar cells resistant to radiation
- VSATs with tracking

In addition the following regulatory question should be pursued.

- Non-GEO interference requirements

2 Reconfigurable Antennas

The technology of MMIC phased arrays should be pursued at C-band and Ku-band in order to reduce the penalty associated with reconfigurable antenna systems.

The changing coverage region area and shape with time (as viewed from non-GEO orbit) require use of reconfigurable satellite antenna designs to control antenna losses and potential interference with ground terminals. The projected 1990 technology is ferrite-in-waveguide variable phase shifters, variable power dividers, and switching circulators. This technology has a substantial mass, volume, power, and cost penalty for multiple element antennas.

3 Intersatellite Links

The development of light weight intersatellite links (ISLs) should be pursued, both at 60 GHz and light wavelength. As discussed in Subsection VI-2.5, projected 1990 technology ISLs are too heavy to be economically incorporated in a satellite system unless they are specifically required by the mission.

Non-GEO systems in particular, with their limited coverage times, could be greatly enhanced by a feasible ISL. The problem with 60 GHz ISLs is their limited RF power and low efficiency. Optical ISLs are even heavier than 60 GHz ISLs.

4 Solar Cells

Satellites in certain non-GEO orbits such as the ACE orbit suffer a heavy penalty in solar array mass due to the adverse radiation environment (Appendix A) and the susceptibility of silicon solar cells to degradation.

Development of GaAs solar cells to be more competitive with the price of silicon cells would be a great help for satellites in these non-GEO orbits. Development of GaAs should concentrate on weight and cost reduction, and not just maximum efficiency.

5 Tracking VSATs

A requirement of non-GEO orbit satellites is that the ground terminal be capable of tracking. Very small aperture terminals (VSATs) of 1.2 m and 1.8 m size need to have developed an innovative tracking mechanism that is low cost in large quantities and requires little maintenance.

This may be a technology development that occurs naturally by industry as the requirement for VSATs and tracking grows. However, it should not be overlooked as it does impact system economic performance as the cost of the ground segment grows relative to the satellite.

6 Non-GEO Interference

The following two interference issues should be pursued.

- Regulations regarding interference among non-GEO and GEO systems.
- Interference of nonGEO-to-nonGEO ISLs with GEO-to-GEO ISLs.

Non-GEO satellites can interfere with equatorially-sited earth stations if the non-GEO satellite antenna pattern is not carefully controlled. Conversely, GEO ground stations may interfere with non-GEO satellites if the non-GEO ground antenna pattern is sloppy out of the equatorial plane.

The other issue is that of non-GEO ISLs sweeping across the GEO arc and potentially interfering with GEO ISLs.

Section X

SUMMARY AND CONCLUSIONS

This section provides a summary and discussion of the study conclusions and recommendations. The following ten points are discussed.

1. Non-GEO satellite-addressable traffic
2. Suitable non-GEO orbits
3. Non-GEO system concepts
4. Non-GEO satellite designs
5. Economic benefits of non-GEO satellites
6. Use of reconfigurable antennas
7. Radiation impact on non-GEO satellites
8. ACE versus STET non-GEO orbits
9. Tracking ground terminals
10. Regulation of non-GEO interference

The bottom line economic result is given in Table X-1, which is a duplicate of Table VIII-3. The projected transponder prices are given for the eight satellite systems modeled, given the constraint of 18% rate of return on money invested. Compared to the baseline GEO concepts, the ACE satellite shows up to a 27% decrease in transponder price.

1 Addressable Traffic

The satellite-addressable traffic has a double peak coinciding with the local business day (see Figure II-5, p. II-10). The majority of CONUS traffic lies in the Eastern and Central time zones. Satellites coverages of 8 hour continuous or two 3 hour separated by 5 hours are desirable.

Satellite Design	Transponder Price (\$M/yr)	
	Trunking	CPS
GEO	1.65	2.14
STET	1.63	1.84
ACE	1.27	1.56
ACE*	1.69	2.05

Table X-1: Transponder Prices (18% Return)

2 Suitable Non-GEO Orbits

Two suitable non-GEO orbits are proposed.

- ACE (Apogee at Constant time-of-day Equatorial) orbit
- STET (Sun-synchronous Twelve-hour Equatorial) orbit

The ACE orbit is a new orbit (patent applied for by Ford Aerospace) devised for the purpose of this study and which may be of use to NASA for other programs such as the *Voice of America* Broadcast Satellite.

These orbits are sun-synchronous to match the traffic throughout the year and require less energy to launch into orbit and less station-keeping fuel than comparable GEO satellites. The ACE orbit is described beginning on page II-23 and the STET orbit on page II-25.

Both these orbits lie in the equatorial plane and thus are only usable by higher latitude geographical locations such as CONUS sites. They can not be used for equatorial region communications since satellites in these orbits pass directly below the GEO arc satellites. The ACE orbit is separated from the GEO arc by $> 5.6^\circ$, and the STET orbit by a constant 3.0° for an

observer in Miami. The separation is greater at higher latitudes.

3 System Concepts

The limited coverage time of the STET and ACE orbits make a single satellite suitable for half CONUS coverage only. The high traffic Eastern/Central time zone region is selected for coverage. Two satellites in slightly different orbits (plus one ground spare) separated by several degrees form one system.

The expense of an intersatellite link between satellites to extend the coverage area or time is not judged to be economical. However, the use of ground terminals with dual feeds or fast slew between satellites could offer operational advantages.

4 Non-GEO Satellite Designs

Six non-GEO satellite designs are given in Section VII and summarized in Tables VII-2 and VII-3, for both ACE and STET orbits and for trunking and CPS applications. Both 3-axis and spin stabilized satellite designs are used.

The main design drivers of the non-GEO designs compared to the GEO are as follows.

- Larger mass can be launched into orbit.
 - 33% more dry mass for STET orbit.
 - 110% more dry mass for ACE orbit.
- “Smart” antenna systems are required to follow changes in coverage region size and shape as the satellite changes position.
- Solar array size increases on account of radiation environment. This is particularly difficult for spinner satellites which already require 2.5 times more solar cell area due to their geometry.
 - Area increases 15% for STET orbit.
 - Area increases 85% and mass doubles for ACE orbit.

- Solar array area can be reduced 50% at the expense of increased battery mass on account of the low communications duty cycle (8 hr per 24 hr).

5 Economic Analysis

Conclusions of the economic analysis are as follows.

- Non-GEO satellites are competitive with GEO satellites.
- The STET orbit used for CPS service allows a 14% transponder price reduction.
- The ACE orbit allows about 25% transponder price reduction for both trunking and CPS service (Table X-1).
- The ground system impact of tracking the non-GEO satellite is not significant economically for the trunking system but can require a 15% lower transponder price for the CPS VSAT system in order to compensate for the increased ground terminal costs of the user.

In addition to pure economic comparison, non-GEO satellites are an alternative to a “full” geostationary arc. The use of small non-GEO satellites could be particularly attractive for a small satellite system that normally would not warrant exclusive assignment of a valuable GEO orbital position.

6 Reconfigurable Antennas

The changing coverage region area and shape with time (as viewed from non-GEO orbit) require use of reconfigurable satellite antenna designs to control antenna losses and potential interference with ground terminals. The projected 1990 technology is ferrite-in-waveguide variable phase shifters, variable power dividers, and switching circulators. This technology has a substantial mass, volume, power, and cost penalty for multiple element antennas.

The technology of MMIC phased arrays should be pursued at C-band and Ku-band in

order to reduce the penalty associated with re-configurable antenna systems.

7 Radiation Impact

The non-GEO radiation environment (Appendix A) poses a severe penalty on two areas of the satellite.

- Shielding of electronics
- Solar cells

Fortunately, radiation-hard technology is an increasing concern and the technology forecast for hardness of 1990 piece parts mitigates the more severe (than GEO) radiation environment. However, the equivalent of an additional 100 mil Al is required for the STET orbit satellite. (The ACE orbit satellite does not need additional shielding.)

For the silicon solar cells used for GEO orbit, an increase of 15% cell area is required for STET orbit satellites to compensate for the increased radiation degradation. The situation is worse in ACE orbit, requiring 85% additional cell area in addition to 5 times (17 kg/kW) the cell cover glass mass. Thus GaAs cells with their greater radiation hardness may be attractive for ACE orbit satellites.

There are also radiation implications for the type of satellite. The more compact spin stabilized design with solar cells wrapped around its body provides better backside protection to its cells. However, the area available for solar cells is limited.

8 ACE Versus STET Orbit

The relative advantages and disadvantages of the ACE and STET orbits for non-GEO communications satellites are summarized below. (The +’s indicate an advantage and the -’s a disadvantage.)

ACE

- + Much less launch fuel
- + Much less station-keeping fuel

- + Smaller size antenna
- More complex antenna
- Short (< 3 hr) coverage time
- Non-uniform motion across the sky
- Radiation impact on solar cells

STET

- + Longer continuous coverage (up to 8 hr) than ACE orbit
- + Uniform motion across sky
- Large antenna size
- Radiation impact on electronics

9 Earth Terminal Tracking

The requirement for tracking the STET or ACE orbit satellite may impose a heavy burden for the small earth terminal. (Larger earth terminals already have two-axis tracking and slew capabilities.) However, with projected VSAT markets in the 10,000’s of terminals per application, private business is likely to act to minimize tracking VSAT costs.

10 Regulation of Interference

A potentially difficult issue is the interaction of GEO and non-GEO satellites with regards to interference. Fortunately, the STET and ACE satellites lie 15,000 to 20,000 km below the GEO satellites and the potential for satellite-to-satellite interference is slight unless intersatellite links (ISLs) are in use.

However, the potential for radiating non-GEO satellites to interfere with receiving earth terminals is great due to their changing position in the sky with time and the fact that for equatorial sites, the non-GEO satellites lie directly in front of the GEO satellites. Careful control of the non-GEO radiation pattern is required to keep sidelobes out of the equatorial regions.

Another issue is the interference of GEO ground terminal transmissions with non-GEO satellites. Since the FCC requirements for earth antenna sidelobes are more stringent in the equatorial plane (where 2° and 1° satellite spacing in

proposed) than perpendicular to the plane, there is significant potential for small GEO ground terminals to interfere with the non-GEO satellite (particularly STET).

Although non-GEO to non-GEO ISLs are not used for the systems of this study, ISLs could be of major value in extending coverage times. However, the non-GEO ISL would sweep along the GEO arc and potentially interfere with GEO-to-GEO ISLs. Regulations need to be developed to protect GEO users while still allowing the possibility of non-GEO to non-GEO ISLs.

APPENDIX A:
RADIATION EFFECTS

Appendix A

RADIATION EFFECTS

	Orbit Type			
	GEO	1	2	3
Name	GEO	STET	8 hr	ACE
Eccentricity	0	0	0	.49
Apogee (R_{\oplus})	6.62	4.17	3.19	3.37
Perigee (R_{\oplus})	-	-	-	1.16
Revs/day	1	2	3	5

Table A-1: Orbital Parameters

1 Radiation Environment

The geostationary communications satellite is positioned in a circular orbit in the equatorial plane at a distance of $6.62 R_{\oplus}$ (earth radii) from the center of the earth. Section III proposes three other lower orbits for communications satellite use:

1. $4.17 R_{\oplus}$ circular orbit; 12 hr period.
2. $3.19 R_{\oplus}$ circular orbit; 8 hr period.
3. $3.37 R_{\oplus}$ apogee, $1.16 R_{\oplus}$ perigee; 4.8 hr period.

Table A-1 summarizes the parameters for the three candidate orbits. All orbits have zero inclination, i.e. lie in the equatorial plane. Orbits 1 and 2 are circular and orbit 3 is elliptical. All orbits are sun-synchronous with differing integer number of orbits per solar day. The parameters for the geosynchronous orbit are included in the table for purposes of comparison.

The problem is to determine the location of these orbits in relation to the charged particles of the Van Allen belts and to assess the effects of the charged particles on the satellite design.

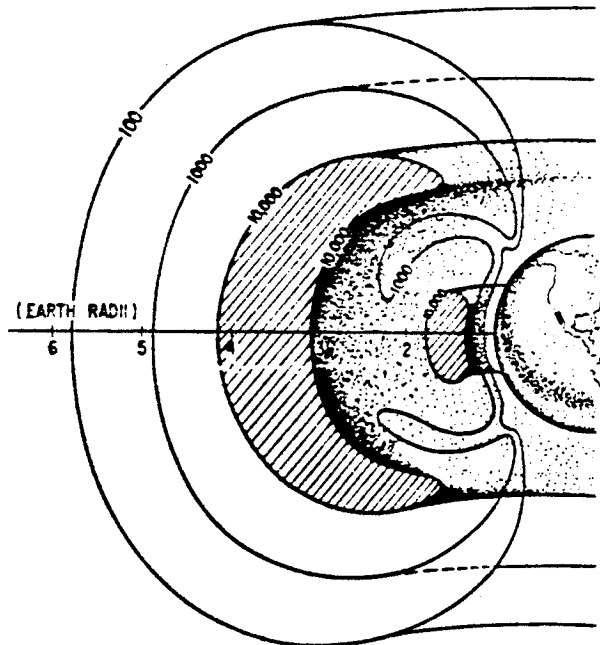


Figure A-1: Inner and Outer Van Allen Belts

1.1 Location of Van Allen Belts

Figure A-1 shows the inner and outer radiation belts as they were first mapped by Van Allen's group [White, 1970]. This figure shows the counting rates of particles energetic enough to penetrate the 1 gr/cm^2 lead shielding which covered the 1 cm^2 window of the Geiger counter.

The high counting rates of the inner belt (1.2 to $1.8 R_{\oplus}$) are produced by energetic protons with energies in the 10 to 100 MeV range. More detailed studies show that the spatial distribution of the trapped protons varies with their energy. The highly energetic protons peak near $1.5 R_{\oplus}$, but for protons of lower energies the belt moves farther out and the width of the belt increases considerably.

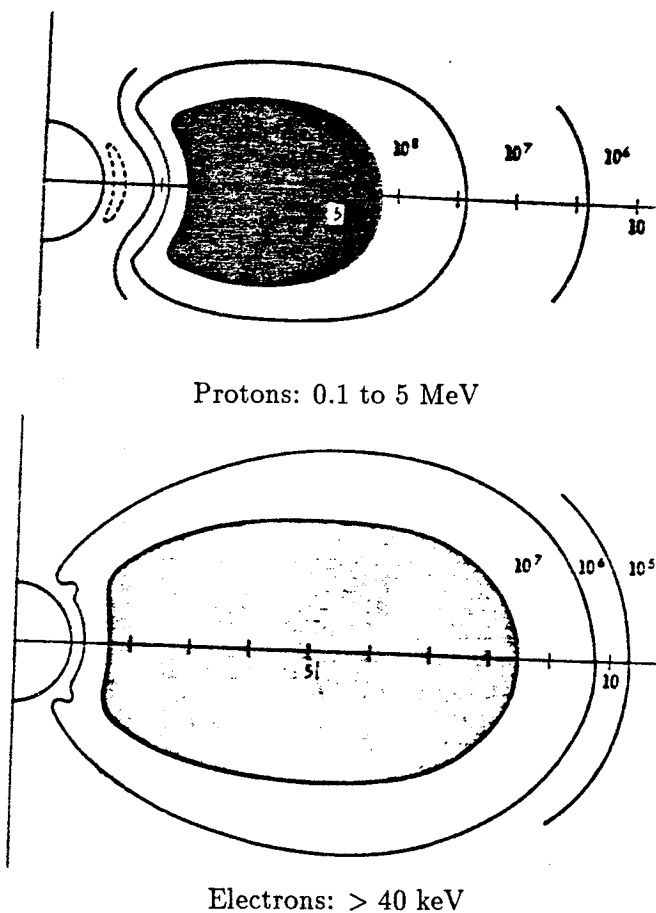


Figure A-2: Trapped Particle Distribution

The high counting rates of the outer belt (3.0 to 4.2 R_E) are produced by high energy electrons with energies in the 1 MeV range and above. For energies above 1 MeV, the belt is relatively narrow and peaks near 4 R_E while for electrons of lower energy the belt spreads out evenly over a much larger volume.

These effects are demonstrated in Figure A-2 which shows the approximate distribution of trapped electrons and protons of lower energy compared to the ones shown in Figure A-1. Contours are in units of particles per cm^2 per sec. For the more plentiful particles of lower energies, the concept of inner and outer belts disappears because the less energetic particles are distributed over a much wider range.

1.2 Influence of Solar Activity

The solar activity, which rises to a maximum every 11 years, affects the outer radiation zone in the following manner:

- The region of maximum intensity moves closer to the earth with increased solar activity.
- The maximum flux increase with solar activity, rising by a factor of 3 to 4 for energies around 500 keV.
- Alpha particles range around 2 to 5 MeV and show a peak around 3 R_E .

1.3 Radiation Dose for Orbits

A quantitative comparison of radiation environments for the different orbits is presented in Tables A-2 and A-3, and plotted in Figure A-3. The common unit of radiation measurement is Rad (Si) which stands for roentgen absorbed dose. The total radiation dose for the 12 year mission is calculated for different shielding thicknesses in mils (.001 in) of aluminum. A particular shielding thickness stops all radiation (particles) less than a certain energy. The typical GEO communications satellite effective shielding is 100 mils aluminum. Note that the effect of a particular shielding thickness depends on the distribution of particle energies in the orbit.

Table A-2 gives the relative dose for the different orbits compared to GEO for different shielding thicknesses. Included in these figures is the dose due to trapped (Van Allen) electrons only.

The typical satellite has 100 mils Al effective shielding divided equally among the satellite skin, the component box, and the component itself. For this 100 mil Al shielding, the STET orbit radiation dose is 17 times that of GEO and the ACE orbit dose is 3.3 times. (The radiation environment presented at the September 25 Review was in error for the ACE orbit in that it did not correctly include the low altitude electron total dose.)

The reason the 200 mil thickness ratios of Table A-2 (117 times GEO for STET and 20 times GEO for ACE) are much higher than the 100

Shielding Thickness (mils Al)	Relative Dose [Rad (Si)]		
	STET	8 hr	ACE
10	2.1	0.8	1.6
50	5.1	1.6	1.4
100	17.1	4.5	3.3
150	46.7	12.1	8.5
200	117.6	33.3	20.1

Table A-2: Normalized Total Radiation Dose

mil ratios is that the relative number of higher energy particles (> 2.8 MeV) is much higher for the STET and ACE orbits.

Table A-3 gives total dose (12 yr) for the GEO orbit and the three other orbits – STET, 8 hr circular, and ACE – described in Table A-1. Table A-3 contains the information from which Table A-2 is derived. Total dose is given in millions of Rad (Si). The satellite geometry is such that there is a slab effect and no back side dose, and the omnidirectional dose is reduced by a factor of four.

Figure A-3 plots the information of Table A-3. The conclusion is that 175 mils Al thickness is required for the ACE orbit in order to reduce the radiation environment to the same as GEO (100 mils Al). For the 8 hr orbit, 230 mils Al thickness is required. For the STET orbit, 330 mils Al thickness is required. Use of such excessive amounts of shielding would be unreasonable in view of the other methods to increase radiation resistance, which are described in the next subsection.

2 Impact on Satellite

There are a number of techniques that can be employed to harden the communications satellite equipment:

- Use thicker shielding
- Use selective piece part shields
- Use radiation hardened parts
- Redesign circuits

Shield Thick (mils)	Energy (MeV)	Total Dose for Orbit [10^6 Rad (Si)]			
		Geo	Stet	8 hr	Ace
10	.26	30.30	64.1	25.4	49.6
50	.85	3.61	18.3	5.7	5.0
100	1.50	.51	8.8	2.3	1.7
150	2.20	.09	4.0	1.0	.7
200	2.80	.02	2.2	.6	.4

Table A-3: Radiation Environment of Orbits

The most effective approach is a combination of the above methods.

2.1 Electronics

Table A-4 gives the projected improvements in hardness level of available piece parts for the 1990 to 2000 time frame. For the baseline year of 1990, GaAs technology and improved CMOS parts will be available that will allow basic wall thicknesses to be reduced by 50% over designs based on present day technology.

Considering the shielding thickness suggested by Figure A-3, the improvement in hardness levels (1990 technology) should allow the ACE and 8 hr orbit satellites to suffer no mass penalty versus a GEO satellite. However, the STET orbit satellite requires the equivalent of 100 mils Al shielding in addition to the harder piece parts. It is not expected that the GEO orbit satellite shielding mass (using 1990 technology) will decrease since the existing shielding is supplied by satellite structure.

Note that the shielding thickness is determined by the electron environment only. The typical 100 mil aluminum satellite shielding stops the much heavier protons and alpha particles.

2.2 Solar Array Design

The four orbit types of Table A-1 are analyzed as to solar array relative sizes (area and cover glass thickness) considering the radiation environments.

ORIGINAL PAGE IS
OF POOR QUALITY

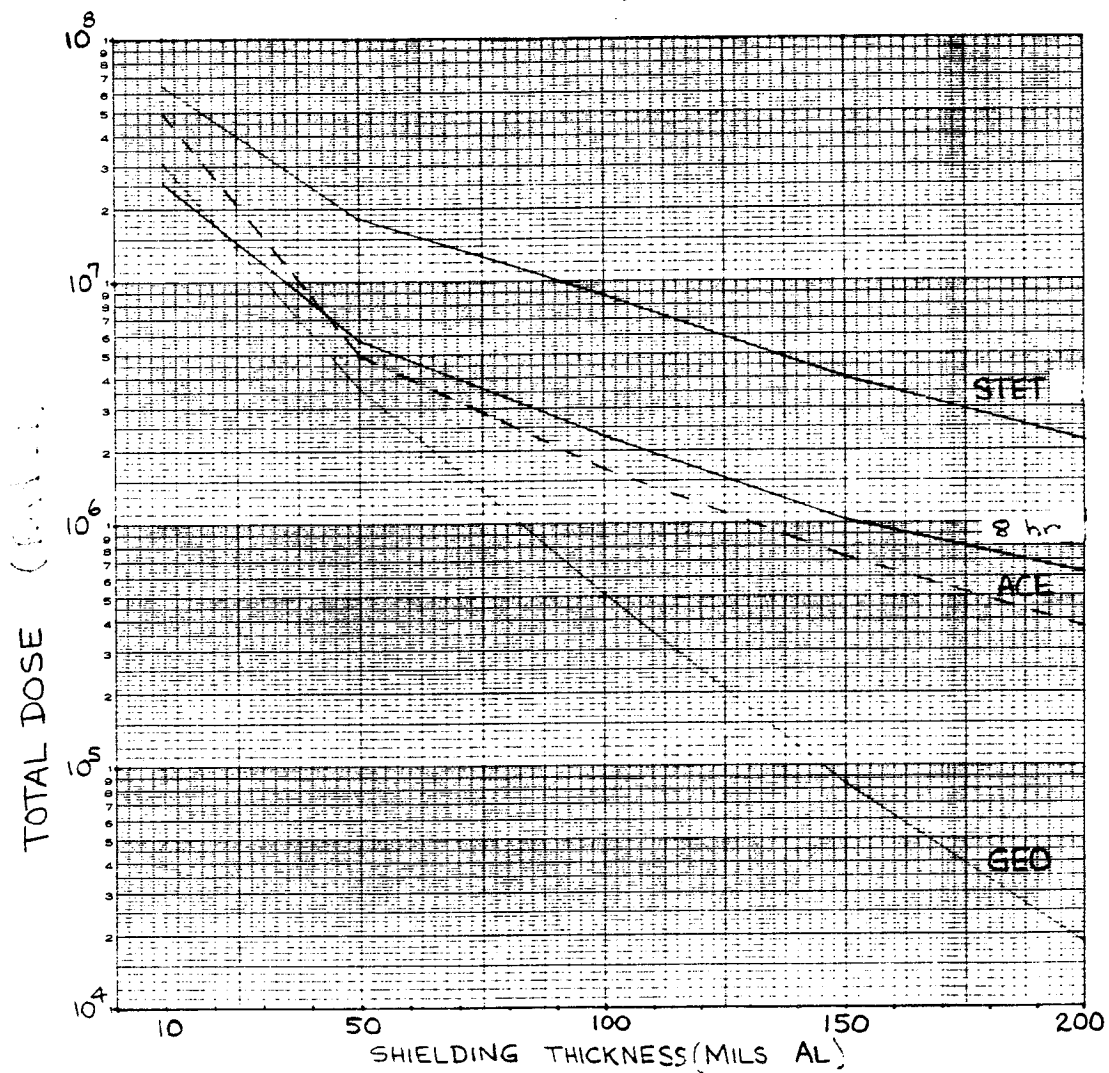


Figure A-3: Total Dose Versus Shielding Thickness for Different Orbits

Parameter/(Units)	1985	1990	1995	2000
Neutron hardness (n/cm ² (eV equiv))	10 ¹⁴	3 x 10 ¹⁴	10 ¹⁵	3 x 10 ¹⁵
Total dose hardness (Rad (material))	10 ⁴ to 2 x 10 ⁵	10 ⁵ to 10 ⁶ [a]	10 ⁷ to 10 ⁸ [b]	3 x 10 ⁸
Dose rate upset (Rad (material)/sec)	10 ⁹ to 10 ¹⁰	10 ⁹ to 3 x 10 ¹⁰	10 ⁹ to 3 x 10 ¹⁰	3 x 10 ¹⁰
Latchup level (Rad (material)/sec)	10 ⁸ to 10 ¹⁰	> 10 ¹¹ [c]	> 10 ¹¹	> 10 ¹¹
Single event upset (upsets/bit)/(particle/cm ²)	> 10 ⁻¹⁴	10 ⁻¹⁶ to 10 ⁻¹³ [d]	0 to 10 ⁻¹²	0 to > 10 ⁻¹⁰
Feature size (μm)	1.25 to 3	1.25	< 1.0	0.5
Operating power (mW)	10 to 50	25 to 50	50 to 100	50 to 200
Size	(16 kb)	(64 kb)	(256 kb)	(1 Mb)
Cycle time (ns)	50 to 200	25 to 100	12 to 50	5 to 20

Table A-4: System Level Projections for Radiation-Hardened Electronics Technology

- a. Improvement in hardened field oxides.
- b. GaAs devices available.
- c. CMOS/SOS devices available.
- d. Layout design solutions versus smaller feature size problem.

The solar cell used for analysis is that which will be used on the GOES series of satellites scheduled for launch in the early 1990s. It is a 200 μm silicon solar cell with antireflective coating to optimize light transmission and a back surface reflector to minimize cell heating. The cover glass used to protect the cell from the radiation environment is a borasilicate glass with cerium dioxide added for ultraviolet filtering. Data supplied by Spectrolab is used to determine radiation degradation factors as a function of coverglass thickness.

The results are summarized in four figures for the different orbits:

Figure A-4: GEO Orbit

Figure A-5: STET Orbit

Figure A-6: 8 Hour Orbit

Figure A-7: ACE Orbit

Results are presented for a 1 kW array, and give curves of array area versus coverglass thickness and coverglass mass versus coverglass thickness. The optimum design points are marked by circles on these figures.

Table A-5 summarizes the results of these figures. The coverglass thickness and mass, and cell area of a 1 kW solar array is given for a 12 year mission in the four different orbits. In each case, the optimum coverglass thickness to minimize array area without excessively increasing coverglass mass is chosen.

The reason the ACE orbit satellite solar array is more impacted than that of the STET (in contrast to the electronic piece parts) is that the proton environment is also included in the total dose. There is no satellite body or box shielding to protect the solar arrays.

The STET orbit satellite array is very similar to the GEO satellite. However, the ACE orbit satellite solar array is almost twice as large and has five times the mass of coverglass as the GEO satellite array.

Satellite Orbit	1 kW Array Parameter		
	Glass Thick (mils)	Glass Mass (kg)	Cell Area (m^2)
GEO	6	4	10.0
STET	6	4	11.5
8 hr	20	13	11.0
ACE	20	21	18.5

Table A-5: Solar Array Parameters (1 kW)

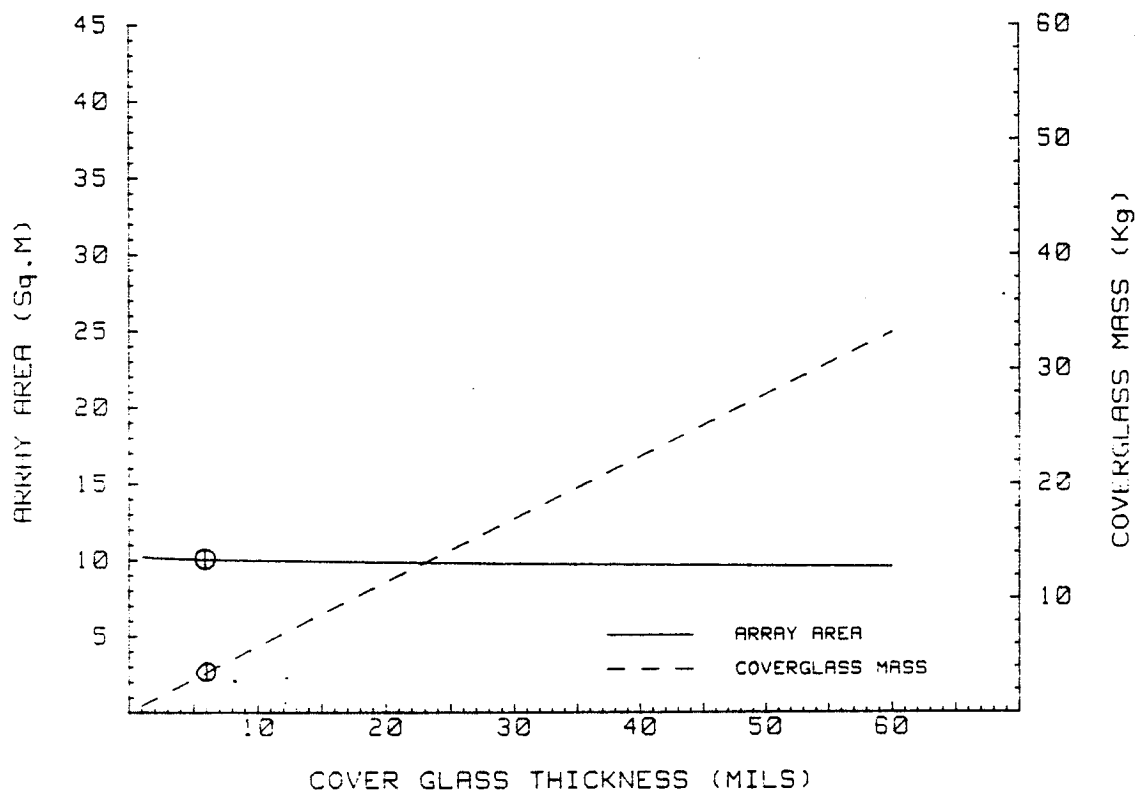


Figure A-4: Solar Array Parameters for GEO Orbit Satellite

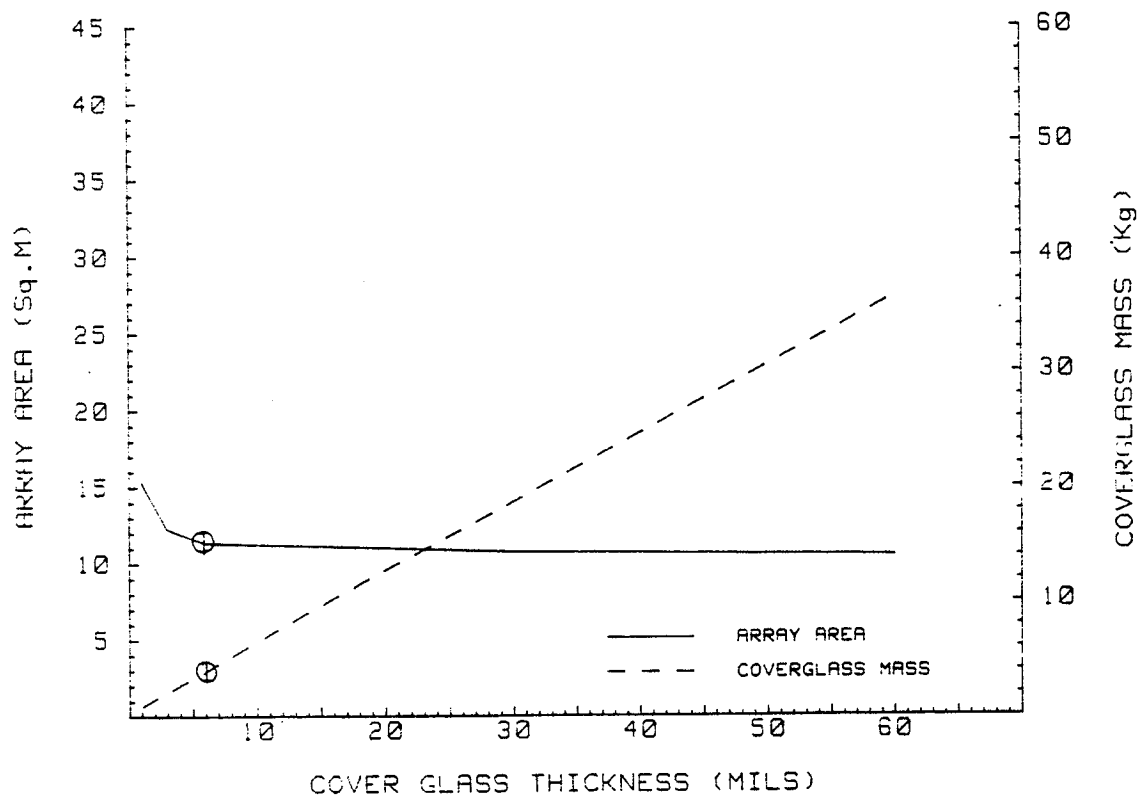


Figure A-5: Solar Array Parameters for STET Orbit Satellite

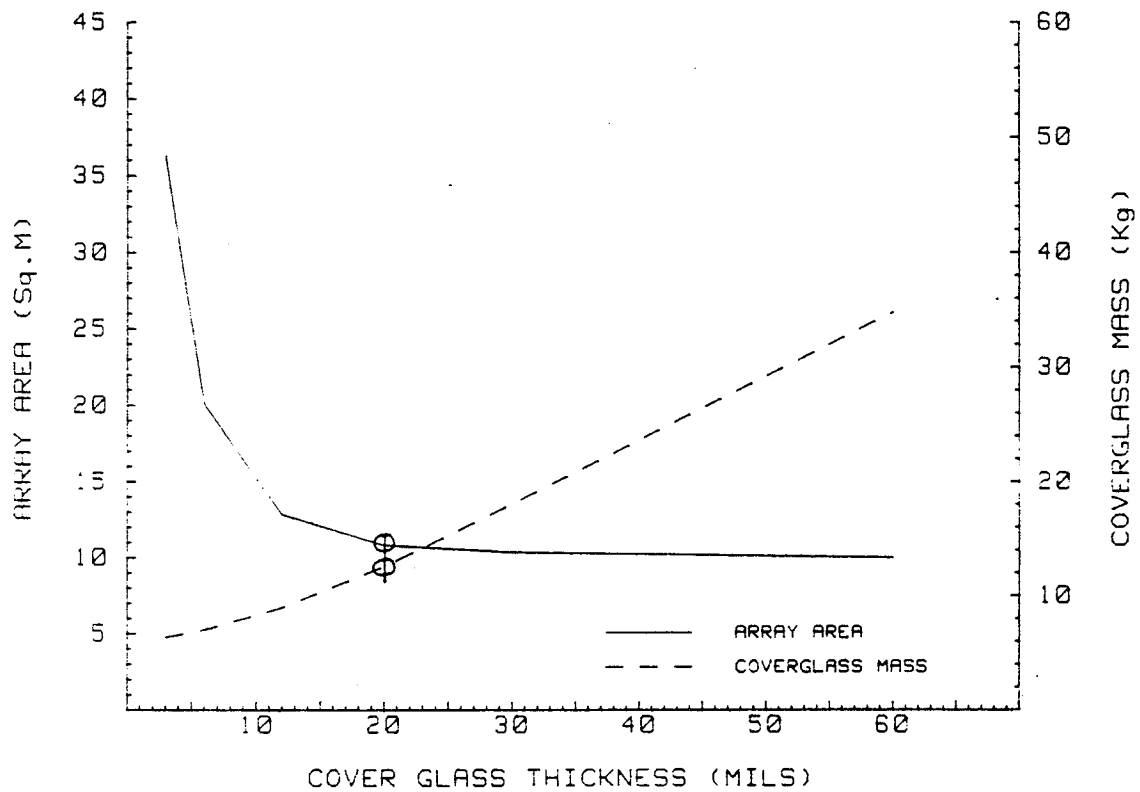


Figure A-6: Solar Array Parameters for 8 Hour Orbit Satellite

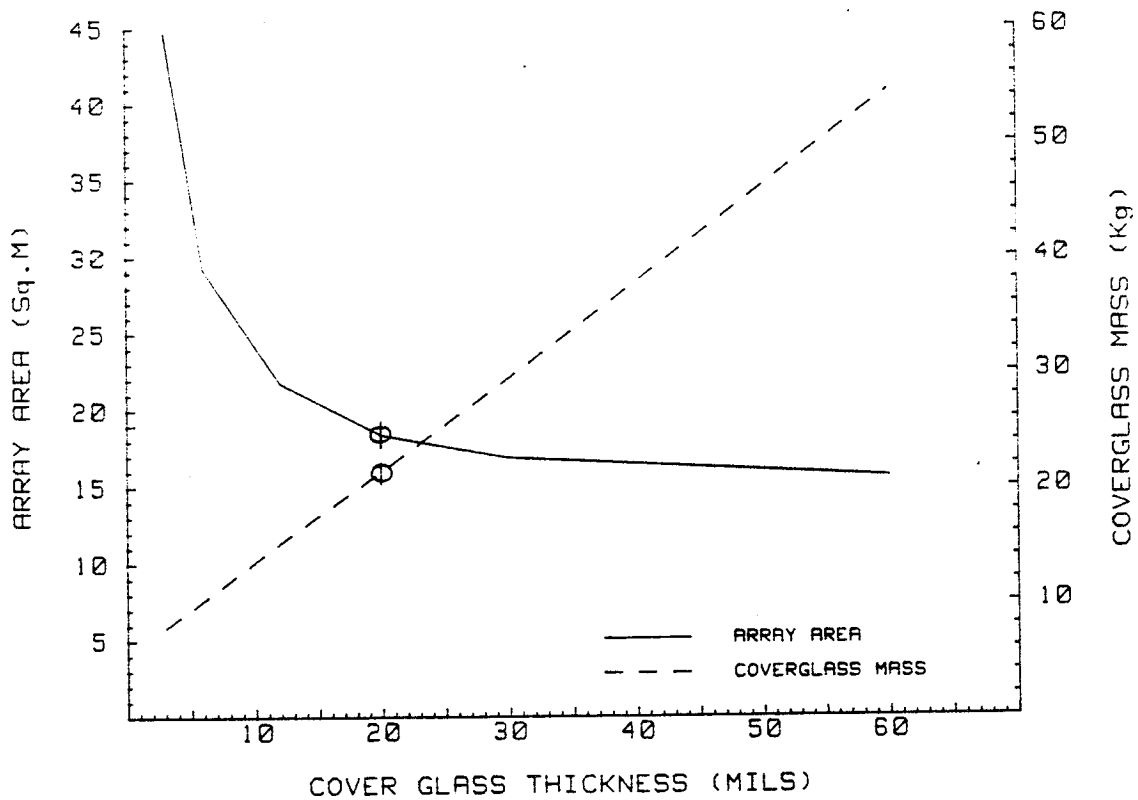


Figure A-7: Solar Array Parameters for ACE Orbit Satellite

APPENDIX B:
ANTENNA COVERAGE

Appendix B

ANTENNA COVERAGE

Figures B-1 thru B-3 compare the apparent size and shape of the eastern CONUS coverage region as viewed from satellites in three different orbital positions:

- B-1. Geosynchronous orbit: $6.62 R_{\oplus}$ (earth radii) from center of earth
- B-2. STET orbit: $4.17 R_{\oplus}$
- B-3. ACE orbit: $2.5 R_{\oplus}$

These three figures are to the same scale, 3° per division.

Figures B-4 thru B-6 show how the apparent shape of the eastern CONUS coverage region changes for the STET satellite as it rises (Boston at 10° elevation angle), passes overhead (80° W meridian), and sets (Chicago at 10° elevation angle).

- B-4. STET orbit satellite rises; 128° W
- B-5. STET orbit satellite overhead; 80° W
- B-6. STET orbit satellite sets; 30° W

These three figures are to the same scale, 1° per division. Since the altitude of the STET satellite remains constant with time, the change in coverage region shape is due to the different satellite viewing positions and the foreshortening of the coverage region when the satellite is low in the sky.

Figures B-7 thru B-12 show how the apparent shape of the eastern CONUS coverage region changes for the ACE satellite as it rises (Boston at 10° elevation angle), passes overhead (80° W meridian), and sets (Chicago at 10° elevation angle) for the morning coverage and repeats for the afternoon coverage period.

- B-7. ACE orbit satellite, AM rising; 98.6° W and $1.94 R_{\oplus}$ distance from center of earth
- B-8. ACE orbit satellite, AM overhead, 66.6° W and $2.90 R_{\oplus}$
- B-9. ACE orbit satellite, AM setting, 36.8° W and $3.14 R_{\oplus}$
- B-10. ACE orbit satellite, PM rising; 123.2° W and $3.36 R_{\oplus}$
- B-11. ACE orbit satellite, PM overhead, 86.6° W and $2.36 R_{\oplus}$
- B-12. ACE orbit satellite, PM setting, 63.8° W and $1.81 R_{\oplus}$

These six figures are to the same scale, 3° per division. Note how the altitude of the ACE satellite changes with time over 0.8 to 2.4 earth radii. This results in dramatic changes in coverage region apparent size as well as shape changes due to the foreshortening of the coverage region when the satellite is low in the sky.

It is apparent that the ACE satellite does not follow the same path through the sky for the morning as for the afternoon coverage. This is because the satellite apogee position changes by 72° on successive orbits. Thus the satellite orbital position is a compromise for providing the morning

and afternoon coverages. However, the coverage repeats itself each day of the year; i.e. all morning coverages are the same and all afternoon coverages are the same.

One solution to changing coverage areas is to use a composite antenna pattern that covers the envelope of all possible coverages. This approach is used by Intelsat for the Intelsat V series of satellites where there are several possible orbital positions for the Atlantic Ocean region satellite. Figures B-13 and B-14 give composite coverages of the eastern half of CONUS for the STET and ACE satellites respectively. It is assumed that the antenna can be pointed such as to give the minimum coverage envelope.

B-13. Composite Coverage Pattern for STET Orbit Satellite Antenna

B-14. Composite Coverage Pattern for ACE Orbit Satellite Antenna

Comparison with the other figures shows that these composite patterns are larger than the individual patterns, particularly for the ACE orbit, and hence have lower gain antennas.

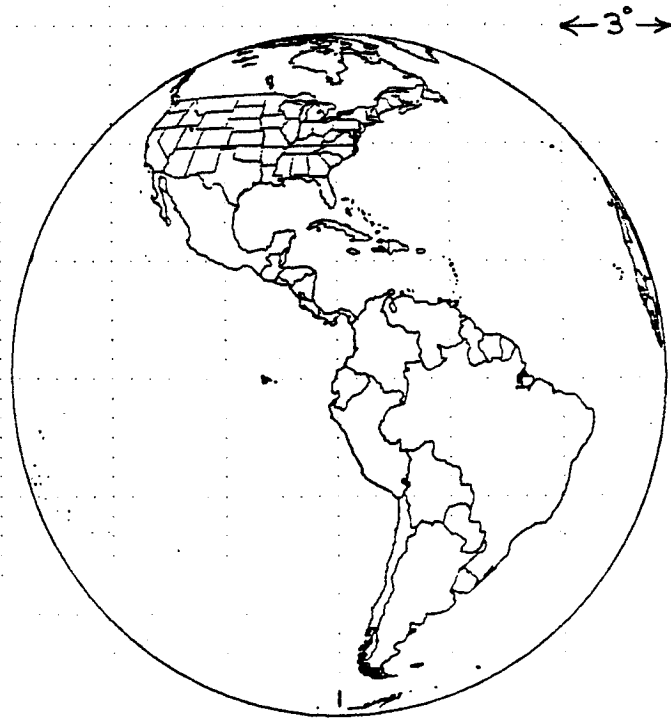


Figure B-1: View of Earth from GEO Orbit (80° W, $R = 6.62 R_\oplus$)

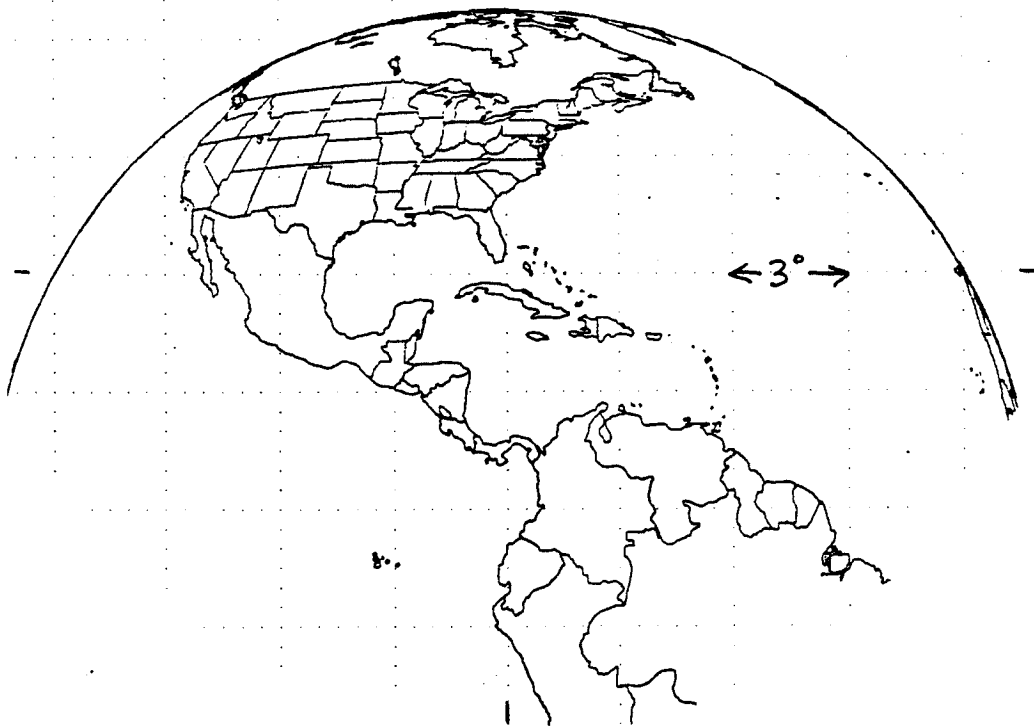


Figure B-2: View of Earth from STET Orbit (80° W, $R = 4.17 R_\oplus$)

ORIGINAL PAGE IS
OF POOR QUALITY

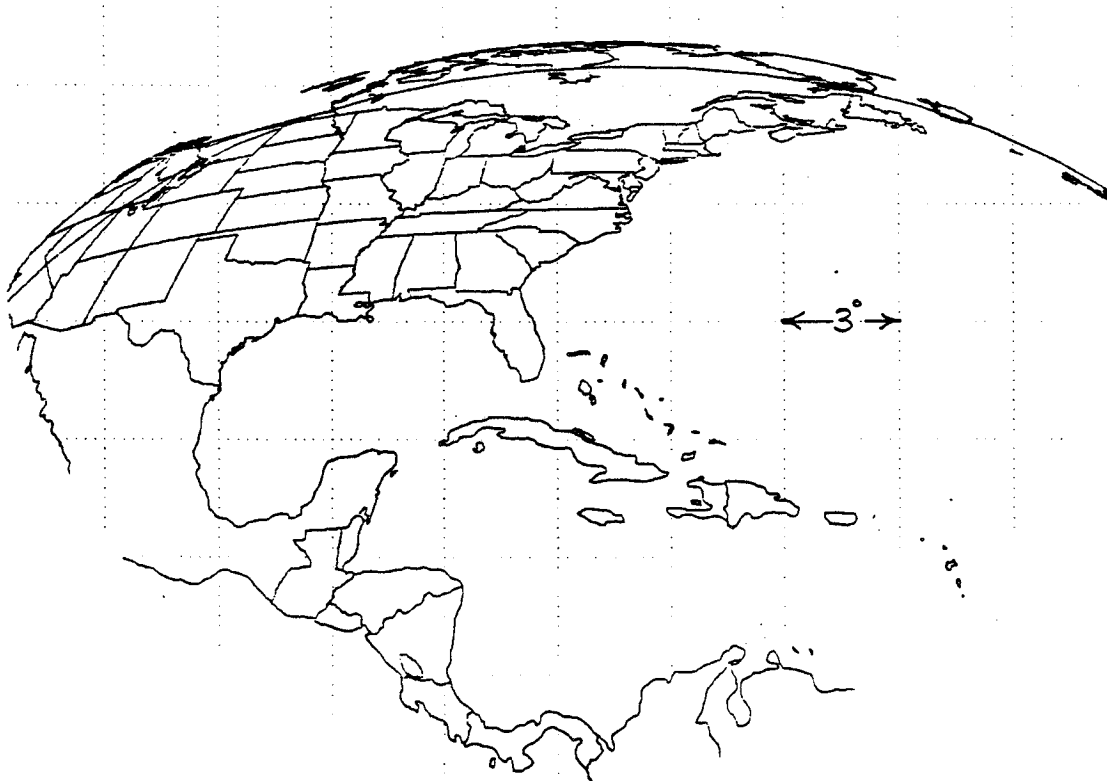


Figure B-3: View of Earth from ACE Orbit (76.6° W, $R = 2.5 R_\oplus$)

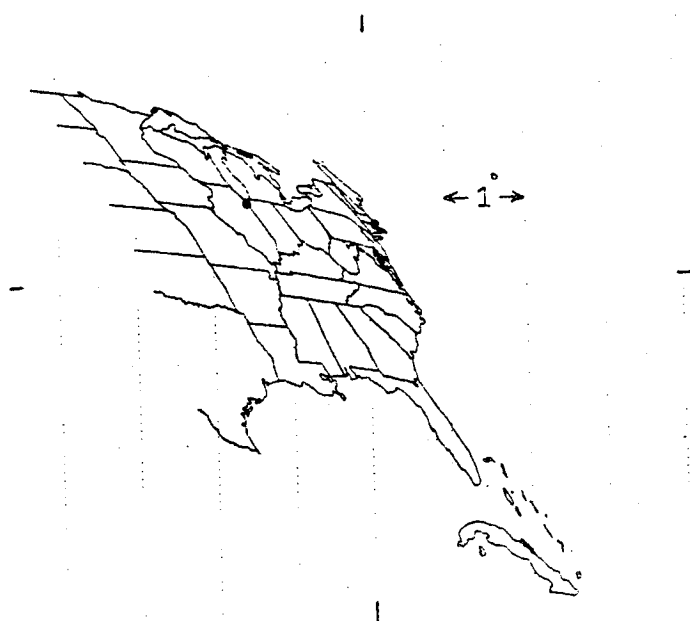


Figure B-4: STET Satellite Rises (128.3° W); Boston at 10° Elevation

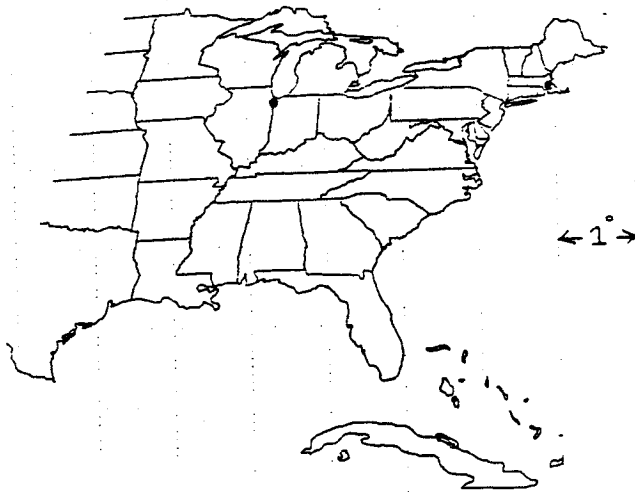


Figure B-5: STET Satellite Overhead (80° W)

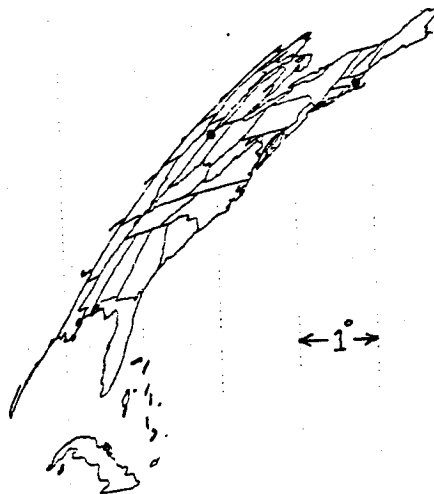


Figure B-6: STET Satellite Sets (29.9° W); Chicago at 10° Elevation